Discovery and properties of enzymes for biocatalytic production of β-amino acids

Crismaru, Ciprian

Discovery and properties of enzymes for biocatalytic production of β-amino acids

Ciprian Gică Crîşmaru

This Ph.D. syudy was carried out in the Biotransformation and Biocatalysis research group, Department of Biochemistry, Groningen Biomolecular Sciences and Biotechnology Institute (GBB) of the University of Groningen, the Netherlands.

This work was financially supported by the Netherlands Ministery of Economic Affairs and the B-Basic partner organizations (www.be-basic.org), through B-Basic, a public-private NOW-ACTS program (ACTS = Advanced Chemical Technologies for Sustainability).

Cover design by Off Page, Ciprian G. Crismaru and Samta Jain

Printing by Off Page, www.offpage.nl, Amsterdam

Printing costs were financially supported by the University Library and the Graduate School of Science Groningen, Faculty of Mathematics and Natural Sciences, University of Groningen.

Cover: the top image on the front shows the crystal structure (monomer) of *Variovorax paradoxus* *β*-phenylalanine aminotransferase (*Vp*AT). The bottom image on the front shows the *β*-phenylalanine docked in the active site of *Vp*AT. The image on the back represents the homodimeric structure of *Vp*AT. Images were taken by Ciprian G. Crismaru.

ISBN: printed version: 978-90-367-6965-5
digital version: 978-90-367-6966-2

rijksuniversiteit
groningen

Discovery and properties of enzymes for biocatalytic production of β-amino acids

Proefschrift

ter verkrijging van de graad van doctor aan de
Rijksuniversiteit Groningen
op gezag van de
rector magnificus prof. dr. E. Sterken
en volgens besluit van het College voor Promoties.

De openbare verdediging zal plaatsvinden op

vrijdag 9 mei 2014 om 14.30 uur

door

Ciprian Gică Crîşmaru

geboren op 5 maart 1982
te Târgu Frumos, Roemenië

Promotores

Prof. dr. D.B. Janssen

Prof. dr. B.W. Dijkstra

Beoordelingscommissie

Prof. dr. W. Kroutil

Prof. dr. L. Dijkhuizen

Prof. dr. ir. A.J. Minnaard

Contents

Chapter 1

Introduction and outline

1. Significance and occurrence of *β*-amino acids in natural products

In nature, non-proteinogenic *β*-amino acids occur as free compounds or as components of various secondary metabolites. In the free form, *β*-amino acids can act as osmoregulators and signaling molecules. As building blocks, they exist in a variety of non-ribosomal peptides that often show interesting bioactivity (Wani *et al.,* 1971; Shih *et al.,* 1999; Namikoshi *et al.,* 1989). For example, some *β*-amino acids are precursors of *β*-lactam antibiotics or of anticancer agents, like taxol (Benaglia *et al.,* 2000; Magriotis, 2001; Steele *et al.,* 2005). It became apparent in the last few decades that *β*-amino acids may be also used as building blocks for the development of synthetic compounds with pharmacological activity, such as peptidomimetics, antibiotics and anti-cancer agents (Juaristi & Soloshonok, 2005; Liu & Sibi, 2002). Due to their potential role in the preparation of pharmaceutical compounds, *β*-amino acids are becoming important targets for research aimed at finding new synthetic routes and new functionalization reactions.

Since *β*-amino acids have two carbon atoms that separate the carboxylate and amino groups, side chains can be present at the *α*-(C2) carbon atom or at the *β*-(C3) carbon atom, either in the (*R*) or (*S*) configuration. This can result in up to four possible isomers for *α,β*-disubstituted *β*-amino acids. Substituted *β*-amino acids are defined as β^2-amino acids, β^3-amino acids and $\beta^{2,3}$-amino acids according to the number and position of the substituents (**Scheme 1.1**).

Examples of *β*-amino acids that are present in bioactive molecules (**Scheme 1.2**) are *β*-tyrosine, a building unit in jasplakinolide, which acts as an antifungal antibiotic (Crews *et al.,* 1986), (*S*)-3-chloro-5-hydroxy-*β*-tyrosine, which is formed by

---

Part of this chapter was published: Wu B., Szymanski W., Crismaru C.G., Feringa B.L. and Janssen D.B. (2012) C-N lyases catalyzing addition of ammonia, amines and amides to C=C and C=O bonds, p 749–778. *In* Drauz K., Groger H., May O. (ed), *Enzyme Catalysis in Organic Synthesis*. Wiley-VCH, New York, NY.

a tyrosine aminomutase and incorporated into the structure of the antitumor antibiotic enediyne C-1027 (Christenson *et al.,* 2003), and (*R*)-2-aza-3-chloro-*β*-tyrosine, a building block in the biosynthesis of the antitumor antibiotic kedarcidin, which is structurally related to enediyne C-1027 (Huang *et al.,* 2013).

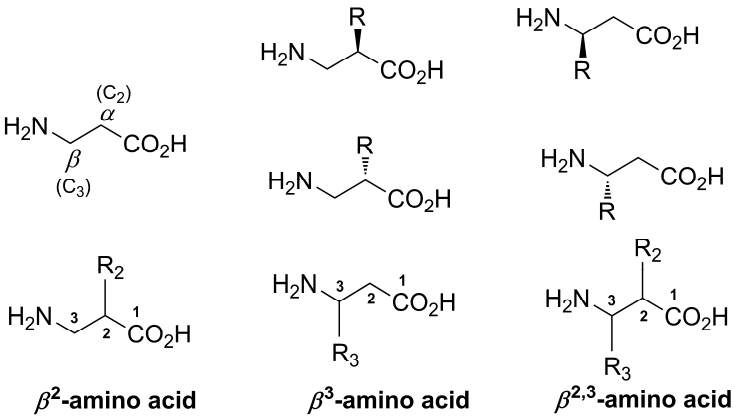

Scheme 1.1 Structures of *β*-amino acids (β^2, β^3, $\beta^{2,3}$) and possible enantiomers.

Another example is *β*-phenylalanine, which occurs in modified form in taxol (paclitaxel), a compound used for the treatment of lung, breast and ovarian cancer (Steele *et al.,* 2005; Mekhail & Markman, 2002). Further on, *β*-alanine occurs in the biosynthesis of pantothenic acid and *α*-methyl-*β*-alanine is present in the skeleton of cryptophycin, an anti-tumor agent (Steer *et al.,* 2002; Seebach *et al.,* 1998a; Seebach *et al.,* 1996). In addition, a β^3-quinoline-*β*-alanine derivative (Elarobifan, RWJ-53033) was found to be a potent non-peptide integrin antagonist (Hoekstra & Poulter, 1998).

A class of *β*-amino acid containing compounds that has drawn significant interest are the *β*-peptides (Seebach *et al.,* 1996; Appella *et al.,* 1996; Seebach *et al.,* 1998a). Optically pure enantiomers of *β*-amino acids have been incorporated into peptides and peptidomimetics with biological and pharmacological activity (Steer *et al.,* 2002). The *β*-peptides that are produced are resistant to proteases such as pepsin, chymotrypsin, and trypsin which rapidly degrade peptides composed of α-amino acids. Incubation of mixtures of *α*-peptides and *β*-peptides with proteases showed that *β*-peptides were resistant to cleavage by proteases, whereas *α*-peptides were degraded, suggesting that *β*-peptides are not inhibiting and do not bind to the proteases (Seebach *et al.,* 1998b). However, it has been shown by enrichment experiments that degradation of *β*-peptides by a consortium of microorganisms can

occur at a low rate. Such microbial consortia can utilize these compounds as sole carbon and energy source (Schreiber *et al.,* 2002).

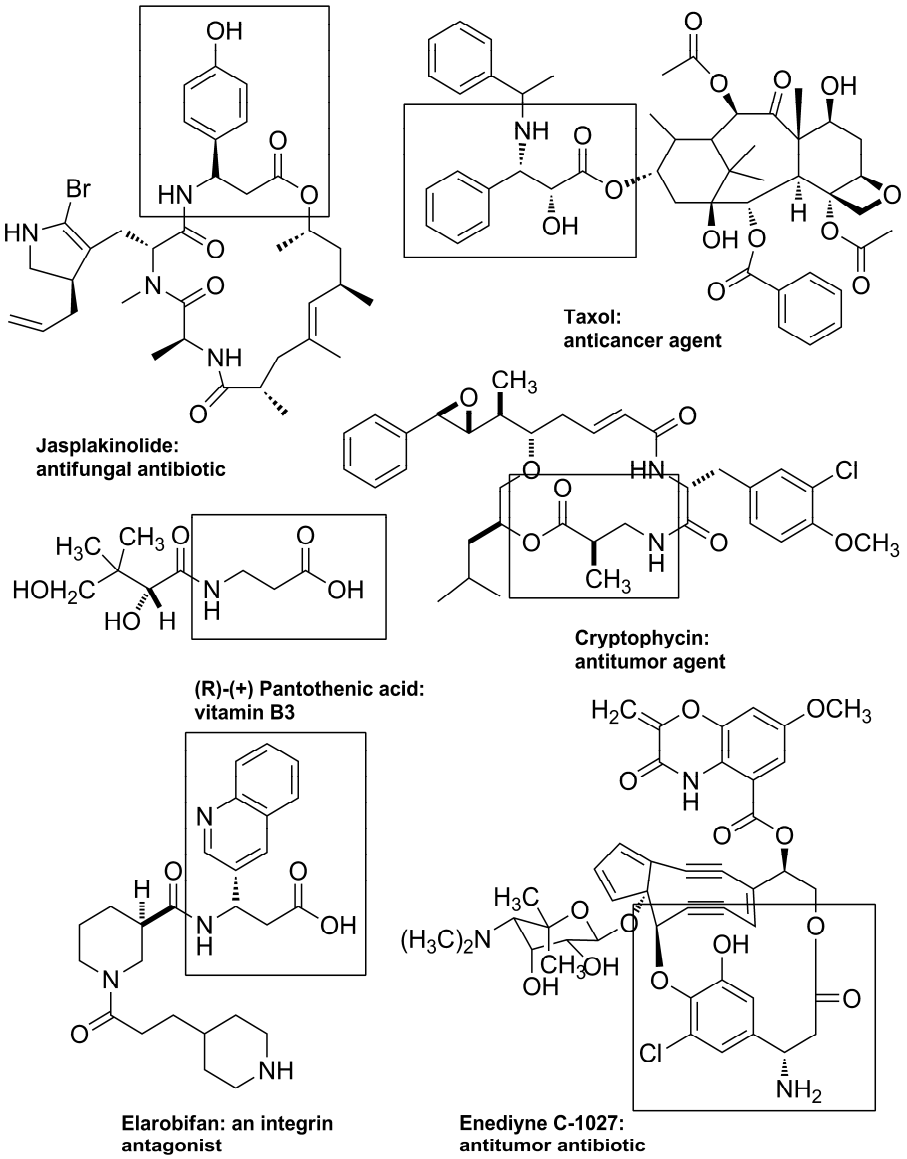

Scheme 1.2 Natural compounds containing *β*-amino acid units.

The enzymatic degradation of various types of *β*-peptides by *β*-peptidyl aminopeptidases that catalyze the N-terminal cleavage of *β*-amino acids from

oligopeptides has been reported (Heck *et al.,* 2006). The natural function of these enzymes is not yet understood (Geueke & Kohler, 2007).

2. Preparation of *β*-amino acids

2.1. Chemical

The most common methods for the chemical synthesis of *β*-amino acids are catalytic asymmetric hydrogenation, conjugate addition of carbon and nitrogen nucleophiles to *α,β*-unsaturated systems, and the Mannich reaction (Seebach *et al.,* 2009; Weiner *et al.,* 2010; Seebach & Gardiner, 2008; Tang & Zang, 2003). An example of a hydrogenation reaction is in synthesis of cispentacin (**Scheme 1.3**) using (*S*)-C3-TunaPhos **1.3.1** as ligand in a ruthenium catalyzed reaction that yields product with excellent enantiomeric excess (*ee* up to 99%, Tang *et al.,* 2003). In the same reaction, TangPhos **1.3.2** and Me-DuPhos **1.3.3** gave the cispentacin derivative with significantly lower *ee*.

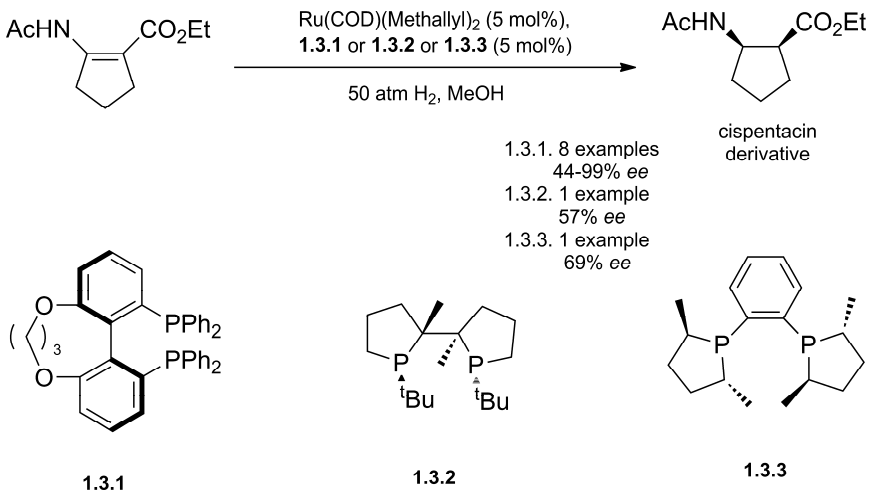

Scheme 1.3 Ru-catalyzed hydrogenation towards cyclic *β*-amino acids.

Chemical synthesis of *β*-amino acids is extensively studied in the PhD thesis of B. Weiner (2009) and described in a recent review (Weiner *et al.,* 2010). This thesis focuses on biochemical transformations.

2.2. Enzymatic

An attractive alternative for chemical preparation of enantiopure *β*-amino acids is enzymatic synthesis. In several cases, enzymatic processes for peptide synthesis appear to have significant advantages over chemical processes, e.g. in the synthesis of semi-synthetic antibiotics (Bruggink *et al.,* 2001; Tramper *et al.,* 2001) and artificial sweetener aspartame (Hanzawa & Kidokoro, 1999; Hanzawa *et al.,* 1999). The main advantages are high enantioselectivity, high regioselectivity, mild reaction conditions and low amounts of catalyst used. This delivers both environmental and economic benefits (Liljeblad & Kanerva, 2006; Swiderska & Stewart, 2006; Szymanski *et al.,* 2009). However, the development of a biocatalytic process can be time consuming since it is critically dependent on the possibility to discover or engineer a good enzyme for the desired conversion. At this moment there are only few biocatalytic options for producing enantiopure *β*-amino acids. The main routes are based on the kinetic resolution of *β*-amino acids or derivatives thereof. Asymmetric transformations starting with non-chiral compounds would yield an even more attractive process.

2.2.1 Preparation of enantiopure β-amino acids by kinetic resolution

In an ideal kinetic resolution process one enantiomer in a racemic mixture is converted into an enantiopure product by selective and complete transformation. Thus, the yield is maximally 50%, unless a dynamic resolution is carried out, in which the starting compound is racemized to continuously provide the enantiomer that is converted. Examples of enzymes used for preparation of *β*-amino acids by biocatalysis are reviewed by Liljeblad & Kanerva (2006). The list includes lipase, lactamase, acylase, nitrilase and nitrile hydratase.

Enantiopure *β*-amino acids can be prepared from their racemic ester derivatives or prochiral precursors by enzymatic catalyzed hydrolysis. Examples are pig liver esterase (PLE, EC 3.1.1.1) and chymotrypsin (EC 3.4.21.1)-catalyzed hydrolysis of *N*-protected *β*-aminoglutarate (Ohno *et al.,* 1981), aspartate (Cohen *et al.,* 1963) and *β*-phenylalanine derivatives (Cohen & Weinstein, 1964). The enzymatic hydrolysis of the prochiral compound dimethyl *β*-aminoglutarate (**1.4.1**) into **(*R*)-1.4.2** proceeds with low product enantioselectivity (**Scheme 1.4**, **panel A**). It was suggested that this is due to pronounced chemical hydrolysis parallel to the enzymatic reaction. By using *N*-benzyloxycarnonyl (Z) as a protecting group, hydrogen bond formation of the amino group to the carbonyl oxygen is prevented, which translates in efficient synthesis of **(*S*)-1.4.3**, with reversed and improved enantioselectivity.

In the second example, α-chymotrypsin exhibits high enantioselectivity towards diethyl *N*-acetyl aspartate (***rac*-1.4.4**) and diethyl *β*-acetamido-glutarate (***rac*-1.4.6**). The α-ester group of diethyl *N*-acetyl aspartate is hydrolyzed rapidly with high enantioselectivity, yielding **(*S*)-1.4.5**. The hydrolysis of meso-diethyl *β*-acetamido-glutarate (***rac*-1.4.6**) proceeded to 83% conversion in 5 h, producing **(*R*)-1.4.2** with high enantioselectivity (**Scheme 1.4**, **panel B**). Lastly, α-chymotrypsin catalyzed the enantioselective hydrolysis of ethyl *β*-acetamido-3-phenylpropionate (***rac*-1.4.8**), yielding the correspondent **(*R*)-1.4.8** and **(*S*)-1.4.9**, with a modest conversion (**Scheme 1.4**, **panel C**).

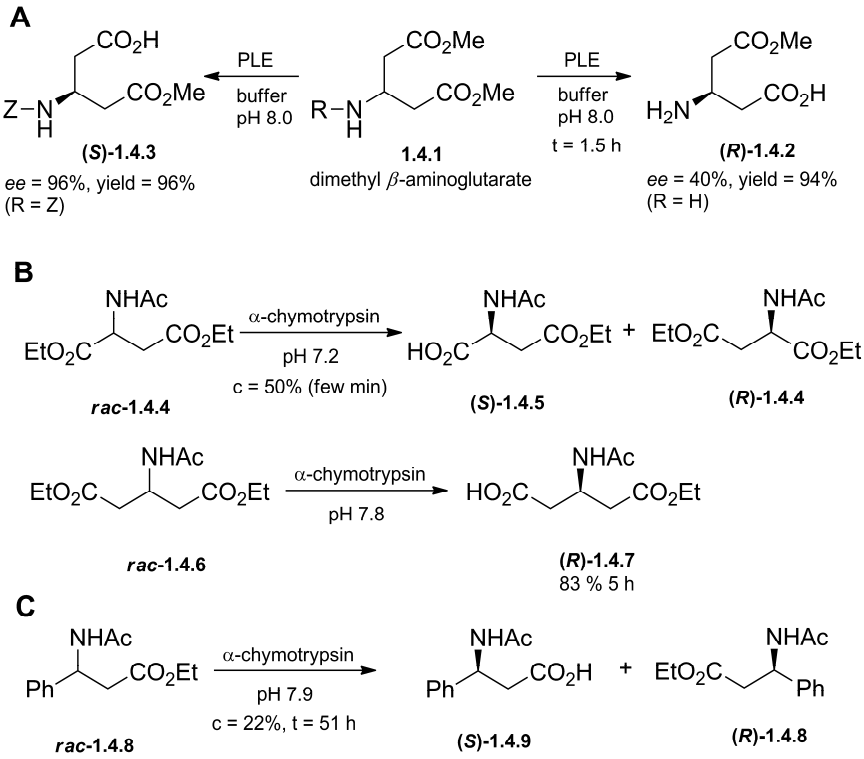

Scheme 1.4 Kinetic resolution of *β*-amino acid esters derivatives using pig liver esterase and chymotrypsin.

A fourth example is the kinetic resolution of racemic *β*-aminobutyric acid derivatives (Sanchez *et al.,* 1997). *Candida antarctica* lipase (EC 3.1.1.3) was used in 1,4-dioxane where ammonolysis of *N*-unprotected **1.5.1** was observed with formation of (*S*)-*β*-aminobutyric ethyl ester **1.5.3** and (*R*)-amide product **1.5.6** (**Scheme 1.5**). However, when the substrate was *N*-benzyloxycarbonyl (Cbz) derivative **1.5.2**, the

(*R*)-hydrolytic product **1.5.5** was formed besides **1.5.4**. When 1 eq. of H_2O was used instead of NH_3, a lower reaction rate and enantioselectivity (*E*) was observed. Further, if besides 1 eq. of H_2O, another 1 eq. of Et_3N was added, a very high *E* was obtained and high conversion. Et_3N was used instead of NH_3 in order to avoid amide formation. Hydrolysis was also attempted in a buffer at pH 7.0, wherein a higher reaction rate and lower *E* were observed.

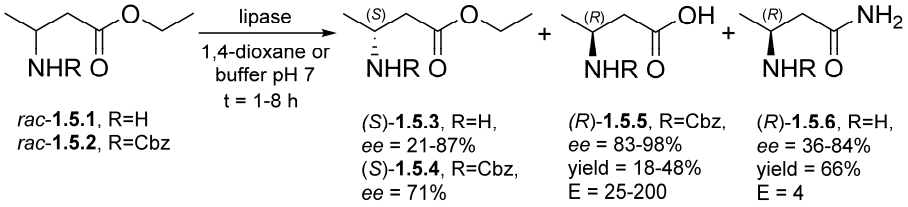

Scheme 1.5 Ammonolysis and hydrolysis of *rac*-*β*-aminobutyric ethyl ester and *N*-Cbz-*β*-aminobutyric ethyl ester by *C. antarctica* lipase (adopted from Sanchez *et al.,* 1997).

A fifth example is the resolution of *rac*-3-aryl-3-aminopropionic acid esters ***rac*-1.6.1 - 1.6.6e** giving (*S*)-3-amino-arylpropionic acid esters **(*S*)-1.6.1 - 1.6.6e** catalyzed by *Pseudomonas cepacia* lipase. Very high enantioselectivities were observed with different aryl substituents (**Scheme 1.6)**. The (*S*)-3-amino-phenylpropionic acid ethyl ester **(*S*)-1.6.1e** was isolated with 99.6% *ee* and yields up to 46% were reported (Faulconbridge *et al.,* 2000; Groger & Werner, 2003).

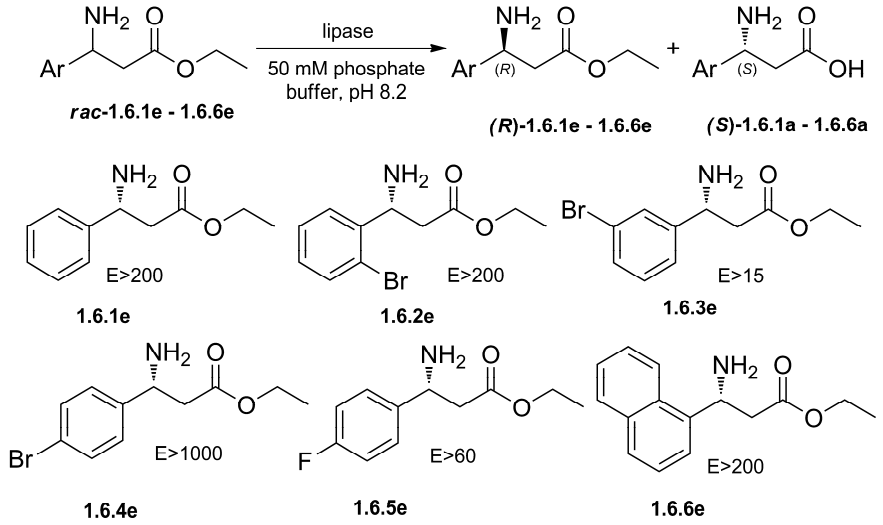

Scheme 1.6 Kinetic resolution of *rac*-3-aryl-3-aminopropionic acid esters by *P. cepacia* lipase.

A sixth example is the kinetic resolution of β^2-amino acids such as *N*-acylation of α-methyl-β-alanine ethyl ester ***rac*-1.7.1** by *Candida antarctica* lipase A (CAL-A) followed by an interesterification catalyzed by CAL-B (Solymar *et al.,* 2002). The step catalyzed by CAL-A with 2,2,2-trifluoroethyl butanoate proceeds with low enantioselectivity (E = 7), in the presence of acetonitrile (ACN) as solvent. The reaction gives **(*R*)-1.7.1** and **(*S*)-1.7.2** with low *ee* at up to 75% conversion (**Scheme 1.7**, **panel A**). Incubation with CAL-B increases the *ee* of the latter by interesterification of the (*R*)-enantiomer with butyl butanoate yielding highly enantioenriched **(*S*)-1.7.2** (**Scheme 1.7**, **panel B**).

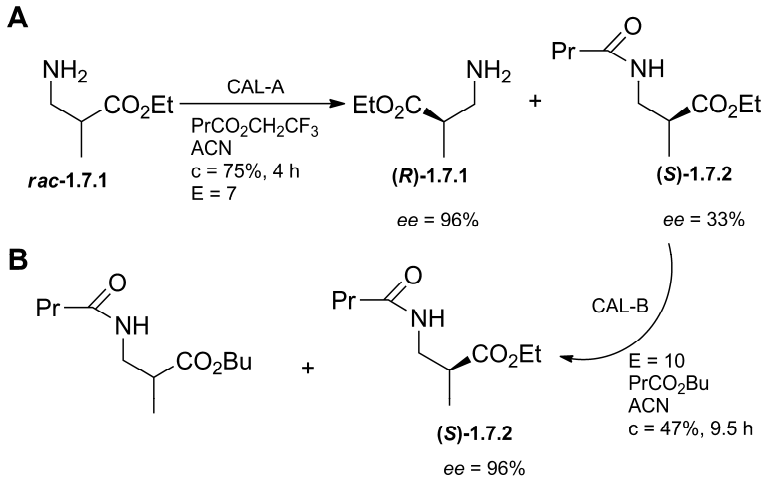

Scheme 1.7 Kinetic resolution of *rac*-α-methyl-β-alanine ethyl ester by CAL-A (**panel A**) and CAL-B (**panel B**).

Other enzymes, such as Baeyer-Villiger monooxygenases (BVMOs), have been proposed as biocatalytic tool for the synthesis of enantiomerically pure β-amino acids and β-amino alcohols (Rehdorf *et al.,* 2010). BVMOs are flavoenzymes (EC 1.14.13.X) that convert cyclic ketones to lactones and aromatic, aliphatic or aryl alkyl ketones into esters, using molecular oxygen. Four enzymes from different bacterial species were used, namely cyclododecanone monooxygenase from *Rhodococcus ruber* SC1 (CDMO) and cyclohexanone monooxygenases from *Arthrobacter* sp. ($CHMO_{Arthro}$), from *Brachymonas* sp. ($CHMO_{Brachy}$) and from *Xanthobacter* sp. ZL5 ($CHMO_{Xantho}$). The enzymes actively converted *N*-protected-β-amino ketone **1.8.1** with high enantioselectivity. Substrate **1.8.1** is oxidized by CDMO into the (*R*)-enantiomer of product **1.8.2**, which is in contrast to the other three enzymes, for which the product

is the (*S*)-enantiomer. In both cases a very high *ee* was obtained (**Scheme 1.8**, **panel A**). After isolation and purification of the Baeyer-Villiger products (*N*-protected *β*-amino esters **1.8.2** and **1.8.3**) hydrolysis was performed with CAL-B (*C. antarctica* lipase B) in a next step to give optically pure *N*-protected *β*-amino acids. Furthermore, *N*-protected *β*-amino alcohols can be obtained (**Scheme 1.8**, **panel B**).

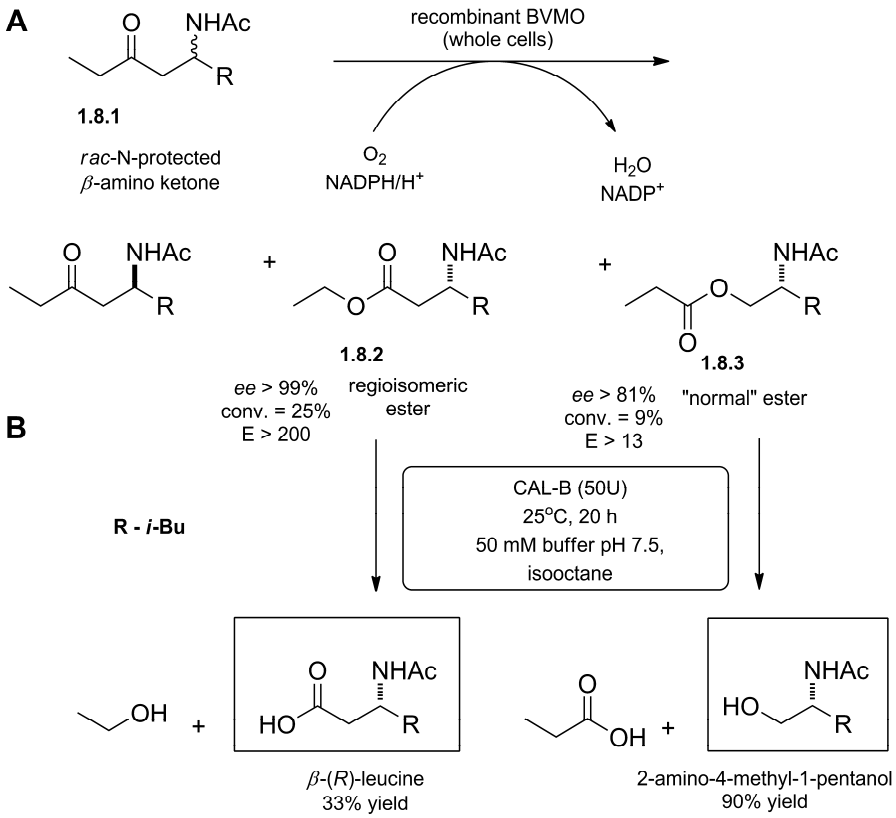

Scheme 1.8 BVMO-catalyzed kinetic resolution of the racemic aliphatic *N*-protected *β*-amino ketone **1.8.1** (**panel A**) and lipase-catalyzed hydrolysis of Baeyer-Villiger esters forming *N*-protected *β*-(*R*)-leucine and 2-amino-4-methyl-1-pentanol (**panel B**).

2.2.2 Synthesis of β-amino acids by asymmetric transformations using C-N bond forming enzymes

Enzymatic asymmetric synthesis is an important alternative to kinetic resolution because its main advantage is that 100% product yield can be obtained if the equilibrium is efficiently directed to the formation of the desired product. Among

the enzymes that can be used in asymmetric synthesis of *β*-amino acids are ammonia lyases (ALs), aminomutases (AMs) and aminotransferases (ATs) (**Scheme 1.9**).

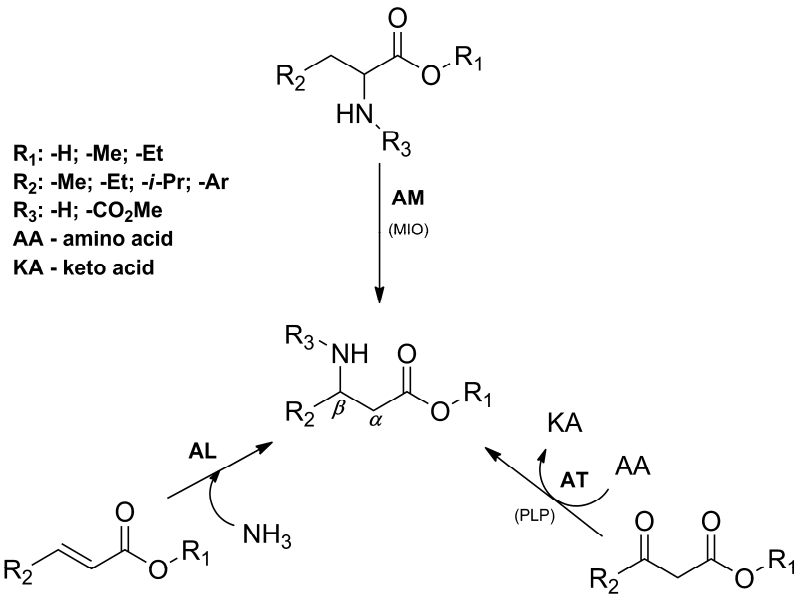

Scheme 1.9 Possible biocatalytic routes towards *β*-amino acids based on by asymmetric synthesis.

Ammonia lyases (EC 4.3.1.X) catalyze the addition of small nucleophiles such as ammonia, to C=C bonds, with L-aspartase as a typical example (aspartase/fumarase superfamily). L-aspartase (EC 4.3.1.1) is present in many bacteria and plants, where it is involved in the catabolism of L-aspartate to produce ammonia and fumarate. From bacteria, well-characterized aspartases are those from *E. coli* (AspA), *Bacillus* sp. YM55-1 (AspB) and *Hafnia alvei* (Mizobata & Kabata, 2007). These enzymes are very specific, having a rather narrow substrate scope. For example, AspA has no activity with D-*α*-aspartic acid, L-*α*-asparagine or other L-*α*-amino acids. In the reverse reaction, there is no activity with unsaturated carboxylic acids other than fumaric acid, and activity with other nucleophiles than ammonia is very limited. These enzymes are homotetrameric proteins with monomers of 52-55 kDa.

The aspartate ammonia lyase-catalyzed addition of ammonia to fumaric acid has been implemented commercially on multi-thousand ton scale for the industrial production of (*S*)-aspartic acid with very high enantiomeric excess (*ee*) and high yield (**Scheme 1.10)** (Wubbolts, 2002; Chibata *et al.,* 1992). Thus, L-aspartase has found

application since the 1970s in the form of a whole-cell biocatalyst (Mizobata & Kawata, 2007).

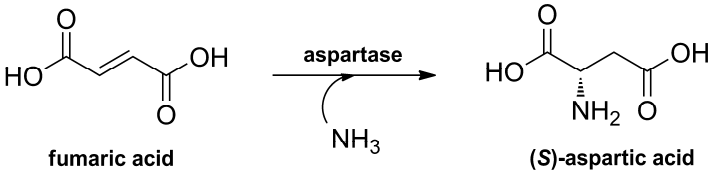

fumaric acid **(*S*)-aspartic acid**

ee = 100%, yield = 100%

Scheme 1.10 Michael addition of ammonia to fumaric acid by aspartase.

Another group of ammonia lyases with potential biocatalytic application, are the **methylaspartate ammonia lyases**, (MALs) (EC 4.3.1.2). They are involved in the anaerobic degradation of glutamate in *Clostridium tetanomorphum* and several other (facultative) anaerobic organisms that initiate glutamate degradation via a mutase reaction that yields L-threo-3-methylaspartic acid ((2*S*,3*R*)-3-methylaspartatic acid). This product is converted by the lyase to mesaconic acid. The enzymes are homodimeric proteins with subunits of 45 kDa of which the structure and sequence indicate that they are members of the enolase superfamily (Gerlt *et al.,* 2005). Enzymes of this class catalyze a wide diversity of reactions, and include lyase-, (de)hydratase, racemase-, and decarboxylase-type conversions. Like other members of the enolase superfamily, methylaspartate ammonia lyase requires Mg^{2+} and K^{+} for activity, and a Mg^{2+} ion located in the active site is involved in substrate binding. Similar methylaspartate ammonia lyases have been obtained from *C. tetanomorphum* (Goda *et al.,* 1992) *Citrobacter amalonaticus* (Kato & Asano, 1988), *E. coli* (Kato & Asano, 1995) and other organisms (see references in cited papers).

Methylaspartate ammonia lyases have a much broader substrate range than aspartases. They catalyze a stereoselective addition of ammonia and other nitrogen compounds not only to mesaconic acid but also to several analogs. Compounds that were used include chloro- and bromo-fumaric acid and, at a very low rate, *n*- and *i*-propylfumaric acid, giving 3 substituted (2*R*,3*R*)-aspartates (Akhtar *et al.,* 1987; Botting *et al.,* 1988). In all cases the same stereochemistry prevailed with *si*-face attack of the amine.

Alternative *N*-nucleophiles that can be used include hydrazine, methylamine, hydroxylamine, methoxylamine, and to some extent ethylamine and dimethylamine (Raj *et al.,* 2012a), and in the presence of excess *N*-nucleophile at high pH (9.0) good conversion of mesaconate (40-90%) was achieved (**Scheme 1.11**, Gulzar *et al.,* 1997). In all cases only a single diastereomer with the expected stereoconfiguration was

obtained. When ethyl-, isopropyl- and propyl-fumaric acids were used with hydrazine the 2-hydrozino-3-alkyl substituted succinates were also found. Most of these reactions occurred very slowly. Even though some alternative substrates are accepted, the active site appears quite small, as indicated by the observation that a combination of a larger 3-substituent (instead of methyl) and a larger *N*-nucleophile abolishes the reaction.

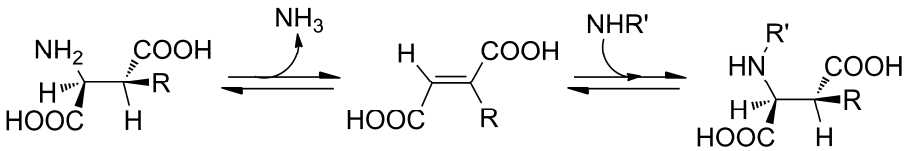

R = -Me; -Et; -*i*-Pr; -Pr; -Cl
R' = -NH_2; -Me; -OH; -OMe; -Et

Scheme 1.11 Reactions catalyzed by MAL.

Of great importance are also aromatic ammonia lyases (ALs), such as L-histidine (EC 4.3.1.3), L-phenylalanine (EC 4.3.1.24) and L-tyrosine ammonia lyases (EC 4.3.1.23). The biological role of microbial L-histidine ammonia lyases and L-phenylalanine ammonia lyases is catabolic. Other aromatic C-N lyases, such as plant L-phenylalanine ammonia lyases and tyrosine ammonia lyases, play a role in biosynthesis by generating the corresponding unsaturated carboxylic acids, which are used for lignin synthesis. Tyrosine ammonia lyase (EC 4.3.1.23) is also involved in the synthesis of coumarate, which can serve as a precursor for cofactors or as a building block for some antibiotics. These are so-called MIO-dependent enzymes because they use during catalysis the cofactor methylideneimidazole-5-one (MIO). The cofactor is formed from a conserved tripeptide in the protein sequence (AlaSerGly). Since some aminomutases (AMs) also contain MIO, these groups of enzymes will be discussed together. The role of MIO has been under debate, but crystal structures of AMs with substrate analogues (Christianson *et al.,* 2007) indicate that MIO reacts with the amino group of the substrate during the mutase reaction (Cooke *et al.,* 2009). Aromatic ammonia lyases and aminomutases have been recently reviewed together with other enzymes that are able to perform addition of ammonia, amines or amides to C=C and C=O bonds (Wu *et al.,* 2012[a]). L-phenylalanine ammonia lyase (EC 4.3.1.24) can be used for the production of L-phenylalanine from cinnamic acid, and is active with several substituted analogs (Poechlauer *et al.,* 2010). The progress of these reactions is dependent on the thermodynamic equilibrium, so high concentrations of ammonia are required (**Scheme 1.12**).

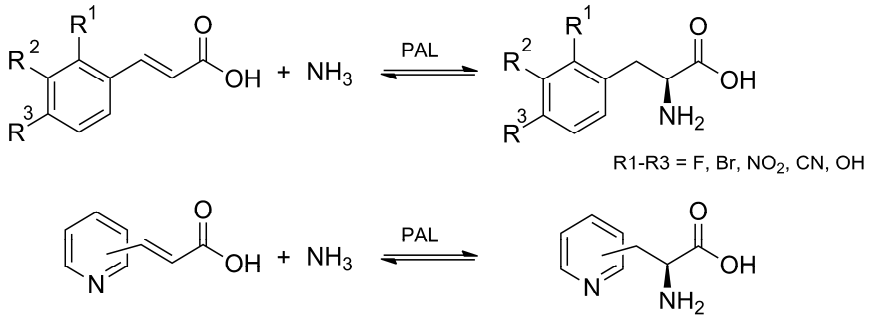

Scheme 1.12 Reactions catalyzed by MIO-type aromatic ammonia lyases.

A number of other amines can possibly be synthesized with these enzymes as well. Further applications will be dependent on the discovery and/or engineering of enzyme variants that show improved conversion kinetics, accept a broader range of substrates, or that are better compatible with the required reaction conditions (Heberling *et al.,* 2013).

Among MIO-dependent aminomutases with potential biotechnological relevance, at least two can be mentioned. Phenylalanine aminomutase (PAM) (EC 5.4.3.10) from *Taxus chinensis* (Wu *et al.,* 2009), is involved in providing the precursor of the N-benzoylphenyl-*iso*-serinoyl side chain of the anti-cancer drug taxol (Steele *et al.,* 2005). Optically pure aromatic *β*-amino acids can be obtained by using PAM in a reaction of *trans*-cinnamic acid with ammonia (Wu *et al.,* 2009). Since the ammonia addition reaction proceeds with low regioselectivity, (*S*)-*α*-phenylalanine and (*R*)-*β*-phenylalanine were obtained in a ratio of 51:49 (*α*:*β*). The *ee* values for the both products were higher than 99% (**Scheme 1.13**). The reaction was performed in 6 M ammonia and pH 10, which could be reached after bubbling the ammonia buffer with CO_2.

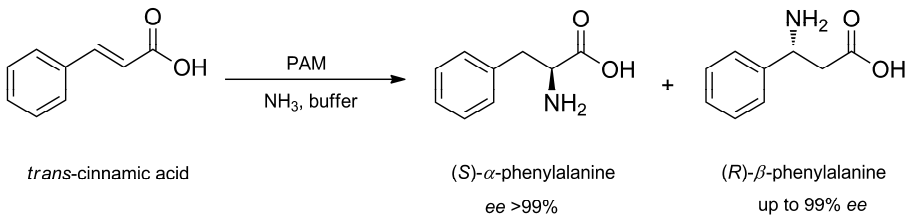

Scheme 1.13 Synthesis of enantiomerically pure (*S*)-*α*-phenylalanine and (*R*)-*β*-phenylalanine by PAM-catalyzed ammonia addition to *trans*-cinnamic acid.

Using the same enzyme, a series of enantiomerically pure (*R*)-*β*-phenylalanine derivatives and (*S*)-*α*-phenylalanine derivatives (18 examples) were prepared from *trans*-cinnamic acid derivatives (**Scheme 1.14**). The absolute configuration of the products was resolved by chiral HPLC using standard compounds (Szymanski *et al.,* 2010). Both for substituted (*S*)-*α*-phenylalanines and (*R*)-*β*-phenylalanines excellent *ee* was achieved (up to >99%). The ratio between (*S*)-*α*-phenylalanine derivatives and (*R*)-*β*-phenylalanine derivatives differs depending upon the nature and position of the substituent on the aromatic ring of cinnamic acid. For instance cinnamic acid derivatives that have electron-donating groups are predominantly converted to *β*-amino acids, which could be justified by a lower capacity of the phenyl ring to accept electrons. For the synthesis of *β*-phenylalanine derivatives, the best results were obtained with cinnamic acid derivatives that have an electron-donating (alkyl and alkoxy) in the *para* position. The cinnamic acid derivative with a NO_2-group (strong electron-withdrawing) on the *para* position is converted almost exclusively to an *α*-amino acid and predominant formation of (*S*)-*α*-amino acids that possess fluoro, cloro, bromo or methyl substituents was also found.

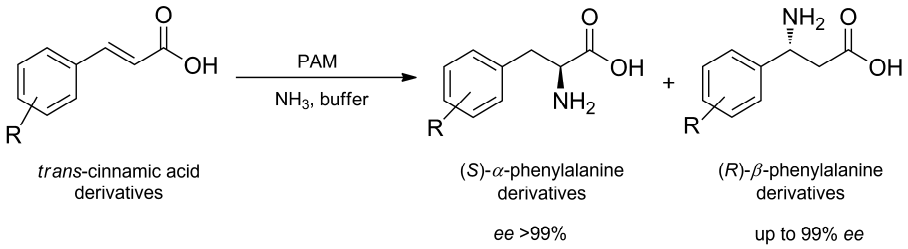

Scheme 1.14 Synthesis of pure enantiomers (*S*)-*α*-phenylalanines (*R*)-*β*-phenylalanines by PAM-catalyzed addition of ammonia to *trans*-cinnamic acid derivatives.

The second promising MIO-dependent AMs are tyrosine aminomutase (TAM) from *Streptomyces globisporus* (SgTAM) and TAM from *Streptoalloteichus* sp. ATCC 53650 (KedY4), which in these microbes provide precursors for the biosynthesis of antitumor antibiotics. SgTAM is responsible for the conversion of L-*α*-tyrosine into (*S*)-*β*-tyrosine, which is used for the biosynthesis of enediyne C-1027 (Christenson *et al.,* 2003), an antitumor antibiotic, whereas TAM from *Streptoalloteichus* sp. ATCC 53650 converts 2-aza-L-*α*-tyrosine into (*R*)-2-aza-*β*-tyrosine, which serves as precursor in the biosynthesis of kedarcidin, an antibiotic structurally related to C-1027 chromophore (Huang *et al.,* 2013) (**Scheme 1.15**).

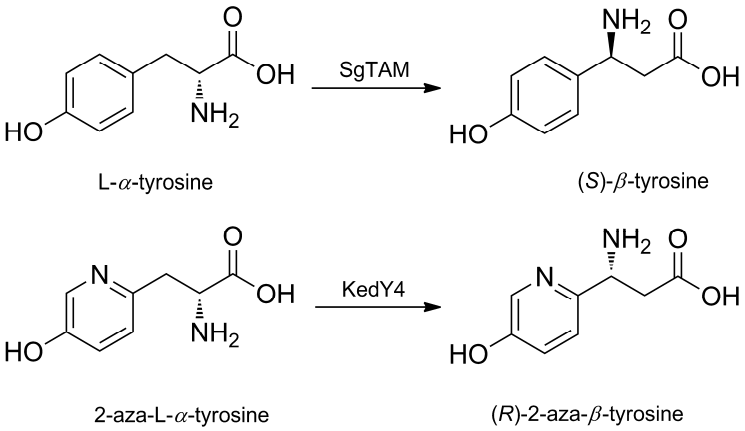

Scheme 1.15 Conversion of L-α-tyrosine and its 2-aza-derivative to (*S*)-β-tyrosine and (*R*)-2-aza-β-tyrosine, respectively by TAMs.

2.2.3 Other transformations

Another group of enzymes that could possibly be used for the preparation of β-amino acids are aminomutases that convert aliphatic amino acids. This group of enzymes (EC 5.4.3.X) catalyzes the conversion of different aliphatic α-amino acids, such as lysine, glutamate, leucine and ornithine into the corresponding β-amino acid analogs. Some members of this group are known as S-adenosyl-L-methionine (SAM)-dependent enzymes, because they require for the enzymatic activity SAM, [4Fe-4S] cluster and PLP (pyridoxal 5'-phosphate).

So far, the best characterized member from this group is lysine 2,3-aminomutase (2,3-LAM) from *C. subterminale, B. subtilis* and *E. coli*. As a potential biocatalyst, the recombinant 2,3-LAM that originates from the previously three mentioned sources, was produced by *C. glutamicum*, which proved to serve as a robust host (Zelder *et al.,* 2009). The wild type enzyme in *C. subterminale* and *B. subtilis* catalyzes the isomerization of (*S*)-α-lysine onto (*S*)-β-lysine and vice-versa depending upon the cell needs (Aberhart *et al.,* 1981). The product of *E. coli* 2,3-LAM using the same substrate is (*R*)-β-lysine (Behshad *et al.,* 2006). However, its low activity limits its application to other amino acid conversions. The enzyme from *C. subterminale* converts other substrates such as (*S*)-α-alanine, (*S*)-α-aspartate, (*S*)-α-glutamate, (*S*)-α-homoserine, (*S*)-α-methionine and (*S*)-α-homocysteine (Frey & Ruzicka, 2008a). However, little information is known about its application in industrial processes.

Other SAM-dependent aminomutases, such as 2,3-glutamate aminomutase (2,3-GAM) was investigated and efficiently used to produce β-glutamate from (*S*)-α-

glutamate (**Scheme 1.16**) (Frey & Ruzicka, 2008b). The 2,3-GAM and the 2,3-LAM are related in amino acid sequence and share relevant amino acid residues, such as the cysteine motif CxxxCxxC that is linked to [4Fe-4S] cluster, or the lysine residue that binds PLP (Ruzicka & Frey, 2007).

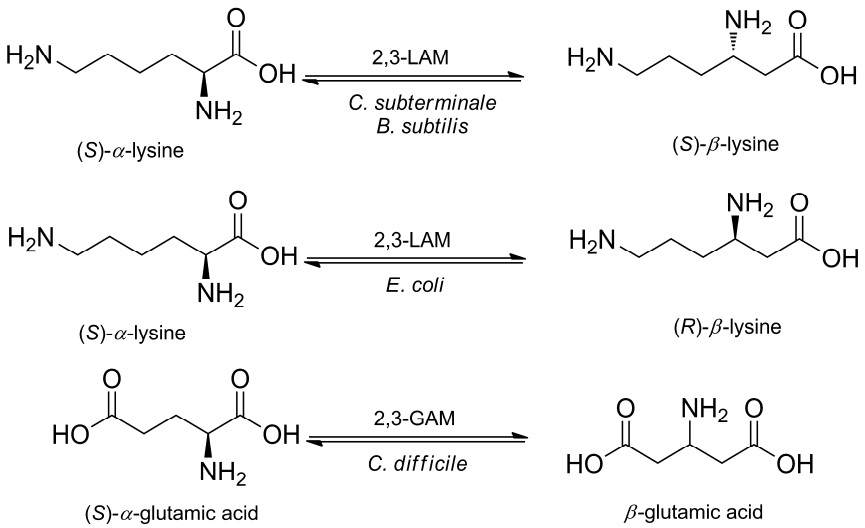

Scheme 1.16 Isomerization of α-amino acids to β-amino acids by SAM-dependent enzymes.

These examples illustrate that SAM-dependent enzymes are potential biocatalysts for the synthesis of various β-amino acids. Still there are some drawbacks in applying SAM-dependent aminomutases in an industrial process. For example, the enzymes are rather unstable and sensitive to oxygen, causing quite rapid inactivation. This would imply that protein isolation and purification needs to be done under anaerobic conditions. Another issue would be the requirement of addition of an external cofactor, which is expensive. Whole cell biotransformations could be more attractive for application to industrial processes because laborious enzyme purification is avoided and because β-amino acids could possibly be formed from α-amino acids by fermentation.

The anaerobic bacterial degradation of uracil and L-aspartate can proceed via β-alanine, which is conjugated to CoA after which it is deaminated in a lyase type reaction that produces acryloyl CoA (**Scheme 1.17**). A highly active ***β*-alanyl-CoA ammonia lyase** (EC 4.3.1.6) is induced to very high level in *Clostridium priopionicum* during growth on β-alanine, and it was purified from this organism. The enzyme is a

homopentamer composed of 16 kDa subunits (Herrmann *et al.,* 2005). Two homologous genes encoding these enzymes in *C. priopionicum* were cloned and expressed in *E. coli*. Homologous sequences are also found in the genomes of various other anaerobes, e.g. bacteria that anaerobically ferment lysine and possess *β*-aminobutyryl-CoA ammonia lyase activity (Kreimeyer *et al.,* 2007). The equilibrium of the *β*-alanyl-CoA ammonia lyase reaction is in the direction of the amine adduct, and amine elimination only proceeds rapidly in the presence of a dehydrogenase that converts acryloyl-CoA to propionyl-CoA.

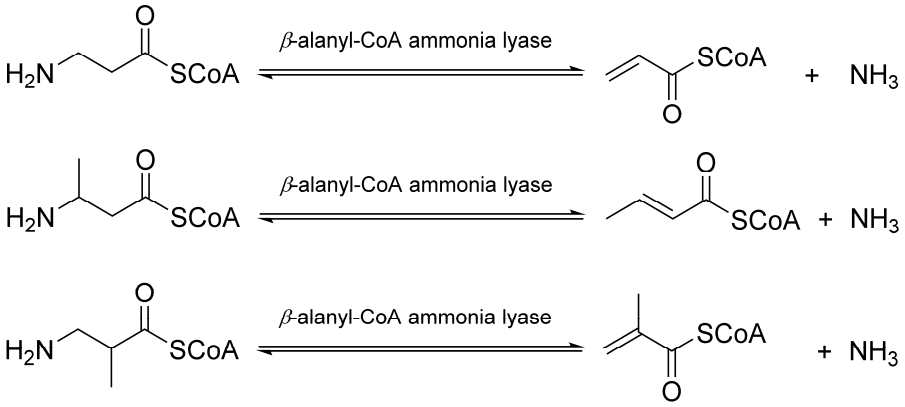

Scheme 1.17 Reactions catalyzed by *β*-alanyl CoA ammonia lyase.

It was suggested that the broad substrate range of the enzyme with respect to the enoyl-CoA derivatives (crotonyl-CoA, methacryloyl-CoA are accepted) allows production of chiral amino compounds such as 3-aminobutyrate and of 3-aminoisobutyrate (Herrmann *et al.,* 2005). Another biotechnological application would be the production of acryloyl-CoA from alanine in a pathway leading to 3-hydroxypyruvate, which has been considered as a bio-based building block for polymers (Jiang *et al.,* 2009). Besides ammonia, also methylamine can be accepted by *β*-aminobutyryl-CoA ammonia lyase, but detailed kinetic data have not been reported.

No structures of (putative) *β*-alanyl-CoA lyases or sequence related enzymes are known, so mechanistic details are lacking. There is slight sequence similarity with a broad-specificity acyl-CoA thioesterase from *Haemophilus influenzae* (PDB code 3BJK). In fact, low sequence similarity can be detected with several members of the HotDog protein family, which encompases enoyl-CoA hydratases, β-hydroxyacyl-ACP dehydratases, and acyl-CoA thioesterases (Dillon & Bateman, 2004), but apart from

the notion that these proteins possess a tight-binding CoA site at the dimer interface, the mechanistic implications of these similarities are not clear at this moment.

Another group of potent enzymes for asymmetric synthesis of β-amino acids are **aminotransferases** (ATs). These are prominent enzymes involved in amino acid metabolism, where they catalyze the reversible transfer of an amino group from an amino donor to an α-keto acid, forming a new amino acid and a new keto compound (or aldehyde) (Mehta & Christen, 2000; Mehta *et al.,* 1993; Christen & Metzler, 1985). ATs are ubiquitously present in nature and use pyridoxal-5'-phosphate (PLP) as cofactor for amino group transfer. Details of the reaction mechanism of aminotransferases (EC 2.6.1.X) are discussed in **chapter 3** and **chapter 4**. ATs occur in at least two fold types of PLP-dependent enzymes, fold type I and fold type IV (Eliot & Kirsch, 2004). Fold type I has as main representative aspartate AT, but includes the aromatic ATs as well. ATs from this group are functional as homodimers, each monomer containing an active center that is present at the interface of the dimer. Each monomer has a small and a large domain that can move significantly upon substrate binding. The fold type IV ATs perform transamination of D-amino acids and are structurally similar to ATs of the fold type I family. However, the main difference is that the PLP cofactor is bound at the interface of the dimer with the *re* face exposed to the solvent rather than the *si* face as seen in the structures of fold type I and II enzymes (Sugio *et al.,* 1995).

ATs have been used for the enzymatic synthesis of chiral amines such as (*S*)-α-methyl benzyl amine and (*S*)-1-methyl-3-phenylpropylamine (Shin & Kim, 1999). Various chiral amines are important building blocks in the pharmaceutical industry as they are incorporated in synthetic routes towards drugs.

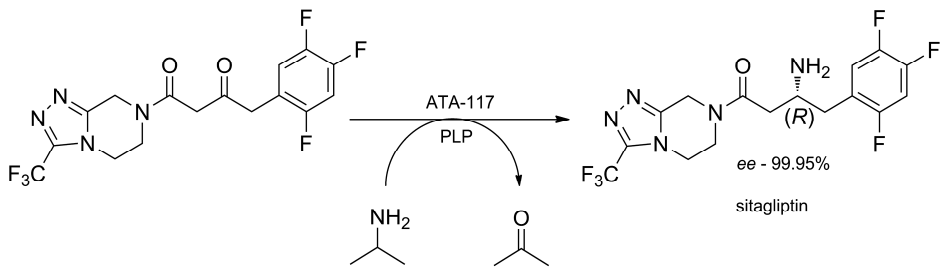

Scheme 1.18 Sitagliptin production by ATA-117 transaminase-catalyzed reaction.

An example of a biocatalyst from this group of enzymes is an engineered transaminase (ATA-117), which is a homologue of an enzyme from *Arthrobacter* sp. (Iwasaki *et al.,*

2006; Koszelewski *et al.,* 2008). ATA-117 was improved by protein engineering for large-scale production of the antidiabetic drug sitagliptin (**Scheme 1.18**) (Savile *et al.,* 2010). To shift the equilibrium towards sitagliptin synthesis, the cheap and accessible amino donor, isopropyl amine was used in large excess.

ATs that catalyze synthesis or conversion of *β*-amino acids could be attractive for biocatalysis if they are enantioselective, stable, and exhibit a wide substrate scope (Rudat *et al.,* 2012). Indeed, preparation of 3-amino-3-phenylpropionic acid by aminotransferases was recently described (Banerjee *et al.,* 2005). Two ATs with opposite enantioselectivity and isolated from different sources were employed, i.e. a D-*β*-aminotransferase from *Variovorax paradoxus* and an L-*β*-aminotransferase from *Alcaligenes eutrophus*. The enzymes catalyze the reductive amination of 3-oxo-3-phenylpropionic acid into (*S*)- and (*R*)-*β*-phenylalanine, respectively. As amino donors (*S*)-glutamic acid and (*S*)-alanine were used. The reactions gave exclusively one enantiomer (**Scheme 1.19**). The enzymes exhibited a wide substrate range.

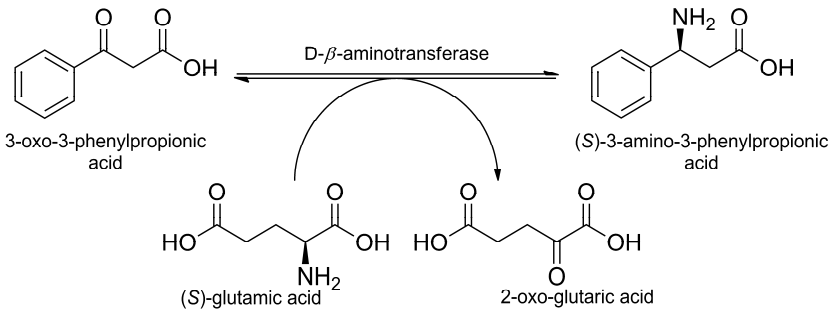

Scheme 1.19 Synthesis of (*S*)-3-amino-3-phenylpropionic acid using D-*β*-aminotransferase from *Variovorax paradoxus.*

Another example is the asymmetric synthesis of (*S*)-3-amino-3-phenyl propionic acid using phenyl substituted *β*-ketoester in a coupled reaction catalyzed by the *β*-transaminase from *Mesorhizobium* sp. strain LUK (*Mes*AT) and a lipase from *Candida rugosa* (Kim *et al.,* 2007). The lipase catalyzes the hydrolysis of the *β*-ketoester to the chemically labile *β*-ketoacid, which is immediately used as the amino acceptor in the transaminase reaction. As amino donor, *rac*-3-amino butyric acid was used which is transformed to aceto-acetic acid, which is converted to acetone by spontaneous decarboxylation (**Scheme 1.20**). However, (*S*)-*β*-phenylalanine was produced with only 20% yield.

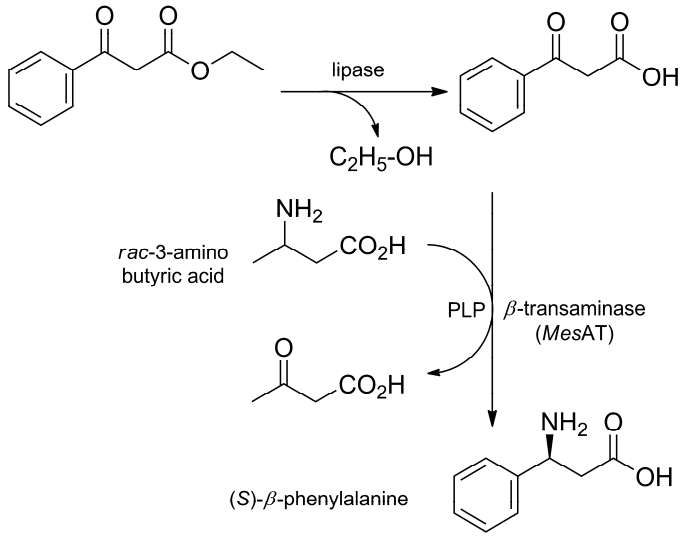

Scheme 1.20 Synthesis of (*S*)-*β*-phenylalanine catalyzed by the tandem lipase - *β*-transaminase (*Mes*AT) system.

A quite unique AT is an acyl-coenzyme A (CoA) *β*-transaminase (Perret *et al.,* 2011) isolated from the genome of an uncultivated bacterium ("*Candidatus Cloacamonas acidaminovorans*"), which has been reconstructed *in silico* (Pelletier *et al.,* 2008). The enzyme was called 3-amino-butyryl-CoA aminotransferase (*β*-AB-CoA-AT), and it acts on a CoA ester intermediate in the lysine fermentation pathway. Because acyl-CoA compounds are difficult to synthesize due to their sensitivity to hydrolysis, *N*-acetylcysteamine (NAC) thioesters were chosen to serve as acyl-CoA mimics. Activity of the novel *β*-AB-CoA-AT was found with NAC thioesters derived from *β*-aminobutyrate, *β*-homoleucine and *β*-phenylalanine as amino donors and *α*-ketoglutarate as amino acceptor (**Scheme 1.21**).

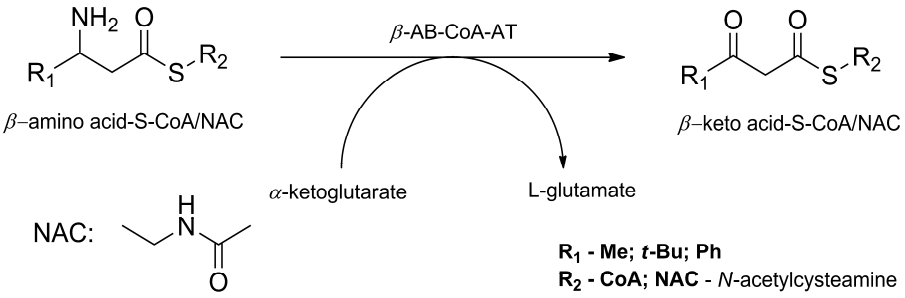

Scheme 1.21 Transamination of different *β*-amino CoA/NAC-thioesters by *β*-AB-CoA-AT into the corresponding 3-oxo-compounds.

Similar to *Mes*AT, *β*-AB-CoA-AT can use pyruvate as an alternative amino acceptor although the rate was 5-fold lower than with *α*-ketoglutarate. In contrast to what was found with *Mes*AT, the free acid form of *β*-aminobutyrate, *β*-homoleucine and *β*-phenylalanine were not converted by *β*-AB-CoA-AT, suggesting that the thioester moiety (CoA or its NAC mimic) is necessary for substrate recognition.

3. Discovery of new *β*-amino acid converting enzymes

3.1. Enrichments

Until a few years ago, microbial cultures isolated from natural habitats were the main biological source for enzyme discovery. Enrichment of microorganisms on the basis of their ability to perform a certain reaction on a specific substrate indeed is an efficient way to discover new biocatalysts. Isolation of new organisms by enrichment experiments is based on the ability of a very limited number of microorganisms from a habitat (e.g. activated sludge, grassland soil etc.) to grow in a defined medium due to the production of a specific enzyme that metabolizes an essential medium component. Usually, this is a selective C-source or N-source. Enrichment cultures can recover organisms that form only a tiny fraction of the microbial diversity present in a certain environment making it an efficient way to discover rare enzymes (Torsvik & Ovreas, 2002).

A few microorganisms that act on *β*-amino acids and related compounds have been isolated by enrichment cultivation. For example, cultures producing aminotransferases that allow utilization of *β*-amino acids as a growth substrate were isolated this way (Kim *et al., 2007*; Shin *et al.,* 2003). Such aminotransferases are interesting because of their potential application in the kinetic resolution of *β*-amino acids and chiral amines (Yun *et al.,* 2004). After isolation of cultures that use specific nitrogen compounds, activity assays for different deamination activities (e.g. ammonia lyase, aminomutase, aminotransferase, amino acid dehydrogenase, amino acid oxidase) can lead to identification of new enzymes. In this thesis, we report the isolation of 18 microorganisms on various *β*-amino acids (*β*-alanine, *β*-glutamate, *β*-asparagine, *β*-leucine, *β*-phenylalanine, *β*-aminobutyric acid, cispentacin, D-aspartic acid and *β*-tyrosine) and the search for new deamination enzymes in some of these cultures (**chapter 2**).

3.2. Metagenomics

Discovery of new enzymes by enrichment cultivation may be more complicated if metabolism of an enrichment substrate is dependent on the activities of mixed cultures (Kaeberlein *et al.,* 2002). Furthermore, microorganisms may exist in a non-cultivable state, e.g. as a result of prolonged starvation conditions, which also hinders enrichment cultivation (Oliver *et al.,* 1991; Roszak *et al.,* 1984). Thus, cultivation-independent techniques for obtaining novel biocatalysts have also been explored. Screening for new enzymes using metagenomic libraries relies solely on the genetic information stored in the collective DNA of all microorganisms present in an environmental sample (Handelsman *et al.,* 1998). In the past years, cloning of the metagenomic DNA followed by expression library screening has become a popular strategy for cultivation-independent enzyme discovery and has led to the recovery of a range of new biocatalysts (Rondon *et al.,* 2000; Lorenz *et al.,* 2001). In general, the success of screening for new activities using metagenomic libraries depends on a number of factors such as: (a) availability of a suitable sample and a matching DNA extraction protocol that yields sufficient amounts of high quality DNA; (b) a suitable host-vector system that allows efficient cloning and good expression of target genes; (c) a fast and easy screening method of reasonable throughput. This approach has its drawbacks. For example, it is not efficient when searching for rare genes or when large inserts or even whole pathways are to be discovered.

3.3 Genome mining

Another tool for enzyme discovery is genome mining. With over 2,500 microbial genomes completely sequenced, a wealth of information is present in databases, including millions of genes that encode putative enzymes that have never been examined for activity. Discovery by genome mining requires knowledge of functional motifs in a polypeptide sequence that can be linked to the catalytic activity of the target enzyme. Consequently, quite some biochemical information is needed on the type of enzyme that is searched for. Crystal structure information on homologous enzymes is very valuable since it provides an understanding of the reaction mechanism, and structural events along the catalytic cycle. Furthermore, it is important to examine and compare homologous protein that catalyze the same reaction especially if they have different catalytic properties. Genome mining can also lead to the discovery of new enzymes, e.g. enzymes that are encoded in biosynthetic gene clusters or in clusters of catabolic genes. Especially the interplay between examination of structures of biosynthetic products and examination of biosynthetic clusters can identify interesting new enzymes.

By combining sequence analysis and protein structure information on a target enzyme activity, *in silico* prediction of substrate range and enantiopreference seems possible (Hohne *et al.,* 2010). Using structural inspection of aminotransferases, specific amino acids around the active site were predicted to be required for an uncommon (*R*)-selectivity of aminotransferases. Database searches identified amino acid sequences that met these criteria, and cloning and expression studies indeed produced enzymes with the desired enantioselectivity and substrate scope. By this approach, 17 (*R*)-selective amine transaminases were discovered and found to catalyze the synthesis of several (*R*)-amines with high stereoselectivity.

Since both genome mining and protein engineering for obtaining improved enzymes benefit from structural information, and because no crystal structure of an aminotransferase that converts *β*-amino acids was available, we solved the structures of two *β*-aminotransferases (*Vp*AT and *Mes*AT) as part of the research described in this thesis (see **chapter 3** and **chapter 4**). Based on the reaction mechanism and by combining sequence data and crystal structure information, we identified sequence motifs that can predict *β*-aminotransferase activity (see **chapter 3**). These sequence signature motifs should make it possible to discover new homologues with the desired activity in sequence databases.

3.4 Protein engineering

Since many years, protein engineering is being used to tailor the biochemical, physical and catalytic properties of enzymes for application in various biotechnological processes. In recent years, approaches from directed evolution and structure-based protein engineering (rational protein engineering) are merging. Crystal structures make it possible to establish reaction mechanisms and to identify residues that shape the substrate binding site and govern activity and selectivity. For example, structure-based protein engineering of methylaspartate ammonia lyase (MAL) yielded enzyme variants for the asymmetric synthesis of unnatural amino acids (Raj *et al.,* 2012b). One active-site mutant (Q73A) accepted a range of amines in addition to ammonia in the amination of mesaconic acid. Another mutant (L384A) accepted a range of mesaconic acid analogs with other substituents than a methyl group. In addition, very high regio- and stereoselectivity were observed and a whole variety of *N*-substituted 3-methylaspartic acids were produced with very high diastereomeric and enantiomeric excess.

In another example, phenylalanine aminomutase (PAM) was engineered for improved *β*-regioselective asymmetric amination of cinnamic acid derivatives (Wu *et al.,* 2012[b]). The WT PAM was able to produce (*S*)-*α*-phenylalanine and (*R*)-*β*-

phenylalanine in a ratio of about 1:1. After employing a protein structure- and enzyme mechanism-based approach, a PAM mutant was obtained, of which the *β*-addition of ammonia was superior (Q319M, 88% *β*-selectivity) compared to that of WT PAM. In addition, the same mutant showed a 2-fold higher affinity for cinnamate and a 2-fold increase in catalytic efficiency in the amination reaction. In a different study, PAM was re-engineered by a single mutation of an active-site residue (C107S) to obtain activity with tyrosine (Wu *et al.,* 2010). The authors used sequence analysis and homology modeling and the mutant became a true tyrosine aminomutase that converted (*S*)-*α*-tyrosine to (*R*)-*β*-tyrosine with excellent *ee* while retaining the aminomutase activity. It was proposed that this mutant might be used for enzymatic synthesis of (*R*)-*β*-tyrosine and its derivatives.

In another case, growth selection was used as a screening method for directed evolution of an ω-transaminase with increased resistance to product inhibition by aliphatic ketones (Yun *et al.,* 2005). The ω-transaminase (ω-TA) from *Vibrio fluvialis* JS17 has prominent properties such as high enantioselectivity for the (*S*) enantiomers of different chiral amines (e.g. *α*-methylbenzyl amine and *sec*-butyl amine), high stability and high catalytic activity. These properties are eclipsed by severe product inhibition by the ketone that is formed (e.g. acetophenone and 2-butanone). In order to increase product tolerance, Yun and coworkers used error-prone PCR mutagenesis and growth selection. The product inhibition constants of an identified P233L+V297A double mutant with 2-butanone and 2-heptanone were 6- and 4.5-fold higher than that of the wild type, respectively. Apparently, the same method could not be applied to enrichment of mutants with increased resistance to aromatic ketones (e.g. acetophenone) due to their toxicity to *E. coli*. A solution would be to a more tolerant host, possibly a *Pseudomonas putida* degrading aromatic compounds, as a host for growth-based screening of error-prone PCR libraries.

Goal and outline of the thesis

This thesis is the outcome of the project “Selection and characterization of novel enantioselective (de)amination enzymes” which was part of B-Basic, a public-private NWO-ACTS program in which the University of Groningen participated. The goal was to discover and characterize novel (de)amination enzymes that are involved and could be applied for the conversion and production of *β*-amino acids. Since some *β*-amino acids occur naturally, either as free molecules or as structural elements of larger structures, it is expected that nature has enzymes responsible for their metabolism. To find these enzymes, we used 2 approaches: (a) microbial enrichment

experiments to isolate organisms that grow on *β*-amino acids as sole nitrogen source; (b) screening of environmental gene libraries and selection on *β*-amino acids as nitrogen source.

As outlined above, the first approach is based on the assumption that the target enzymes can produce metabolic intermediates or inorganic nitrogen that can support microbial growth. In the batch enrichments, a *β*-amino acid was used as the sole nitrogen source in the presence of the corresponding unsaturated carboxylic acid as the carbon source. The latter was expected to increase the possibility of finding organisms that can grow on the unsaturated carbon source and consequently benefit from conversion of the *β*-amino acid by a lyase reaction. We also tested environmental gene libraries, expressed in *E. coli*, with growth selection on plates containing a *β*-amino acid as sole nitrogen source, but with little success.

In the work described in **Chapter 2**, enrichment experiments were used to obtain bacterial strains that possess various deamination activities. We describe the isolation and partial characterization of 18 bacterial strains that are able to degrade *β*-alanine, *β*-asparagine, *β*-glutamate, *β*-leucine, *β*-phenylalanine, *β*-aminobutyric acid, D-aspartic acid and *β*-tyrosine. A *Variovorax paradoxus* strain growing on *β*-phenylalanine was selected for further study.

The discovery of a novel *β*-phenylalanine aminotransferase from *V. paradoxus* (*Vp*AT) is described in **Chapter 3.** The gene encoding the enzyme was found after screening a cosmid library for growth and by testing for clones that catalyze acetophenone formation from *β*-phenylalanine. The enzyme was overexpressed in *E. coli* and biochemically and structurally characterized in collaboration with Gjalt G. Wybenga of the X-Ray Crystallography group, University of Groningen. Based on sequence analysis and structural comparisons, an active site sequence motif is proposed for the discovery of further aminotransferases acting on *β*-amino acids.

In **Chapter 4**, the *β*-phenylalanine aminotransferase from *Mesorhizobium* sp. strain LUK (*Mes*AT), originally reported by Kim *et al.* (2006), was examined and used for comparative studies in terms of catalytic activity and 3D structure, again in collaboration with Gjalt G. Wybenga. The results reveal that the enzyme belongs to the fold-type I PLP enzymes, but has an inverted orientation of *β*-phenylalanine in the active site as compared to the positioning of *α*-amino acids in other members of this family of aminotransferases.

Chapter 5 describes the degradation of *β*-valine by *Pseudomonas* sp. strain SBV1, a bacterial strain obtained by enrichment cultivation and provided by Dr. Stefaan de Wildeman, DSM. The organism is able to convert *β*-valine in minimal medium at very high rates and use it as sole nitrogen source. The substrate is a so-

called blocked amino acid: since the amino substituent is on a tertiary carbon atom, the most common deamination mechanisms (aminotransferase, amino acid dehydrogenase, amine oxidase) are prevented, increasing the likelihood of finding a mutase or lyase reaction. A lyase-based deamination route is proposed and a genetic analysis of the suspected *β*-valine pathway is presented. A novel type of lyase, acting on the CoA-conjugate of *β*-valine and related to enoyl-CoA hydratases, is proposed to catalyze the deamination reaction.

In **Chapter 6** the results of this thesis are summarized and discussed in the context of current challenges and possibilities in the area of discovery of (de)amination enzymes for biocatalysis.

References

Aberhart, D.J., Lin, H.J. and Weiller, B.H. (1981) Stereochemistry of lysine 2,3-aminomutase. *J Am Chem Soc* 103: 6750–6752.

Appella, D.H., Christianson, L.A., Karle, I.L., Powell, D.R. and Gellman, S.H. (1996). "β-Peptide foldamers: robust helix formation in a new family of β-amino acid oligomers". *J Am Chem Soc* 118: 13071–13072.

Akhtar, M., Botting, N.P., Cohen, M.A. and Gani, D. (1987) Enantiospecific synthesis of 3-substituted aspartic acids via enzymic amination of substituted fumaric acids. *Tetrahedron* 43: 5899–5908.

Akhtar, M., Cohen, M.A. and Gani, D. (1987) Stereochemical course of the enzymic amination of chloro- and bromo fumaric acid by 3-methylaspartate ammonia-lyase. *Tetrahedron Lett* 28: 2413–2416.

Banerjee, A., Chase, M., Calyton, A. and Landis, B. (2005) Methods for the stereoselective synthesis and enantiomeric enrichment of *β*-amino acids. *PCT international application patent* WO2005005633.

Behshad, E., Ruzicka, F.J., Mansoorabadi, S.O., Chen, D., Reed, G.H. and Frey, P.A. (2006) Enantiomeric free radicals and enzymatic control of stereochemistry in a radical mechanism: the case of lysine 2,3-aminomutases. *Biochemistry* 45: 12639–12646.

Benaglia, M., Cinquini, M. and Cozzi, F. (2000) The S-thioester enolate/imine condensation: a shortcut to β-lactams *Eur J Org Chem* 4: 563–572.

Botting, N.P., Akhtar, M., Cohen, M. and Gani, D. (1988) Substrate-specificity of the 3-methylaspartate ammonia-lyase reaction: observation of differential relative reaction-rates for substrate product pairs. *Biochemistry* 27: 2953–2955.

Bruggink, A. and Roy, P.D. (2001) Industrial synthesis of semisynthetic antibiotics. In: Bruggink, A. (ed.), Synthesis of β-Lactam Antibiotics: Chemistry, biocatalysis, and process integration, Dordrecht: Kluwer 12–55.

Chibata, I., Tosa, T. and Shibatani, T. (1992) Chirality in industry collins, A. N., Sheldrake, G. N., Crosby, J. *Eds Wiley*: Chichester, UK: Chapter 19, p. 358.

Christen, P. and Metzler, D.E. (1985) Transaminases. Wiley, New York, N.Y.

Christenson, S.D., Liu, W., Toney, M.D. and Shen, B. (2003) A novel 4-methylideneimidazole-5-one-containing tyrosine aminomutase in enediyne antitumor antibiotic C-1027 biosynthesis. *J Am Chem Soc* 125: 6062–6063.

Christianson, C.V., Montavon, T.J., Van Lanen, S.G., Shen, B. and Bruner, S.D. (2007) The structure of L-tyrosine 2,3-aminomutase from the C-1027 enediyne antitumor antibiotic biosynthetic pathway. *Biochemistry* 46: 7205–7214.

Cohen, S.G and Weinstein, S.Y. (1964) Hydrolysis of D(-)-ethyl β-phenyl-β-hydroxypropionate and D(-)-ethyl β-phenyl-β-acetamidopropionate by α-chymotrypsin. *J Amer Chem Soc* 86: 725–727.

Cohen, S.G., Crossley, J. and Khedouri, E. (1963) Action of α-cymotrypsin on diethyl N-acetylaspartate and on diethyl N-methyl-N-acetylaspartate. *Biochemistry* 2: 820–823.

Cooke, H.A., Christianson, C.V. and Bruner, S.D. (2009) Structure and chemistry of 4-methylideneimidazole-5-one containing enzymes. *Curr Opin Chem Biol* 13: 453–461.

Crews, P., Manes, L.V. and Boehler, M. (1986) Jasplakinolide, a cyclodepsipeptide from the marine sponge, *Jaspis* sp. *Tetrahedron Lett* 27: 2797–2800.

Dillon, S.C. and Bateman, A. (2004) The Hotdog fold: wrapping up a superfamily of thioesterases and dehydratases. *BMC Bioinformatics* 12: 109.

Eliot, A.C. and Kirsch, J.F. (2004) Pyridoxal phosphate enzymes: mechanistic, structural, and evolutionary considerations. *Annu Rev Biochem* 73: 383–415.

Faulconbridge, S.J., Holt, K.E., Sevillano, L.G., Lock, C.J., Tiffin, P.D., Tremayne, N. and Winter, S. (2000) Preparation of enantiomerically enriched aromatic β-amino acids via enzymatic resolution. *Tetrahedron Lett* 41: 2679–2681.

Frey, P.A and Ruzicka, F.J. (2008a) Methods for the preparation of β-amino acids US *patent* 7,452,701 B2.

Frey, P.A and Ruzicka, F.J. (2008b) Glutamate 2,3-aminomutases and methods of use thereof US *patent* 7,456,271 B2.

Gerlt, J.A., Babbitt, P.C. and Rayment, I. (2005) Divergent evolution in the enolase superfamily: the interplay of mechanism and specificity. *Arch Biochem Biophys* 433: 59–70.

Geueke, B. and Kohler, H.P. (2007) Bacterial beta-peptidyl aminopeptidases: on the hydrolytic degradation of beta-peptides. *Appl Microbiol Biotechnol* 74: 1197–204.

Goda, S.K., Minton, N.P., Botting, N.P. and Gani, D. (1992) Cloning, sequencing, and expression in *Escherichia coli* of the *Clostridium tetanomorphum* gene encoding beta-methylaspartase and characterization of the recombinant protein. *Biochemistry* 31: 10747–10756.

Groger, H. and Werner, H. (2003) CA 02428163 *patent*.

Gulzar, M.S., Akhtar, M. and Gani, D. (1997) Preparation of *N*-substituted aspartic acids via enantiospecific conjugate addition of *N*-nucleophiles to fumaric acids using methylaspartase: synthetic utility and mechanistic implications. *J Chem Soc Perkin Trans* 1: 649–655.

Handelsman, J., Rondon, M.R., Brady, S.F., Clardy, J. and Goodman, R.M. (1998) Molecular biological access to the chemistry of unknown soil microbes: a new frontier for natural products. *Chem Biol* 5: 245–249.

Hanzawa, S. and Kidokoro, S.I. (1999) Thermolysin. M.C. Flickinger, S.W. Drew (Eds.), Encyclopedia of Bioprocess Technology: Fermentation, Biocatalysis, and Bioseparation, John Wiley and Sons, New York (1999), pp. 2527–2535.

Hanzawa, S. (1999) Aspartame. M.C. Flickinger, S.W. Drew (Eds.), Encyclopedia of Bioprocess Technology: Fermentation, Biocatalysis, and Bioseparation, John Wiley and Sons, New York (1999), pp. 201–210. Comprehensive review on the production of aspartame by DSM/Tosoh and alternative processes. It includes the history of the discovery of the process and some process characteristics.

Heberling, M.M., Wu, B., Bartsch, S. and Janssen, DB. (2013) Priming ammonia lyases and aminomutases for industrial and therapeutic applications. *Curr Opin Chem Biol* 17: 250–260.

Heck, T., Limbach, M., Geueke, B., Zacharias, M., Gardiner, J., Kohler, H.P. and Seebach, D. (2006) Enzymatic degradation of beta- and mixed alpha,beta-oligopeptides. *Chem Biodivers* 3: 1325–1348.

Herrmann, G., Selmer, T., Jessen, H.J., Gokarn, R.R., Selifonova, O., Gort, S.J. and Buckel, W. (2005) Two beta-alanyl-CoA:ammonia lyases in *Clostridium propionicum*. *FEBS J* 272: 813–821.

Hoekstra, W.J. and Poulter, B.L. (1998) Combinatorial chemistry techniques applied to nonpeptide integrin antagonists. *Curr Med Chem* 5: 195–204.

Hohne, M., Schatzle, S., Jochens, H., Robins, K., and Bornscheuer, U.T. (2010) Rational assignment of key motifs for function guides *in silico* enzyme identification. *Nat Chem Biol* 6: 807–813.

Huang, S.X., Lohman, J.R., Huang, T. and Shen, B. (2013) A new member of the 4-methylideneimidazole-5-one-containing aminomutase family from the enediyne kedarcidin biosynthetic pathway. *Proc Natl Acad Sci* U S A. 110: 8069–8074.

Iwasaki, A., Yamada, Y., Kizaki, N., Ikenaka Y. and Hasegawa, J. (2006) Microbial synthesis of chiral amines by (*R*)-specific transamination with *Arthrobacter* sp. KNK168. *Appl Microbiol and Biotechnol* 69: 499–505.

Jiang, X., Meng, X. and Xian, M. (2009) Biosynthetic pathways for 3-hydroxypropionic acid production. *Appl Microbiol Biotechnol* 82: 995–1003.

Juaristi, E. and Soloshonok, V. (2005) Enantioselective synthesis of β-amino acids. *Wiley-Interscience*, New York, 2nd ed.

Kaeberlein, T., Lewis, K. and Epstein, S.S. (2002) Isolating "uncultivable" microorganisms in pure culture in a simulated natural environment. *Science* 296: 1127–1131.

Kato, Y. and Asano, Y. (1995) 3-Methylaspartate ammonia-lyase from a facultative anaerobe, strain YG-1002. *Appl Microbiol Biotechnol* 43: 901–907.

Kato, Y. and Asano, Y. (1988) Cloning, nucleotide sequencing, and expression of the 3-methylaspartate ammonia-lyase gene from *Citrobacter amalonaticus* strain YG-1002. *Appl Microbiol Biotechnol* 50: 468–474.

Kawasaki, H., Koyama, K., Kurokawa, S., Watanabe, K., Nakazawa, M., Izawa, K. and Nakamatsu, T. (2006) Production of (*R*)-3-amino-3-phenylpropionic acid and (*S*)-3-amino-3-

phenylpropionic acid from (*R,S*)-N-acetyl-3-amino-3-phenylpropionic acid using microorganisms having enantiomer-specific amidohydrolyzing activity. *Biosci Biotechnol Biochem* 70: 99–106.

Kim, J., Kyung, D., Yun, H., Cho, B.K., Seo, J.H., Cha, M. and Kim, B.G. (2007) Cloning and characterization of a novel β-transaminase from *Mesorhizobium* sp. strain LUK: a new biocatalyst for the synthesis of enantiomerically pure β-amino acids. *Appl Environ Microbiol* 73: 1772–1782.

Kim, J., Kyung, D., Yun, H., Cho, B.K. and Kim, B.G. (2006) Screening and purification of a novel transaminase catalyzing the transamination of aryl β-amino acid from *Mesorhizobium* sp. LUK. *J Microbiol Biotechnol* 16: 1832–1836.

Koszelewski, D., Lavandera, I., Clay, D., Guebitz, G., Rozzell, D. and Kroutil, W. (2008) Formal asymmetric biocatalytic reductive amination. *Angew Chem Int Ed* 47: 9337–9340.

Kreimeyer, A., Perret, A., Lechaplais, C., Vallenet, D., Medigue, C., Salanoubat, M. and Weissenbach, J. (2007) Identification of the last unknown genes in the fermentation pathway of lysine. *J Biol Chem* 282: 7191–7197.

Liljeblad, A. and Kanerva, L.T. (2006) Biocatalysis as a profound tool in the preparation of highly enantiopure β-amino acids. *Tetrahedron* 62: 5831–5854.

Liu, M. and Sibi, M.P. (2002) Recent advances in the stereoselective synthesis of β-amino acids. *Tetrahedron* 58: 7991–8035.

Lorenz, P., Liebeton, K., Niehaus, F., Eck, J. and Zinke, H. (2001) Novel enzymes from unknown microbes – direct cloning of the metagenome. Darmstadt (Germany): 5th International Symposium on Biocatalysis and Biotransformation.

Magriotis, P.A. (2001) Recent progress in the enantioselective synthesis of β-lactams: development of the first catalytic approaches. *Angew Chem Int Ed* 40: 4377–4379.

Mehta, P.K. and Christen, P. (2000) The molecular evolution of pyridoxal-5'-phosphate-dependent enzymes. *Adv Enzymol Relat Areas Mol Biol* 74: 129–184.

Mehta, P.K., Hale, T.I. and Christen, P. (1993) Aminotransferases – demonstration of homology and division into evolutionary subgroups. *Eur J Biochem* 214: 549–561.

Mekhail, T.M. and Markman, M. (2002) Paclitaxel in cancer therapy. *Expert Opin Pharmacother* 3: 755–66.

Mizobata, T., Kawata, Y. (2007) Aspartases, in industrial enzymes - structure, functions and applications (eds J. Polaina and A.P. MacCabe), Springer, Dordrecht, pp. 549 –565.

Namikoshi, M., Rinehart, K.L., Dahlem, A.M., Beasley, V.R. and Carmichael, W.W. (1989) Total synthesis of Adda, the unique C20 amino acid of cyanobacterial hepatotoxins. *Tetrahedron Lett* 30: 4349–4352.

Ohno, M., Kobayashi, S., Limori, T., Wang, Y.F. and Izawa, T. (1981) Synthesis of (*S*)- and (*R*)-4-[(Methoxycarbonyl)methyl]-2-azetidinone by chemicoenzymatic approach *J Am Chem Soc* 103: 2405–2406.

Oliver, J.D., Nilsson, L. and Kjelleberg, S. (1991) Formation of non-culturable *Vibrio vulnificus* cells and its relationship to the starvation state. *Appl Environ Microbiol* 57: 2640–2644.

Pelletier, E., Kreimeyer, A., Bocs, S., Rouy, Z., Gyapay, G., Chouari, R., Riviere, D., Ganesan, A., Daegelen, P., Sghir, A., Cohen, G.N., Medigue, C., Weissenbach, J. and Le Paslier, D. (2008)

"*Candidatus Cloacamonas acidaminovorans*": genome sequence reconstruction provides a first glimpse of a new bacterial division. *J Bacteriol* 190: 2572–2579.

Perret, A., Lechaplais, C., Tricot, S., Perchat, N., Vergne, C., Pelle, C., Bastard, K., Kreimeyer, A., Vallenet, D., Zaparucha, A., Weissenbach, J. and Salanoubat, M. (2011) A novel acyl-CoA beta-transaminase characterized from a metagenome. *PLoS One* 6: e22918.

Poechlauer, P., Braune, S., de Vries A. and May, O. (2010) Sustainable route design for pharmaceuticals. Why, how and when. *Chim Oggi* 28: 14–17.

Raj, H., Puthan Veetil, V., Szymanski, W., Dekker, F.J., Quax, W.J., Feringa, B.L., Janssen, D.B. and Poelarends, G.J. (2012a) Characterization of a thermostable methylaspartate ammonia lyase from *Carboxydothermus hydrogenoformans*. *Appl Microbiol Biotechnol* 94: 385–397.

Raj, H., Szymanski W., de Villiers, J., Rozeboom, H.J., Veetil, V.P., Reis, C.R., de Villiers, M., Dekker, F.J., de Wildeman, S., Quax, W.J., Thunnissen, A.M., Feringa, B.L., Janssen, D.B. and Poelarends, GJ. (2012b) Engineering methylaspartate ammonia lyase for the asymmetric synthesis of unnatural amino acids. *Nat Chem* 4: 478–484.

Rehdorf, J., Mihovilovic, M.D. and Bornscheuer, U.T. (2010) Exploiting the regioselectivity of Baeyer–Villiger monooxygenases for the formation of β-amino acids and β-amino alcohols. *Angew Che Internat Ed* 49: 4506–4508.

Rondon, M.R., August, P.R., Bettermann, A.D., Brady, S.F., Grossman, T.H., Liles, M.R., Loiacono, K.A., Lynch, B.A., MacNeil, I.A., Minor, C., Tiong, C.L., Gilamn, M., Osburne, M.S., Clardy, J., Handelsman, J. and Goodman, R.M. (2000) Cloning the soil metagenome: a strategy for accessing the genetic and functional diversity of uncultured microrganisms. *Appl Environ Microbiol* 66: 2541–2547.

Roszak, D.B., Grimes, D.J. and Colwell, R.R. (1984) Viable but non-recoverable stage of *Salmonella enteritidis* in aquatic systems. *Can J Microbiol* 30: 334–338.

Rudat, J., Brucher, B.R. and Syldatk, C. (2012) Transaminases for the synthesis of enantiopure beta-amino acids. *AMB Express* 2:11.

Ruzicka, F.J. and Frey, P.A. (2007) Glutamate 2,3-aminomutase: a new member of the radical SAM superfamily of enzymes. *Biochim Biophys Acta* 1774: 286–296.

Sanchez, V.M., Rebolledo, F. and Gotor, V. (1997) *Candida antarctica* lipase catalyzed resolution of ethyl (+/-)-3-aminobutyrate. *Tetrahedron: Asymmetry* 8: 37–40.

Savile, C.K., Janey J.M., Mundorff, E.C., Moore, J.C., Sarena, Tam, S., Jarvis, W.R., Colbeck, J.C., Krebber, A., Fleitz, F.J., Brands, J., Devine, P.N., Huisman, G.W. and Hughes, G.J. (2010) Biocatalytic asymmetric synthesis of chiral amines from ketones applied to sitagliptin manufacture. *Science* 329: 305–309.

Schreiber J.V., Frackenpohl, J., Moser, F., Fleischmann, T., Kohler, H.P. and Seebach, D. (2002) On the biodegradation of beta-peptides. *ChemBioChem* 3: 424–432.

Seebach, D., Beck, A.K., Capone, S., Deniau, G., Groselj, U. and Zass, E. (2009) Enantioselective preparation of β^2-amino acid derivatives for β-peptide synthesis. *Synthesis* 1: 1–33.

Seebach, D. and Gardiner, J. (2008) β-Peptidic peptidomimetics. *Acc Chem Res* 41: 1366–1375.

Seebach, D., Abele, S., Gademann, K., Guichard, G., Hintermann, T., Jaun, B., Matthews, J.L. and Schreiber, J.V. (1998a) β^2- and β^3-peptides with proteinaceous side chains: synthesis and solution structures of constitutional isomers, a novel helical secondary structure and the

influence of solvation and hydrophobic interactions on folding. *Helv Chim Acta* 81: 932–982.

Seebach, D., Abele, S., Schreiber, J. V., Martinoni, B., Nussbaum, A. K., Schild, H., Schulz, H., Hennecke, H.,Woessner, R. and Bitsch, F. (1998b) Biological and pharmacokinetic studies with β-peptides. *Chimia* 52: 734–739.

Seebach, D., Overhand, M,, Kühnle, F.N.M., Martinoni, B., Oberer, L., Hommel, U. and Widmer, H. (1996) β-Peptides: synthesis by Arndt-Eistert homologation with concomitant peptide coupling. Structure determination by NMR and CD spectroscopy and by X-ray crystallography. Helical secondary structure of a β-hexapeptide in solution and its stability towards pepsin. *Helv Chim Acta* 76: 913–941.

Shih, C., Gossett, L.S., Gruber, J.M., Grossman, C.S., Andis, S.L., Schultz, R.M., Worzalla, J.F., Corbett, T.H. and Metz, J.T. (1999) Synthesis and biological evaluation of novel cryptophycin analogs with modification in the β-alanine region. *Bioorg Med Chem Lett* 9: 69–74.

Shin, J.S., Yun, H., Jang, J.W., Park, I. and Kim, B.G. (2003) Purification, characterization, and molecular cloning of a novel amine: pyruvate transaminase from *Vibrio fluvialis* JS17. *Appl Microbiol Biotechnol* 61: 463–471.

Shin, J.S. and Kim, B.G. (1999) Asymmetric synthesis of chiral amines with omega-transaminase. *Biotechnol Bioeng* 65: 206–211.

Steele, C.L., Chen, Y., Dougherty, B.A., Li, W., Hofstead, S., Lam, K.S., Xing, Z. and Chiang, S.J. (2005) Purification, cloning, and functional expression of phenylalanine aminomutase: the first committed step in taxol side-chain biosynthesis. *Arch Biochem Biophys* 438: 1–10.

Steer, D.L., Lew, R.A., Perlmutter, P., Smith, A.I. and Aguilar, M.I. (2002) Beta-amino acids: versatile peptidomimetics. *Curr Med Chem* 9: 811–822.

Solymar, M., Liljeblad, A., Lazar, L., Fulop, F. and Kanerva, L.T. (2002) Lipase-catalysed kinetic resolution in organic solvents: an approach to enantiopure α-methyl-β-alanine esters. *Tetrahedron: Asymmetry* 13: 1923–1928.

Sugio, S., Petsko, G.A., Manning, J.M., Soda, K. and Ringe, D. (1995) Crystal structure of a D-amino acid aminotransferase: how the protein controls stereoselectivity. Biochemistry 34: 9661–9669.

Swiderska, M.A. and Stewart, J.D. (2006) Asymmetric bioreductions of β-nitro acrylates as a route to chiral β^2-amino acids. *Organic Letters* 8: 6131–6133.

Szymanski, W., Wu, B., Weiner, B., de Wildeman, S., Feringa, B.L. and Janssen, D.B. (2009) Phenylalanine aminomutase-catalyzed addition of ammonia to substituted cinnamic acids: a route to enantiopure α- and β-amino acids. *J Org Chem* 74: 9152–9157.

Tang, W.J. and Zhang, X.M. (2003) New chiral phosphorus ligands for enantioselective hydrogenation. *Chem Rev* 103: 3029–3069.

Tang, W., Wu, S. and Zhang, X. (2003) Enantioselective hydrogenation of tetrasubstituted olefins of cyclic *β*-(acylamino)acrylates. *J Am Chem Soc* 125: 9570–9571.

Torsvik, V. and Ovreas, L. (2002) Microbial diversity and function in soil: from genes to ecosystems. *Curr Opin Microbiol* 5: 240–245.

Torsvik, V., Ovreas, L. and Thingstad, T.F. (2002) Prokaryotic diversity – magnitude, dynamics, and controlling factors. *Science* 296: 1064–1066.

Tramper, J., Beeftink, H.H., Janssen, A.E.M., Ooijkaas, L.P., Van Roon, J.L., Stubel, M., and Schroen, C.G.P.H. (2001) Biocatalytic production of semi-synthetic cephalosporins: process technology and integration. In: Bruggink, A. (ed.), Synthesis of β-Lactam Antibiotics, Dordrecht: Kluwer, 206–249.

Wani, M.C., Taylor, H.L., Wall, M.E., Coggon, P. and McPhail, A.T. (1971) Plant antitumor agents. VI. Isolation and structure of taxol, a novel antileukemic and antitumor agent from *Taxus brevifolia*. *J Am Chem Soc* 93: 2325–2327.

Weiner, B., Szymanski, W., Janssen, D.B., Minnaard A.J. and Feringa, B.L. (2010) Recent advances in the catalytic asymmetric synthesis of β-amino acids. *Chem Soc Rev* 39: 1656–1691.

Weiner, B., Poelarends, G.J., Janssen, D.B. and Feringa, B.L. (2008) Biocatalytic enantioselective synthesis of *N*-substituted aspartic acids by aspartate ammonia lyase. *Chem Eur J* 14: 10094–10100.

Wu, B., Szymanski, W., Crismaru, C.G., Feringa B.L. and Janssen, D.B. (2012[a]) C-N lyases catalyzing addition of ammonia, amines and amides to C=C and C=O bonds, p 749–778. *In* Drauz K, Groger H, May O (ed), *Enz Catal Org Synth* Wiley-VCH, New York, NY.

Wu, B., Szymanski, W., Wietzes, P., de Wildeman, S., Poelarends, G.J., Feringa, B.L. and Janssen, D.B. (2009) Enzymatic synthesis of enantiopure α- and β-amino acids by phenylalanine aminomutase-catalyzed amination of cinnamic acid derivatives. *ChemBioChem* 10: 338–344.

Wu, B., Szymanski, W., Wybenga, G.G., Heberling, M.M., Bartsch, S., de Wildeman, S., Poelarends, G.J., Feringa, B.L., Dijkstra, B.W. and Janssen, D.B. (2012[b]) Mechanism-inspired engineering of phenylalanine aminomutase for enhanced β-regioselective asymmetric amination of cinnamates. *Angew Chem Int Ed Engl* 51: 482–486.

Wu, B., Szymanski, W., Wijma, H.J., Crismaru, C.G., de Wildeman, S., Poelarends, G.J., Feringa, B.L. and Janssen, D.B. (2010) Engineering of an enantioselective tyrosine aminomutase by mutation of a single active site residue in phenylalanine aminomutase. *Chem Commun (Camb)* 46: 8157–8159.

Wubbolts, M. (2002) Addition of Amines to C=C Bonds. *In* enzyme catalysis in organic synthesis. Drauz, K. and H Waldmann *Eds Wiley-VCH*: Weinheim 2: 866–872.

Yun, H., Lim, S., Cho, B.K. and Kim, B.G. (2004) ω-amino acid: pyruvate transaminase from *Alcaligenes denitrificans* Y2k-2: a new catalyst for kinetic resolution of β-amino acids and amines. *Appl Environ Microbiol* 70: 2529–2534.

Yun, H., Hwang, B.Y., Lee, J.H. and Kim, B.G. (2005) Use of enrichment culture for directed evolution of the *Vibrio fluvialis* JS17 omega-transaminase, which is resistant to product inhibition by aliphatic ketones. *Appl Environ Microbiol* 71: 4220–4224.

Zelder, O., Jeong, W.K., Klopprogge, C., Herold, A. and Schroder, H. (2009) US application patent No. US2009/0029425 A1.

Chapter 2

Enrichment of *β*-amino acid-degrading microorganisms

Ciprian G. Crismaru,[a] Gerrit J. Poelarends[b] and Dick B. Janssen[a]

[a]*Department of Biochemistry, Groningen Biomolecular Sciences and Biotechnology Institute, and* [b]*Department of Pharmaceutical Biology, Groningen Research Institute of Pharmacy, University of Groningen, The Netherlands*

Abstract

Discovery of new enzymes for applied biocatalysis from microorganisms often starts with selective enrichment of cultures growing on a specific target compound. In this chapter we describe the isolation and partial characterization of 18 bacterial strains that were obtained by an enrichment procedure using the following *β*-amino acids as sole nitrogen source: *β*-alanine, *β*-asparagine, *β*-glutamate, *β*-leucine, *β*-phenylalanine, *β*-amino butyric acid, D-aspartic acid, *β*-tyrosine and cispentacin [(1*R*,2*S*)-2-aminocyclopentane-1-carboxylic acid)]. On the basis of activity screening two types of enzymatic activity were observed: amide hydrolase activity for *β*-asparagine-degrading microorganisms (CBN1-3) and aminotransferase activity for *β*-phenylalanine degraders. Because of its promising enzymatic activity, one of the *β*-phenylalanine degrading cultures was characterized by 16S rRNA gene sequencing and appeared to be a *Variovorax paradoxus* strain. The *β*-phenylalanine aminotransferase (*Vp*AT) was partially purified (133 mU/mg) and activity tests showed that *Vp*AT is highly enantioselective for (*S*)-*β*-phenylalanine. Additionally, *Vp*AT can use *α*-ketoglutarate and pyruvate as amino acceptors with comparable reactivities.

Introduction

In order to obtain new enzymes for biotechnological applications, selective enrichment of microorganisms with specific target substrates is often used. Enrichment experiments are designed such that the desired enzymatic activity is essential for growth of the culture. Often, the target substrate is a nitrogenous or organic compound that serves as sole nitrogen or carbon source, respectively.

The *β*-amino acids are naturally occurring compounds that occur both as free metabolites and as biosynthetic precursors of natural products with various bioactivities (Seebach *et al.,* 2004). The bioactivity of secondary metabolites containing *β*-amino acids as building blocks has stimulated research into their chemical synthesis. Several routes for the preparation of *β*-amino acids have been described, including chemical (Cole, 1994; Weiner *et al.,* 2010), chemo-enzymatic (Liljeblad & Kanerva, 2006) or fully enzymatic methods (Koeller & Wong, 2001). Enzymatic routes often have some advantages compared to chemical methods, such as high regio- and enantioselectivity, high activity and use of mild reaction conditions. Integration of enzymes into engineered biosynthetic pathways may also provide elegant synthetic approaches.

Biocatalytic routes towards optically active *β*-amino acids obviously depend on enzymes that can produce or in an enantioselective manner degrade these chiral compounds. The metabolism of *α*-amino acids has been extensively characterized. Various deamination reactions are known and similar routes may exist for *β*-amino acids. At least five different types of reactions known for *α*-amino acids are theoretically possible for the degradation of *β*-amino acids (**Fig. 2.1**).

Reaction 1 is catalyzed by an amino acid oxidase (AAO), which belongs to the oxidoreductase class of enzymes. These oxidases are known for L- and D-*α*-amino acids and use FAD as cofactor and O_2 as electron acceptor, and release ammonia and H_2O_2. The deaminated product is a 2-oxo acid. These enzymes (EC 1.4.3.2) are involved in the metabolism of L-*α*-amino acids such as alanine, aspartate, methionine, valine, leucine, isoleucine, tyrosine, phenylalanine and tryptophan, but also play a role in biosynthetic reactions (Boyer *et al.,* 1963). There are also D-*α*-amino acid oxidases (D-AAOs) (EC 1.4.3.3), e.g. in peroxisomes. They occur in organisms ranging from yeast to human (Pollegioni *et al.,* 2007), but have not been reported to be present in bacteria and plants. Similarly to L-AAOs, D-AAOs contain FAD as cofactor and use molecular oxygen as electron acceptor. Both for L-AAOs and D-AAOs, crystal structures are available (Pawelek *et al.,* 2000; Moustafa *et al.,* 2006; Faust *et al.,* 2007).

Reaction 2 is a typical aminotransferase (AT) (EC 2.6.1.X) reaction. Aminotransferases contain pyridoxal-5'-phosphate (PLP) as cofactor which is covalently bound to the ε-amino group of a lysine residue in the active site of the enzyme. During the aminotransferase reaction an amino acid (amino donor) transfers via the enzyme an amino group to a keto acid (amino acceptor) forming a new amino acid and a new keto acid. The transamination reaction consists of two half reactions (Hayashi *et al.,* 2003; Eliot & Kirsch, 2004). Each half reaction encompasses three steps. The first step is transaldimination, where the internal Schiff base between the PLP and an ε-NH_2 of the lysine residue is replaced by the same bond type between the amino substrate and the PLP, forming an external aldimine. The second step is a 1,3 hydrogen migration, which involves the abstraction of the α-proton (β-proton in the case of β-amino acids) from the external aldimine and reprotonation to the imine of the PLP to yield a ketimine intermediate. The final step in the first half reaction is hydrolysis of the ketimine to release the 2-oxo acid and the pyridoxamine 5'-phosphate (PMP) enzyme. The second half reaction involves the keto acid (amino acceptor) and is the reverse of the first half reaction. It yields the corresponding new amino acid and regenerates the PLP form of the enzyme (**Fig. 2.2**) (Hwang *et al.,* 2005).

Aminotransferases for the preparation of β-amino acids have been recently reviewed (Rudat *et al.,* 2012). Pyruvate is a suitable amino acceptor in known transaminase reactions involving a β-amino acid. Activity was found with β-amino butyric acid and β-leucine (Yun *et al.,* 2004). Aminotransferases acting on α-amino acids generally have a preference for either pyruvate or 2-oxoglutarate and oxaloacetate (Yun *et al.,* 2004; Shin *et al.,* 2003; Shin & Kim, 2001; Sung *et al.,* 1990; Lowe *et al.,* 1985). However, the β-transaminase from a *Mesorhizobium* strain shows similar activities with 2-oxoglutarate, pyruvate, pyruvate ethyl ester and pyruvate methyl ester (Kim *et al.,* 2007).

PLP-dependent enzymes whose structures have been solved belong to one of five fold types (Eliot & Kirsch, 2004). The fold type I group contains the majority of PLP-containing enzymes and includes the well-known aspartate aminotransferase. It also includes the aromatic aminotransferases (e.g. tyrosine aminotransferase). These enzymes function as homodimers, each dimer containing two active sites (one active site per monomer). The active sites lie on the interface of the dimer, and each monomer contains essential residues for both active sites. The monomers have a large and a small domain. In some cases (e.g. aspartate aminotransferase) these domains move significantly upon substrate binding, creating a closed conformation that may play a role in substrate specificity and influence the type of reaction that is catalyzed.

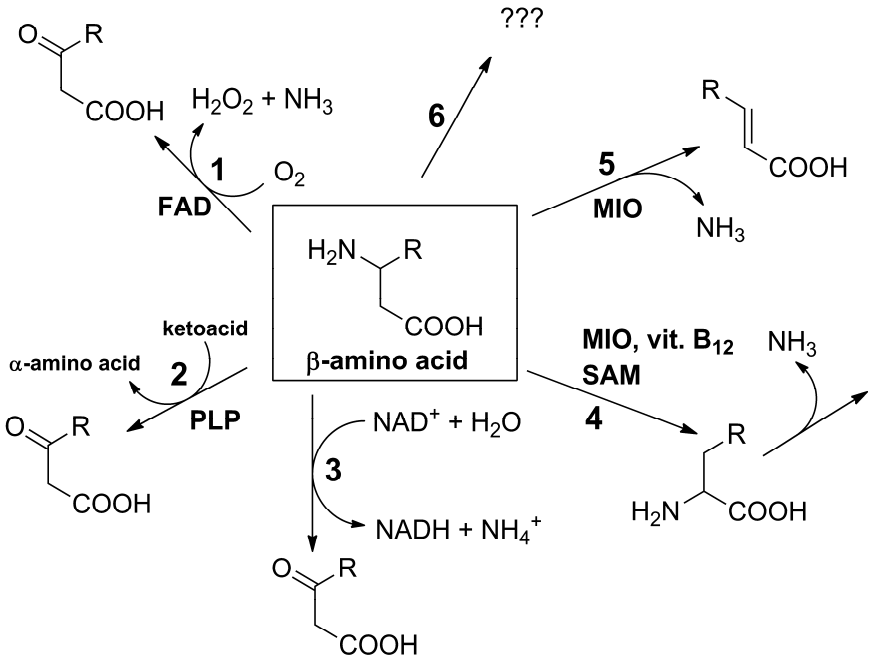

Figure 2.1 Expected reactions for deamination of *β*-amino acids: 1, amine oxidase; 2, aminotransferase; 3, amine dehydrogenase; 4, aminomutase; 5, ammonia lyase; 6, other still unknown reactions.

The structures of fold type II PLP-dependent enzymes (tryptophan synthase family) are closely related to those of fold type I but the proteins are evolutionarily different (Mehta & Christen, 2000). A distinct feature of the fold type II enzymes that contrasts with the enzymes from fold type I family are the active sites residues, which belong entirely to one monomer, though the functional state of the proteins remains a homodimer or higher-order oligomer. Additionally, enzymes of the fold type II family possess regulatory domains, e.g. threonine synthase and cystathionine synthase, which are allosterically regulated by S-adenosylmethionine.

The fold type IV (D-amino acid aminotransferase family) enzymes are very similar to fold type I and II enzymes, because they are also functional as homodimers of which each monomer is composed of a small and a large domain. The main structural feature of the fold type IV enzymes is the orientation of the PLP cofactor, which is bound at the interface of the dimer with the *re*-face exposed to the solvent rather than the *si*-face, as seen in the structures of fold type I and II enzymes (Sugio *et al.,* 1995).

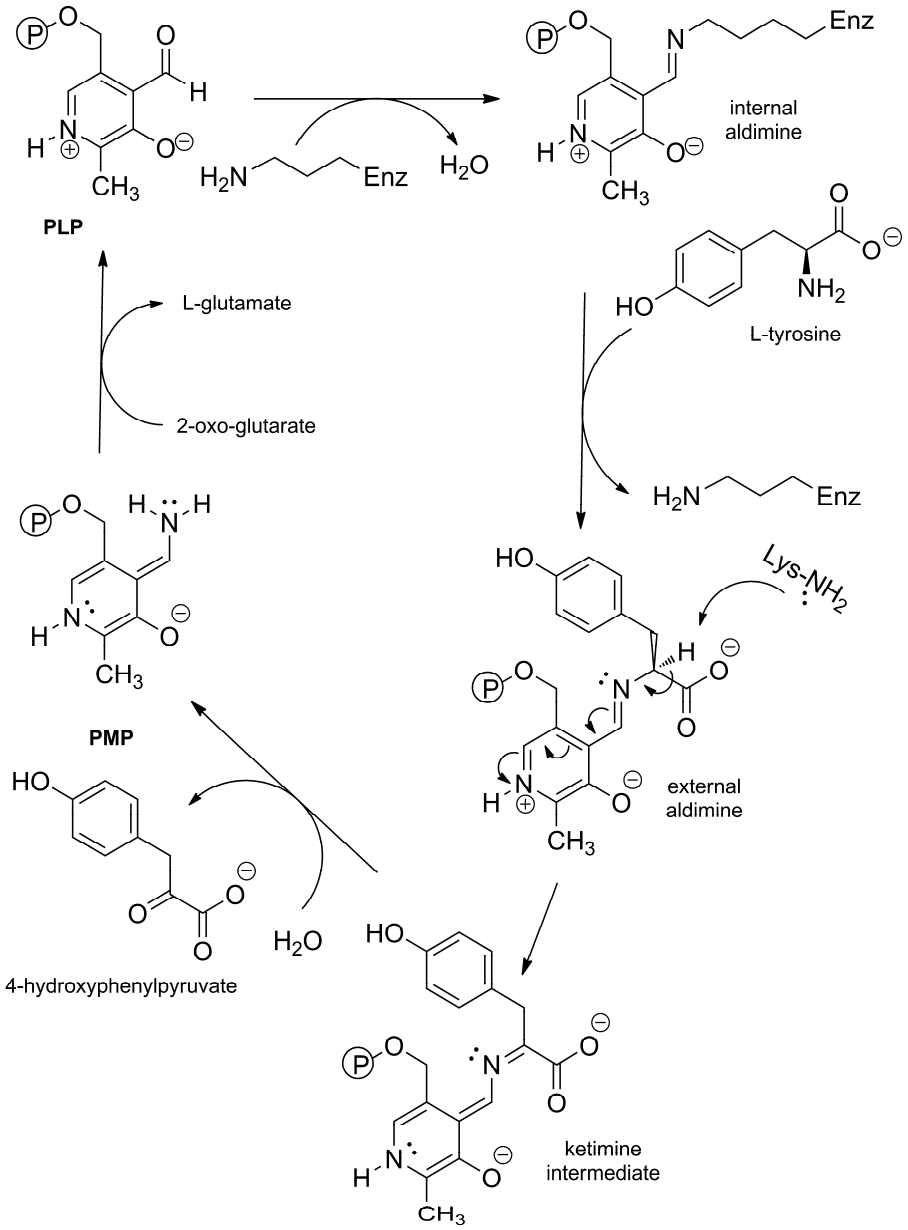

Figure 2.2 Reaction mechanism of tyrosine aminotransferase (Eliot & Kirsch, 2004).

Fold type III (alanine racemase family) and V (glycogen phosphorylase family) PLP enzymes are structurally very different from other PLP enzymes. The fold type V enzymes make use of the phosphate group of PLP for catalysis in a distinct

manner, which is not discussed further. The enzymes that are part of the fold type III class (e.g. ornithine decarboxylase) display the well-known α/β barrel fold and a second β-sheet domain. The enzymes belonging to fold type III and V PLP enzymes, are biologically active as homodimers. The PLP binding mode is similar to that in enzymes of other fold types and amino acid residues of each monomer contribute to both active sites (Kern *et al.,* 1999).

Aminotransferases are found in the fold type I and IV groups of PLP-dependent enzymes.

Amino acid dehydrogenases (AADHs) (NAD-dependent) catalyze **reaction 3**, forming a keto acid, NADH and ammonia. Amino acid dehydrogenases (EC 1.4.1.X) thus belong to a group of oxidoreductases that catalyze the reversible oxidative deamination of an amino acid to its keto acid and ammonia with the simultaneous reduction of either NAD^+, $NADP^+$ or FAD. AADHs are used for the synthesis of L-amino acids that serve as building blocks for different bioactive compounds and are used as coenzyme regeneration systems (Brunhuber & Blanchard, 1994; Hummel & Kula, 1989; Krix *et al.,* 1997; Ohshima & Soda, 1990). Enrichment experiments yielded bacteria that produce AADHs, including enzymes that possess NAD^+-dependent dehydrogenase activity toward L-*α*-isoleucine, L-*α*-methionine, L-*α*-cysteine, L-*α*-serine and L-*α*-glutamine (Mohammadi *et al.,* 2007). Several structures are available, including those of glutamate dehydrogenase (GluDH) (Rice *et al.,* 1987) and alanine dehydrogenase (AlaDH) (Baker *et al.,* 1998).

Based on coenzyme specificity, glutamate dehydrogenases were divided in three groups. The first group of GluDHs are $NADP^+$-dependent, the second group of GluDHs are NAD^+-dependent, whereas the third group of GluDHs are non-specific for either of the coenzymes NAD^+ or $NADP^+$ (Hudson & Daniel, 1993). For overall structure of these enzymes, various oligomeric states were reported. GluDHs occur in four oligomeric classes depending on their monomeric size and on their subunit composition (Minambres *et al.,* 2000). As a consequence glutamate dehydrogenases exist as either hexameric proteins with subunits of 50 or 180 kDa, or tetramers with monomers having a molecular weight of 50 kDa or 115 kDa (Peterson & Smith, 1999).

Similarly to some glutamate dehydrogenases, alanine dehydrogenases are mainly biologically active as hexamers (Sawa *et al.,* 1994), but they exist also as dimers (Schroder *et al.,* 2004), tetramers (Vancura *et al.,* 1989) or octamers (Vancurova et al., 1988) with a typical subunit size of 40 kDa. Furthermore, AlaDHs can be NAD^+- or $NADP^+$-dependent.

Reaction 4 is catalyzed by aminomutases (AMs) that shift the *β*-amino group to the *α*-position of their substrates. The product may be deaminated via one of the

other enzymes. Aminomutases are involved in the biosynthesis of various biologically active molecules, e.g. antibiotics (Prabhakaran *et al.,* 1988; Yin *et al.,* 2003; Walker *et al.,* 2004). Currently, AMs are divided in 3 classes based on the catalytic mechanism and the involvement of specific cofactors. Class I contains adenosylcobalamin (AdoCbl) -dependent AMs, such as lysine 5,6-aminomutase and D-ornithine 4,5-aminomutase from *Clostridium sticklandii*. These enzymes possess an AdoCbl-binding domain and a PLP-binding site (Berkovitch *et al.,* 2004; Wolthers *et al.,* 2010; Tang *et al.,* 2003; Chen *et al.,* 2001). A second group includes S-adenosylmethionine (SAM)-dependent enzymes. Lysine 2,3-aminomutase (2,3-LAM) from *Clostridium subterminale* (Aberhart *et al.,* 1981) and 2,3-LAM from *Escherichia coli* (Behshad *et al.,* 2006) are the best characterized enzymes from this class of aminomutases. The main difference is that while 2,3-LAM from *Clostridium* converts (*S*)-*α*-lysine to (*S*)-*β*-lysine, the product of *Escherichia* 2,3-LAM is (*R*)-*β*-lysine (Behshad *et al.,* 2006). Other members of this class are arginine 2,3-aminomutase from *Streptomyces griseochromogenes* (Prabhakaran *et al.,* 1988) and glutamate 2,3-aminomutase from *Clostridium difficile* (Ruzicka & Frey, 2007). Mechanistically, the enzymes from this group have in common the use of S-adenosylmethionine as cofactor, and also a [4Fe-4S]$^{2+}$ cluster and PLP. They are sensitive to oxidative conditions (Lepore *et al.,* 2005). The third class of aminomutases are MIO-dependent enzymes (MIO – 4-methylene-imidazol-5-one) which catalyze the migration of the amine group of aromatic amino acids. In plants, such as the *Taxus* tree, a MIO-dependent phenylalanine aminomutase catalyzes the conversion of *α*-phenylalanine to *β*-phenylalanine, which is the biosynthetic precursor of the N-benzoylphenyl-*iso*-serinoyl side chain of the anti-cancer drug taxol (Steele *et al.,* 2005). Another MIO-dependent AM is tyrosine aminomutase (TAM), which is responsible for conversion of *α*-tyrosine to *β*-tyrosine. TAM from *Streptomyces globisporus* and TAM from *Cupriavidus crocatus* have different kinetically preferred products, (*S*)-*β*-tyrosine and (*R*)-*β*-tyrosine, which are further incorporated into the antibiotic enediyne C-1027 and into cytostatic actin-targeting chondramides, respectively (Christenson *et al.,* 2003; Krug & Muller, 2009). In terms of mechanism, MIO-dependent aminomutases are related to MIO-dependent ammonia lyases. The MIO cofactor involved in catalysis is autocatalytically formed through internal cyclization of three amino acids of the mutase peptide, namely alanine, serine and glycine. All known MIO-containing enzymes share similar structures and are phylogenetically related (Schwede *et al.,* 1999).

Reaction 5 corresponds to an ammonia lyase (AL) that releases ammonia and forms the corresponding unsaturated acid. Several enzymes from the ammonia

lyase group can be used in the reverse direction and can add ammonia to C=C double bond (EC 4.3.1.X).

A very common ammonia lyase is L-aspartase (EC 4.3.1.1), which occurs in many bacteria and plants, where it is involved in the catabolism of L-aspartate to produce ammonia and fumarate, the latter being channeled into the tricarboxylic acid cycle or, in some bacteria, used as an electron acceptor for fermentative growth. Well-studied aspartases are those from *E. coli*, *Bacillus* sp. YM55-1 and *Hafnia alvei* (Mizobata & Kabata, 2007). These enzymes are very specific. For example, the *E. coli* aspartase has no activity with D-aspartic acid, L-asparagine or other L-*α*-amino acids. In the reverse reaction, there is no activity with unsaturated carboxylic acids other than fumaric acid, and activity with other nucleophiles than ammonia is very restricted. These enzymes are homotetrameric proteins with monomers of 52-55 kDa. Well-studied enzymes are *E. coli* aspartase (AspA) (Shi *et al.,* 1997) and the thermostable *Bacillus* sp. YM55-1 enzyme (AspB) (Fibriansah *et al.,* 2011). The *H. alvei* aspartase is used industrially for L-aspartate synthesis from fumarate and ammonia (Nuiry *et al.,* 1984). Based on sequence similarities and structural comparison, aspartases are classified as members of aspartase-fumarase superfamily. Other members of this superfamily that have been recently reviewed (Puthan Veetil *et al.,* 2012) are fumarase, argininosuccinate lyase (EC 4.3.2.1), adenylosuccinate lyase (EC 4.3.2.2) and (*S,S*)-ethylenediamine disuccinate (EDDS, a structural isomer of EDTA) lyase. The sequence similarity between these enzymes is low, but structural data indicate that the three regions (called C1, C2 and C3) that shape the active site are highly conserved. Argininosuccinate lyase plays a role in arginine metabolism by catalyzing the cleavage of argininosuccinate to arginine and fumarate, which is part of the urea cycle in liver. Adenylosuccinate lyase is involved in purine biosynthesis, where it catalyzes the conversion of succinyladenosine monophosphate to adenosine monophosphate (AMP) and fumarate. The reaction is important for the transfer of an amino group from aspartate to inosine monophosphate to produce AMP. The EDDS lyase was found in strains of *Agrobacterium tumefaciens* and *Ralstonia* sp., which are bacteria growing on EDDS as sole nitrogen and carbon source (Bauerle *et al.,* 2006). The lyase from *A. tumefaciens* converts EDDS to fumarate and N-(2-aminoethyl) aspartate.

Another ammonia lyase, which is not a member of the aspartase-fumarase superfamily, is L-methylaspartase (EC 4.3.1.2) (de Villiers *et al.,* 2012). Based on structure and sequence, this enzyme is part of the enolase superfamily. Enzymes of this class catalyze a large diversity of reactions such as lyase-, (de)hydratase, racemase-, and decarboxylase-type conversions (Gerlt *et al.,* 2005). Methylaspartate

ammonia lyases are involved in the anaerobic breakdown of glutamate by bacteria from the genus *Clostridium*. The activity is present in several (facultative) anaerobic microorganisms, where degradation of glutamate starts with a mutase reaction yielding L-*threo*-3-methylaspartic acid. In the next step, this product is deaminated by the lyase to mesaconic acid. Methylaspartate ammonia lyases are homodimeric proteins with subunits of 45 kDa, and like other members of the enolase superfamily, they require Mg^{2+} and K^{+} for activity, and an Mg^{2+} ion located in the active site is involved in substrate binding (Levy *et al.,* 2002).

Histidine ammonia lyase (EC 4.3.1.3) and related enzymes that act on aromatic amino acids, such as phenylalanine ammonia lyase (PAL, EC 4.3.1.24) and tyrosine ammonia lyase (TAL, EC 4.3.1.23), form a distinct group of proteins that share the 4-methylidene-imidazole-5-one cofactor (MIO). As mentioned above for the group of MIO-dependent aminomutases (**reaction 4**), this cofactor is derived from an internal Ala-Ser-Gly tripeptide by cyclization and dehydration reactions (Schwede *et al.,* 1999). The amino acids that autocatalytically form the MIO cofactor are strictly conserved, both in aromatic ammonia lyases and aromatic aminomutases. The aromatic ammonia lyases catalyze reversible amine elimination from histidine, tyrosine or phenylalanine. Mechanistically, the important feature of the MIO cofactor is the ethylene group that was assumed to carry out a Friedel-Crafts like attack on the aromatic ring, but according to more recent evidence, it reacts with the amino group of the substrate (Cooke *et al.,* 2009). A likely reaction mechanism is an E1cb-like elimination, involving abstraction of a proton from the *β*-carbon, which is activated by γ-carboxyl group, and subsequent removal of the amino group (**Fig. 2.3**). Most information about the mechanisms of the MIO enzymes indeed points to an electrophilic attack of the MIO group on the amino group of the substrate. The evidence can be summarized as follows: a covalent adduct involving MIO and an amine function has been observed by X-ray crystallography of the closely related MIO-enzyme tyrosine aminomutase (Christianson *et al.,* 2007); computational studies indicate that the alternative Friedel-Crafts mechanism is energetically unlikely (Wu *et al.,* 2012; Wang *et al.,* 2013); and the MIO cofactor is required for the re-addition of amine in the aminomutase reaction (Wu *et al.,* 2009). The biological function of microbial L-histidine and L-phenylalanine ammonia lyases is catabolic. Ammonia lyases from plants, such as L-phenylalanine ammonia lyase and L-tyrosine ammonia lyase, play a role in biosynthesis by providing unsaturated carboxylic acids that are channeled into lignin synthesis. Additionally, L-tyrosine ammonia lyase occurs in the synthesis of coumarate, which can be used as building block for some antibiotics.

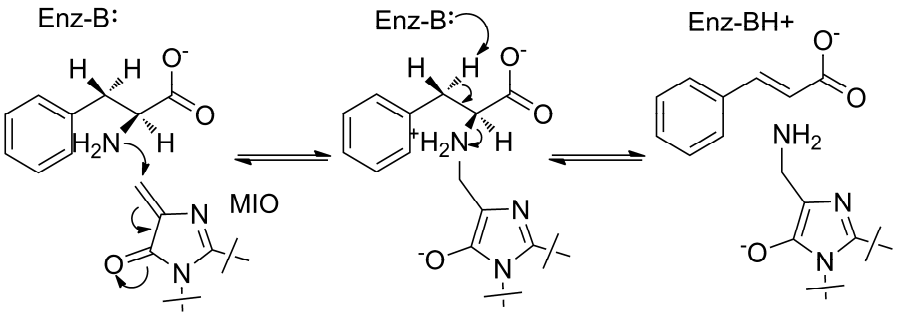

Figure 2.3 Proposed mechanism of MIO-type ammonia lyase.

Degradation of some *β*-amino acids, such as *β*-alanine, can also proceed by an ammonia lyase reaction after activation to the coenzyme A (CoA) thioester, a reaction catalyzed by a CoA-dependent ligase that requires ATP. Formation of the CoA adduct is followed by deamination catalyzed by a CoA-dependent ammonia lyase (Herrmann *et al.,* 2005) (**Fig. 2.5, panel B**). The equilibrium of the *β*-alanyl-CoA ammonia lyase reaction was proposed to be towards the formation of the amine adduct, and ammonia elimination occurred rapidly only in the presence of a dehydrogenase that converts the formed acrylyl-CoA to propionyl-CoA.

The above illustrates that different reaction types are possible for removing an amino group from *α*-amino acids. To what extent these reactions play a role in the metabolism of *β*-amino acids as well is not known. Still other mechanisms than those included in **Fig. 2.2** cannot be excluded. Few organisms growing on *β*-amino acids have been described and information on deamination reactions with these compounds is scarce. In view of the potential use of deamination enzymes in applied biocatalysis, the generation of more knowledge on the metabolism of *β*-amino acids is desirable. In this chapter we explore the use of enrichment cultures for obtaining bacteria that grow on *β*-amino acids and report a partial characterization of the deamination reactions that occur in the organisms that were identified.

Materials and methods

Chemicals and media

An overview of the *β*-amino acids used in enrichment cultures is presented in **Fig. 2.4**. *rac*-*β*-Phenylalanine (**2.4i**), phenazine methosulfate, nitro blue tetrazolium (NBT), pyridoxal 5'-phosphate (PLP), L-*α*-glutamic acid, L-*α*-alanine acid and crotonic

acid (**2.4n**) were purchased from Acros Organics. Glutaconic acid (**2.4b**), 2-oxo-glutaric acid disodium salt and *β*-alanine (**2.4e**) were purchased from Fluka.

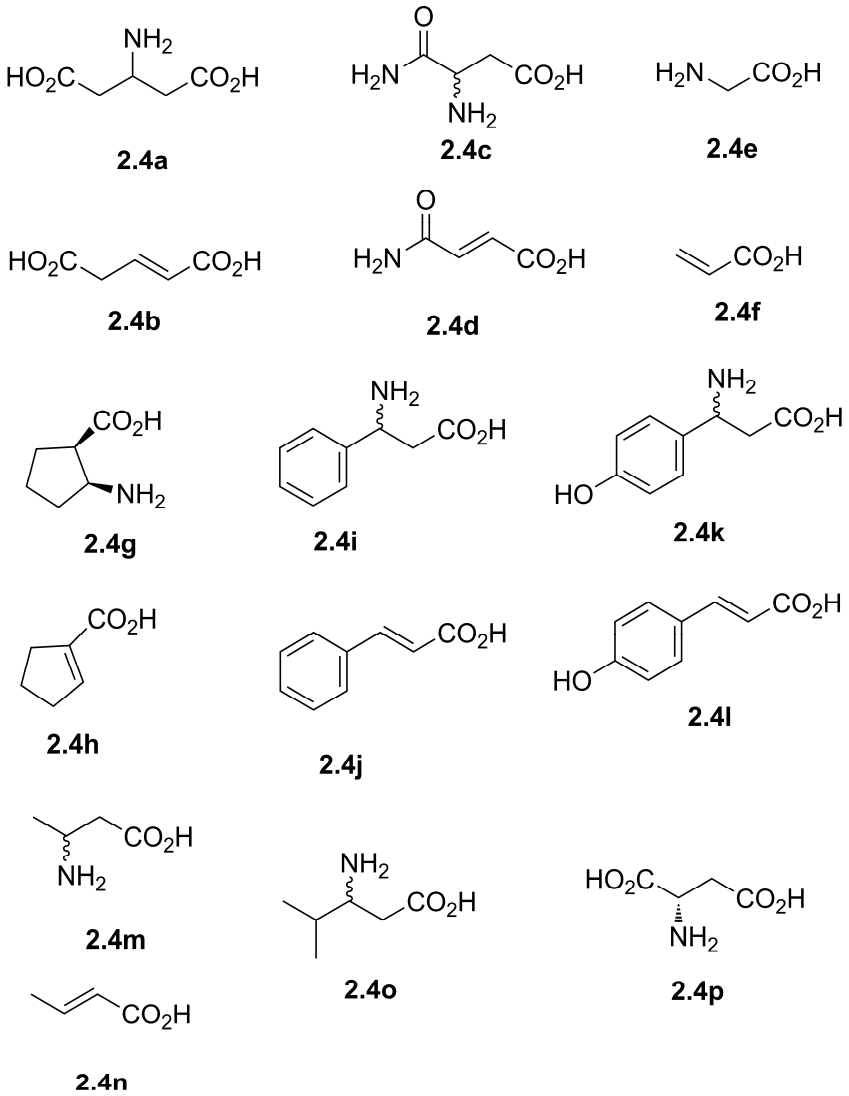

Figure 2.4 Overview of *β*-amino acids and corresponding unsaturated acids used in enrichment cultures.

Maleamic acid (**2.4d**), *trans*-cinnamic acid (**2.4j**), *rac*-*β*-leucine (**2.4o**), S-(5'-adenosyl)-L-methionine (SAM), coenzyme B_{12} (AdoCbl), *β*-nicotinamide adenine dinucleotide (NAD), adenosine 5'-triphosphate (ATP), coenzyme A, glutamic acid

dehydrogenase from bovine liver, *p*-coumaric acid (**2.4l**), *β*-glutamic acid (**2.4a**), sodium pyruvate, *ortho*-phthalaldehyde (OPA), MOPS, CHES, and Tris were purchased from Sigma-Aldrich. Other chemicals were purchased as follows: *β*-asparagine (**2.4c**) (Bachem), *rac*-*β*-tyrosine (**2.4k**) (InnoChimie GmbH), D-aspartic acid (**2.4p**) (Lancaster Synthesis), Nessler's reagent and phenylmethanesulfonyl fluoride (PMSF) solution (Fluka).

Enrichment and growth of *β*-amino acid degrading bacteria

Enrichment cultures were inoculated with samples collected of soil and sludge from various locations in the Netherlands. Samples (1-2 g) were added to flasks containing 50 ml minimal medium of pH 7.0 comprising per l 5.3 g $Na_2HPO_4 \cdot 12H_2O$, 1.4 g KH_2PO_4, 0.2 g $MgSO_4 \cdot 7H_2O$, 0.1 ml vitamin solution and 0.5 ml trace elements solution (Neidhardt *et al.,* 1974). The trace elements solution consisted of a number of important metals important for bacterial growth (Gabor *et al.,* 2004).

In the enrichment cultures, the nitrogen source was a *β*-amino acid (1 mM) whereas its corresponding unsaturated acid was used as carbon source (5 mM). This was assumed to stimulate enrichment of lyase-producing organisms. In some experiments a *β*-amino acid was used as the sole nitrogen and carbon source (e.g. D-aspartic acid and *β*-alanine), whereas in other experiments glucose was employed as more accessible carbon source instead of a potentially toxic unsaturated acid (e.g. acrylic acid).

Enrichment cultures were incubated at room temperature in the dark without shaking. After bacterial growth was visible, 5 ml of the culture was transferred to a new flask containing the same medium. Growth was observed within 2-4 days. After 3-4 cycles, a sample from the liquid culture was streaked on agar plates containing the same medium and incubated at room temperature. Single colonies that appeared were isolated as potential *β*-amino acid-degrading microorganisms. Pure cultures were isolated, labeled, and stored as 15% glycerol stocks at -80 °C to be used for subsequent analysis. Growth on the respective *β*-amino acid as nitrogen source was verified in liquid culture.

Screening of alternative carbon sources and growth of *β*-amino acid degraders

In order to test whether the isolates obtained on various *β*-amino acids can also (efficiently) metabolize other carbon sources than the corresponding unsaturated acids, several potential carbon sources were used. Alternative carbon sources were expected to allow more rapid growth and give higher cell densities, which facilitates preparation of cell-free extracts for enzyme assays. Carbon sources such as sucrose,

glucose, cinnamic acid, glycerol, citrate, benzoate and ethanol were tested on minimal medium plates but also in liquid culture in concentrations varying from 5 to 20 mM.

16S rRNA gene analysis

All chemicals used in DNA manipulation procedures were purchased from Roche Diagnostics (Mannheim, Germany) and Qiagen NV (Venlo, The Netherlands) and used as recommended by the manufacturer. Genomic DNA of few *β*-amino acid degraders was isolated by a published protocol (Poelarends *et al.,* 1998). A PCR reaction was performed on this DNA using two universal 16S rRNA gene primers: 27F (5'-AGAGTTTGATCMTGGCTCAG–3') and 1492R (5'-GGYTACCTTGTTACGACTT-3') and gDNA of the strain of interest. The PCR product was sequenced by GATC Biotech AG (Konstanz, Germany) and the nucleotide sequences were analyzed using the Blastn program from NCBI.

Cultivation and preparation of cell-free extracts

For all whole-cell deamination assays and assays done with cell-free extracts (CFE), cells were cultivated aerobically for about 48 h at 22 °C and 160 rpm unless mentioned otherwise. To obtain a high yield of cells the unsaturated acid (expected deamination product from a lyase reaction) was replaced by an accepted alternative carbon source, such as glucose, sucrose or glycerol. Bacterial strains were grown to an optical density (OD) at 600 nm of 1 or higher. After harvesting the cells by centrifugation, they were washed and disrupted by sonication. CFE was obtained by centrifugation of the lysate for 45 min at 15,000 rpm and 4 °C. The buffer for obtaining CFE consisted of 50 mM Tris-SO_4, pH 8, 0.5 mM PMSF and 0.01% *β*-mercaptoethanol.

Enzyme deamination assays

Deamination assays (**reactions 1, 3** and **5**) were performed in sodium phosphate buffer, pH 8.0, and Tris buffer, pH 8.0, with or without addition of Mg^{2+} and K^{+}, ions known to activate or stabilize some deamination enzymes, *e.g.* ammonia lyases (Raj *et al.,* 2011). **Reaction 2** was assayed in 50 mM MOPS buffer, pH 7.6, and **reaction 4**, in 50 mM CHES buffer, pH 9.0. Specific cofactors were added in all tested reactions to a final concentration of 0.1 mM, e.g. FAD, NAD^{+}, PLP, SAM, B_{12} and ATP. Reactions were monitored over time and at temperatures between 25 and 30 °C. For CFE prepared from strain CBA1, CoA ligase activity was tested by adding coenzyme A (CoA-SH) and ATP.

For reactions **1**, **3** and **5** (**Fig. 2.1**) deamination assays consisted of a colorimetric procedure for detecting ammonia, using Nessler's reagent (potassium

tetraiodomercurate alkaline solution). Because of interference with NAD^+, which gave a dark grey color, Nessler's reagent was not used for **reaction 3**. Instead, AADH activity was assayed by monitoring the formation of NADH from NAD^+ by UV spectroscopy at 340 nm. Ammonia detection assays were done in microtiter plates (MTPs), using 150 µl of sample to which one drop of 1.5 M trichloroacetic acid (TCA) and three drops of Nessler's reagent were added with a Pasteur pipette. Formation of an orange to brown precipitate indicates the presence of ammonia. Incubations were done with CFE and with whole-cells at 30 °C for about 16 h. All substrate solutions (*β*-amino acids) were tested for any free ammonia present.

Reaction 5 was also monitored by UV spectroscopy at 240-290 nm, which detects the formation of a double bond (unsaturated acid) by a lyase reaction.

Reaction 2 (AT) and **reaction 4** (AM) were assayed by HPLC using OPA (*ortho*-phthalaldehyde) for prederivatization of amino compounds (e.g. the *β*-amino acid substrate) and amino acid formed (L-*α*-alanine or L-*α*-glutamate)). Aminomutase activity was measured by separation and detection of the *β*-isomer formed from the *α*-isomer of an amino acid (substrate). Enantioselectivity of the enzyme was studied using reaction mixtures consisting of 5 mM of *β*-amino acid in 50 mM CHES buffer pH 9, containing appropriate cofactors (S-adenosyl methionine, PLP, ATP or vitamin B_{12}) and a suitable amount of freshly prepared cell-free extract. Reaction mixtures were incubated at 30 °C and samples were taken with different time intervals (e.g. at 0 min, 15 min, 30 min, 60 min, 120 min and 240 min). Reaction mixtures were quenched by addition of 2 M HCl. Proteins were removed by centrifugation and the pH was neutralized by adding a suitable amount of 2 M NaOH. Samples were then analyzed by the OPA-HPLC-based method as described below.

Quantitative HPLC was performed with a C18 Alltech OPA-HS Adsorbosphere column (5 µm, 4.6 mm x 100 mm) connected to a Jasco HPLC system with prederivatization of the sample with OPA. The thio-substituted isoindole derivatives formed from *α*- and *β*-amino acids with OPA have different retention times, so they can be separated and quantified. L-*α*-glutamate, L-*α*-alanine and *rac*-*β*-phenylalanine were separated by HPLC using 20 mM sodium acetate in 5% THF, pH 5.5, as buffer A and acetonitrile as buffer B, with a flow rate of 1 ml/min. Fluorescence was followed with a Jasco fluorescence detector using excitation 350 nm and emission 450 nm at 25 °C. Retention times for the derivatized L-*α*-glutamate, L-*α*-alanine and *rac*-*β*-phenylalanine derivatives were 2.3 min, 7.8 min and 23.3 min, respectively.

Chiral HPLC analyses were carried out on a Crownpak CR(+) column (4 mm x 150 mm). (*S*)- and (*R*)-*β*-phenylalanine were eluted isocratically with aqueous $HClO_4$ in 15% MeOH, pH 1.8, at a flow rate of 0.3 ml/min and a temperature of -7 °C.

Retention times for (*S*)- and (*R*)-*β*-phenylalanine were 45.4 min and 56.3 min, respectively.

One unit of *β*-phenylalanine aminotransferase is defined as the amount of enzyme that catalyzes the formation of one µmol of L-*α*-glutamate from 10 mM *rac*-*β*-phenylalanine and 5 mM 2-oxoglutarate in 1 min in 50 mM MOPS buffer (pH 7.6) at 30 °C.

Partial purification of *β*-phenylalanine AT from CBF3

In order to isolate the *β*-aminotransferase detected in CFE of strain CBF3, cells were grown in a 2 l volume. Cells were harvested by centrifugation and pellets (about 8 g, wet weight) were resuspended in 40 ml of lysis buffer containing 50 mM Tris-SO_4 (pH 8.0), 0.5 mM EDTA, 1 tablet of protease inhibitor cocktail (Roche) and 0.01% (vol/vol) *β*-mercaptoethanol. Cells were disrupted by sonication at 4 °C. The supernatant obtained after centrifugation (15,000 rpm, 45 min) at 4 °C was used as cell-free extract. This was loaded onto a Q-Sepharose FF column (150 ml, 2.6 cm x 34 cm; Pharmacia) preequilibrated with the same buffer as the sonication buffer. After washing, an elution gradient was applied composed of 0 to 100% of 1.5 M NaCl in Tris buffer. The active fractions were pooled, concentrated and dialyzed against 20 mM HEPES buffer (pH 7.8) containing 0.2 mM EDTA and 0.01% (vol/vol) *β*-mercaptoethanol. The pooled active fractions were loaded onto a monoQ column (10 µm, 1 ml, 0.5 cm x 5 cm; GE Healthcare). After washing, elution was done with 0 to 100% 1 M NaCl in HEPES buffer. Active fractions were concentrated and dialyzed against 50 mM sodium phosphate buffer (pH 7.2) containing 150 mM NaCl. This material was subjected to gel filtration using a Superdex 200 column (24 ml, 13 µm, 1 cm x 30 cm; GE Healthcare) and sodium phosphate buffer (pH 7.2) containing 150 mM NaCl.

For preparative native gel electrophoresis, partially purified *β*-phenylalanine AT was run on a 4 to 20% gradient polyacrylamide gel (Bio-Rad) for 2 h at 4 °C. The gel was stained with native gel activity staining solution as described (Kim et *al.,* 2007), except that we used 2-oxoglutaric acid and glutamate dehydrogenase instead of pyruvate and alanine dehydrogenase. An active *β*-aminotransferase produces a purple band in the gel (Pedraza *et al.,* 2004).

Protein concentrations were determined using Coomassie brilliant blue and bovine serum albumin as protein standard.

Results

Enrichment of β-amino acid degraders

Isolation of β-amino acid degrading microorganisms was accomplished after four to seven serial transfers in shake-flask batch cultures and followed by streaking on minimal medium agar plates. In most cases, growth in liquid culture was visible after 3-4 days of incubation with the substrate of interest. Attempts to isolate strains from grassland soil or garden soil samples were more often successful than those using sludge or deep soil samples.

The following β-amino acids were attempted: β-alanine, β-glutamate, β-asparagine, β-leucine, β-phenylalanine, β-amino butyric acid, D-aspartic acid, β-tyrosine and cispentacin. In total 18 bacterial strains were isolated using these β-amino acids as sole nitrogen source. In the case of cispentacin and β-amino butyric acid we could not obtain pure cultures due to the persistent formation of bacteria-fungi mixed cultures. All the isolated strains were stored as frozen stocks in 15% glycerol at -80 °C (**Table 2.1**).

Table 2.1 Overview of β-amino acid degrading microorganisms obtained by enrichment culture.

N-source[a]	C-source[b]	Pure cultures[d]	Strains
β-glutamate	glutaconic acid	+	CBE1
β-asparagine	maleamic acid	+	CBN1-3
β-leucine	glucose	+	CBL1
β-phenylalanine	*trans*-cinnamic acid	+	CBF1-4
β-aminobutyric acid	crotonic acid	-[d]	-
cispentacin	1-cyclopentene-1-carboxylic acid	-[d]	-
β-alanine	-	+	CBA1
D-aspartate[c]	-	+	CDD1-3
β-tyrosine	*p*-coumaric acid	+	CBY1, 3-6

[a] Concentration 1 mM; [b] Concentration 5 mM; [c] Regarded as a β-amino acid; [d] -, occurrence of a persistent bacteria-fungi mixed culture.

Screening for deamination reactions

Since most of the unsaturated acids used as C-source in the enrichment cultures were not rapidly metabolized, alternative C-sources for growing the isolated

bacterial strains were tested. For most organisms a carbon source was found that gave faster growth and higher biomass yield than the deaminated analog of the nitrogen source that was used for selection (**Table 2.2**). For enzyme assays, cells were cultivated with this compound as carbon source and the *β*-amino acid for enrichment as nitrogen source.

Table 2.2 Screening for alternative C-sources for *β*-amino acid degraders[a].

Strains	C-source[b,c]						
	Sucrose	Glucose	Cinnamic acid	Glycerol	Citrate	Benzoate	Et-OH
CBA1	+++	-	-	++	+	+++	+
CBE1	+++	+	-	+++	+	+++	+
CBN1	+	-	-	+	-	++	-
CBN2	++	-	-	+	+	++	-
CBN3	++	-	-	+	+	++	-
CBL1	+	++	-	-	-	+++	+
CBF1	-	+	++	+	-	+++	+
CBF2	+	+	++	+	-	+++	+
CBF3	+	+++	+++	+	+	+++	+++
CBF4	+++	++	++	+++	+	-	+++
CDD1	++	-	-	-	-	-	-
CDD2	-	-	-	-	+	+++	++
CDD3	-	-	-	-	+	+++	++
CBY1	++	++	+++	-	+	+++	++
CBY3	-	+	-	++	-	-	++
CBY4	++	-	++	++	+	-	+
CBY5	+++	-	+	+++	+	-	+
CBY6	-	-	-	+	+	-	+++

[a] $(NH_4)_2SO_4$ (1 mM) used as N-source; [b] C-source 5-20 mM; growth was tested on minimal medium plates; [c] Growth is expressed as follows: growth (+), good growth (++), rich growth (+++), no growth (-).

Enzymatic routes for amino acid deamination

We tested whether amine oxidase (**Fig. 2.1,** reaction **1**), amino acid dehydrogenase (**Fig. 2.1,** reaction **3**), or ammonia lyase (**Fig. 2.1,** reaction **5**) activities were present in the isolated *β*-amino acid degraders. For this, each strain was grown under selective conditions (**Table 2.3**) and where it was required for rapid growth the

unsaturated acid used as a C-source in the enrichment was replaced by an alternative C-source. Cell-free extracts (CFE) were prepared and used in enzyme assays.

Table 2.3 Growth conditions and substrates used for detecting enzymatic activities in CFEs prepared from pure cultures grown on β-amino acids. The last five columns indicate ammonia release[a] in cell-free extracts under appropriate assay conditions.

Strains	Growth substrate(s)	Assay substrate (5-10 mM)	AAO	AT	AADH	AL	AM
CBA1	15 mM β-Ala	β-Ala	-	-	-	-	-
		α-Ala	-	-	-	-	-
CBE1	1 mM β-Glu + 20 mM sucrose	β-Glu	-	-	-	-	-
		α-Glu	-	nt	-	-	nt
CBN1-3	1 mM β-Asn + 20 mM sucrose	β-Asn	A[?]	-	-	A	-
		α-Asn	A[?]	-	-	A	-
		β-Ala	-	nt	-	-	nt
		L-Asp	nt	nt	nt	A	nt
		D-Asp	nt	nt	nt	A	nt
CBL1	1 mM β-Leu + 20 mM glucose	β-Leu	-	-	-	-	nt
CBF1-4	1 mM β-Phe + 20 mM glucose	β-Phe	-	A[b]	-	-	-
		α-Phe	-		-	-	-
CDD1-3	10 mM D-Asp	D-Asp	-	-	-	-	nt
		L-Asp	-	nt	-	-	nt
		β-Asn	A?	nt	-	A	nt
		β-Glu	-	nt	-	-	nt

[a] A, ammonia detected; nt, not tested; -, no activity.

[b] Aminotransferase was also detected in strains CBF2 and CBF3.

Degradation of β-alanine

β-Alanine is a naturally occurring β-amino acid found in animals, plants (Stinson *et al.,* 1969) and microorganisms. In metabolism, β-alanine occurs in the biosynthesis of pantothenic acid and α-methyl-β-alanine is present in the skeleton of cryptophycin (Steer *et al.,* 2002; Seebach *et al.,* 1998; Seebach *et al.,* 1996).

The bacterial strain CBA1 uses β-alanine as sole nitrogen and carbon source. The organism appeared as white-yellowish colonies on minimal medium agar plates. The strain did not use acrylic acid (**Fig. 2.4**, compound **2.4f**) as C-source, possibly due to toxicity or lack of a catabolic pathway. Strain CBA1 was also able to use L-α-alanine as sole nitrogen source.

For determining the mechanism of deamination, cells of CBA1 were grown in the presence of 15 mM β-alanine as nitrogen and carbon source for about 48 h at 22 °C and 160 rpm. Cell-free extract was prepared and enzyme activities were tested. Possible pathways for β-alanine degradation are shown in **Fig. 2.5**. One could expect

conversion of *β*-alanine to malonate semialdehyde by transamination (Hayaishi *et al.,* 1961). For the AT assay, different keto acids such as pyruvate and α-ketoglutarate were tested as amino acceptors (**Fig. 2.5, route A**). Another possibility is that *β*-alanine degradation proceeds by a lyase reaction that acts on the CoA adduct (Herrmann *et al.,* 2005) (**Fig. 2.5, route B**). In this case, deamination would be CoA-dependent and require ATP. Other options are an oxidase, a lyase or an aminomutase activity (**Fig. 2.1**).

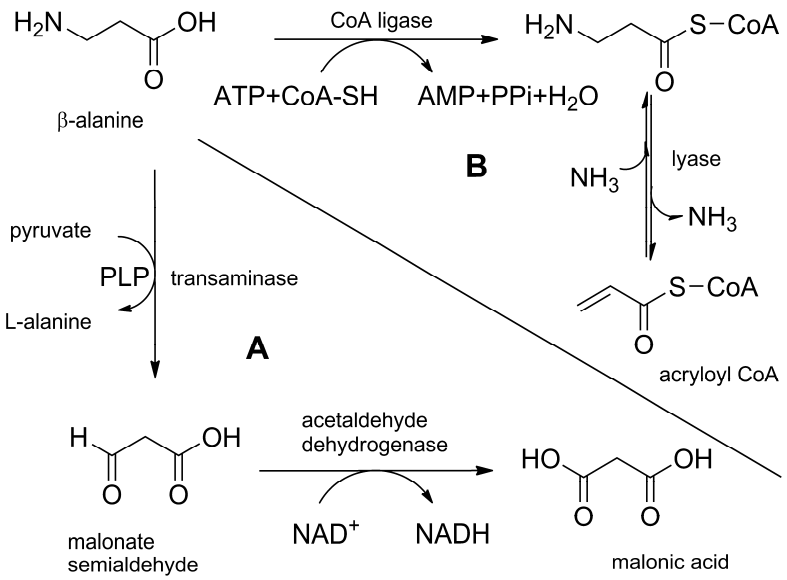

Figure 2.5 Deamination of *β*-alanine by a transaminase (**route A**) or a lyase that acts on a CoA adduct (**route B**).

Using CFE or whole-cells of CBA1 we did not detect any of these five enzyme activities depicted in **Fig. 2.1**. No formation of *α*-alanine or *α*-glutamate was detected with pyruvate or ketoglutarate as amine acceptor, indicating the absence of an aminotransferase acting on *β*-alanine. We tested also the possibility of *β*-alanine degradation via an acrylyl-CoA adduct (**Fig. 2.5, route B**), but the CoA adduct could not be detected by means of UV spectroscopy at about 254 nm. No release of ammonia was detected under these conditions using the Nessler assay. Assays in the presence of NAD^+ or $NADP^+$ also did not reveal activity, suggesting a dehydrogenase is not involved in the degradation of *β*-alanine. The route thus remains unclear.

Degradation of *β*-asparagine

The bacterial strains CBN1, CBN2 and CBN3 were isolated by enrichment culture using *β*-asparagine and maleamic acid (**2.4d**) as nitrogen and carbon source, respectively. All three organisms grew rapidly under these conditions and formed similar white opaque creamy colonies on plates. The three *β*-asparagine degraders could use as sole nitrogen source *β*-alanine, *β*-phenylalanine and *β*-glutamate (**Table 2.2**).

Not much information is available on *β*-asparagine catabolism. We considered 2 potential routes (**Fig. 2.6**). **Route A** implies the presence of an asparaginase (amidase) that would yield aspartic acid. Asparaginases are well studied enzymes that occur in many organisms including bacteria, archaea and plants. **Route B** consists of an ammonia lyase that would liberate the amino group from the *β*-position, forming maleamic acid. Both routes can be tested by means of an ammonia release assay, whereas a spectrophotometric analysis can detect maleamic acid formation.

For testing these activities, the *β*-asparagine degrading organisms were grown on minimal medium supplemented with 1 mM *β*-asparagine and 20 mM sucrose. Cell-free extracts (CFEs) prepared from strains CBN1, CBN2 and CBN3 did show ammonia release upon incubation with both L-*α*- and *rac*-*β*-asparagine, which was not stimulated by addition of FAD. The activity probably is due to an amide hydrolase (amidase), rather than an ammonia lyase, since the release of ammonia is not accompanied by the formation of an unsaturated acid, as monitored by UV spectroscopy.

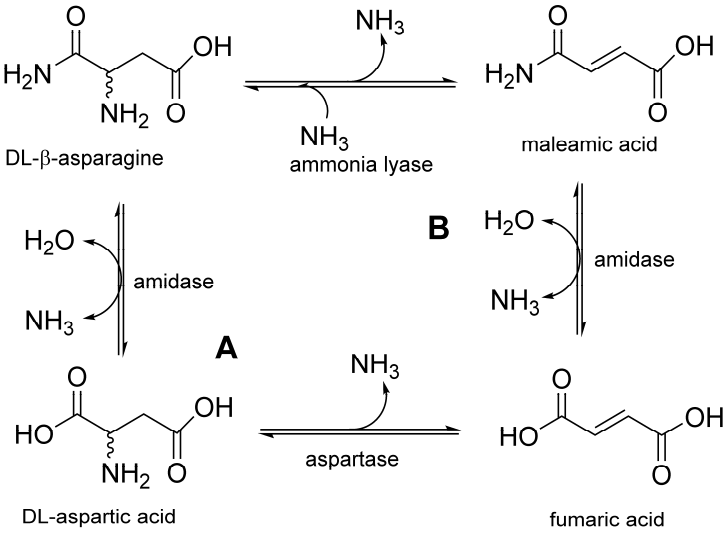

Figure 2.6 Possible routes for *β*-asparagine deamination.

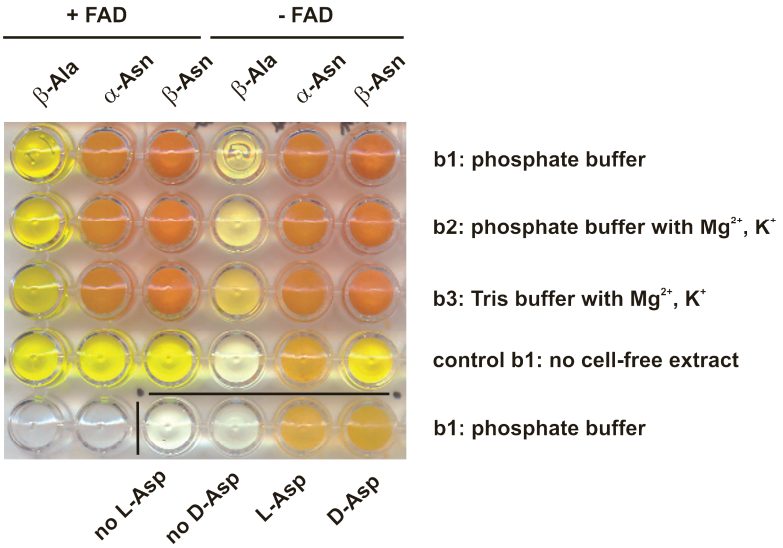

Figure 2.7 Ammonia detection assay by Nessler reagent using CFE of strain CBN3 and *α*- and *β*-asparagine, *β*-alanine, D- and L-aspartic acid. Three buffer conditions were used both with (+) and without (-) 0.1 mM FAD.

This makes **route B** (**Fig. 2.6**) unlikely. The most likely route for *β*-asparagine conversion is **route A**, which produces aspartic acid. Cell-free extract contained activity for release of ammonia from L- and D-aspartate as well, further supporting **route A** (**Fig. 2.7**). However, we did not observe formation of fumarate as monitored by UV spectroscopy at 240 nm.

Degradation of *β*-glutamate

β-Glutamate acts as an osmolyte in marine methanogenic bacteria (Robertson *et al.,* 1990). Using *β*-glutamate as sole nitrogen source and its corresponding unsaturated acid (glutaconic acid, **2.4b**) as carbon source, one bacterial strain was isolated (CBE1). On agar plates, strain CBE1 formed creamy white colonies. Since the growth on glutaconic acid was rather slow, we tested other potential carbon sources. The results indicated that strain CBE1 grows faster when sucrose, glycerol or benzoate was used as sole carbon source (**Table 2.2**). For preparation of cell-free extract for activity assays, strain CBE1 was aerobically cultivated on minimal medium supplemented with 1 mM *β*-glutamate and 20 mM sucrose.

A catabolic pathway for *β*-glutamate that starts with an aminomutase (AM) reaction producing L-*α*-glutamate has been described (Ruzicka & Frey, 2007). The latter can be deaminated by a dehydrogenase or by a transaminase (**Fig. 2.8**). The

mutase reaction was tested by following the conversion of *β*-glutamate to *α*-glutamate using HPLC. Another possibility is a coupled assay with added glutamate dehydrogenase and NAD^+, with spectrophotometric monitoring of the formation of NADH at 340 nm (**Fig. 2.8, route A**). A coupled assay for **route B** would rely on the addition of aspartate ammonia lyase and follow the release of ammonia or fumarate. The latter can be detected by UV spectroscopy at 240 nm (**Fig. 2.8, route B**).

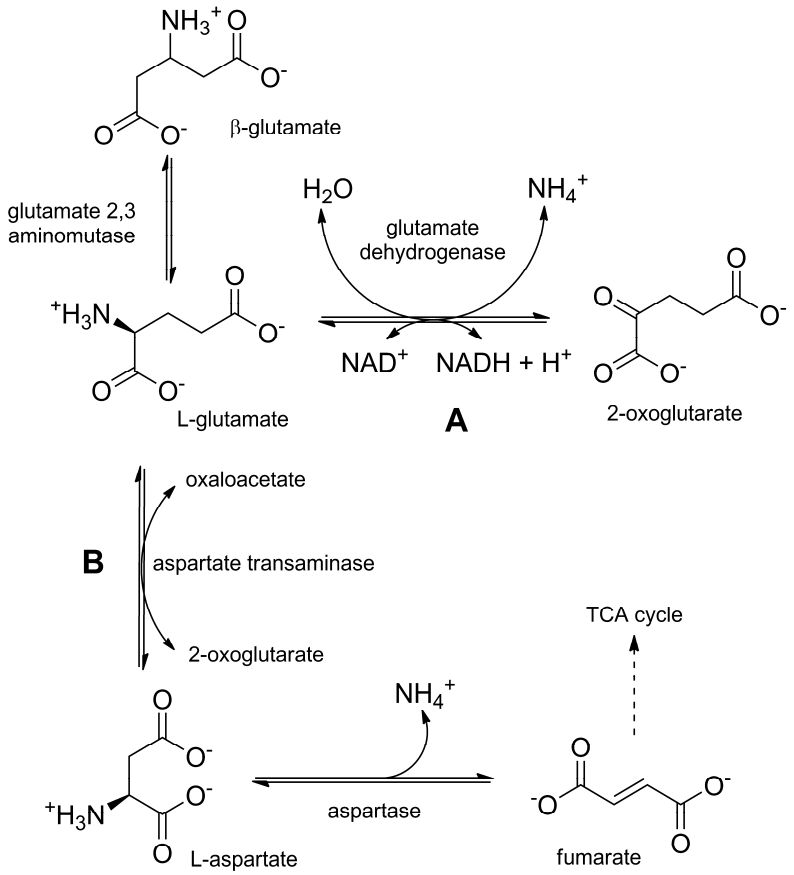

Figure 2.8 Possible routes for conversion of *β*-glutamate by aminomutase reactions. **Routes A** and **B** show aminomutase routes that can be detected in coupled assays.

When *β*-glutamate was incubated with cell-free extracts of strain CBE1, no ammonia release was found, indicating that no oxidase (FAD added) or lyase was present. Also after addition of NAD^+, no ammonia release was found and no NADH was produced. Using HPLC assays no aminomutase or transaminase activity could be detected, even upon addition of known mutase cofactors (SAM, B_{12}, PLP and ATP).

Thus, although the mutase activity for *β*-glutamate has been described in anaerobic bacteria (Ruzicka & Frey, 2007), no such activity was found in CBE1. Using a coupled assay (**Fig. 2.8, route A**) with addition of glutamate DH and NAD^+, no NADH formation could be detected by UV spectroscopy at 340 nm. Thus, the assays did not reveal a pathway for *β*-glutamate degradation in strain CBE1.

Catabolism of *β*-leucine

No microorganism growing on *β*-leucine has been described. However, this compound occurs in a metabolic pathway of L-leucine. Most organisms degrade L-leucine via initial transamination by a branched chain aminotransferase (BCAT) (EC 2.6.1.42) to produce *α*-ketoisocaproate (Norton *et al.,* 1970), or by an NAD^+-dependent leucine dehydrogenase (L-LDH) that gives the same product (Baker *et al.,* 1995; Sanwal *et al.,* 1961). The keto acid is then converted to acetoacetate and acetyl-CoA. A different pathway was found in the anaerobic bacterium *Clostridium sporogenes* (**Fig. 2.9**). This organism first converts L-leucine to *β*-leucine, which is deaminated by a transaminase to ketoisocaproate and then converted to isobutyrate and acetate (Poston *et al.,* 1976). The only enzyme that has been characterized from this pathway is leucine 2,3-aminomutase (LAM) (EC 5.4.3.7) (Poston *et al.,* 1976). The enzyme also was reported to be present in mammalian tissues (Poston *et al.,* 1980), green plants (Freer *et al.,* 1981) and chicken (Ward *et al.,* 1988). The latter study provides also data indicating conversion of *β*-leucine by LAM to *α*-leucine in the presence of coenzyme B_{12} (adenosylcobalamin).

Another report describes the occurrence of *β*-leucine as a product of a *β*-peptidyl aminopeptidase (EC 3.4.11.25) converting the non-natural *β*-tripeptide *β*-leucine-*β*-homoalanine-*β*-homoleucine (Geueke *et al.,* 2005). A Gram-negative bacterium, identified as *Sphingosinicella xenopeptidilytica*, was able to use the *β*-tripeptide but also the dipeptide *β*-homoalanine-*β*-homoleucine as sole nitrogen and carbon source. The same *β*-peptidyl hydrolase cleaved the *β*-dipeptide into *β*-homoalanine and *β*-homoleucine. The sequence of the gene coding for *β*-peptidyl aminopeptidase (BapA) identified the enzyme as a new member of the *N*-terminal nucleophile hydrolase superfamily.

We obtained by selective enrichment an organism that grows on *β*-leucine as sole nitrogen source (CBL1). The organism appeared on plates as small white colonies. Since the corresponding unsaturated acid (4-methyl-2-pentenoic acid) was not available, enrichment was performed with glucose as carbon source. Growth experiments showed that strain CBL1 could also use sucrose, but not glycerol (**Table 2.2**).

Enzyme activities were tested using cell-free extracts prepared from cultures grown on 1 mM *β*-leucine and 20 mM glucose. Assays with cell-free extracts in the absence of an external coenzyme revealed that there is no ammonia release from *β*-leucine, indicating no activity of an ammonia lyase or amine oxidase. Further assays were carried out to test other enzymatic activities (**Fig. 2.1**). AADH activity tested by monitoring NADH formation from NAD^+ was not detected in CFE of strain CBL1. Furthermore, no AT activity was detected when using 2-oxoglutarate or pyruvate as amino acceptors and *β*-leucine as amino donor. No further assays were performed since we were primarily interested in ammonia lyase and aminotransferase activities.

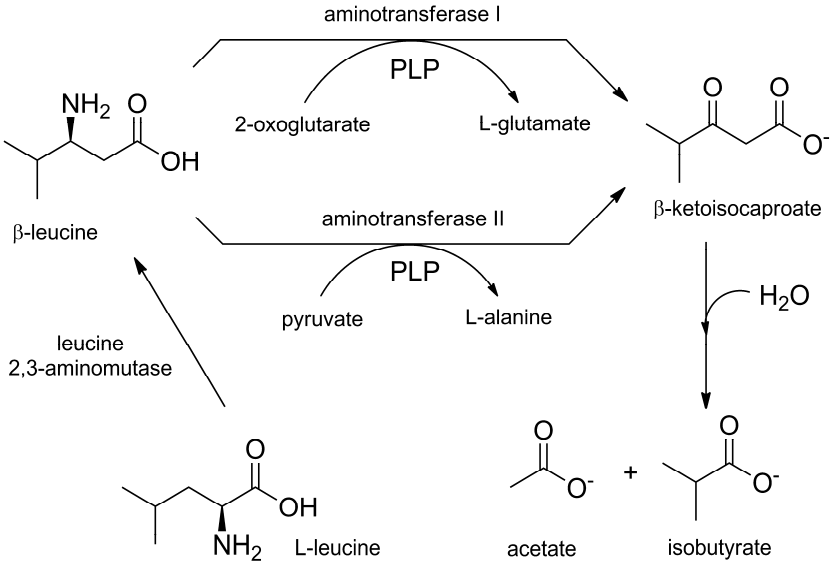

Figure 2.9 Possible routes for conversion of *β*-leucine.

Degradation of *β*-phenylalanine

β-Phenylalanine occurs in nature as a building block in the biosynthesis of the N-benzoyl phenylisoserinoyl side chain of the anticancer drug taxol (Steele *et al.,* 2005). In this pathway, *β*-phenylalanine is produced from *α*-phenylalanine by phenylalanine aminomutase (PAM). This activity can be assayed by following the interconversion of *β*-phenylalanine and *α*-phenylalanine, but also in a coupled assay with phenylalanine ammonia lyase (PAL) which converts *α*-phenylalanine to *trans*-cinnamic acid, which can be detected by following the absorbance at 290 nm, and ammonia, detectable via the colorimetric assay (**Fig. 2.10**).

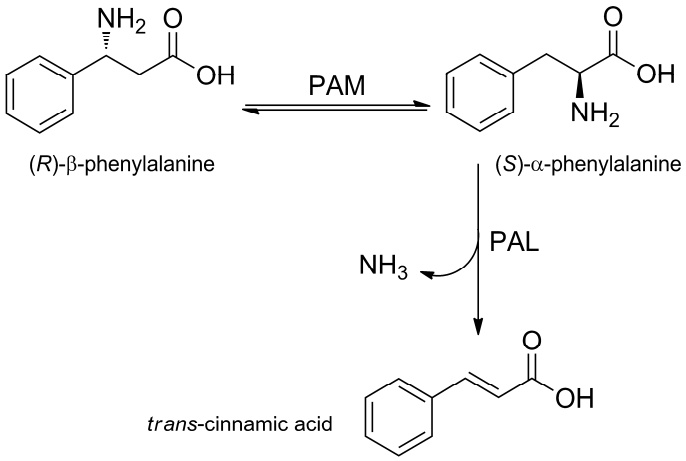

Figure 2.10 Conversion of *β*-phenylalanine by aminomutase and ammonia lyase activities.

Another deamination pathway would start with an aminotransferase, as is the case for its *α*-analogue L-*α*-phenylalanine and would yield 3-phenylpyruvate (Vuralhan *et al.,* 2003). For L-*α*-phenylalanine, this step can be performed by two aromatic transaminases. The first is an aromatic aminotransferase that acts as a catabolic enzyme and accepts phenylpyruvate, pyruvate or *p*-hydroxyphenylpyruvate, but not *α*-ketoglutarate, as the amino acceptor (Kradolfer *et al.,* 1982; Urrestaraz *et al.,* 1998). A different aminotransferase may be involved in a reaction utilizing *α*-ketoglutarate (Kradolfer *et al.,* 1982; Urrestaraz *et al.,* 1998; Iraqui *et al.,* 1998). Also for *β*-phenylalanine an aminotransferase has been reported (Kim *et al.,* 2006). The product of this transaminase reaction, 3-oxo-3-phenylpropionic acid, is chemically unstable and decarboxylates, forming acetophenone (**Fig. 2.11**), which is detectable at 245 nm (Schatzle *et al.,* 2009). Qualitatively, acetophenone can be detected by reaction with 2,4-dinitrophenylhydrazine (2,4-DNPH) (Brady & Elsmie, 1926). This is a condensation reaction forming the respective hydrazone, which forms an orange-red precipitate.

By selective enrichment using *β*-phenylalanine as sole nitrogen source and *trans*-cinnamic acid as carbon source, four bacterial strains (CBF1-4) were isolated. On minimal medium agar plates CBF1, CBF2 and CBF4 grew very slowly with small white colonies colonies appearing after 7-10 days, whereas strain CBF3 showed lemon-yellow colonies and grew somewhat faster (3-4 days). All four *β*-phenylalanine degraders were capable of using glucose as carbon source, which gave faster growth than *trans*-cinnamic acid.

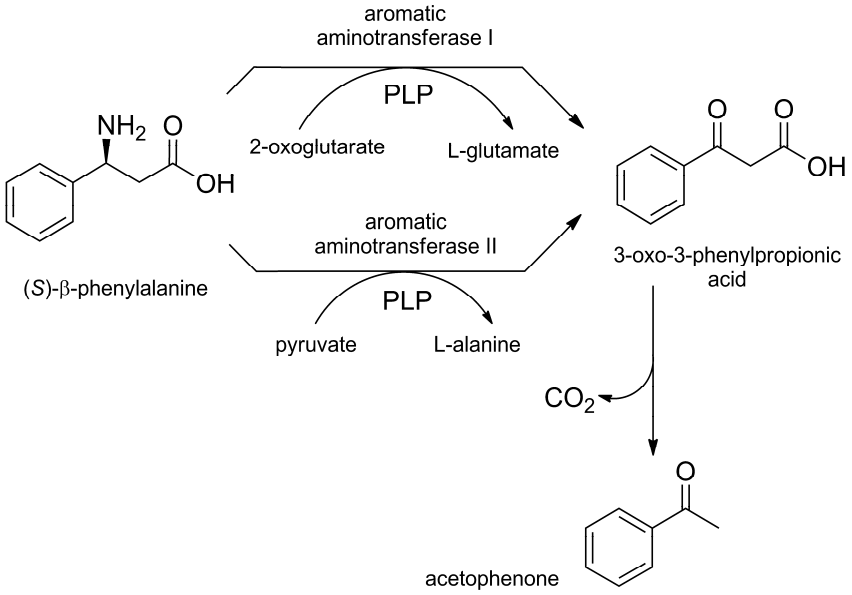

Figure 2.11 The degradation of *β*-phenylalanine by aminotransferases.

Therefore, cell-free extracts were prepared from cells that were aerobically grown on 1 mM *β*-phenylalanine and 20 mM glucose.

None of the enzyme activities (**Fig. 2.1**) were detected for any of the *β*-phenylalanine degraders, except for CBF2 and CBF3 where AT activity was observed in assays with whole cells. The partial 16S rRNA gene sequences of strains CBF2 and CBF3 were obtained. A BLAST search showed that strain CBF2 is a *Pseudomonas* sp. and CBF3 is a member of *Variovorax paradoxus*. With both strains, we detected by HPLC (OPA-method) the formation of the new amino acid, i.e. L-glutamate or L-alanine, depending on the amino acceptor used for the assay (*α*-ketoglutarate and pyruvate, respectively). Since strain CBF3 was a faster degrader than CBF2, we decided to continue with CBF3.

Partial purification of aminotransferase from strain CBF3

V. paradoxus strain CBF3 was grown for seven days at 28 °C using 1-2 mM *β*-phenylalanine and 20 mM glucose in 2 l minimal medium supplemented with vitamins and trace elements solution. The concentration of *β*-phenylalanine was followed by HPLC and the growth of strain CBF3 by OD_{600} measurements (**Fig. 2.12**). Small amounts of *β*-phenylalanine were gradually added up to 1-2 mM final concentration.

Inhibition of growth was observed if higher concentration of *β*-phenylalanine (5-10 mM) were present in the medium, possibly due to formation of acetophenone.

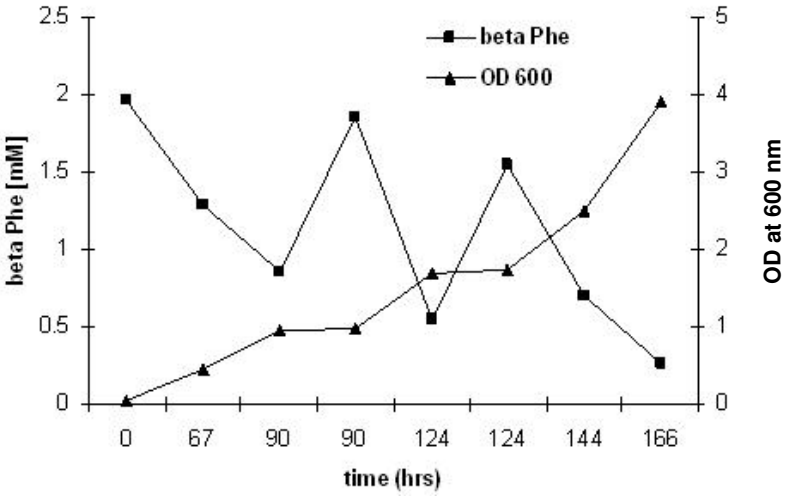

Figure 2.12 Growth of CBF3 in minimal medium using *β*-phenylalanine as nitrogen source. β-Phe was added several times.

The results of a partial purification by three chromatographic steps are summarized in **Table 2.4**. The amount of *Vp*AT recovered was quite low. SDS-PAGE gel gave no clearly dominant band that suggested enrichment of an aminotransferase. The final preparation still contained several different proteins. In addition, activity staining following a protocol described by Kim and coworkers (2007) with PLP and *rac*-*β*-phenylalanine, *α*-ketoglutarate, glutamate dehydrogenase, NAD+, phenazine methosulfate, and nitro blue tetrazolium as reagents did not give a band. As a consequence, it was not possible to obtain peptide sequence information that could support discovery of the gene coding for the transaminase.

In order to obtain the gene coding for *Vp*AT, we changed the strategy to a genetic approach. After preparation of a cosmid DNA library, followed by a sub-library, the gene encoding *Vp*AT was discovered by a screening assay based on acetophenone formation, which is produced by spontaneous decarboxylation of *β*-keto-3-phenyl propionic acid, the keto acid formed from *β*-phenylalanine. A biochemical characterization including a 3D structure determination of the recombinant *Vp*AT is described in **Chapter 3**.

Activity assays with chiral substrates showed that the enzyme is highly enantioselective toward (*S*)-*β*-phenylalanine. Another interesting result was that *Vp*AT accepts *α*-ketoglutarate and pyruvate as amino acceptors with similar reactivities. This is in line with the activity of a *β*-transaminase (*Mes*AT) from *Mesorhizobium* sp. strain LUK (Kim *et al.,* 2007). Mechanistic studies together with the crystal structure of *Mes*AT are described in **Chapter 4**.

Table 2.4 Partial purification of aminotransferase from *V. paradoxus* CBF3.

Step	Volume (ml)	Protein (mg/ml)	Total protein (mg)	Total activity (mU)	Specific activity (mU/mg)	Yield (%)
CFE	35	11.5	402	4709	11.7	100
Q-Sepharose	30	0.7	21	640	30.5	13.6
MonoQ	18	0.3	9.4	370	39.4	7.9
Superdex 200	0.5	5.2	2.6	344	132	7.3

Degradation of D-aspartic acid

D-aspartic acid occurs naturally as a building block in the biosynthesis of the peptidoglycan layer of the bacterial cell wall (Staudenbauer & Strominger, 1972) but it also acts as a neurotransmitter in animals (D'Aniello *et al.,* 2011). The two most common pathways (**Fig. 2.13**) by which the degradation of D-aspartic acid takes place are conversion to L-aspartic acid, catalyzed by a racemase (EC 5.1.1.13) (Rahmanian et *al.,* 1971), and oxidation to oxaloacetate by a specific oxidase (EC 1.4.3.1) (Yamamoto *et al.,* 2007). The D-aspartate oxidase is FAD-dependent, whereas aspartate racemase is a PLP-dependent enzyme (Yoshimura & Esak, 2003). Although D-aspartate oxidases have not been reported in bacteria, an easy test is to measure ammonia release after incubation of cells or cell-free extract with D-aspartate and FAD.

The aspartate racemase activity (**Fig. 2.13, reaction A**) can be tested directly by chiral HPLC following conversion of D-aspartate to L-aspartate or via a coupled assay with an aspartate ammonia lyase specific for L-aspartate. The latter assay includes detection of ammonia release and/or formation of fumarate by UV spectroscopy at 240 nm (**Fig. 2.13, reaction B**).

Three bacterial strains (CDD1-3) were obtained by enrichment using D-aspartic acid as sole nitrogen and carbon source. The type, color and consistency of the colonies of strains CDD2 and CDD3 were similar (light-yellow opaque). Furthermore, strains CDD2 and CDD3 could use as sole carbon source benzoate, ethanol and citrate.

In contrast, CDD1 had yellow-orange colonies and grew faster than CDD2 and CDD3 on minimal medium agar plates supplemented with D-aspartic acid but also in combination with sucrose as carbon source.

For preparation of cell-free extracts, cells of CDD1, CDD2 and CDD3 were grown under aerobic conditions on selective minimal medium supplemented with 10 mM D-aspartic acid. For all three D-aspartic acid degraders (CDD1-3), we found a slight ammonia release with L-aspartic acid and more abundant ammonia release with *β*-asparagine, as shown for strain CDD3 in **Fig. 2.14** and no ammonia release with D-aspartic acid as substrate.

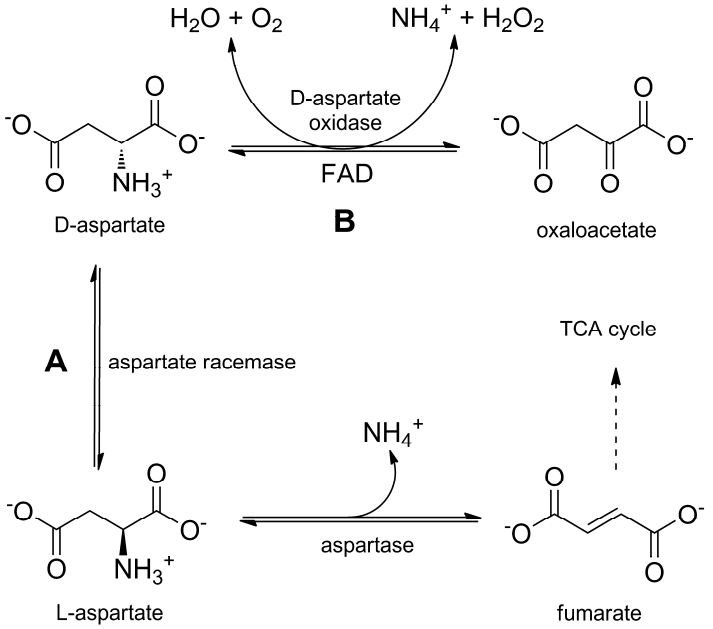

Figure 2.13 Deamination of D-aspartic acid by a racemase (**reaction A**) or by an oxidase (**reaction B**).

With L-aspartic acid and *β*-asparagine as substrates, ammonia release was not stimulated by addition of FAD or Mg^{2+}. Furthermore, when NAD^+ was added, no NADH formation was observed at 340 nm which would have indicated the presence of an amino acid dehydrogenase activity. The ammonia release with L-aspartic acid was not accompanied by the formation of fumarate, as no specific absorbance was observed by UV spectroscopy at 240 nm. Thus, an ammonia lyase seems also unlikely. We concluded that at least for *β*-asparagine ammonia release is more likely due to an amide hydrolase activity.

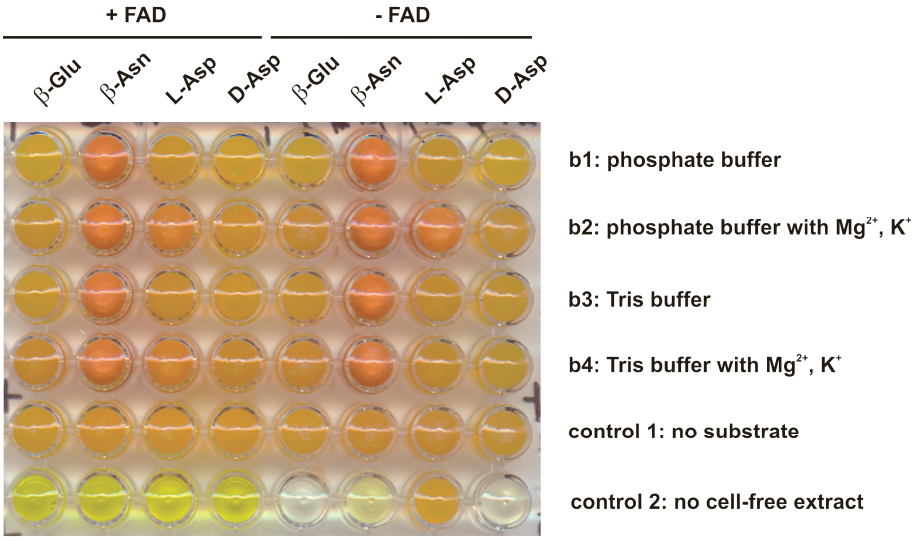

Figure 2.14 Ammonia detection by the Nessler reagent using CFE of strain CDD3 and D- and L-aspartic acid, *β*-asparagine, and *β*-glutamic acid as substrate. Four different buffer conditions were used, each with (+) and without (-) addition of 0.1 mM FAD.

The results do not indicate the presence of a D-aspartate ammonia lyase, and the mechanism of D-aspartate metabolism was not explored further.

Discussion

In this chapter, we report the isolation of various *β*-amino acid-degrading microorganisms and their partial characterization and tests for deamination activities. We isolated 18 microorganisms that are able to degrade *β*-alanine, *β*-glutamate, *β*-asparagine, *β*-leucine, *β*-phenylalanine, D-aspartic acid and/or *β*-tyrosine. For some *β*-amino acids such as *β*-amino butyric acid and cispentacin, it was not possible to obtain pure cultures since the fungi stayed closely associated with bacteria and were not removed by plate streaking. For cispentacin this is surprising because the compound is known to be an antifungal antibiotic (Konishi *et al.,* 1989). Nevertheless, the results demonstrated that classical enrichment cultivation is still a very useful tool for isolating new microorganisms with desired biotransformation properties. In this context, it should be noted that for several compounds enrichment cultivation appeared more successful than the use of environmental gene libraries. Previous work suggested that the use of enrichment cultures would be superseded by metagenomic

library construction and screening. This is based on the notion that the discovery of a specific catabolic activity by enrichment cultivation can be hindered by strict dependence of growth on other organisms (Kaeberlein *et al.,* 2002) or because organisms are (temporarily) in a non-culturable state. The latter may be due to exposure to salts, low temperature or prolonged starvation conditions (Oliver *et al.,* 1991; Roszak *et al.,* 1984).

In the metagenomic approach, DNA is isolated from environmental samples and randomly cloned in an expression vector, after which screening is carried out by functional assays. We subjected several of the libraries that were constructed earlier and successfully used for the discovery of amidases, acylases and other hydrolases (Gabor *et al.,* 2004) for the presence of clones that are capable of growth on *β*-amino acids as nitrogen source. For the same *β*-amino acids used for the enrichment experiments (e.g. *β*-glutamate, *β*-phenylalanine), we screened the libraries on minimal medium agar plates supplemented with various *β*-amino acids (1 mM) and glucose or citrate. In total, about 100,000 clones from each of the 5 different libraries constructed in the pZErO-2 expression vector (Invitrogen) were tested with *E. coli* as the host. However, not a single positive clone was observed. The most likely explanation is that genes encoding enzymes that metabolize *β*-amino acids are too rare to be recovered using non-enriched metagenomic libraries.

Another way to access new enzymes for biocatalytic applications is genome mining. Due to the enormous abundance of genome sequences present in public databases, it should be rather easy to find new biocatalysts based on annotated enzymes sequences. However, sequences are often wrongly annotated to have a particular function based on sequence comparison (Furnham *et al.,* 2009). Furthermore, completely new genes are not readily discovered by homology-based genome analysis. Another application of sequence analysis in biocatalysis is the use of alignments of proteins that are experimentally characterized in order to discover conserved regions or sequence motifs that are indicative of certain catalytic activities or selectivities. Based on sequence analysis and structural inspection, an example of a motif characteristic for aminotransferases that are active with *β*-amino acids is described in **Chapter 3**.

From the enzyme activities found in this study, the most interesting one is the aminotransferase of the *β*-phenylalanine-degrading microorganisms CBF2 and CBF3. Since strain CBF3 grows faster than CBF2, the aminotransferase of this organism was selected for further study. The aminotransferase from *V. paradoxus* strain CBF3 (*Vp*AT) is enantioselective for (*S*)-*β*-phenylalanine and can use both *α*-ketoglutarate and pyruvate as amino acceptors with no clear preference. This type of behavior has

also been reported for two homologous enzymes, (*Mes*AT) from *Mesorhizobium* sp. strain LUK (Kim *et al.,* 2007) and glutamate 2,1-semialdehyde aminomutase from *Polaromonas* sp. strain JS666 (Bea *et al.,* 2011). The applicability of aminotransferases in industrial processes has been already proven (Savile *et al.,* 2010). A toolbox of aminotransferases acting on *β*-amino acids would allow exploration of those enzymes for new processes in applied biocatalysis. It also enables mechanistic and structural studies.

Although we were mainly interested in aminotransferases and ammonia lyases converting *β*-amino acids, we found also other deamination activities, such as amide hydrolase. The strains that degrade *β*-asparagine- (CBN1-3) and D-aspartic acid (CDD1-3) likely contain such an activity. We did not investigate further the amide hydrolase activity. For all other *β*-amino acid-degrading organisms (e.g., *β*-alanine, *β*-glutamate and *β*-leucine) none of the well-known deamination reactions for α-amino acids (**Fig. 2.1**) tested gave a positive result when tested with *β*-amino acids.

Possibly aminomutases are involved in the metabolism of *β*-amino acids. It has been already reported that these enzymes have low activities (e.g., MIO enzymes in particular) and require a laborious purification procedure under anaerobic conditions since they are sensitive to oxidative conditions and often they need activation by reduction of the cofactors (Ruzicka & Frey, 2007; Chen *et al.,* 2000; Lieder *et al.,* 1998). The observation that in most cases activity detection in cell-free extracts was not straightforward suggests a role of labile enzymes, possibly dependent on unstable cofactors, or the involvement of multistep reactions. The latter is illustrated in **Chapter 5** for metabolism of *β*-valine.

Acknowledgements

This research was financially supported by the Dutch Ministry of Economic Affairs and B-Basic partner organizations, through B-Basic, a public-private research organization. The authors acknowledge prof. Jan Dirk van Elsas (Department of Microbial Ecology, University of Groningen, NL) for providing samples of grassland soil used for enrichment cultivation.

References

Aberhart, D.J., Lin, H.J. and Weiller, B.H. (1981) Stereochemistry of lysine 2,3-aminomutase. *J Am Chem Soc* 103: 6750–6752.

Baker, P.J., Sawa, Y., Shibata, H., Sedelnikova, S.E. and Rice, D.W. (1998) Analysis of the structure and substrate binding of *Phormidium lapideum* alanine dehydrogenase. *Nat Struct Biol* 5: 561–567.

Baker, P.J., Turnbull, A.P., Sedelnikova, S.E., Stillman, T.J. and Rice, DW. (1995) A role for quaternary structure in the substrate specificity of leucine dehydrogenase. *Structure* 3: 693–705.

Bauerle B., Cokesa, Z., Hofmann, S. and Rieger P.G. (2006) Sequencing and heterologous expression of an epimerase and two lyases from iminodisuccinate-degrading bacteria. *Appl Environ Microbiol* 72: 2824–2828.

Bea, H.S., Park, H.J., Lee, S.H., Yun, H. (2011) Kinetic resolution of aromatic beta-amino acids by omega-transaminase. *Chem Commun* 47: 5894–5896.

Behshad, E., Ruzicka, F.J., Mansoorabadi, S.O., Chen, D., Reed, G.H. and Frey, P.A. (2006) Enantiomeric free radicals and enzymatic control of stereochemistry in a radical mechanism: the case of lysine 2,3-aminomutases. *Biochemistry* 45: 12639–12646.

Berkovitch, F., Behshad, E., Tang, K.H., Enns, E.A., Frey, P.A. and Drennan, C.L. (2004) A locking mechanism preventing radical damage in the absence of substrate, as revealed by the x-ray structure of lysine 5,6-aminomutase. *Proc Natl Acad Sci* 101: 15870–15875.

Boyer, P.D., Lardy, H. and Myrback, K. (1963) (Eds.), The Enzymes, 2nd ed., vol. 7, Academic Press, New York: 609–648.

Bradford, M.M. (1976) A rapid and sensitive method for the quantitation of microgram quantities of protein utilizing the principle of protein-dye binding. *Anal Biochem* 72: 248–254.

Brady, O.L. and Elsmie, G.V. (1926) The use of 2:4-dinitrophenylhydrazine as a reagent for aldehydes and ketones. *Analyst* 51: 77–78.

Brunhuber, N.M.W. and Blanchard, J.S. (1994) The biochemistry and enzymology of amino acid dehydrogenases. *Crit Rev Biochem Mol Biol* 29: 415–467.

Chen, H.P., Wu, S.H., Lin, Y.L., Chen, C.M. and Tsay, S.S. (2001) Cloning, sequencing, heterologous expression, purification, and characterization of adenosylcobalamin-dependent D-ornithine aminomutase from *Clostridium sticklandii*. *J Biol Chem* 276: 44744–44750.

Chen, D., Ruzicka, F.J. and Frey, P.A. (2000) A novel lysine 2,3-aminomutase encoded by the yodO gene of *Bacillus subtilis*: characterization and the observation of organic radical intermediates. *Biochem J* 348: 539–549.

Christenson, S.D., Liu, W., Toney, M.D. and Shen, B. (2003) A novel 4-methylideneimidazole-5-one-containing tyrosine aminomutase in enediyne antitumor antibiotic C-1027 biosynthesis. *J Am Chem Soc* 125: 6062–6063.

Christianson, C.V., Montavon, T.J., Van Lanen, S.G., Shen, B. and Bruner, S.D. (2007) The structure of L-tyrosine 2,3-aminomutase from the C-1027 enediyne antitumor antibiotic biosynthetic pathway. *Biochemistry* 46: 7205–7214.

Cole, D.C. (1994) Recent stereoselective synthetic approaches to β-amino acids. *Tetrahedron* 50: 9517–9582.

Cooke, H.A., Christianson, C.V. and Bruner, S.D. (2009) Structure and chemistry of 4-methylideneimidazole-5-one containing enzymes. *Curr Opin Chem Biol* 13: 453–461.

D'Aniello. S., Somorjai, I., Garcia-Fernandez, J., Topo, E. and D'Aniello, A. (2011) D-Aspartic acid is a novel endogenous neurotransmitter. *FASEB J* 25: 1014–1027.

de Villiers, M., Puthan Veetil, V., Raj, H., de Villiers, J. and Poelarends, G.J. (2012) Catalytic mechanisms and biocatalytic applications of aspartate and methylaspartate ammonia lyases. *ACS Chem Biol* 7: 1618–1628.

Eliot, A.C. and Kirsch, J.F. (2004) Pyridoxal phosphate enzymes: mechanistic, structural, and evolutionary considerations. *Annu Rev Biochem* 73: 383–415.

Faust, A., Niefind, K., Hummel, W. and Schomburg, D. (2007) The structure of a bacterial L-amino acid oxidase from *Rhodococcus opacus* gives new evidence for the hydride mechanism for dehydrogenation. *J Mol Biol* 367: 234–248.

Fibriansah, G., Veetil, V.P., Poelarends, G.J. and Thunnissen, A.M. (2011) Structural basis for the catalytic mechanism of aspartate ammonia lyase. *Biochemistry* 50: 6053–6062.

Freer, I., Pedrocchi-Fantoni, G., Picken, D.J. and Overton, K.H. (1981) Stereochemistry of the leucine 2,3-aminomutase from tissue-cultures of *Andrographis paniculata*. *J Chem Soc Chem Commun* 3: 80–82.

Furnham, N., Garavelli, J.S., Apweiler, R. and Thornton, J.M. (2009) Missing in action: enzyme functional annotations in biological databases. *Nat Chem Biol* 5: 521–525.

Gabor, E.M, de Vries, E.J. and Janssen, D.B. (2004) Construction, characterization, and use of small-insert gene banks of DNA isolated from soil and enrichment cultures for the recovery of novel amidases. *Environ Microbiol* 6: 948–958.

Gerlt, J.A., Babbitt, P.C. and Rayment, I. (2005) Divergent evolution in the enolase superfamily: the interplay of mechanism and specificity. *Arch Biochem Biophys* 433: 59–70.

Geueke, B., Namoto, K., Seebach, D. and Kohler, H.P. (2005) A novel beta-peptidyl aminopeptidase (BapA) from strain 3-2W4 cleaves peptide bonds of synthetic beta-tri- and beta-dipeptides. *J Bacteriol* 187: 5910–5917.

Hayaishi, O., Nishizuka, Y., Tatibana, M., Takeshita, M. and Kuno, S. (1961) Enzymatic studies on the metabolism of beta-alanine. *J Biol Chem* 236: 781–790.

Hayashi, H., Mizuguchi, H., Miyahara, I., Islam, M.M., Ikushiro, H., Nakajima, Y., Hirotsu, K. and Kagamiyama, H. (2003) Strain and catalysis in aspartate aminotransferase. *Biochim Biophys Acta* 1647: 103–109.

Herrmann, G., Selmer, T., Jessen, H.J., Gokarn, R.R., Selifonova, O., Gort, S.J. and Buckel, W. (2005) Two beta-alanyl-CoA:ammonia lyases in *Clostridium propionicum*. *FEBS J* 272: 813–821.

Hudson, R.C. and Daniel, R.M. (1993) L-glutamate dehydrogenases: distribution, properties and mechanism. *Comp Biochem Physiol B* 106: 767–792.

Hummel, W. and Kula, M. (1989) Dehydrogenases for the synthesis of chiral compounds. *Eur J Biochem* 184: 1–13.

Hwang, B.Y., Cho, B.K., Yun, H., Koteshwar, K. and Kim, B.G. (2005) Revisit of aminotransferase in the genomic era and its application to biocatalysis. *J Mol Catal B-Enzym* 37: 47–55.

Iraqui, I., Vissers, S., Cartiaux, M. and Urrestarazu, A. (1998) Characterisation of *Saccharomyces cerevisiae* ARO8 and ARO9 genes encoding aromatic aminotransferases I and II reveals a new aminotransferase subfamily. *Mol Gen Genet* 257: 238–248.

Kaeberlein, T., Lewis, K. and Epstein, S.S. (2002) Isolating "uncultivable" microorganisms in pure culture in a simulated natural environment. *Science* 296: 1127–1131.

Kern, A.D., Oliveira, M.A., Coffino, P. and Hackert, M.L. (1999) Structure of mammalian ornithine decarboxylase at 1.6 A resolution: stereochemical implications of PLP-dependent amino acid decarboxylases. *Structure* 7: 567–581.

Kim, J., Kyung, D., Yun, H., Cho, B.K., Seo, J.H., Cha, M. and Kim, B.G. (2007) Cloning and characterization of a novel β-transaminase from *Mesorhizobium* sp. strain LUK: a new biocatalyst for the synthesis of enantiomerically pure *β*-amino acids. *Appl Environ Microbiol* 73: 1772–1782.

Kim, J., Kyung, D., Yun, H., Cho, B.K. and Kim, B.G. (2006) Screening and purification of a novel transaminase catalyzing the transamination of aryl beta-amino acid from *Mesorhizobium* sp. LUK. *J Microbiol Biotechnol* 16: 1832–1836.

Koeller, K.M. and Wong, C.H. (2001) Enzymes for chemical synthesis. *Nature* 409: 232–240.

Konishi, M., Nishio, M., Saitoh, K., Miyaki, T., Oki, T. and Kawaguchi, H. (1989) Cispentacin, a new antifungal antibiotic. Production, isolation, physico-chemical properties and structure. *J Antibiot* 42: 1749–1755.

Kradolfer, P., Niederberger, P. and Hutter, R. (1982) Tryptophan degradation in *Saccharomyces cerevisiae*: characterization of two aromatic aminotransferases. *Arch Microbiol* 133: 242–248.

Krix, G., Bommarius, A.S., Drauz, K., Kottenhahn, M., Schwarm, M. and Kula, M.R. (1997) Enzymatic reduction of keto acids leading to L-amino acids, D- or L-hydroxy acids. *J Biotech* 53: 29–39.

Krug, D. and Muller, R. (2009) Discovery of additional members of the tyrosine aminomutase enzyme family and the mutational analysis of CmdF. *ChemBiochem* 10: 741–750.

Lepore, B.W., Ruzicka, F.J., Frey, P.A. and Ringe, D. (2005) The x-ray crystal structure of lysine-2,3-aminomutase from *Clostridium subterminale*. *Proc Natl Acad Sci* 102: 13819–13824.

Levy, C.W., Buckley, P.A., Sedelnikova, S., Kato, Y., Asano, Y., Rice, D.W. and Baker, P.J. (2002) Insights into enzyme evolution revealed by the structure of methylaspartate ammonia lyase. *Structure* 10: 105–113.

Lieder, K.W., Booker, S., Ruzicka, F.J., Beinert, H., Reed, G.H. and Frey, P.A. (1998) S-Adenosylmethionine-dependent reduction of lysine 2,3-aminomutase and observation of the catalytically functional iron-sulfur centers by electron paramagnetic resonance. *Biochemistry* 37: 2578–2585.

Liljeblad, A. and Kanerva, L.T. (2006) Biocatalysis as a profound tool in the preparation of highly enantiopure β-amino acids. *Tetrahedron* 62: 5831–5854.

Lowe, P.N. and Rowe, A.F. (1985) Aspartate-2-oxoglutarate aminotransferase from *Trichomonas vaginalis* - identity of aspartate-aminotransferase and aromatic amino-acid aminotransferase. *Biochem J* 232: 689–695.

Mehta, P.K. and Christen P. (2000) The molecular evolution of pyridoxal-5'-phosphate-dependent enzymes. *Adv Enzymol Relat Areas Mol Biol* 74: 129–184.

Minambres, B., Olivera, E.R., Jensen, R.A. and Luengo, J.M. (2000) A new class of glutamate dehydrogenases (GDH). Biochemical and genetic characterization of the first member,

the AMP-requiring NAD-specific GDH of *Streptomyces clavuligerus*. *J Biol Chem* 275: 39529–39542.

Mizobata, T., Kawata, Y. (2007) Aspartases, in Industrial Enzymes - Structure, Functions and Applications (eds J. Polaina and A.P. MacCabe), Springer, Dordrecht, pp. 549 –565.

Mohammadi, H.S., Omidinia, E., Lotfi, A.S. and Saghiri, R. (2007) Preliminary report of NAD^+-dependent amino acid dehydrogenase producing bacteria isolated from soil. *Iran Biomed J* 11: 131–135.

Moustafa, I.M., Foster, S., Lyubimov, A.Y. and Vrielink, A. (2006) Crystal structure of LAAO from *Calloselasma rhodostoma* with an L-phenylalanine substrate: insights into structure and mechanism. *J Mol Biol* 364: 991–1002.

Neidhardt, F.C., Bloch, P.L. and Smith, D.F. (1974) Culture medium for enterobacteria. *J Bacteriol* 119: 736–747.

Norton, J.E. and Sokatch, J.R. (1970) Purification and partial characterization of the branched chain amino acid transaminase of *Pseudomonas aeruginosa*. *Biochim Biophys Acta* 206: 261–269.

Nuiry, I.I., Hermes, J.D., Weiss, P.M., Chen, C.Y. and Cook, P.F. (1984) Kinetic mechanism and location of rate-determining steps for aspartase from *Hafnia alvei*. *Biochemistry* 23: 5168–5175.

Ohshima, T. and Soda, K. (1990) Biochemistry and biotechnology of amino acid dehydrogenases. *Adv Biochem Eng Biotechnol* 42: 181-209.

Oliver, J.D., Nilsson, L. and Kjelleberg, S. (1991) Formation of non-culturable *Vibrio vulnificus* cells and its relationship to the starvation state. *Appl Environ Microbiol* 57: 2640–2644.

Pawelek, P.D., Cheah, J., Coulombe, R., Macheroux, P., Ghisla, S. and Vrielink, A. (2000) The structure of L-amino acid oxidase reveals the substrate trajectory into an enantiomerically conserved active site. *EMBO J* 19: 4204–4215.

Pedraza, R.O., Ramírez-Mata, A., Xiqui, M.L. and Baca, B.E. (2004) Aromatic amino acid aminotransferase activity and indole-3-acetic acid production by associative nitrogen-fixing bacteria. *FEMS Microbiol Lett* 233: 15–21.

Peterson, P.E. and Smith, T.J. (1999) The structure of bovine glutamate dehydrogenase provides insights into the mechanism of allostery. *Structure* 7: 769–782.

Poelarends, G.J., Wilkens, M., Larkin, M.J., van Elsas, J.D. and Janssen, D.B. (1998) Degradation of 1,3-dichloropropene by pseudomonas cichorii 170. *Appl Environ Microbiol* 64: 2931–2936.

Pollegioni, L., Piubelli, L., Sacchi, S., Pilone, M.S. and Molla, G. (2007) Physiological functions of D-amino acid oxidases: from yeast to humans. *Cell Mol Life Sci* 64: 1373–1394.

Poston, J.M. (1986) Beta-leucine and the beta-keto pathway of leucine metabolism. *Adv Enzymol Relat Areas Mol Biol* 58: 173–189.

Poston, J.M. (1980) Distribution of leucine 2,3-aminomutase activity in various organs of the rat and in subcellular organelles of rat liver. *Biochem Biophys Res Commun* 96: 838–843.

Poston, J.M. (1976) Leucine 2,3-aminomutase, an enzyme of leucine catabolism. *J Biol Chem* 251: 1859–1863.

Prabhakaran, P.C., Woo, N.T., Yorgey, P.S. and Gould, S.J. (1988) Biosynthesis of blasticidin S from L-α-arginine. Stereochemistry in the arginine-2,3-aminomutase reaction. *J Am Chem Soc* 110: 5785–5791.

Puthan Veetil, V., Fibriansah, G., Raj, H., Thunnissen, A.M. and Poelarends GJ (2012) Aspartase/fumarase superfamily: a common catalytic strategy involving general base-catalyzed formation of a highly stabilized aci-carboxylate intermediate. *Biochemistry* 51: 4237–43.

Rahmanian, M., Waller, G.R. and Smith, W.G. (1971) Biosynthesis of D-aspartic acid by *Streptococcus faecalis*. *J Biol Chem* 246: 823–830.

Raj, H., Puthan Veetil, V., Szymanski, W., Dekker, F.J., Quax, W.J., Feringa, B.L., Janssen, D.B. and Poelarends, G.J. (2012) Characterization of a thermostable methylaspartate ammonialyase from *Carboxydothermus hydrogenoformans*. *Appl Microbiol Biotechnol* 94: 385–397.

Rice, D.W., Baker, P.J., Farrants, G.W. and Hornby, D.P. (1987) The crystal structure of glutamate dehydrogenase from *Clostridium symbiosum* at 0.6 nm resolution. *Biochem J* 242: 789–795.

Robertson, D.E., Roberts, M.F., Belay, N., Stetter, K.O. and Boone, D.R. (1990) Occurrence of β-glutamate, a novel osmolyte, in marine methanogenic bacteria. *Appl Environ Microbiol* 56: 1504–1508.

Roszak, D.B., Grimes, D.J. and Colwell, R.R. (1984) Viable but non-recoverable stage of *Salmonella enteritidis* in aquatic systems. *Can J Microbiol* 30: 334–338.

Rudat, J., Brucher, B.R. and Syldatk, C. (2012) Transaminases for the synthesis of enantiopure beta-amino acids. *AMB Express* 2: 11.

Ruzicka, F.J. and Frey, P.A. (2007) Glutamate 2,3-aminomutase: a new member of the radical SAM superfamily of enzymes. *Biochim Biophys Acta* 1774: 286–296.

Sanwal, B.D. and Zink, M.W. (1961) L-Leucine dehydrogenase of *Bacillus cereus*. *Arch Biochem Biophys* 94: 430–435.

Savile, C.K., Janey J.M., Mundorff, E.C., Moore, J.C., Sarena, Tam, S., Jarvis, W.R., Colbeck, J.C., Krebber, A., Fleitz, F.J., Brands, J., Devine, P.N., Huisman, G.W. and Hughes, G.J. (2010) Biocatalytic Asymmetric Synthesis of Chiral Amines from Ketones Applied to Sitagliptin Manufacture. *Science* 329: 305–309.

Sawa, Y., Tani, M., Murata, K., Shibata, H. and Ochiai, H. (1994) Purification and characterization of alanine dehydrogenase from a cyanobacterium, *Phormidium lapideum*. *J Biochem* 116: 995–1000.

Schatzle, S., Hohne, M., Redestad, E., Robins, K. and Bornscheuer, U.T. (2009) Rapid and sensitive kinetic assay for characterization of omega-transaminases. *Anal Chem* 81: 8244–8248.

Schroder, I., Vadas, A., Johnson, E., Lim, S. and Monbouquette, H.G. (2004) A novel archaeal alanine dehydrogenase homologous to ornithine cyclodeaminase and mu-crystallin. *J Bacteriol* 186: 7680–7689.

Schwede, T.F., Retey, J. and Schulz, G.E. (1999) Crystal structure of histidine ammonia-lyase revealing a novel polypeptide modification as the catalytic electrophile. *Biochemistry* 38: 5355–5361.

Seebach, D., Beck, A. and Bierbaum, D. (2004) The world of beta- and gamma-peptides comprised of homologated proteinogenic amino acids and other components. *Chem & Biodiv* 1: 1111–1239.

Seebach, D., Abele, S., Gademann, K., Guichard, G., Hintermann, T., Jaun, B., Matthews, J.L. and Schreiber, J.V. (1998) β^2- and β^3-peptides with proteinaceous side chains: synthesis and solution structures of constitutional isomers, a novel helical secondary structure and the influence of solvation and hydrophobic interactions on folding. *Helv Chim Acta* 81: 932–982.

Seebach, D., Overhand, M., Kühnle, F.N.M., Martinoni, B., Oberer, L., Hommel, U. and Widmer, H. (1996) β-Peptides: synthesis by Arndt-Eistert homologation with concomitant peptide coupling. Structure determination by NMR and CD spectroscopy and by X-ray crystallography. Helical secondary structure of a β-hexapeptide in solution and its stability towards pepsin. *Helv Chim Acta* 76: 913–941.

Shi, W., Dunbar, J., Jayasekera, M.M., Viola, R.E. and Farber, G.K. (1997) The structure of L-aspartate ammonia-lyase from *Escherichia coli*. *Biochemistry* 36: 9136–9144.

Shin, J.S., Yun, H., Jang, J.W., Park, I. and Kim, B.G. (2003) Purification, characterization, and molecular cloning of a novel amine: pyruvate transaminase from *Vibrio fluvialis* JS17. *Appl Microbiol Biotechnol* 61: 463–471.

Shin, J.S. and Kim, B.G. (2001) Comparison of the ω-transaminases from different microorganisms and application to production of chiral amines. *Biosci Biotechnol Biochem* 65: 1782–1788.

Staudenbauer, W. and Strominger, J.L. (1972) Activation of D-aspartic acid for incorporation into peptidoglycan. *J Biol Chem* 247: 5095–5102.

Steele, C.L., Chen, Y., Dougherty, B.A., Li, W., Hofstead, S., Lam, K.S., Xing, Z. and Chiang, S.J. (2005) Purification, cloning, and functional expression of phenylalanine aminomutase: the first committed step in taxol side-chain biosynthesis. *Arch Biochem Biophys* 438: 1–10.

Steer, D.L., Lew, R.A., Perlmutter, P., Smith, A.I. and Aguilar, M.I. (2002) Beta-amino acids: versatile peptidomimetics. *Curr Med Chem* 9: 811–822.

Stinson, R.A. and Spencer, M.S. (1969) Beta alanine aminotransferase(s) from a plant source. *Biochem Biophys Res Commun* 34: 120–127.

Sugio, S., Petsko, G.A., Manning, J.M., Soda, K. and Ringe, D. (1995) Crystal structure of a D-amino acid aminotransferase: how the protein controls stereoselectivity. Biochemistry 34: 9661–9669.

Sung, M.H., Tanizawa, K., Tanaka, H., Kuramitsu, S., Kagamiyama, H. and Soda, K. (1990) Purification and characterization of thermostable aspartate aminotransferase from a thermophilic *Bacillus* species. *J Bacteriol* 172: 1345–1351.

Tang, K.H., Casarez, A.D., Wu, W. and Frey, P.A. (2003) Kinetic and biochemical analysis of the mechanism of action of lysine 5,6-aminomutase. *Arch Biochem Biophys* 418: 49–54.

Urrestarazu, A., Vissers, S., Iraqui, I. and Grenson, M. (1998) Phenylalanine- and tyrosine-auxotrophic mutants of *Saccharomyces cerevisiae* impaired in transamination. *Mol Gen Genet* 257: 230–237.

Vancura, A., Vancurova, I., Volc, J., Jones, S.K., Flieger, M., Basarova, G. and Behal, V. (1989) Alanine dehydrogenase from *Streptomyces fradiae*. Purification and properties. *Eur J Biochem* 179: 221–227.

Vancurova, I., Vancura, A., Volc, J., Neuzil, J., Flieger, M., Basarova, G. and Behal, V. (1988) Purification and partial characterization of alanine dehydrogenase from *Streptomyces aureofaciens*. *Arch Microbiol* 150: 438–440.

Vuralhan, Z., Morais, M.A., Tai, S.L., Piper, M.D. and Pronk, J.T. (2003) Identification and characterization of phenylpyruvate decarboxylase genes in *Saccharomyces cerevisiae*. *Appl Environ Microbiol* 69: 4534–4541.

Walker, K.D., Klettke, K., Akiyama, T. and Croteau, R. (2004) Cloning, heterologous expression, and characterization of a phenylalanine aminomutase involved in taxol biosynthesis. *J Biol Chem* 279: 53947–53954.

Wang, K., Hou, Q. and Liu, Y. (2013) Insight into the mechanism of aminomutase reaction: A case study of phenylalanine aminomutase by computational approach. *J Mol Graphics Modell* 46: 65–73.

Wang, L.J., Li, C.X., Ni, Y., Zhang, J., Liu, X. and Xu, J.H. (2011) Highly efficient synthesis of chiral alcohols with a novel NADH-dependent reductase from *Streptomyces coelicolor*. *Bioresour Technol* 102: 7023–7028.

Ward, N.E., Jones, J. and Maurice, D.V. (1988) Essential role of adenosylcobalamin in leucine synthesis from beta-leucine in the domestic chicken. *J Nutr* 118: 159–164.

Weiner, B., Szymanski, W., Janssen, D.B., Minnaard A.J. and Feringa, B.L. (2010) Recent advances in the catalytic asymmetric synthesis of β-amino acids. *Chem Soc Rev* 39: 1656–1691.

Wolthers, K.R., Levy, C., Scrutton, N.S. and Leys, D. (2010) Large-scale domain dynamics and adenosylcobalamin reorientation orchestrate radical catalysis in ornithine 4,5-aminomutase. *J Biol Chem* 285: 13942–13950.

Wu, B., Szymanski, W., Wybenga, G.G., Heberling, M.M., Bartsch, S., de Wildeman, S., Poelarends, G.J., Feringa, B.L., Dijkstra, B.W. and Janssen, D.B. (2012) Mechanism-inspired engineering of phenylalanine aminomutase for enhanced β-regioselective asymmetric amination of cinnamates. *Angew Chem Int Ed Engl* 51: 482–486.

Wu, B., Szymanski, W., Crismaru, C.G, Feringa, B.L. and Janssen, D.B. (2012) C-N lyases catalyzing addition of ammonia, amines and amides to C=C and C=O bonds, p. 749–778. *In* Drauz K, Groger H, May O (ed), Enzyme catalysis in organic synthesis. Wiley-VCH, New York, NY.

Wu, B., Szymanski, W., Wietzes, P., de Wildeman, S., Poelarends, G.J., Feringa, B.L. and Janssen, D.B. (2009) Enzymatic synthesis of enantiopure alpha- and beta-amino acids by phenylalanine aminomutase-catalysed amination of cinnamic acid derivatives. *ChemBiochem* 10: 338–344.

Yamamoto, A., Tanaka, H., Ishida, T. and Horiike, K. (2007) Functional and structural characterization of D-aspartate oxidase from porcine kidney: non-Michaelis kinetics due to substrate activation. *J Biochem* 141: 363–376.

Yin, X., O'Hare, T., Gould, S.J. and Zabriskie, T.M. (2003) Identification and cloning of genes encoding viomycin biosynthesis from *Streptomyces vinaceus* and evidence for involvement of a rare oxygenase. *Gene* 312: 215–224.

Yoshimura, T. and Esak, N. (2003) Amino acid racemases: functions and mechanisms. *J Biosci Bioeng* 96: 103–109.

Yun, H., Lim, S., Cho B.K. and Kim, B.G. (2004) ω-Amino acid: pyruvate transaminase from *Alcaligenes denitrificans* Y2k-2: a new catalyst for kinetic resolution of β-amino acids and amines. *Appl Environ Microbiol* 70: 2529–2534.

Chapter 3

Biochemical properties and crystal structure of a *β*-phenylalanine aminotransferase from *Variovorax paradoxus*

Ciprian G. Crismaru,[a,#] Gjalt G. Wybenga,[b,#] Wiktor Szymanski,[c] Hein J. Wijma,[a] Bian Wu,[a] Sebastian Bartsch,[a] Stefaan de Wildeman,[d] Gerrit J. Poelarends,[e] Ben L. Feringa,[c] Bauke W. Dijkstra [b] and Dick B. Janssen [a]

[a]*Department of Biochemistry, Groningen Biomolecular Sciences and Biotechnology Institute, University of Groningen*

[b]*Laboratory of Biophysical Chemistry, Groningen Biomolecular Science and Biotechnology Institute, University of Groningen*

[c]*Center for Systems Chemistry, Stratingh Institute for Chemistry, University of Groningen*

[d]*DSM Pharmaceutical Products, Geleen, The Netherlands*

[e]*Department of Pharmaceutical Biology, Groningen Research Institute of Pharmacy, University of Groningen*

[#] These two authors contributed equally to this study.

Published in *Applied and Environmental Microbiology* (2013) 79: 185–195.

Abstract

By selective enrichment we isolated a bacterium that can use *β*-phenylalanine as sole nitrogen source. It was identified by 16S rRNA gene sequencing as a strain of *Variovorax paradoxus*. Enzyme assays revealed an aminotransferase activity. Partial genome sequencing and screening of a cosmid DNA library resulted in the identification of a 1,302 bp aminotransferase gene, which encodes a 46,416 Da protein. The gene was cloned and overexpressed in *Escherichia coli*. The recombinant enzyme was purified and showed a specific activity of 17.5 U mg^{-1} for (*S*)-*β*-phenylalanine at 30 °C and 33 U mg^{-1} at the optimum temperature of 55 °C. The *β*-specific aminotransferase exhibits a broad substrate range, accepting *ortho*-, *meta*- and *para*-substituted *β*-phenylalanine derivatives as amino donors and 2-oxoglutarate and pyruvate as amino acceptors. The enzyme is highly enantioselective towards (*S*)-*β*-phenylalanine (E>100) and derivatives thereof with different substituents on the phenyl-ring, allowing the kinetic resolution of various racemic *β*-amino acids to yield (*R*)-*β*-amino acids with >95% *ee*. The crystal structures of the holo-enzyme and of the enzyme in complex with the inhibitor 2-aminooxyacetate revealed structural similarity to the *β*-phenylalanine aminotransferase from *Mesorhizobium* sp. LUK. The crystal structure was used to rationalize the stereo- and regioselectivity of *V. paradoxus* aminotransferase and to define a sequence motif with which new aromatic *β*-amino acid converting aminotransferases may be identified.

Introduction

Various non-proteinogenic *β*-amino acids occur naturally as free metabolites and as components of biosynthetic products (Seebach *et al.,* 2004). The simplest *β*-amino acid, *β*-alanine, occurs in carnosine, coenzyme A and pantothenic acid. Other *β*-amino acids are present in bioactive peptides, such as the protease inhibitor bestatin, which contains a (2*S*,3*R*)-3-amino-2-hydroxy-4-phenylbutanoyl group, and microcystin, a cyclic non-ribosomal peptide that acts as a phosphatase inhibitor and contains both an aliphatic and an aromatic *β*-amino acid moiety (Burley *et al.,* 1991; Geueke *et al.,* 2007; Juaristi *et al.,* 2005). Further examples are cryptophycins, which are anti-tumor agents containing an *α*-methyl-*β*-alanine group (Shih *et al.,* 1999) and taxol, an anti-tumor agent from *Taxus brevifolia* that contains a (2*R*,3*S*)-*N*-benzoyl-3-phenylisoserine group that is derived from (*R*)-*β*-phenylalanine (Mekhail *et al.,* 2002). Other *β*-amino acids occur as building blocks in β-lactam antibiotics (Juaristi *et al.,* 2005; Ojima *et al.,* 1999) and in antifungal compounds such as jasplakinolide (Crews *et al.,* 1986). In view of the growing importance of pharmaceutical compounds containing *β*-amino acid groups, there is demand for new tools for their production in enantiopure form. Chemical and biochemical reactions yielding enantiopure *β*-amino acids have recently been reviewed (Weiner *et al.,* 2010). However, the possibilities for biocatalytic processes are scarce and most existing options rely on kinetic resolution of racemates instead of the more attractive asymmetric conversions (Liljeblad *et al.,* 2006; Rehdorf *et al.,* 2010).

Microorganisms that can synthesize or degrade specific organic compounds are a rich source of enzymes for application in biocatalytic processes. However, the microbial metabolism of *β*-amino acids has been poorly investigated. Some information is available about the formation of aliphatic *β*-amino acids such as *β*-lysine, *β*-leucine or *β*-glutamate, which can be formed from α-amino acids by catabolic bacterial aminomutases and are subject to deamination by aminotransferases or ammonia lyases (Chirpich *et al.,* 1970; Ruzicka *et al.,* 2007; Wu *et al.,* 2011). The formation of *β*-alanine in *E. coli* proceeds by decarboxylation of aspartate (Cronan *et al.,* 1980). Aromatic *β*-amino acids that occur in secondary metabolite biosynthesis can be formed from proteinogenic *α*-amino acids by MIO (4-methylideneimidazole-5-one)-dependent aminomutases that have a biosynthetic function. The uncommon MIO cofactor also plays a key role in catabolic ammonia lyases that act upon *α*-histidine, *α*-phenylalanine and *α*-tyrosine (Christianson *et al.,* 2007).

Attractive enzymes for asymmetric synthesis are aminotransferases (ATs). These are pyridoxal 5′-phosphate (PLP)-dependent enzymes that transfer amino

groups between different metabolites and are ubiquitously present in prokaryotic and eukaryotic cells (Christen *et al.,* 1985; Stirling *et al.,* 1992). There is evidence for a role of aminotransferases (also known as transaminases) in the biodegradation of *β*-amino acids by microorganisms. For example, a study on a *β*-phenylalanine-utilizing strain of *Mesorhizobium* led to the discovery of a transaminase that converts *β*-phenylalanine into 3-oxo-3-phenylpropionic acid (Kim *et al.,* 2006; Shin *et al.,* 2001; Yun *et al.,* 2004).

Based on the latest update of the B6 database that compiles information on PLP-dependent enzymes, seven fold types can be distinguished (Percudani *et al.,* 2009). The ATs occur in fold type I and IV. Typical examples of fold type I ATs are aspartate AT, aromatic AT and ω-ATs (Finn *et al.,* 2010). According to a broader classification introduced in the 1980s, based on the reaction that is catalyzed, ATs are divided in two subgroups: (I) α-ATs, which catalyze transamination of amino groups at the α-carbon, and (II) ω-ATs, which perform transamination at a *β*-, *γ*-, or another more distal amino group of the substrate (Yonaha *et al.,* 1983). According to this older non-phylogenetic classification, all ATs that convert *β*-amino acids are confusingly considered to be ω-ATs. Enzymes from subgroup II include β-alanine AT, 4-aminobutyrate AT, ornithine AT, acetylornithine AT and 7,8-diaminopelargonic acid AT (Christen *et al.,* 2001; Mehta *et al.,* 1993), as well as a *β*-transaminase from *Mesorhizobium* sp. strain LUK (*Mes*AT) (Kim *et al.,* 2007).

Application of ATs in biocatalysis has mainly been investigated for the production of proteinogenic amino acids, unnatural amino acids, and various other amines and amino alcohols (Hwang *et al.,* 2005; Koszelewski *et al.,* 2008; Koszelewski *et al.,* 2010; Rozzell *et al.,* 1985; Stewart *et al.,* 2001; Taylor *et al.,* 1998; Wu *et al.,* 2010). The catalytic activities can be quite high (apparent k_{cat} values up to 50 s^{-1}) (Nowicki *et al.,* 2001), and apart from PLP, which is sometimes added, there is no requirement for an external cofactor. Aminotransferases that catalyze synthesis or conversion of *β*-amino acids could be attractive for biocatalysis if they are enantioselective (Rudat *et al.,* 2012), stable, and exhibit a wide substrate scope. Here, we describe the gene cloning, the biochemical properties and the 3D structure of *Vp*AT, an aromatic *β*-amino acid aminotransferase discovered in a strain of *Variovorax paradoxus* isolated from soil. Based on the crystal structure, we offer a rationale for the regio- and stereoselectivity of *β*-transaminases and identify a signature sequence motif that allows the discovery of new aromatic *β*-amino acid-converting aminotransferases.

Materials and methods

Chemicals

Pyridoxal-5′-phosphate (PLP) and *rac*-3-amino-3-phenylpropionic acid (*β*-phenylalanine) were purchased from Acros Organics, 2-oxoglutarate (*α*-ketoglutarate) disodium salt and Brij 35 were purchased from Fluka. *Ortho*-phthalaldehyde (OPA), dimethyl sulfoxide (DMSO), *trans*-cinnamic acid, sodium pyruvate, *rac*-*β*-leucine, and 2-aminooxyacetic acid (AOA) were purchased from Sigma-Aldrich. (*S*)-*β*-phenylalanine and (*R*)-*β*-phenylalanine were purchased from PepTech Corp. Racemic and enantiomerically pure *ortho*-, *meta*-, and *para*-substituted *β*-phenylalanines and *α*-phenylalanines were either purchased from PepTech Corp. or synthesized according to published procedures (Szymanski *et al.,* 2009). Other chemicals were purchased as follows: (*R*)-3-amino-butyric acid (Chemcube), (*R*)-3-amino-5-methyl-hexanoic acid (Fluorochem), *β*-asparagine (Bachem), and *rac*-3-amino-3-(4-hydroxyphenyl)-propionic acid (*β*-tyrosine) (Innochemie GmbH).

Enrichment of a *β*-phenylalanine-degrading microorganism

Samples of grassland soil (1-2 g) were used as a source of microorganisms. Minimal medium of pH 7.0 contained per liter 5.3 g $Na_2HPO_4 \cdot 12H_2O$, 1.4 g KH_2PO_4, 0.2 g $MgSO_4 \cdot 7H_2O$, 1.0 g $(NH_4)_2SO_4$, 1 ml vitamin solution (Janssen *et al.,* 1984) and 5 ml trace element solution (Gabor *et al.,* 2004). In nitrogen-free minimal medium, $(NH_4)_2SO_4$ was replaced by Na_2SO_4 and $Ca(NO_3)_2 \cdot 4H_2O$ was omitted from the trace element solution. Stock solutions of carbon source (cinnamic acid, glucose) and nitrogen source (*rac*-*β*-phenylalanine) were prepared in 50 mM sodium phosphate buffer (pH 7.5). Inoculated flasks containing 50 ml minimal medium supplemented with 5 mM cinnamic acid and 1 mM *rac*-*β*-phenylalanine were incubated in the dark at 20 °C without shaking. After 2-3 transfers, pure cultures were isolated on minimal medium agar plates supplemented with *β*-phenylalanine as sole nitrogen source and cinnamic acid as carbon source. A fast-growing strain, named CBF3, was chosen for further study.

Bacterial strains, plasmids

E. coli strains VCS257, DH5α, MC1061 and C41(DE3) were used as hosts for the construction of a cosmid library, a sublibrary, for proliferation of cloned genes, and for overexpression of protein, respectively. Plasmids pLAFR3, pZErO-2 (Invitrogen) and pET28b+ (Novagen) were used for DNA libraries, subcloning and overexpression, respectively.

Preparation of cell-free extracts

For obtaining a high yield of cells expressing aminotransferase, strain CBF3 was grown on glucose (10 mM) with *rac*-*β*-Phe (2 mM) as nitrogen source. From a 1 liter culture, about 1 g of wet cells was obtained. Cells were washed with 50 mM Tris-SO_4 buffer (pH 8.0) and then suspended in 3 ml of this buffer containing 0.01% (vol/vol) β-mercaptoethanol. Sonication was performed with a Sonic Wibra cell, followed by centrifugation at 15,000 rpm and 4 °C for 1 h. The supernatants were used as cell-free extracts (CFEs).

Enzyme assays and amino acid analysis

To test the enzyme activity, an aminotransferase (AT) assay cocktail was prepared, consisting of 10 mM *rac*-*β*-phenylalanine, 5 mM 2-oxoglutarate (or pyruvate) and 50 µM PLP in 50 mM MOPS, pH 7.6. Reactions were started by addition of purified enzyme or CFE and incubated at 30 °C. The conversion was monitored by taking samples at different times. To 50 µl sample, 50 µl 2 M HCl was added to quench the reaction, and the mixture was kept on ice for 5 min. Then, 45 µl 2 M NaOH was added to neutralize the pH and 50 µl of water for dilution. Immediately prior to injection, 1 µl of sample was mixed with 2 µl *ortho*-phthalaldehyde (OPA) solution and 5 µl of 0.4 M $NaBO_3$, pH 10.4, in an HPLC autosampler (Hill *et al.,* 1979). The OPA solution was prepared by first dissolving 15 mg OPA in 50 µl absolute ethanol, which then was added to a mixture of 4.42 ml of 0.4 M $NaBO_3$, pH 10.4, 15 µl of 30% (wt/vol) Brij 35 and 11 µl of β-mercaptoethanol.

Quantification of glutamate, alanine and *β*-phenylalanine was performed with a C18 OPA Adsorbosphere column connected to a Jasco HPLC system after pre-derivatization with OPA. Elution was done with 20 mM sodium acetate, pH 5.5, containing 5% (vol/vol) tetrahydrofuran (THF) as eluent A and acetonitrile as eluent B, with a flow rate of 1 ml/min. Eluent A and eluent B were used with a gradient program as follows: 0-5 min, 100:0; 5-12 min, from 100:0 to 80:20; 12-16 min 80:20; 16-24 min from 80:20 to 40:60; 24-28 min 40:60; from 28-30 min 40:60 to 100:0; from 30-35 min re-equilibration at 100:0. Detection was done with a fluorescence detector, using excitation at 350 nm and measuring emission at 450 nm. Retention times for derivatized L-α-glutamate, L-α-alanine and *β*-phenylalanine were 2.3 min, 7.7 min and 23.2 min, respectively. One unit is defined as the amount of enzyme that catalyzes the formation of one µmol of L-α-glutamate min^{-1} at concentrations of 10 mM *rac*-*β*-phenylalanine and 5 mM 2-oxoglutarate. Protein concentrations were determined with Coomassie brilliant blue.

To determine the pH optimum of *Vp*AT, Britton-Robinson buffer was used with a pH range from pH 2 to pH 12. The buffer consists of a mixture of 0.04 M H_3BO_3,

0.04 M H_3PO_4 and 0.04 M CH_3COOH that is titrated to the desired pH with 0.2 M NaOH. A sufficient amount of enzyme was added and its activity was assayed using *rac-β*-phenylalanine (10 mM) as the amino donor and 2-oxoglutarate (5 mM) as the amino acceptor. The initial reaction rates were plotted against pH.

The optimum temperature was determined by measuring the specific activity of *Vp*AT in MOPS buffer (50 mM, pH 7.6) at temperatures between 20 °C and 65 °C. Enzyme was added and activity was assayed with *rac-β*-phenylalanine (10 mM) as the amino donor and 2-oxoglutarate (5 mM) as the amino acceptor.

For following the kinetic resolution of *rac-β*-phenylalanines with *Vp*AT, separation of enantiomers was performed using a Crownpak CR(+)HPLC column connected to a UV detector (210 nm), as described elsewhere (Szymanski *et al.,* 2009). Because of the low solubility of the racemates, they were tested in 50 mM MOPS (pH 7.6) at a concentration of 3 mM, using 5 mM 2-oxoglutarate and 50 μM PLP, at 30 °C.

Cloning and sequence analysis

All chemicals used in DNA manipulation procedures were purchased from Roche Diagnostics (Mannheim, Germany) and Qiagen NV (Venlo, The Netherlands) and used as recommended by the manufacturer.

The 16S rRNA gene of strain CBF3 was sequenced after PCR amplification. For amplification, two universal primers of the 16S rRNA gene were used, namely 27F as the forward primer (5′–AGAGTTTGATCMTGGCTCAG–3′) and 1492R as the reverse primer (5′–GGYTACCTTGTTACGACTT–3′) and genomic DNA as the template (Woese *et al.,* 1987). The PCR product was sequenced by GATC Biotech AG (Konstanz, Germany).

Genomic DNA was isolated from bacterial cells as described elsewhere (Poelarends *et al.,* 1998), and subjected to paired-end sequencing by Baseclear BV (Leiden, The Netherlands), using an Illumina GA*IIx* platform to obtain about 50 bp reads as raw data. The DNA reads were assembled into contigs using CLC Genomics Workbench software (CLC Bio).

For library construction, chromosomal DNA was partially digested with Sau3A, resulting in DNA fragments of 15 kb to 40 kb, which were cloned in BamHI-digested and dephosphorylated cosmid vector pLAFR3 (Sambrook *et al.,* 2001; Staskawicz *et al.,* 1987). Ligated DNA was packaged *in vitro* and transfected to *E. coli* VCS257 according to the recommendations supplied with the kit (Stratagene). Recombinant clones were stored as glycerol stocks at -20 °C. Transformants were grown in 96-well microtiter plates (MTPs) containing 1 ml of LB medium and tetracycline (25 μg/ml) at 30 °C and 900 rpm. After 24 h, *rac-β*-phenylalanine was

added to a final concentration of 7.5-10 mM to each well of the MTP. Screening for AT activity was performed by testing for the formation of acetophenone, which is formed by spontaneous decarboxylation of the expected transaminase product 3-oxo-3-phenylpropionic acid. The assay is based on the reaction of acetophenone with 2,4-dinitrophenylhydrazine (DNPH), forming a hydrazone that appears as an orange-red precipitate (Brady, 1926). For screening, MTPs were covered with a paper filter impregnated with a DNPH solution and incubated for 2 days at 30 °C and 900 rpm.

For subcloning, the vector pZErO-2 and the pLAFR3 positive clone were digested with EcoRI, and fragments were ligated. DNA was transformed to *E. coli* DH5α ElectroMAX cells (Invitrogen) and screening was performed as described for the pLAFR3 cosmid library. A 5 kb insert containing the CBF3 *Vp*AT-encoding gene was isolated and sequenced by primer walking (GATC Biotech AG, Konstanz, Germany). Sequence comparisons were performed with Clustal Ω (Sievers *et al.,* 2011) and Geneious Pro software version 5.5 (Drummond *et al.,* 2010).

For amplification of the entire *Vp*AT gene, two primers were designed, a forward primer (5′-GCGCG<u>CAT</u>**ATG**ACCCATGCCGCCATAG–3′) (NdeI site underlined, start codon in bold) and a reverse primer (5′–CGCGCG<u>CTCGAG</u>**TTA**GTTCG-CGCGGGGCAGC–3′) (XhoI site underlined, stop codon in bold). The 1.3 kb PCR product was cloned using the NdeI and XhoI sites of the pET28b+ plasmid. The *Mes*AT triple mutant I56V/A312S/M414F was expressed and purified as previously reported for *Mes*AT WT (Wybenga & Crismaru *et al.,* 2012).

The *Vp*AT R41A mutant was prepared by site-directed mutagenesis (QuikChange, Stratagene). The R41A forward primer (5′–GGAGCCAACAGC**GCC**TCCGTGCTGTTC–3′) and R41A reverse primer (5′–GAACAGCACGGA**GGC**GCTGTTGGCTCC–3′) (mutated codons in bold) were used according to the manufacturer's recommendations. All constructs were confirmed by sequencing (GATC Biotech AG, Konstanz, Germany). The *Mes*AT I56V/A312S/M414F triple mutant was prepared by site-directed mutagenesis (QuikChange, Stratagene) in three rounds.

Overexpression and purification of *Vp*AT in *E. coli*

The pET28b+ construct containing the gene for *Vp*AT was used to produce the enzyme with an *N*-terminal His_6-tag (MGSSHHHHHH) followed by a 10 amino acid linker (SSGLVPRGSH) in *E. coli* C41(DE3). Cells were grown at 37 °C in LB medium with 50 μg/ml of kanamycin. Expression of *Vp*AT was induced by adding 0.8 mM isopropyl-β-D-thiogalactopyranoside (IPTG) to the growing cells when the OD_{600} reached 0.6. Cultivation was continued for 16 h at 28 °C and 170 rpm. Cells were

obtained by centrifugation and disrupted by sonication at 4 °C followed by centrifugation for 45 min at 15,000 rpm to obtain cell-free extract (CFE). The enzyme was purified in two steps using immobilized metal affinity chromatography (IMAC, HisTrap HP column 5 ml, GE Healthcare) and ion-exchange chromatography (IEXC, Q-Sepharose HP column 5 ml, GE Healthcare). In case of IMAC, *Vp*AT was eluted at a flow rate of 1 ml/min with 15 column volumes of a linear gradient of 0-0.5 M imidazole in a buffer containing 20 mM Tris-HCl, pH 8.0, 0.5 M NaCl, and 0.01% (vol/vol) β-mercaptoethanol, whereas for IEXC elution was performed with 15 column volumes of a gradient of 0-1 M NaCl in a buffer containing 20 mM Tris-HCl, pH 8.0, and 0.01% (vol/vol) β-mercaptoethanol. For use in crystallization experiments, the fractions containing active enzyme were pooled, concentrated (Ultracel 30K MWCO, Amicon) and applied to a Superdex 200 10/300 GL size exclusion chromatography column (GE Healthcare), equilibrated in 20 mM Tris-HCl, pH 7.5, containing 200 mM NaCl. After elution the fractions corresponding to the protein peak were pooled, concentrated (Amicon) and dialyzed overnight against a buffer containing 20 mM Tris-HCl, pH 7.5 and 10 μM of PLP, and concentrated to 20 mg/ml.

Protein crystallization

Crystallization experiments were set up at 20 °C, and a single crystal was obtained under the condition of 0.02 M sodium/potassium phosphate, 0.1 M 1,3-bis(tris(hydroxyl-methyl)-methylamino)-propane, pH 6.5, and 20% (wt/vol) PEG 3350K. Crystals of *Vp*AT grew within a week after which they were transferred to a cryo-protection solution consisting of the mother liquor with 20% (vol/vol*)* glycerol. This was achieved in 4 steps of 5 min each, starting with a solution containing 2% (vol/vol*)* glycerol followed by solutions with 5, 10 and finally 20% glycerol. Crystals from this last solution were cooled in liquid nitrogen. For the 2-aminooxyacetate (AOA) binding study, the same steps were followed, but with the cryo-protection solutions supplemented with 2, 5, 10 and 20 mM AOA.

Diffraction data collection and processing

Diffraction data were collected at beamline ID14-4 of the European Synchrotron Radiation Facility (ESRF, Grenoble, France). Indexing and integration of reflections was done using XDS (Evans *et al.,* 2006) and scaling and merging of the data was achieved using SCALA (Kabsch *et al.,* 2010) from the CCP4 software suite (Bailey *et al.,* 1994). For molecular replacement the Phaser program (McCoy *et al.,* 2007) was used with *Mes*AT (PDB code: 2YKU, (Wybenga & Crismaru *et al.,* 2012)) as the input model. The resulting model structure was subjected to successive rounds of

automatic model building using ARP/wARP (Langer *et al.,* 2008) at 1.7 Å resolution followed by manual model building and manipulation in Coot (Emsley *et al.,* 2004). Refmac5 was used for refinement of the atomic coordinates and atomic B-factors (Murshudov *et al.,* 1997). After refinement the model quality was validated with MolProbity (Chen *et al.,* 2010). Hetero-compound coordinate files were obtained from the HIC-Up server (Kleywegt *et al.,* 1998) while the PRODRG2 server (Schuttelkopf *et al.,* 2004) was used to generate the stereochemical restraints. Structural homologues of *Vp*AT were obtained with the Dali server (Holm *et al.,* 2010). PISA from the CCP4 software suite was used for protein interface analysis (Krissinel *et al.,* 2007) while PyMOL (http://www.pymol.org/) was used for making images of the protein structure. Data collection and refinement statistics are given in the supplemental material (**Table S1**).

Substrate docking

Docking of the PLP-(*S*)-*β*-phenylalanine intermediate was carried out with Rosetta software which allows both side-chain and backbone flexibility during docking (Davis *et al.,* 2009[a]; Davis *et al.,* 2009[b]). Rosetta's redesign specificity application (Richter *et al.,* 2011) was used (without permitting mutations); this application allowed for optimizing the surrounding protein structure to bind the (*S*)-*β*-phenylalanine intermediate while preserving the known binding orientation of the PLP (*Mes*AT, PDB code: 2YKY). To model the flexibility of the protein, Monte Carlo optimizations of side chain rotamers (collections of thermodynamically accessible conformations) were carried out three times. Each of these optimization rounds was followed by an energy minimization, which also allowed backbone atoms to move. Residues up to 8 Å from the intermediate were allowed to change conformation. Rotamers for the PLP-(*S*)-*β*-phenylalanine intermediate were prepared with Yasara (www.yasara.org) (Krieger *et al.,* 2002). AM1-BM3 charges of the PLP-intermediate were assigned by OEchem (OpenEye Scientific Software, Inc., 2010). A total of 1,040 docking runs were carried out of which the lowest energy solution was selected.

Accession numbers

The 16S rRNA gene sequence of *V. paradoxus* CBF3 has been deposited at GenBank under accession number JN990697. The sequences of the DNA contig containing the *Vp*AT encoding gene and of the *Vp*AT enzyme are deposited at EMBL under accession numbers HE608883 and CCE46017, respectively. Atomic coordinates and structure factors have been deposited in the Protein Data Bank

(http://www.pdb.org) under accession codes 4AO9 for the *Vp*AT holo-enzyme and 4AOA for *Vp*AT complexed with 2-aminooxyacetic acid.

Results

Isolation of a *β*-phenylalanine-degrading bacterium

The isolation of a bacterial strain possessing *β*-phenylalanine transaminase activity was carried out by an enrichment procedure using *rac*-*β*-phenylalanine as the sole nitrogen source. After growth was observed, a pure culture was obtained by repeated transfer to fresh medium and streaking onto minimal medium plates supplemented with *β*-phenylalanine and *trans*-cinnamic acid. The most rapidly growing strain (named CBF3) was selected for further investigation. The 16S rRNA gene (1,517 bp) of strain CBF3, identified by PCR and paired-end genome sequencing, has 99% sequence identity to the 16S rRNA genes of *Variovorax paradoxus* S110 (CP001635.1) and *V. paradoxus* EPS (CP002417.1) (Zhang *et al.,* 2000). This affiliates strain CBF3 to the genus of *V. paradoxus*.

Activity assays with HPLC analysis showed that strain CBF3 possesses a *β*-phenylalanine AT activity that converts *β*-phenylalanine and 2-oxoglutarate (or pyruvate) to 3-oxo-3-phenylpropionic acid and L-α-glutamate (or L-α-alanine). Attempts to purify the *Vp*AT using wild-type CBF3 as the source of enzyme failed due to low protein recovery after partial purification.

Isolation of the *vpAT* gene

A DNA library, consisting of about 4,000 clones, was constructed in cosmid pLAFR3. The insert size of the DNA fragments was between 15-25 kb. The genome size of *V. paradoxus* is about 6.7 Mb (Han *et al.,* 2011), thus the number of obtained clones was sufficient for 9-fold coverage of the whole genome. Screening individual clones for AT activity yielded two positive clones of which one was investigated further. The insert was subcloned into vector pZErO-2 and rescreening for acetophenone formation yielded six positive hits. Restriction analysis identified a shared 5 kb EcoRI fragment that likely contains the AT-encoding gene.

DNA sequence analysis showed the presence of a 1,302 bp gene encoding an aminotransferase, which was subsequently transferred to the pET28b+ expression vector. The encoded 434 amino acid protein has a theoretical pI of 6.06 and a calculated molecular mass of 46.42 kDa (http://web.expasy.org/compute_pi/). The sequence of a 20.6 kb contig found by paired-end genome sequencing indicated that

around the *vpAT* gene there were no regulatory regions or open reading frames related to other enzymes of amino acid metabolism.

Protein sequence analysis

Sequence analysis showed that *Vp*AT has 55% sequence identity to glutamate-1-semialdehyde-2,1-aminomutase from *Polaromonas* sp. JS666 (*Po*GSAM), which has been reported to have activity with aromatic *β*-amino acids (ABE43415.1) (**Fig. 3.1**), 51% sequence identity to the aromatic *β*-phenylalanine aminotransferase (*Mes*AT) (ABL74379.1) from *Mesorhizobium* sp. LUK, and 35% sequence identity to a glutamate-1-semialdehyde-2,1-aminomutase from *Synechococcus elongatus* (*Se*GSAM) (ABB56677.1). These data suggest that *Vp*AT, just as *Mes*AT and *Po*GSAM, is a fold type I aminotransferase and furthermore that *Vp*AT belongs to subgroup II transaminases which is based on an enzyme's substrate specificity (Bea *et al.,* 2011; Kim *et al.,* 2007; Wybenga & Crismaru *et al.,* 2012). *Vp*AT has 19% sequence identity to a transaminase from *Alcaligenes denitrificans* that has been reported to have activity towards aliphatic *β*-amino acids (*Ad*bpAT) (AAP92672.1) (Yun *et al.,* 2004). A sequence comparison between *Vp*AT, *Mes*AT, *Po*GSAM and *Ad*bpAT shows that the amino acid residues that are involved in cofactor binding are conserved in addition to several residues that, based on the structures of *Vp*AT and *Mes*AT, are involved in substrate and cofactor binding (**Fig. 3.1**).

Purification of *Vp*AT expressed in *E. coli*

The recombinant protein was overproduced with an *N*-terminal His_6-tag in *E. coli* strain C41(DE3). *Vp*AT was mainly present as a soluble protein. The enzyme was purified by three chromatography steps. Size exclusion chromatography indicated a molecular mass of approximately 100 kDa, suggesting that *Vp*AT exists as a dimer in solution. The purified protein showed a single band of about 48 kDa in an SDS-PAGE gel (**Fig. 3.2**). The overall yield from 1 L of culture was 40-50 mg (**Table 3.1**). The specific activity of the purified enzyme was 17.5 U mg^{-1} at 30 °C, corresponding to a k_{cat} of 11.8 s^{-1} per monomer. The *Vp*AT R41A mutant was overexpressed and purified under the same conditions as the wild-type enzyme, resulting in similar amounts of purified protein.

Catalytic properties

The pH-activity profile of *Vp*AT showed that the enzyme has a high activity over a broad pH range (4 to 11.2) at 30 °C. The optimum temperature of the enzyme was tested by measuring the specific activity at temperatures between 20 °C and 65

°C. *Vp*AT exhibits a maximum specific activity of 33 U mg^{-1} at 55 °C, which is about 2-fold higher than the specific activity at 30 °C (**Fig. 3.3**). These data show that *Vp*AT is more active toward (*S*)-*β*-phenylalanine than other *β*-transaminases reported earlier (Bea *et al.,* 2011; Kim *et al.,* 2007; Yun *et al.,* 2004). The activity of *Vp*AT with pyruvate is 85% of that with *α*-ketoglutarate as the amino acceptor.

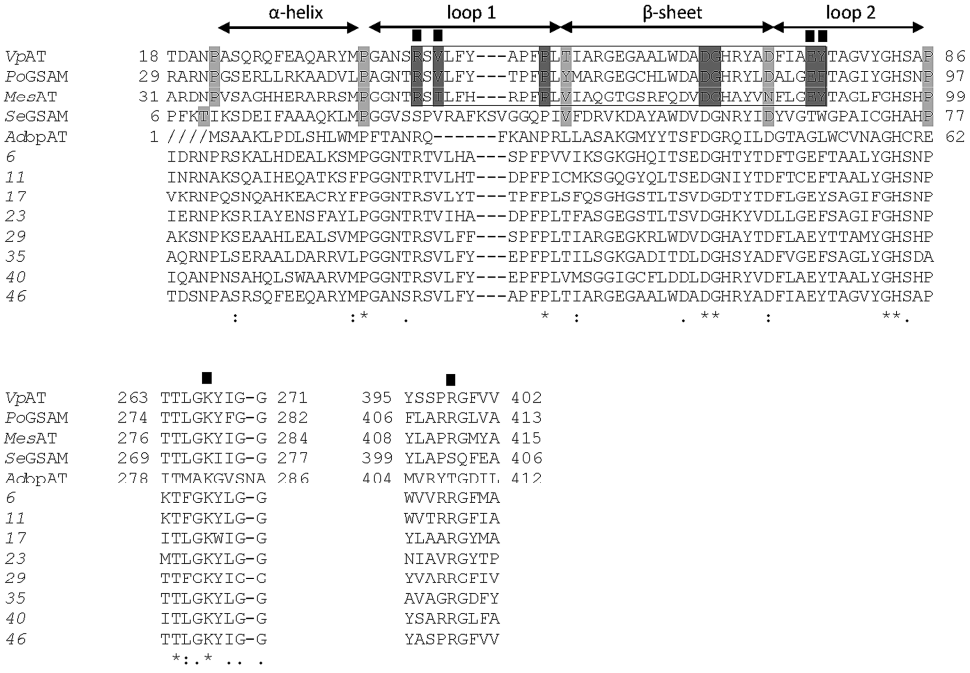

Figure 3.1 Partial sequence alignment of *Vp*AT with other aminotransferases made with Clustal Ω (Sievers *et al.,* 2011). The structure of *Mes*AT and *Se*GSAM are known and α-helices have been assigned based on these structures. For *Po*GSAM, this has been assigned on the basis of sequence conservation. Since the structure of *Adb*pAT has not been elucidated and since the sequence identity to *Vp*AT is low, secondary structural elements are not indicated. The proposed aromatic *β*-transaminase signature sequence is shown in the enclosed box and its residues are highlighted in dark grey boxes. Square black boxes indicate relevant residues for substrate and cofactor binding. Proteins: *Vp*AT, *β*-transaminase of *Variovorax paradoxus* (this study; CCE46017.1, PDB code: 4AO9); *Po*GSAM, glutamate-1-semialdehyde 2,1-aminomutase of *Polaromonas* sp. strain JS666 (ABE43415.1); *Mes*AT, *β*-transaminase of *Mesorhizobium* sp. strain LUK (ABL74379.1, PDB code: 2YKY); *Se*GSAM, glutamate-1-semialdehyde 2,1-aminomutase from *Synechoccus elongatus* (ABB56677.1, PDB code: 2HOZ); *Adb*pAT, *β*-alanine:pyruvate transaminase of *Alcaligenes denitrificans* (AAP92672.1). The numbers 6, 11, 17, 23, 29, 35, 40 and 46 refer to the proteins that are listed in Supplemental Material, **Table S2**.

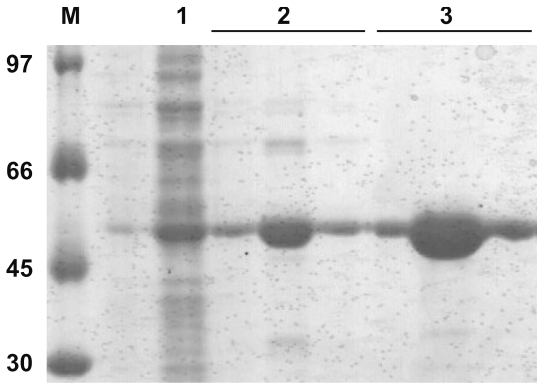

Figure 3.2 SDS-PAGE of *Vp*AT at different steps of purification. The gel contained 10% polyacrylamide. Lanes: M, molecular weight marker (kDa); 1, cell-free extract of *E. coli* strain C41(DE3) expressing the recombinant enzyme; 2, HisTrap fraction; 3, Q-Sepharose HP fraction.

Table 3.1 Purification of the recombinant *Vp*AT from *E. coli* strain C41(DE3).

Purification step	Sp. activity (U • mg^{-1})	Total protein (mg)	Total activity (U)	Purification (fold)	Recovery (%)
Cell-free extract	2.9	1134	3288	1	100
HisTrap chromatography	7.4	248	1835	2.5	56
Q-Sepharose chromatography	17.5	90.4	1582	6	48

The relationship between reaction rate and the substrate concentration displayed Michaelis-Menten kinetics with substrate inhibition (Tipton *et al.,* 1996). The apparent K_m and k_{cat} values (per monomer) for (*S*)-*β*-phenylalanine in the presence of 10 mM α-ketoglutarate were 1.5 mM and 11.8 s^{-1}, respectively, with an apparent substrate inhibition constant (K_i) of 40.3 mM. When using 10 mM (*S*)-*β*-phenylalanine, the apparent K_m and k_{cat} for α-ketoglutarate were 0.3 mM and 10.6 s^{-1}, respectively, with an apparent K_i of 82.4 mM.

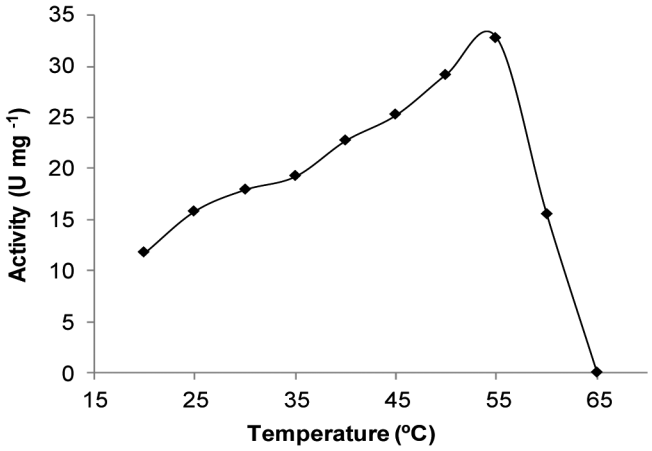

Figure 3.3 Effect of temperature on the specific activity of *Vp*AT.

Substrate scope and enantioselectivity of *Vp*AT

To investigate the substrate scope of the enzyme, a number of *β*-amino acids and *α*-amino acids, were tested (**Table 3.2**). The results show that *Vp*AT acts exclusively on *β*-amino acids and that the enzyme prefers aromatic *β*-amino acids (**Table 3.2**, **entries 1-3, 8-20**) over aliphatic *β*-amino acids (**Table 3.2, entries 21-27**). The most favorable substituent positions on the phenyl ring of *β*-phenylalanine for activity were *para*- and *meta*-, while *ortho*-substituted analogues were poorly converted. The *β*-phenylalanine derivatives bearing linear alkyl substituents at the *para* position, *i.e.* ethyl or propyl (**Table 3.2, entries 13-14**), were converted more efficiently than other substituted substrates (**Table 3.2, entries 12, 16-20**). However, introduction of a branched alkyl substituent, *i.e. iso*-propyl, at the *para* position results in a decrease of activity (**Table 3.2, entry 15**). The enzyme showed no activity for α-phenylalanine or its *meta*-chloro, *meta*-bromo and *para*-hydroxy substituted (α-tyrosine) derivatives, which contrasts with *Mes*AT for which activity was reported with α-phenylalanine and other *α*-amino acids (Kim *et al.,* 2007). The activity of *Mes*AT towards α-phenylalanine however could not be confirmed by us.

*Vp*AT further preferentially converts the (*S*)-enantiomers of aromatic *β*-amino acids, (**Table 3.2, entries 1-3, 9, 10, 12** and **16**) and the (*R*)-enantiomers of aliphatic *β*-amino acids (which have a similar configuration of functional groups around the chiral carbon atom but a change in Cahn–Ingold–Prelog priority). However, the activity of *Vp*AT towards several aliphatic *β*-amino acids was quite low (**Table 3.2, entries 22-23**). We also investigated the regio- and enantioselectivity of *Vp*AT with

several racemic substrates (**Table 3.2, entries 1, 9, 10, 12** and **16**). The enzyme appeared highly enantioselective towards the (*S*)-enantiomers of *β*-phenylalanine and its *meta*- and *para* ring-substituted derivatives thereby producing highly pure (*R*)-enantiomer preparations (*ee* >95%).

Table 3.2 Substrate range of *Vp*AT[a].

Entry	Amino donor	Relative activity (%)	Conversion (%)	*ee* (%), *E*
I.	*β*-phenylalanine derivatives			
1	*rac*-*β*-phenylalanine	100	49	>99 (*R*), >200
2	(*S*)-*β*-phenylalanine	100	99[c]	–
3	(*R*)-*β*-phenylalanine	NA[b]	–[d]	–
4	*rac*-2-methyl-*β*-phenylalanine	5	19	ND[e]
5	*rac*-2-fluoro-*β*-phenylalanine	15	26	ND[e]
6	*rac*-2-chloro-*β*-phenylalanine	4	32	ND[e]
7	*rac*-2-bromo-*β*-phenylalanine	4	25	ND[e]
8	*rac*-3-methyl-*β*-phenylalanine	54	64	ND[e]
9	*rac*-3-fluoro-*β*-phenylalanine	48	48	>98 (*R*), >200
10	*rac*-3-chloro-*β*-phenylalanine	56	47	>95 (*R*), >100
11	*rac*-3-bromo-*β*-phenylalanine	53	99	ND[e]
12	*rac*-4-methyl-*β*-phenylalanine	100	53	>95 (*R*), >200
13	*rac*-4-ethyl-*β*-phenylalanine	134	47	ND[e]
14	*rac*-4-propyl-*β*-phenylalanine	126	48	ND[e]
15	*rac*-4-*iso*-propyl-*β*-phenylalanine	61	25	ND[e]
16	*rac*-4-trifluoromethyl-*β*-phenylalanine	73	49	>95 (*R*), >100
17	*rac*-4-fluoro-*β*-phenylalanine	87	59	ND[e]
18	*rac*-4-bromo-*β*-phenylalanine	62	61	ND[e]
19	*rac*-4-nitro-*β*-phenylalanine	32	6	ND[e]

Table 3.2 Substrate range of *Vp*AT[a] (*continued*).

Entry	Amino donor	Relative activity (%)	Conversion (%)	*ee* (%), *E*
I. *β*-phenylalanine derivatives				
20	*rac*-4-hydroxy-*β*-phenylalanine	61	39	ND[e]
II. Other *β*-amino acids				
21	*rac*-3-amino-butyric acid	1	6	ND[e]
22	(*R*)-3-amino-butyric acid	3.1	11	–
23	(*R*)-3-amino-5-methyl-hexanoic acid	48	75	–
24	*rac*-*β*-asparagine	1	4	ND[e]
25	*rac*-*β*-leucine	38	51	ND[e]
26	*β*-alanine	NA[b]	–[d]	–
27	*β*-glutamic acid	NA[b]	–[d]	–
III. *α*-amino acids				
29	(*S*)-*α*-phenylalanine	NA[b]	–[d]	–
30	*rac*-3-chloro-*α*-phenylalanine	NA[b]	–[d]	–
31	*rac*-3-bromo-*α*-phenylalanine	NA[b]	–[d]	–
32	(*S*)-*α*-tyrosine	NA[b]	–[d]	–

[a] Reaction mixtures (0.4 ml volume) contained amino donor (3 mM) and *α*-ketoglutarate (5 mM) as acceptor. Initial rates were measured and conversion was determined after 16 h at 30 °C. The activity for *β*-phenylalanine, corresponding to 17.5 U mg^{-1}, was taken as 100%. [b] No activity (less than 0.001 U mg^{-1}); [c] Conversion after 0.5 h; [d] No conversion observed after 16 h; [e] ND, not determined.

3D-structure of *Vp*AT

The crystal structure of the *Vp*AT holo-enzyme was solved by molecular replacement, using the structure of *Mes*AT (PDB code: 2YKU, (Wybenga & Crismaru *et al.,* 2012)) as a search model, and subsequently refined at 1.5 Å resolution. *Vp*AT crystallizes in space group $P2_12_12_1$ with two molecules (chains A and B) per asymmetric unit, which are related by non-crystallographic two-fold symmetry. Chains A and B are very similar to each other with RMSD values of C*α* atom positions

of approximately 0.2 Å. For both monomers, electron density is absent for the first 21 *N*-terminal residues. This includes the *N*-terminal His_6-tag, 10 amino acids included as a linker in the expression construct, and the first amino acid (methionine) of the *Vp*AT polypeptide. The interface between the monomers buries an area of about 4,400 $Å^2$, which equals a quarter of the total surface area of the monomer pair (**Fig. 3.4**). Since the active sites of chains A and B are located at this interface and shaped by residues from both monomers, this suggests that the two monomers in the asymmetric unit form the functional *Vp*AT dimer observed in solution (see above).

The structure of the *Vp*AT monomer

The *Vp*AT monomer has a curved shape and consists of a PLP-binding domain and a domain formed by the *N*- and *C*-termini of the polypeptide chain (NC-domain; residues 1-86 and 320-434) (**Fig. 3.4**). The two domains line a cleft into which the PLP cofactor protrudes. The monomer consists of 11 α-helices of at least 2 turns and 13 β-strands that form a central 7-stranded mixed β-sheet in the PLP-binding domain and two 3-stranded anti-parallel β-sheets in the NC-domain. The overall structure of the enzyme is similar to that of aspartate aminotransferase, the archetype of a fold type I aminotransferase (Z score 22, RMSD of 4.3 Å for 308 C*α* atoms, 17 % sequence identity, PDB code 1BKG) (Grishin *et al.,* 1995; Schneider *et al.,* 2000), but is most similar to that of *Mes*AT (Z-score 60, RMSD of 1.1 Å for 429 C*α* atoms, 50 % sequence identity, PDB code: 2YKU) (Wybenga & Crismaru *et al.,* 2012).

The PLP cofactor

Each *Vp*AT dimer contains one PLP cofactor per monomer, which is positioned close to the surface (**Fig. 3.5**). The PLP cofactor is anchored to the protein *via* a covalent imine bond with the ε-amino group of residue K267, which is conserved in the sequence alignment of homologous PLP-dependent enzymes. In addition, the three phosphate oxygen atoms are at hydrogen bonding distance to the amide protons of residues G132, T133 and T300* (monomer B). Two of the phosphate oxygen atoms also make a hydrogen bond to a water molecule, which in turn is hydrogen-bonded to peptide backbone atoms. The phosphate ester oxygen atom is not involved in hydrogen bond formation. The PLP cofactor is positioned in between V242 (at the *si*-face of the C4' of the aldimine) and Y159 (at the *re*-face of the C4' of the aldimine) while the pyridine nitrogen makes a hydrogen bond with the side chain of D240. The interactions of the PLP cofactor with residues K267, V242, Y159 and D240 keep the PLP cofactor fixed in the active site (**Fig. 3.5A**).

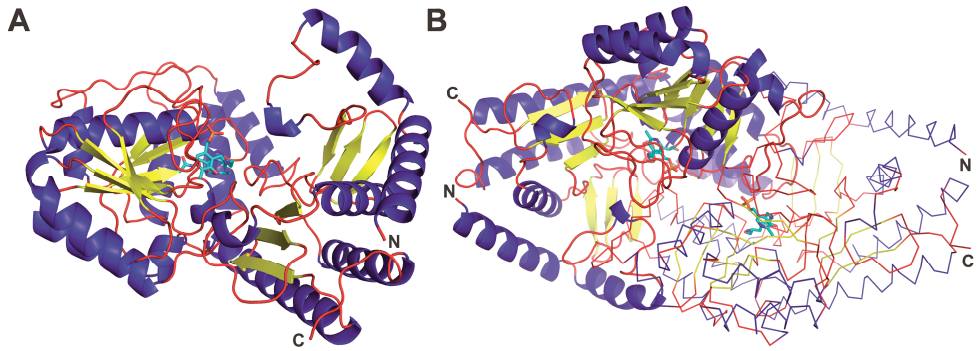

Figure 3.4 Structures of monomer and dimer of *Vp*AT. **A)** The monomer of *Vp*AT with the PLP cofactor (magenta) positioned in the cleft in between the PLP-binding domain (left half of the monomer, containing the 7-stranded mixed β-sheet) and the NC-domain (right half of the monomer, containing the two 3-stranded anti-paralell β-sheets and the N- as well as the C-termini of the polypeptide chain indicated by N and C, respectively). **B)** Two monomers of *Vp*AT assemble into a dimer, here viewed along the two-fold non-crystallographic axis relating the two monomers. The two PLP cofactors are shown in magenta and are linked to the polypeptide backbone *via* a Schiff base with K267. The α-helices are colored blue, the β-strands are colored yellow and the the loops are colored red. N and C indicate the N- and C-termini, respectively.

The PLP cofactor

Each *Vp*AT dimer contains one PLP cofactor per monomer, which is positioned close to the surface (**Fig. 3.5**). The PLP cofactor is anchored to the protein *via* a covalent imine bond with the ε-amino group of residue K267, which is conserved in the sequence alignment of homologous PLP-dependent enzymes. In addition, the three phosphate oxygen atoms are at hydrogen bonding distance to the amide protons of residues G132, T133 and T300* (monomer B). Two of the phosphate oxygen atoms also make a hydrogen bond to a water molecule, which in turn is hydrogen-bonded to peptide backbone atoms. The phosphate ester oxygen atom is not involved in hydrogen bond formation. The PLP cofactor is positioned in between V242 (at the *si*-face of the C4' of the aldimine) and Y159 (at the *re*-face of the C4' of the aldimine) while the pyridine nitrogen makes a hydrogen bond with the side chain of D240. The interactions of the PLP cofactor with residues K267, V242, Y159 and D240 keep the PLP cofactor fixed in the active site (**Fig. 3.5A**).

The binding of 2-aminooxyacetic acid

Aminooxyacetic acid (AOA), a mimic of *β*-alanine, is a known inhibitor of aminotransferases (John *et al.,* 1978) and also inhibits *Vp*AT. To investigate how AOA

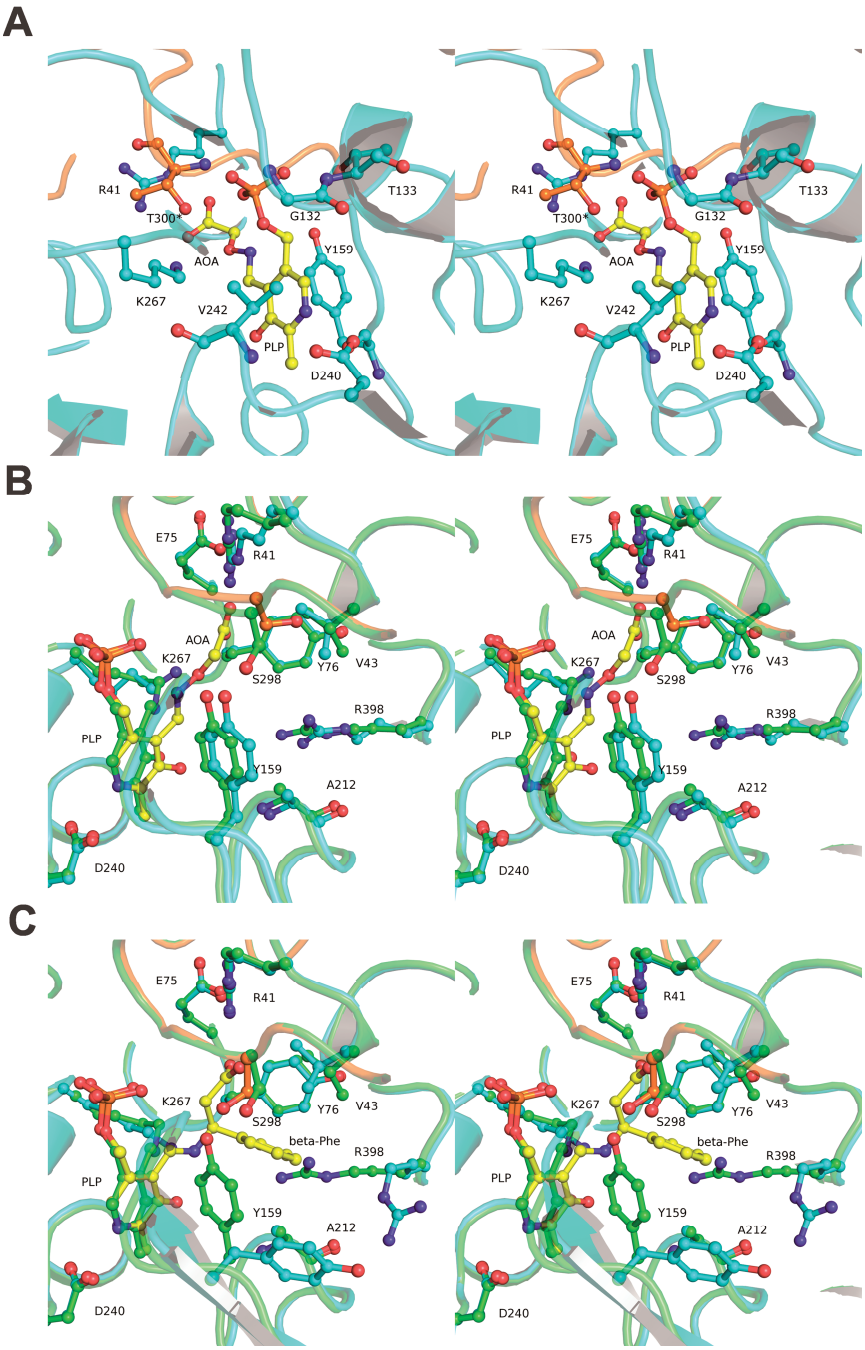

Figure 3.5 Wall-eyed stereo presentation of *Vp*AT bound with an inhibitor and a docked intermediate.

Figure 3.5 Wall-eyed stereo presentation of *Vp*AT bound with an inhibitor and a docked intermediate (*continued*). **A)** The PLP cofactor (yellow) is shown bound to 2-aminooxyacetate (AOA) (yellow). The monomer A of *Vp*AT is shown in light blue, whereas monomer B is shown in orange. **B)** The inhibitor 2-aminooxyacetate (AOA) bound in *Vp*AT. The holo-enzyme without inhibitor is shown in green. The X-ray structure with AOA bound is shown with different colors for monomer A (light blue), monomer B (orange), and the inhibitor (yellow). **C)** X-ray structure of holo-*Vp*AT with docked (*S*)-*β*-phenylalanine. The X-ray structure of the holo-enzyme is shown in green, while the modeled structure with docked (*S*)-*β*-phenylalanine is in light blue for monomer A, and orange for monomer B. The docked intermediate is shown in yellow. The side chains of residues interacting with the docked intermediate and the backbone atoms of A212 are also shown. R41 (P-pocket) is the residue that binds the *α*-carboxylate of *β*-phenylalanine. In the O-pocket, R398 is the arginine switch residue (compare panel B with C).

binds in *Vp*AT, enzyme crystals were soaked with AOA. The structure of *Vp*AT with AOA (**Fig. 3.5A, B**) shows that the amino group of the inhibitor covalently binds to the C4A atom of the PLP cofactor, as also described for aspartate aminotransferase (Markovic-Housley *et al.,* 1996), and recently for *Mes*AT (Wybenga & Crismaru *et al.,* 2012). The ether-oxygen atom (Oχ1) of AOA is positioned close (3.0 Å) to the ε-amino group of residue K267. The carboxylate group binds *via* a salt bridge to the Nε- and Nη2-atoms of R41. The binding of AOA in the active site of *Vp*AT is similar to how AOA binds in the active site of *Mes*AT (PDB code: 2YKV). AOA inhibits aminotransferase activity because the amine-ether oxygen bond of AOA cannot be weakened by K267, and hence hydrolysis and formation of the PMP intermediate does not occur (**Fig. 3.5B**).

Docking of PLP-(*S*)-*β*-phenylalanine in the active site of *Vp*AT

To investigate how an aromatic *β*-amino acid such as (*S*)-*β*-phenylalanine binds in the active site of *Vp*AT, initially a structure was determined after a *Vp*AT crystal had been soaked with (*S*)-*β*-phenylalanine. However, this structure only revealed the presence of a pyridoxamine 5′-phosphate (PMP) intermediate in the active site of the enzyme. Since trapping of (*S*)-*β*-phenylalanine in the active site of *Vp*AT apparently had not occurred, the external (*S*)-*β*-phenylalanine aldimine intermediate was modeled into the active site of *Vp*AT using Rosetta, which allows docking with flexible backbone and side chains. In the docked structure, the aromatic ring of the substrate is bound between V43, Y76, Y159, and A212 (**Fig. 3.5C**), similar to the way (*S*)-*β*-phenylalanine is bound to *Mes*AT (Wybenga & Crismaru *et al.,* 2012). This region was previously termed by us as the O-pocket, because it is positioned on the 3-hydroxyl side of the PLP cofactor ((Wybenga & Crismaru *et al.,* 2012), see below). Similar to the conformational changes observed in *Mes*AT upon formation of the external aldimine intermediate with (*S*)-*β*-phenylalanine (Wybenga & Crismaru *et*

al., 2012), *Vp*AT the arginine switch residue R398 in the O-pocket is displaced during the docking, freeing space for the phenyl ring of the substrate. Instead, the R398 side chain Nη2 atom forms a hydrogen bond to the carbonyl oxygen of A212. Also V43 and Y159 have reoriented to better accommodate the docked external aldimine intermediate. In the absence of (*S*)-*β*-phenylalanine the docking procedure resulted in minor shifts of less than 0.5 Å of the backbone atoms around the active site. While the *ortho* hydrogen atoms of the phenyl ring of the bound intermediate are buried, the *para* and *meta* hydrogen atoms of the phenyl ring are solvent exposed in the docked structure. The carboxylate of the docked (*S*)-*β*-phenylalanine is buried in a region we term the P-pocket, which is at the phosphate group side of the PLP cofactor. Here, residue R41 is directly involved in binding of (*S*)-*β*-phenylalanine by making a salt-bridge to the carboxylate group (**Fig. 3.5C**). The importance of R41 for the binding of (*S*)-*β*-phenylalanine is underscored by the observation that the R41A mutant was inactive when tested with (*S*)-*β*-phenylalanine as amino donor and α-ketoglutarate as amino acceptor.

Identification of aromatic *β*-amino acid aminotransferases

The *Vp*AT structure with bound AOA, a *β*-alanine mimic, and the docking results with *β*-phenylalanine show that R41 is important for binding the *α*-carboxylate of *β*-amino acids, as is the corresponding residue R54 in *Mes*AT (Wybenga & Crismaru *et al.,* 2012). The side chain of R41 interacts with E75, which may assist the function of R41 by orienting its side chain and shaping the carboxylate-binding P-pocket. We therefore hypothesized that the presence of an R41-E75 pair in an aminotransferase protein sequence indicates enzymatic activity with *β*-amino acids. A comparison of the crystal structures of *Vp*AT and *Mes*AT showed that the R41-E75 salt bridge is conserved in *Mes*AT (R54-E88). In addition, a sequence alignment between *Vp*AT and a glutamate-1-semialdehyde-2,1-aminomutase from *Polaromonas* sp. JS666 (*Po*GSAM), for which no structure is available but which has activity towards aromatic *β*-amino acids (Bea *et al.,* 2011), also showed conservation of R41 and E75 (as R51 and E85, respectively) (**Fig. 3.1**). In contrast, the crystal structure of *Synechococcus elongatus* glutamate-1-semialdehyde-2,1-aminomutase (*Se*GSAM, PDB code: 2HOZ) (Stetefeld *et al.,* 2006), which is structurally very similar to that of *Vp*AT (Z-score 47; RMSD of 1.8 Å for 404 C*α* atoms, 35 % sequence identity), shows that no Arg and Glu residues equivalent to R41 and E75 of *Vp*AT are present, in agreement with the enzyme's lack of activity on *β*-amino acids.

We subsequently tested whether R41 and E75 could be used to define a sequence motif with which aromatic *β*-amino acid aminotransferases can be

distinguished from aminotransferases with a similar fold but with a different substrate specificity. For this, BLAST searches were performed using the *Vp*AT, *Mes*AT, and *Po*GSAM (ABE43415.1) protein sequences. For each query sequence, 2,000 homologous sequences were retrieved with ≥ 18% sequence identity. After omitting duplicates, the resulting 2,222 sequences were included in a multiple sequence alignment, and inspected for residues that are important for substrate binding.

We used the P-pocket R41-E75 pair as the starting point to identify a motif with which aminotransferases with activity towards aromatic *β*-amino acids may be distinguished from aminotransferases with a similar fold but a different activity. The R41-E75 starting pair was subsequently broadened by including the O-pocket residues V43 and Y76 since the equivalent residues in *Mes*AT (I56 and Y89) were shown to be involved in substrate binding. At position 43 Val, Ile, and Ala were allowed, but hydrophobic residues with more bulky side chains such a Leu, Phe, Tyr and Trp were excluded since they were expected to prevent aromatic substrate binding for steric reasons. At position 75, apart from Glu, we also allowed Asp, Gln and Asn since these may still be able to interact with the side chain of R41. At position 76, Phe and Trp were also allowed since they are frequently found in the same position as Tyr in other fold type I aminotransferases. We next extended the motif with conserved residues at positions that appear structurally important by adding a conserved Pro at position 50, which is in the center of a hydrophobic cluster in the *Vp*AT and *Mes*AT structures, and an Asp at position 65 and a Gly at position 66, which form a β-turn, of which the Asp is hydrogen bonded to A23 and S24, residues that are located in the α-helix that precedes loop 1.

The motif that was finally defined, R-X-[AVI]-X(6)-P-X(14)-D-G-X(8)-[EDNQ]-[YFW] (**Fig. 3.1**), retrieved 46 unique sequences (Supplemental Material, **Table S2**) that we hypothesize may represent fold type I aminotransferases with activity towards aromatic *β*-amino acids.

Discussion

Catalytic properties and enantioselectivity of *Variovorax* AT

Isolation of microorganisms that use *β*-phenylalanine as sole nitrogen source yielded a gram-negative bacterium of the genus *Variovorax paradoxus* that produces a *β*-amino acid selective aminotransferase. The gene encoding this enzyme was cloned, sequenced and overexpressed to a high level in *E. coli*. Sequence analysis showed that the enzyme is a fold type I AT, just as several other subgroup II ω-ATs. *Vp*AT shares highest sequence identity with biochemically characterized *β*-phenylalanine ATs (Bea *et al.,* 2011; Kim *et al.,* 2007), including the *Mesorhizobium* aminotransferase (*Mes*AT) described by Kim *et al.* (2007), of which the structure was recently solved (Wybenga & Crismaru *et al.,* 2012). *Mes*AT and *Vp*AT have similar activities with *α*-ketoglutarate and pyruvate as amino acceptors (Kim *et al.,* 2007), but differ from *α*-transaminases, which generally show a clear preference for either pyruvate, *α*-ketoglutarate, or oxaloacetate (Lowe *et al.,* 1985; Shin *et al.,* 2003; Sung *et al.,* 1990). Striking differences between *Mes*AT and *Vp*AT are that *Vp*AT has a higher catalytic activity, is active over a very broad range of pH values, and only accepts *β*-amino acids. On the other hand, *Vp*AT shows the same enantiopreference for (*S*)-*β*-phenylalanine and a very high enantioselectivity (E>100), just as *Mes*AT (Kim *et al.,* 2006) and *Po*GSAM (Bea *et al.,* 2011). This allows a biotechnologically relevant kinetic resolution of racemic mixtures, from which the remaining (*R*)-*β*-phenylalanines can be obtained with very high *ee* (**Table 3.2**, **entries 1, 9, 10, 12** and **16**).

Although the differences in activity are difficult to explain, a comparison of the residues surrounding the active site of *Vp*AT with those of *Mes*AT shows that V43, S298* (monomer B) and F400, which line the hydrophobic O-pocket of the active site of *Vp*AT, differ from the residues found at these positions in *Mes*AT (I56, A312* and M414). A triple mutant of *Mes*AT (I56V/A312S/M414F) was generated and showed a two-fold increase (3.3 U mg^{-1}) in activity with (*S*)-*β*-phenylalanine compared to *Mes*AT WT (1.6 U mg^{-1}) (Kim *et al.,* 2007)), indicating an important role of these residues in activity with (*S*)-*β*-phenylalanine.

Structure of *Vp*AT and architecture of the active site

The structure of *Vp*AT revealed the overall topology of the enzyme, the position of the cofactor, and provided insight into the architecture of the active site of *Vp*AT. A comparison with the structure of *Mes*AT shows that the two enzymes are structurally similar (RMSD of 1.0 Å for 423 C*α* atoms, 51 % sequence identity) and confirms that they both belong to the fold type I aminotransferase family (Grishin *et*

al., 1995). As in *Mes*AT, both monomers in *Vp*AT contribute to the binding of the PLP cofactor, suggesting that dimerization is essential for catalytic activity (**Fig. 3.5**).

Previously, we proposed to use the notation P-pocket (pointing in the same direction as the PLP phosphate) and O-pocket (at the side of the hydroxyl substituent of the PLP) to define substrate binding sites of amino acid converting fold type I ATs (Wybenga & Crismaru *et al.,* 2012). This notation is more generally applicable than using L(arge) and S(mall) pocket (Shin *et al.,* 2002), since the size of a pocket at a topologically conserved position may vary, whereas the O-pocket and the P-pocket are topologically fixed (**Fig. 3.6**).

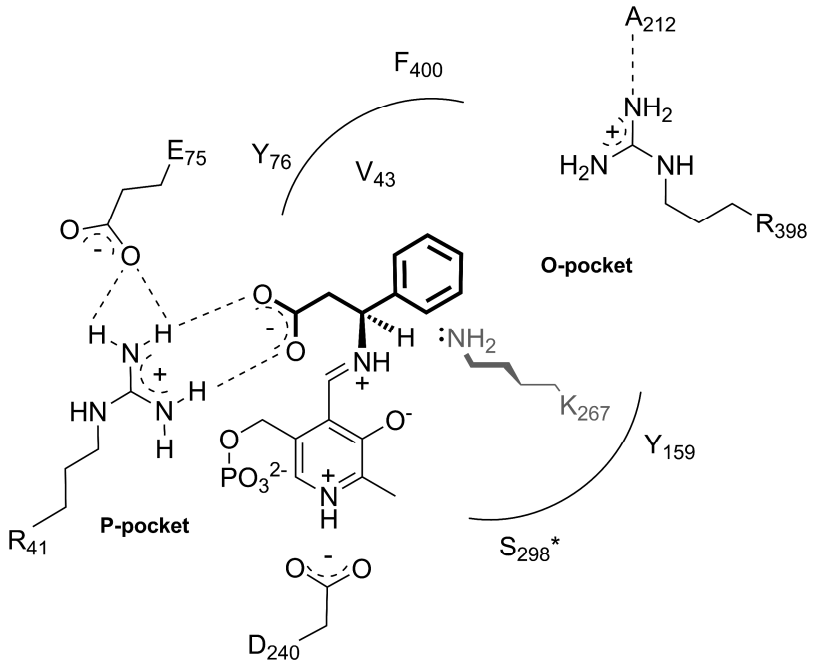

Figure 3.6 Schematic representation of (*S*)-*β*-phenylalanine (structure in bold) bound to PLP (external aldimine) docked in the active site of *Vp*AT. A number of relevant amino acid residues for binding and catalysis are shown.

Computer-aided docking of (*S*)-*β*-phenylalanine suggested binding of *β*-phenylalanine with the carboxylate group in the P-pocket, which is opposite to the binding mode of the α-phenylalanine analogue 3-phenylpropionate in the active site of aromatic amino acid aminotransferase from *Paracoccus denitrificans* (PDB code: 1AY8) (Okamoto *et al.,* 1998), but similar to the binding mode of *β*-phenylalanine in *Mes*AT (Wybenga & Crismaru *et al.,* 2012). The docking results further indicated that

several residues in the O-pocket, including R398, must rearrange to enable binding of the phenyl ring of *β*-phenylalanine (**Fig. 3.5C**). This switch was also observed for *Mes*AT complexed with (*S*)-*β*-phenylalanine (PDB code: 2YKY) and 2-oxoglutarate (PDB code: 2YKX), and appears necessary to allow binding of both the phenyl group of (*S*)-*β*-phenylalanine AT and the α-carboxylate of 2-oxoglutarate (Wybenga & Crismaru *et al.,* 2012). In class I ATs accepting aromatic *α*-amino acids, a so-called arginine switch has also been identified (e.g. R292 in AroAT), but here the arginine switch and co-substrate non-*α*-carboxylate binding site are located in the P-pocket, in agreement with reverse mode of substrate binding of *β*-Phe in *Vp*AT and *Mes*AT as compared to α-phenylalanine in AroAT (Eliot *et al.,* 2004). The docking further indicated that the *para*- and *meta*-positions of the phenyl ring are solvent exposed while the *ortho* position is buried in the O-pocket of the protein (**Fig. 3.5C**). This is in agreement with the observed higher catalytic activities for substrates substituted at the *para*- and *meta*-positions relative to *ortho*-substituted substrates (**Table 3.2, entries 4-7**), for which steric hindrance by S298* (monomer B) and Y76 may prevent productive binding (**Fig. 3.5C**). The importance of steric crowding at the *ortho* position is confirmed by the relatively high activity with the *ortho*-fluorine substituted substrate as compared to the compounds with larger substituents, *i.e.* chlorine and bromine (**Table 3.2, entries 5-7**). Thus, it appears that the substrate specificity of *Vp*AT with regard to substituted *β*-phenylalanine derivatives is mainly determined by the residues that line the hydrophobic O-pocket.

A sequence motif for aromatic *β*-amino acid aminotransferases

A combination of sequence analysis, structural data and information on substrate range may be used to define aminotransferase sequence motifs that can be applied to identify enzymes with certain substrate specificity (Hohne *et al.,* 2010). As observed in the *Vp*AT structure bound with AOA (**Fig. 3.5A, B**), as well as in the modeled *Vp*AT-(*S*)-*β*-phenylalanine structure (**Fig. 3.5C**), residues R41 in loop1 and E75 in loop2 of the NC-domain contribute to shaping the carboxylate binding site for *β*-amino acids in the P-pocket. For this reason, and also taking into account that E75 is conserved in *Mes*AT and *Po*GSAM but not in *Se*GSAM (**Fig. 3.1**), we used the conserved functional P-pocket R41/E75 pair as the starting point to identify a motif that may distinguish aminotransferases with activity towards aromatic *β*-amino acids from aminotransferases with a similar fold but a different activity. Extension of the R41/E75 motif with residues selected on the basis of sequence conservation or position in the structure yielded a motif R-X-[AVI]-X(6)-P-X(14)-D-G-X(8)-[EDNQ]-[YFW] that comprises 36 residues in the N-terminal segment of the NC domain. When

used to screen a set of over 2,200 (putative) class I aminotransferases, it allowed the selection of 46 sequences (Supplemental Material, **Table S2**), among which the sequences of the conserved *β*-selective enzymes *Vp*AT, *Mes*AT and *Po*GSAM. Although several retrieved sequences have been annotated as glutamate-1-semialdehyde 2,1-aminomutase (Supplemental Material, **Table S2**), we propose that the sequences selected by the motif are ATs with activity towards aromatic *β*-amino acids. Although our motif may be applied to identify aminotransferases in a set of fold type I aminotransferases it can probably not predict *β*-aminotransferase activity in less related sequences or enzymes lacking activity with aromatic substrates. For example, *Ad*bpAT (Yun *et al.,* 2004), which is inactive with aromatic *β*-amino acids and has an opposite enantiopreference for aliphatic *β*-amino acids as compared to *Vp*AT (**Table 3.2**) and *Mes*AT (Kim *et al.,* 2007), is not covered by the motif. This may suggest that *Ad*bpAT belongs to a different phylogenetic cluster and may have a different mode of substrate binding.

Outlook

Although more experiments or structure and modeling studies are needed, we are confident that the newly discovered *β*-phenylalanine aminotransferase from *V. paradoxus* strain CBF3, along with its promising biocatalytic properties and its 3D structure, is an attractive template for future *β*-aminotransferase engineering efforts towards the synthesis of enantiomerically pure *β*-amino acids.

Acknowledgements

We thank Dr. O. May and Dr. B. Kaptein from DSM for helpful discussions. This research was financially supported by the Netherlands Ministry of Economic Affairs and the B-Basic partner organizations (www.b-basic.nl) through B-Basic, a public-private NWO-ACTS programme. The work of S. Bartsch was supported by the EU FP7 under Grant Agreement Number 266025 (BIONEXGEN). Hein J. Wijma was supported by NWO (Netherlands Organization for Scientific Research) through an ECHO grant. We acknowledge the European Synchrotron Radiation Facility (ESRF) for provision of synchrotron radiation facilities and thank the beamline staff of ID14-4 for their assistance.

References

Bailey, S. (1994 The CCP4 Suite - programs for protein crystallography. *Acta Crystallogr Sect D: Biol Crystallogr* 50: 760–763.

Bea, H.S., Park, H.J., Lee, S.H. and Yun, H. (2011) Kinetic resolution of aromatic beta-amino acids by omega-transaminase. *Chem Commun* 47: 5894–5896.

Brady, O.L.E.G. (1926) The use of 2:4-dinitrophenylhydrazine as a reagent for aldehydes and ketones. *Analyst* 51: 77–78.

Burley, S.K., David, P.R. and Lipscomb, W.N. (1991) Leucine aminopeptidase: bestatin inhibition and a model for enzyme-catalyzed peptide hydrolysis. *Proc Natl Acad Sci* 88: 6916–6920.

Chen, V.B., Arendall, W.B., Headd, J.J., Keedy, D.A., Immormino, R.M., Kapral, G.J., Murray, L.W., Richardson, J.S. and Richardson, D.C. (2010) MolProbity: all-atom structure validation for macromolecular crystallography. *Acta Crystallogr Sect D: Biol. Crystallogr* 66: 12–21.

Chirpich, T.P., Zappia, V., Costilow, R.N. and Barker, H.A. (1970) Lysine 2,3-aminomutase. Purification and properties of a pyridoxal phosphate and S-adenosylmethionine-activated enzyme. *J Biol Chem* 245: 1778–1789.

Christen, P., and Metzler, D.E. (1985) *Transaminases*. Wiley, New York.

Christen, P., and Mehta, P. (2001) From cofactor to enzymes. The molecular evolution of pyridoxal-5'-phosphate-dependent enzymes. *Chem Rec* 1: 436–447.

Christianson, C.V., Montavon, T.J., Festin, G.M., Cooke, H.A., Shen, B. and Bruner, S.D. (2007) The mechanism of MIO-based aminomutases in beta-amino acid biosynthesis. *J Am Chem Soc* 129: 15744–15745.

Crews, P., Manes, L.V. and Boehler, M. (1986) Jasplakinolide, a cyclodepsipeptide from the marine sponge, *Jaspis* sp. *Tetrahedron Lett* 27: 2797–2800.

Cronan, J. E., Jr. (1980) Beta-alanine synthesis in *Escherichia coli*. *J Bacteriol* 141: 1291–1297.

Davis, I.W. and Baker, D. (2009[a]) RosettaLigand docking with full ligand and receptor flexibility. *J Mol Biol* 385: 381–392.

Davis, I.W., Raha, K., Head, M.S. and Baker, D. (2009[b]) Blind docking of pharmaceutically relevant compounds using RosettaLigand. *Prot Sci* 18: 1998–2002.

Drummond, A.J., Buxton, A.B.S., Cheung, M., Cooper, A., Duran, C., Field, M., Heled, J., Kearse, M., Markowitz, S., Moir, R., Stones-Havas, S., Sturrock, S., Thierer, T. and Wilson, A. (2010) Geneious v5.5, 5.5.3 ed.

Eliot, A.C. and Kirsch, J.F. (2004) Pyridoxal phosphate enzymes: mechanistic, structural, and evolutionary considerations. *Annu Rev Biochem* 73: 383–415.

Emsley, P. and Cowtan, K. (2004) Coot: model-building tools for molecular graphics. *Acta Crystallogr Sect D: Biol Crystallogr* 60: 2126–2132.

Evans, P. (2006) Scaling and assessment of data quality. *Acta Crystallogr Sect D: Biol Crystallogr* 62: 72–82.

Finn, R.D., Mistry, J., Tate, J., Coggill, P., Heger, A., Pollington, J.E., Gavin, O.L., Gunasekaran, P., Ceric, G., Forslund, K., Holm, L., Sonnhammer, E.L., Eddy, S.R. and Bateman, A. (2010) The Pfam protein families database. *Nuc Acids Res* 38: D211–222.

Gabor, E., de Vries, E. and Janssen, D.B. (2004) Construction, characterization, and use of small-insert gene banks of DNA isolated from soil and enrichment cultures for the recovery of novel amidases. *Environ Microbiol* 6: 948–958.

Geueke, B., and Kohler, H. (2007) Bacterial beta-peptidyl aminopeptidases: on the hydrolytic degradation of beta-peptides. *Appl Microbiol Biotechnol* 74: 1197–1204.

Grishin, N.V., Phillips, M.A. and Goldsmith, E.J. (1995) Modeling of the spatial structure of eukaryotic ornithine decarboxylases. *Prot Sci* 4: 1291–1304.

Han, J.I., Choi, H.K., Lee, S.W., Orwin, P.M., Kim, J., Laroe, S.L., Kim, T.G., O'Neil, J., Leadbetter, J.R., Lee, S.Y., Hur, C.G., Spain, J.C., Ovchinnikova, G., Goodwin, L. and Han, C. (2011) Complete genome sequence of the metabolically versatile plant growth-promoting endophyte *Variovorax paradoxus* S110. *J Bacteriol* 193: 1183–1190.

Hill, D.W., Walters, F.H., Wilson, T.D. and Stuart, J.D. (1979) High performance liquid chromatographic determination of amino acids in the picomole range. *Anal Chem* 51: 1338–1341.

Hohne, M., Schatzle, S., Jochens, H., Robins, K. and Bornscheuer, U.T. (2010) Rational assignment of key motifs for function guides in silico enzyme identification. *Nat Chem Biol* 6: 807–813.

Holm, L. and Rosenstrom, P. (2010) Dali server: conservation mapping in 3D. *Nuc Acids Res* 38: W545–549.

Hwang, B.Y., Cho, B.K., Yun, H., Koteshwar, K. and Kim, B.G. (2005) Revisit of aminotransferase in the genomic era and its application to biocatalysis. *J Mol Catal B: Enzym* 37: 47–55.

Janssen, D.B., Scheper, A. and Witholt, B. (1984) Biodegradation of 2-chloroethanol and 1,2-dichloroethane by pure bacterial cultures. *Prog Ind Microbiol* 20: 169–178.

John, R.A. and Charteris, A. (1978) The reaction of amino-oxyacetate with pyridoxal phosphate-dependent enzymes. *Biochem J* 171: 771–779.

Juaristi, E., and V. Soloshonok. 2005. Enantioselective synthesis of β-amino acids. Wiley-VHC, New York.

Kabsch, W. (2010) Integration, scaling, space-group assignment and post-refinement. *Acta Crystallogr Sect D: Biol Crystallogr* 66: 133–144.

Kim, J., Kyung, D., Yun, H., Cho, B.K. and Kim, B.G. (2006) Screening and purification of a novel transaminase catalyzing the transamination of aryl beta-amino acid from *Mesorhizobium* sp LUK. *J Microbiol Biotechnol* 16: 1832–1836.

Kim, J., Kyung, D., Yun, H., Cho, B.K., Seo, J.H., Cha, M. and Kim, B.G. (2007) Cloning and characterization of a novel beta-transaminase from *Mesorhizobium* sp. strain LUK: a new biocatalyst for the synthesis of enantiomerically pure beta-amino acids. *Appl Environ Microbiol* 73: 1772–1782.

Kleywegt, G.J. and Jones, T.A. (1998) Databases in protein crystallography. *Acta Crystallogr Sect D: Biol Crystallogr* 54: 1119–1131.

Koszelewski, D., Lavandera, I., Clay, D., Guebitz, G.M., Rozzell, D. and Kroutil, W. (2008) Formal asymmetric biocatalytic reductive amination. *Angew Chem Int Ed* 47: 9337–9340.

Koszelewski, D., Tauber, K., Faber, K. and Kroutil, W. (2010) omega-Transaminases for the synthesis of non-racemic alpha-chiral primary amines. *Trends Biotechnol* 28: 324–332.

Krieger, E., Koraimann, G. and Vriend, G. (2002) Increasing the precision of comparative models with YASARA NOVA--a self-parameterizing force field. *Proteins* 47: 393–402.

Krissinel, E., and Henrick, K. (2007) Inference of macromolecular assemblies from crystalline state. *J Mol Biol* 372: 774–797.

Langer, G., Cohen, S.X., Lamzin, V.S. and Perrakis, A. (2008) Automated macromolecular model building for X-ray crystallography using ARP/wARP version 7. *Nat Protoc* 3: 1171–1179.

Liljeblad, A., and Kanerva, L.T. (2006) Biocatalysis as a profound tool in the preparation of highly enantiopure beta-amino acids. *Tetrahedron* 62: 5831–5854.

Lowe, P.N., and Rowe, A.F. (1985) Aspartate-2-oxoglutarate aminotransferase from *Trichomonas vaginalis* - Identity of aspartate-aminotransferase and aromatic amino-acid aminotransferase. *Biochem J* 232: 689–695.

Markovic-Housley, Z., Schirmer, T., Hohenester, E., Khomutov, A.R., Khomutov, R.M., Karpeisky, M.Y., Sandmeier, E., Christen, P. and Jansonius, J.N. (1996) Crystal structures and solution studies of oxime adducts of mitochondrial aspartate aminotransferase. *Eur J Biochem* 236: 1025–1032.

McCoy, A.J., Grosse-Kunstleve, R.W., Adams, P.D., Winn, M.D., Storoni, L.C. and Read, R.J. (2007) Phaser crystallographic software. *J Appl Crystallogr* 40: 658–674.

Mehta, P.K., Hale, T.I. and Christen, P. (1993) Aminotransferases - demonstration of homology and division into evolutionary subgroups. *Eur J Biochem* 214: 549–561.

Mekhail, T.M., and Markman, M. (2002) Paclitaxel in cancer therapy. *Expert Opin Pharmacother* 3: 755–766.

Murshudov, G.N., Vagin, A.A. and Dodson, E.J. (1997) Refinement of macromolecular structures by the maximum-likelihood method. *Acta Crystallogr Sect D: Biol Crystallogr* 53: 240–255.

Nowicki, C., Hunter, G.R., Montemartini-Kalisz, M., Blankenfeldt, W., Hecht, H. and Kalisz, H.M. (2001) Recombinant tyrosine aminotransferase from *Trypanosoma cruzi*: structural characterization and site directed mutagenesis of a broad substrate specificity enzyme. *Biochim Biophys Acta* 1546: 268–281.

Ojima, I., Lin, S. and Wang, T. (1999) Recent advances in the medicinal chemistry of taxoids with novel beta-amino acid side chains. *Curr Med Chem* 6: 927–954.

Okamoto, A., Nakai, Y., Hayashi, H., Hirotsu, K. and Kagamiyama, H. (1998) Crystal structures of *Paracoccus denitrificans* aromatic amino acid aminotransferase: a substrate recognition site constructed by rearrangement of hydrogen bond network. *J Mol Biol* 280: 443–461.

OpenEye Scientific Software, Inc. (2010) OEChem TK Programming Library for Chemistry and Cheminformatics. Santa Fe, New Mexico, USA.

Percudani, R., and Peracchi, A. (2009) The B6 database: a tool for the description and classification of vitamin B6-dependent enzymatic activities and of the corresponding protein families. *BMC Bioinformatics* 10: 273.

Poelarends, G.J., Wilkens, M., Larkin, M.J., van Elsas, J.D. and Janssen, D.B. (1998) Degradation of 1,3-dichloropropene by *Pseudomonas ccichorii* 170. *Appl Environ Microbiol* 64: 2931–2936.

Rehdorf, J., Mihovilovic, M.D. and Bornscheuer, U.T. (2010) Exploiting the regioselectivity of Baeyer-Villiger monooxygenases for the formation of beta-amino acids and beta-amino alcohols. *Angew Chem Int Ed* 49: 4506–4508.

Richter, F., Leaver-Fay, A., Khare, S.D., Bjelic, S. and Baker, D. (2011) De Novo enzyme design using Rosetta3. *Plos One* 6: e19230.

Rozzell, J.D. (1985) Production of amino acids by transamination. U.S. patent 4518692.

Rudat, J., Brucher, B.R. and Syldatk, C. (2012) Transaminases for the synthesis of enantiopure beta-amino acids. *AMB Express* 2: 11.

Ruzicka, F.J. and Frey, P.A. (2007) Glutamate 2,3-aminomutase: a new member of the radical SAM superfamily of enzymes. *Biochim Biophys Acta* 1774: 286–296.

Sambrook, J.R.D. (2001) Molecular cloning: A laboratory manual 3rd edition. Cold Spring Harbor Laboratory, New York.

Schneider, G., Kack, H. and Lindqvist, Y. (2000) The manifold of vitamin B6 dependent enzymes. *Structure* 8: R1–6.

Schuttelkopf, A.W. and van Aalten, D.M. (2004) PRODRG: a tool for high-throughput crystallography of protein-ligand complexes. *Acta Crystallogr Sect D: Biol Crystallogr* 60: 1355–1363.

Seebach, D., Beck, A. and Bierbaum, D. (2004) The world of beta- and gamma-peptides comprised of homologated proteinogenic amino acids and other components. *Chem Biodiv* 1: 1111–1239.

Shih, C., Gossett, L.S., Gruber, J.M., Grossman, C.S., Andis, S.L., Schultz, R.M., Worzalla, J.F., Corbett, T.H. and Metz, J.T. (1999) Synthesis and biological evaluation of novel cryptophycin analogs with modification in the beta-alanine region. *Bioorg Med Chem Lett* 9: 69–74.

Shin, J.S. and Kim, B.G. (2001) Comparison of the omega-transaminases from different microorganisms and application to production of chiral amines. *Biosci Biotechnol Biochem* 65: 1782–1788.

Shin, J.S., and Kim, B.G. (2002) Exploring the active site of amine: pyruvate aminotransferase on the basis of the substrate structure-reactivity relationship: How the enzyme controls substrate specificity and stereo selectivity. *J Org Chem* 67: 2848–2853.

Shin, J.S., Yun, H., Jang, J.W., Park, I. and Kim, B.G. (2003) Purification, characterization, and molecular cloning of a novel amine:pyruvate transaminase from *Vibrio fluvialis* JS17. *Appl Microbiol Biotechnol* 61: 463–471.

Sievers, F., Wilm, A., Dineen, D., Gibson, T.J., Karplus, K., Li, W.Z., Lopez, R., McWilliam, H., Remmert, M., Soding, J., Thompson, J.D. and Higgins, D.G. (2011) Fast, scalable generation of high-quality protein multiple sequence alignments using Clustal Omega. *Mol Syst Biol* 7: 539.

Staskawicz, B., Dahlbeck, D., Keen, N. and Napoli, C. (1987) Molecular characterization of cloned avirulence genes from race 0 and race 1 of *Pseudomonas syringae* pv. *glycinea*. *J Bacteriol* 169: 5789–5794.

Stetefeld, J., Jenny, M. and Burkhard, P. (2006) Intersubunit signaling in glutamate-1-semialdehyde-aminomutase. *Proc Natl Acad Sci* 103: 13688–13693.

Stewart, J.D. (2001) Dehydrogenases and transaminases in asymmetric synthesis. *Curr Opin Chem Biol* 5: 120–129.

Stirling, D.I. (1992) The use of aminotransferases for the production of chiral amino acids and amines. In A. N. Collins, G. N. Sheldrake, and J. Crosby (ed.), Chirality in industry. Wiley, New York.

Sung, M.H., Tanizawa, K., Tanaka, H., Kuramitsu, S., Kagamiyama, H. and Soda, K. (1990) Purification and characterization of thermostable aspartate-aminotransferase from a thermophilic *Bacillus* species. *J Bacteriol* 172: 1345–1351.

Szymanski, W., Wu, B., Weiner, B., de Wildeman, S., Feringa, B.L. and Janssen, D.B. (2009) Phenylalanine aminomutase-catalyzed addition of ammonia to substituted cinnamic acids: a route to enantiopure alpha- and beta-amino acids. *J Org Chem* 74: 9152–9157.

Taylor, P.P., Pantaleone, D.P., Senkpeil, R.F. and Fotheringham, I.G. (1998) Novel biosynthetic approaches to the production of unnatural amino acids using transaminases. Trends Biotechnol 16: 412–418.

Tipton, K.F. (1996) Patterns of enzyme inhibition. In P. C. Engel (ed.). Enzymology. LABFAX. Academic Press, San Diego, CA.

Weiner, B., Szymanski, W., Janssen, D.B., Minnaard, A.J. and Feringa, B.L. (2010) Recent advances in the catalytic asymmetric synthesis of beta-amino acids. *Chem Soc Rev* 39: 1656–1691.

Woese, C.R. (1987) Bacterial evolution. *Microbiol Rev* 51: 221–271.

Wu, B., Szymanski, W., Heberling, M.M., Feringa, B.L. and Janssen, D.B. (2011) Aminomutases: mechanistic diversity, biotechnological applications and future perspectives. *Trends Biotechnol* 29: 352–362.

Wu, B., Szymanski, W., Crismaru, C.G., Feringa, B.L. and Janssen, D.B. (2010) C-N lyases catalyzing addition of ammonia, amines and amides to C=C and C=O bonds. *Enzyme Catalysis in Organic Synthesis* (Wiley-VCH Ed.).

Wybenga, G.G., Crismaru, C.G., Janssen, D.B. and Dijkstra, B.W. (2012) Structural determinants of the beta-selectivity of a bacterial aminotransferase. *J Biol Chem* 287: 28495–28502.

Yonaha, K., Suzuki, K., Minei, H. and Toyama, S. (1983) Distribution of omega-amino acid - pyruvate transaminase and aminobutyrate - alpha-ketoglutarate transaminase in microorganisms. *Agr Biol Chem* Tokyo 47: 2257–2265.

Yun, H., Lim, S., Cho, B.K. and Kim, B.G. (2004) omega-Amino acid:pyruvate transaminase from *Alcaligenes denitrificans* Y2k-2: a new catalyst for kinetic resolution of beta-amino acids and amines. *Appl Environ Microbiol* 70:2529–2534.

Zhang, Z., Schwartz, S., Wagner, L. and Miller, W. (2000) A greedy algorithm for aligning DNA sequences. J Comput Biol 7: 203–214.

Supplemental Material

Biochemical properties and crystal structure of a *β*-phenylalanine aminotransferase from *Variovorax paradoxus*

Ciprian G. Crismaru,[a,#] Gjalt G. Wybenga,[b,#] Wiktor Szymanski,[c] Hein J. Wijma,[a] Bian Wu,[a] Sebastian Bartsch,[a] Stefaan de Wildeman,[d] Gerrit J. Poelarends,[e] Ben L. Feringa,[c] Bauke W. Dijkstra[b] and Dick B. Janssen[a,]

[a]*Department of Biochemistry,* [b]*Laboratory of Biophysical Chemistry, Groningen Biomolecular Science and Biotechnology Institute,* [c]*Center for Systems Chemistry, Stratingh Institute for Chemistry, University of Groningen, The Netherlands,* [d]*DSM Pharmaceutical Products, Geleen, The Netherlands,* [e]*Department of Pharmaceutical Biology, Groningen Research Institute of Pharmacy, University of Groningen, The Netherlands*

[#] These two authors contributed equally to this study.

Table S1. Data collection and refinement statistics of *Vp*AT crystal structures.

Parameters	*Vp*AT holo	*Vp*AT + AOA
Beamline	ID14-4	ID14-4
Data collection		
Resolution (Å) [a]	46.42-1.5 (1.58-1.5)	66.31-2.28 (2.4-2.28)
Space group	$P2_12_12_1$	$P2_12_12_1$
Cell dimensions		
a, b, c (Å)	88.74, 100.1, 104.8	88.67, 99.88, 104.7
R_{merge} [b]	0.043 (0.136)	0.095 (0.158)
Wavelength (Å)	0.9395	0.9395
I/σ (*I*)	21.9 (9.3)	10.9 (7.5)
Completeness (%)	99.7 (100.0)	99.8 (99.8)
No. unique reflections	148964 (21628)	43283 (6220)
Multiplicity	4.8	4.0
Refinement		
Resolution (Å)	1.5	2.3
R_{work} [c]	0.17	0.18
R_{free} [d]	0.18	0.23
Rmsd		
Bond lengths (Å)	0.08	0.08
Bond angles (^{o})	1.22	1.11
Ramachandran (Molprobity)		
Favored (%)	98	97.0
Outliers (%)	0.0	0.0
PDB code	4AO9	4AOA

[a] Values in the parentheses are for the highest resolution shell.
[b] $R_{merge} = \Sigma_h\Sigma_i |I(h)_i - \langle I(h)\rangle| / \Sigma_h\Sigma_i \langle I(h)_i\rangle$, where I is the observed intensity and $\langle I\rangle$ is the average intensity of multiple observations of symmetry-related reflections.
[c] $R_{work} = \Sigma_h||F_{obs}| - |F_{calc}|| / \Sigma_h|F_{obs}|$, where $|F_{obs}|$ and $|F_{calc}|$ are the observed and calculated structure factor amplitudes, respectively.
[d] R_{free} is calculated as R_{work} using 5 % of all reflections randomly chosen and excluded from structure calculation and refinement.

Table S2. List of putative aromatic *β*-amino acid aminotransferases.

no	NCBI reference sequence	annotation	strain	seq. id.
1	CCF34891	aminotransferase class-III	*Colletotrichum* higginsianum	41
2	EFQ30679	aminotransferase class-III	*Glomerella graminicola* M1.001	41
3	EFW16762	conserved hypothetical protein	*Coccidioides posadasii* str. Silveira	39
4	EFW99062	aminotransferase class 3	*Grosmannia clavigera* kw1407	38
5	EFZ00111	glutamate-1-semialdehyde 2,1-aminomutase, putative	*Metarhizium anisopliae* ARSEF 23	42
6	EGU77831	hypothetical protein FOXB_11695	*Fusarium oxysporum* Fo5176	44
7	EGX43269	hypothetical protein AOL_s00215g5	*Arthrobotrys oligospora* ATCC 24927	38
8	EGX48176	hypothetical protein AOL_s00081g39	*Arthrobotrys oligospora* ATCC 24927	42
9	EGY14282	glutamate-1-semialdehyde 2,1-aminomutase	*Verticillium dahliae* VdLs.17	41
10	EHA25332	hypothetical protein ASPNIDRAFT_186860	*Aspergillus niger* ATCC 1015	37
11	EHK26440	hypothetical protein TRIVIDRAFT_36134	*Trichoderma virens* Gv29-8	43
12	EHK45279	hypothetical protein TRIATDRAFT_138933	*Trichoderma atroviride* IMI 206040	40
13	EIM84416	aminotransferase class-III	*Stereum hirsutum* FP-91666 SS1	49
14	GAA86562	aminotransferase class-III	*Aspergillus kawachii* IFO 4308	37
15	GAA93170	aminotransferase class-III	*Aspergillus kawachii* IFO 4308	37
16	XP_001218204	predicted protein	*Aspergillus terreus* NIH2624	37
17	XP_001248198	hypothetical protein CIMG_01969	*Coccidioides immitis* RS	40
18	XP_001824703	acetylornithine aminotransferase	*Aspergillus oryzae* RIB40	41
19	XP_001930822	glutamate-1-semialdehyde 2,1-aminomutase	*Pyrenophora tritici-repentis* Pt-1C-BFP	39
20	XP_002145750	glutamate-1-semialdehyde 2,1-aminomutase, putative	*Penicillium marneffei* ATCC 18224	33
21	XP_002150372	glutamate-1-semialdehyde 2,1-aminomutase, putative	*Penicillium marneffei* ATCC 18224	43
22	XP_002383909	acetylornithine aminotransferase, putative	*Aspergillus flavus* NRRL3357	41
23	XP_002483365	acetylornithine aminotransferase, putative	*Talaromyces stipitatus* ATCC 10500	38
24	XP_003040355	hypothetical protein NECHADRAFT_34859	*Nectria haematococca* mpVI 77-13-4	39

Table S2. List of putative aromatic *β*-amino acid aminotransferases (*continued*).

no	NCBI reference sequence	annotation	strain	seq. id.
25	XP_003065334	aminotransferase class III family protein	*Coccidioides posadasii* C735 delta SOWgp	39
26	XP_003295515	hypothetical protein PTT_01400	*Pyrenophora teres f. teres* 0-1	39
27	XP_003711910	glutamate-1-semialdehyde 2,1-aminomutase	*Magnaporthe oryzae* 70-15	39
28	XP_381362	hypothetical protein FG01186.1	*Gibberella zeae* PH-1	42
29	YP_001862264	class III aminotransferase	*Burkholderia phymatum* STM815	55
30	YP_001890102	class III aminotransferase	*Burkholderia phytofirmans* PsJN	58
31	YP_002944294	class III aminotransferase	*Variovorax paradoxus* S110	87
32	YP_003481853	aminotransferase class-III	*Natrialba magadii* ATCC 43099	35
33	YP_004154921	class III aminotransferase	*Variovorax paradoxus* EPS	87
34	YP_004978979	class III aminotransferase	*Burkholderia sp.* YI23	56
35	YP_006397172	glutamate-1-semialdehyde 2,1-aminomutase	*Sinorhizobium fredii* USDA 257	43
36	ZP_02187576	aminotransferase class-III	*alpha proteobacterium* BAL199	50
37	ZP_02885261	aminotransferase class-III	*Burkholderia graminis* C4D1M	56
38	ZP_06895587	possible glutamate-1-semialdehyde 2,1-aminomutase	*Roseomonas cervicalis* ATCC 4995	42
39	ZP_07281103	glutamate-1-semialdehyde 2,1-aminomutase	*Streptomyces* sp. AA4	41
40	ZP_07777755	aminotransferase class-III	*Pseudomonas fluorescens* WH6	52
41	ZP_08528159	threonine dehydratase	*Agrobacterium* sp. ATCC 31749	27
42	ZP_09395248	glutamate-1-semialdehyde 2,1-aminomutase	*Acetobacteraceae bacterium* AT-5844	50
43	ZP_10156387	class III aminotransferase	*Hydrogenophaga* sp. PBC	50
44	ZP_10393152	glutamate-1-semialdehyde aminotransferase	*Acidovorax* sp. CF316	56
45	ZP_10477025	class III aminotransferase	*Pseudomonas* sp. Ag1	54
46	ZP_10571586	glutamate-1-semialdehyde aminotransferase	*Variovorax* sp. CF313	90

Seq. id. = percentage sequence identity to the protein sequence of *Vp*AT.

Chapter 4

Structural determinants of the *β*-selectivity of a bacterial aminotransferase

Gjalt G. Wybenga[1,a], Ciprian G. Crismaru[2,a], Dick B. Janssen[2] and Bauke W. Dijkstra[1,*]

[1]*Laboratory of Biophysical Chemistry, University of Groningen, Nijenborgh 7, 9747 AG Groningen, The Netherlands and*
[2]*Department of Biochemistry, University of Groningen, Nijenborgh 4, 9747 AG Groningen, The Netherlands*

Background: *β*-Transaminases are promising biocatalysts for the synthesis of *β*-amino acids.
Results: First 3D structures were obtained of a native *β*-transaminase, and complexes with a keto-acid and two covalently bound *β*-amino acids.
Conclusion: Dual functionality of the carboxylate and side-chain binding pockets allows binding of *β*- and *α*-amino acids.
Significance: These structures may facilitate the development of improved *β*-amino acid biocatalysts.

[a] These two authors contributed equally to this study.

Published in *Journal of Biological Chemistry* (2012) 287: 28495–28502.

Abstract

Chiral *β*-amino acids occur as constituents of various natural and synthetic compounds with potentially useful bioactivities. The pyridoxal-5'-phosphate dependent (*S*)-selective transaminase from *Mesorhizobium* sp. LUK (*Mes*AT) is a fold type I aminotransferase that can be used for the preparation of enantiopure *β*-phenylalanine and derivatives thereof. Using X-ray crystallography, we solved structures of *Mes*AT in complex with (*S*)-*β*-phenylalanine, (*R*)-3-amino-5-methylhexanoic acid, 2-oxoglutarate, and the inhibitor 2-aminooxyacetic acid, which allowed us to unveil the molecular basis of the amino acid specificity and enantioselectivity of this enzyme. The binding pocket of the side chain of a *β*-amino acid is located on the 3'-O side of the PLP cofactor. The same binding pocket is utilized by *Mes*AT to bind the *α*-carboxylate group of an *α*-amino acid. A *β*-amino acid thus binds in a reverse orientation in the active site of *Mes*AT as compared to an *α*-amino acid. Such a binding mode has not been reported before for any PLP-dependent aminotransferase and shows that the active site of *Mes*AT has specifically evolved to accommodate both *β*- and *α*-amino acids.

Introduction

β-Amino acids occur as precursors of many natural and synthetic compounds that display a wide range of pharmacological activities. Altering and improving the pharmacological properties of these compounds critically depends on the availability of *β*-amino acids and their derivatives as building blocks. Therefore, several strategies for the synthesis of *β*-amino acids have been explored over the years, involving either synthetic (Cole *et al.,* 1994; Weiner *et al.,* 2010) or combined chemo-enzymatic (Liljeblad et al., 2006) methods. However, fully enzyme-based synthesis methods have clear advantages over synthetic or chemo-enzymatic methods (Koeller *et al.,* 2001) and have the potential to increase the feasibility of biocatalytic or fermentative routes towards *β*-amino compounds.

Pyridoxal-5'-phosphate (PLP) dependent aminotransferases (also called transaminases) are attractive for the production of amino acids since they have a broad substrate range, can be highly enantioselective, show a high catalytic activity, and are relatively stable (Taylor *et al.,* 1998). Aminotransferases catalyze the transfer of an amino group from an amino compound to a keto-acid. In the first half reaction, the amino group of the amino compound substitutes the covalent Schiff base linkage, or imine bond, between the ε-amino group of a lysine and the C4A-atom of the PLP cofactor, generating an external aldimine (**Fig. 4.1**). Lysine-assisted transfer of a proton from the external aldimine to the C4A-atom of the cofactor results in a ketimine intermediate, which is hydrolyzed to yield pyridoxamine-5'-phosphate (PMP). Subsequently, in the second half reaction, the amino group of PMP is transferred to a keto-acid which generates a new amino compound (**Fig. 4.1**) (Braunstein *et al.,* 1964).

The production of *β*-amino acids using PLP-dependent aminotransferases has been demonstrated for an ω-transaminase from *Polaromonas* sp. JS666 (Bea *et al.,* 2011) and a *β*-transaminase from *Mesorhizhobium* sp. LUK (*Mes*AT) (Kim *et al.,* 2007). The genes of these two enzymes were successfully cloned and expressed in *E. coli* BL21(DE3) using pET-based expression systems (Bea *et al., 2011*; Kim *et al.,* 2007) and *Mes*AT has been crystallized (Kim *et al.,* 2011).

*Mes*AT is an enzyme of 445 amino acids with an M_r of 45 kDa, which forms dimers in solution and which accepts *β*- as well as *α*-amino acids (Kim *et al.,* 2007; Kim *et al.,* 2006). The enzyme can convert the aliphatic *β*-amino acids (*R*)-3-amino-5-methylhexanoic acid and (*R*)-3-aminobutyric acid as well as the aromatic *β*-amino acid (*S*)-*β*-phenylalanine ((*S*)-*β*-Phe) to the corresponding *β*-keto acids using pyruvate or 2-oxoglutarate as the amino-acceptor.

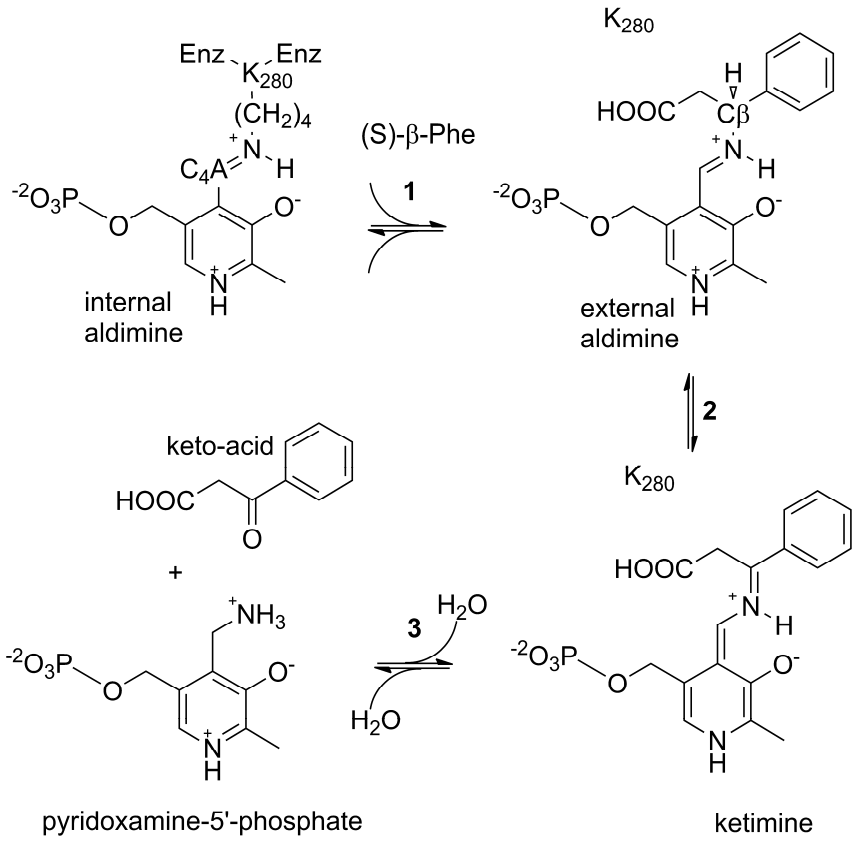

Figure 4.1 Half reactions catalyzed by *Mes*AT, a *β*-specific PLP-dependent transaminase. An amino acid ((*S*)-*β*-Phe) enters the active site of the enzyme (**1**) and an external aldimine is generated. K280, a base, abstracts the C*β*-proton (**2**) and transfers the proton to the C4A-atom (1,3-prototropic shift, not shown), which results in the ketimine intermediate. Hydrolysis of the ketimine intermediate results in the formation of pyridoxamine-5′-phosphate (PMP) and a keto-acid (3-oxo-3-phenylpropanoic acid) (**3**).

In the reverse reaction, *Mes*AT can be used to produce (*S*)-*β*-Phe from its *β*-keto acid esthylester in a coupled enzyme reaction containing a lipase to generate the keto-acid *in situ* and *rac*-3-aminobutyric acid as amino-donor (Kim *et al.,* 2007). Unfortunately, the more stable keto-ester is a very poor substrate for aminotransferase-mediated conversion to (*S*)-*β*-Phe.

Information on 3D-structures of *β*-aminotransferases is currently lacking. To enable rational protein engineering approaches for improving the activity of the enzyme for application in the biosynthesis of *β*-amino acids, we have elucidated the crystal structure of *Mes*AT in the native state, as well as in complex with *β*-amino acids, a keto-acid, and an inhibitor. The structure of the enzyme conforms to a fold type I

aminotransferase structure, but the hydrophobic binding pocket is located on the 3'-O side of the PLP cofactor rather than on its phosphate side as found in other amino-transferases. On the other hand, an *α*-amino acid binds in a normal orientation, with the *α*-carboxylate on the 3'-O side and the side chain of the amino acid on the phosphate side of the PLP cofactor. The architecture of the active site explains how *Mes*AT can accept *β*- as well as *α*-amino acids (Kim *et al.,* 2007), while the aromatic *α*-amino acid aminotransferase (AroAT) (Oue *et al.,* 1997) and most other aminotransferases only accept *α*-amino acids. The structure also explains the stereo-preference of the enzyme for *α*- and *β*-amino acids.

Materials and methods

Protein expression and purification

The *Mes*AT gene was codon optimized for *E. coli*, synthesized by DNA2.0 Inc., and cloned into the expression plasmid pET28b+ with an *N*-terminal His_6-tag using *Nde*I/*Hind*III restriction sites. After transformation into *E. coli* strain BL21(DE3) cells were grown at 37 °C in 1.4 l TBS medium (Terrific Broth Sorbitol) (Barth *et al.,* 2000) containing 50 µg/ml of kanamycin. Protein expression was induced with 0.4 mM IPTG (isopropyl-β-D-1-thiogalactopyranoside) when the optical density of the culture at 600 nm reached 0.6-0.8, and the temperature was adjusted to 17 °C. The cells were grown for another 48 h, then harvested and resuspended in a buffer containing 20 mM Tris-HCl, pH 8.0, 500 mM NaCl, 20 mM imidazole, 1 mg of DNaseI (Roche) and a cOmplete EDTA-free protease inhibitor tablet (Roche). The cells were disrupted at 4 °C by sonication followed by centrifugation for 1 h at 31,000 × g at 4 °C.

The supernatant was applied to a HisTrap HP affinity chromatography column (GE Healthcare) and, after washing, *Mes*AT was eluted with 15 column volumes of a linear gradient of 20 – 500 mM imidazole in elution buffer (20 mM Tris-HCl, pH 8.0, 500 mM NaCl). The fractions corresponding to the peak were pooled and the imidazole was removed by a buffer exchange using a HiPrep 26/10 desalting column (GE Healthcare) equilibrated with 25 mM Tris-HCl, pH 8.0, 0.01% *v/v* β-mercaptoethanol. The resulting protein fractions were applied to a Q-Sepharose HP anion exchange column (GE Healthcare) and eluted with 15 column volumes of a linear gradient of 0 – 1 M NaCl in 25 mM Tris-HCl, pH 8.0. The fractions containing active enzyme were pooled, concentrated (Ultracel 30K MWCO, Amicon) and applied to a Superdex 200 10/300 GL size exclusion chromatography column (GE Healthcare), equilibrated in 20 mM Tris-HCl, pH 8.0, containing 200 mM NaCl. After elution the

fractions corresponding to the protein peak were pooled, concentrated (Amicon) and dialyzed overnight against a buffer containing 20 mM Tris-HCl, pH 7.5. The sample was subsequently concentrated to 10 mg/ml as judged from a protein assay and the purity of the sample was checked with silver-stained SDS-PAGE gels using a Phast system (GE Healthcare).

Mutagenesis

The R412A mutant gene of *Mes*AT was constructed by site-directed mutagenesis (QuikChange kit, Stratagene). Arg412 was mutated to Ala with the primer 5′-ATCTATCTGGCTCCG**GCT**GGTATGTATGCACTGAGC-3′and its complementary primer, 5′-CTCAGTGCATACATACC**AGC**CGGAGCCAGATAGATG-3′ (mutated codon in bold and underlined). The resulting pET28b+ *Mes*AT R412A was transformed into *E. coli* DH5α ElectroMAX electrocompetent cells (Invitrogen). For overexpression *E. coli* BL21(DE3) was used. The mutant construct was confirmed by sequence analysis (GATC Biotech AG, Konstanz, Germany).

Protein crystallization

A Mosquito crystallization robot (TTP LabTech) was used to search for suitable crystallization conditions. Crystallization experiments were set up at 20 °C. Crystals were found in a JCSG+ Suite (QIAGEN) condition containing 0.1 M HEPES (4-(2-hydroxyethyl)-1-piperazineethanesulfonic acid), pH 7.5, 8% *v/v* ethylene glycol and 10% *w/v* PEG 8K. After optimization, it was found that this was also the optimal condition for crystal growth, with crystals reaching sizes of 80x50x30 μm. Crystals were transferred to a cryoprotection solution consisting of mother liquor with 20% *v/v* ethylene glycol. This was done in 4 steps of 5 min each, starting with a solution containing 2% (*v/v*) ethylene glycol, followed by solutions of 5, 10 and finally 20% (*v/v*) ethylene glycol. Crystals from this last solution were cryo-cooled in liquid nitrogen. For amino acid binding studies, the same steps were followed, but with the cryoprotection solutions supplemented with 2, 5, 10 and 20 mM (*S*)-*β*-Phe (Peptech Corp.), (*R*)-3-amino-5-methylhexanoic acid (Fluorochem), 2-oxoglutarate disodium salt (Fluka), or 2-aminooxyacetic acid (AOA) (Aldrich).

Diffraction data collection and processing

Diffraction data were collected at beam lines ID14-1 and ID14-2 of the European Synchrotron Radiation Facility (ESRF, Grenoble) and at beam line X13 of the EMBL outstation at the Deutsches Elektronen-Synchrotron (DESY, Hamburg). Reflections were indexed and integrated using XDS (Evans *et al.,* 2006), and scaling

and merging of the data was done with the program SCALA (Kabsch *et al.,* 2010) from the CCP4 software suite (1994). Phaser (McCoy *et al.,* 2007) was used for molecular replacement with a mixed input model generated by the FFAS03 server (Jaroszewski *et al.,* 2005) on the basis of the structures of glutamate-1-semialdehyde-2,1-aminomutase from *Thermus thermophilus* HB8 (PDB code: 2E7U; Mizutani, H., Kunishima, N., RIKEN Structural Genomics/Proteomics Initiative, to be published), D-phenylglycine aminotransferase from *Pseudomonas stutzeri* ST-201 (PDB code: 2CY8; Kongsaeree, P., Shirouzu, M., Yokoyama, S., RIKEN Structural Genomics/Proteomics Initiative, to be published) and 4-aminobutyrate aminotransferase from pig (PDB code: 1OHV (Storici *et al.,* 2004)). The resulting model was subjected to successive rounds of automatic model building with ARP/wARP (Langer *et al.,* 2008) followed by manual model building in Coot (Emsley *et al.,* 2010). Refmac5 was used for refinement of the atomic coordinates and atomic B-factors (Murshudov *et al.,* 1997). Data collection and refinement statistics are given in the Supplemental Material, **Table S1**. After refinement the model was validated with MolProbity (Chen *et al.,* 2010). Stereochemical restraints for the amino acid analogues were generated using the PRODRG2 server (Schuttelkopf *et al.,* 2004). RMSD values were calculated with the RMSDcalc tool of the CaspR server (Claude *et al.,* 2004) and structural homologues of *MesAT* were obtained from the Dali server (Holm *et al.,* 2010). PISA from the CCP4 software suite was used for protein interface analysis (Krissinel *et al.,* 2007). Simulated annealing composite omit maps where generated with PHENIX (Adams *et al.,* 2010). Chemical structure drawings were made using the ChemDraw program (CambridgeSoft) and PyMOL (version 1.2r3pre) was used for making images of the protein structure.

Atomic coordinates and structure factors have been deposited in the Protein Data Bank, www.pdb.org, with PDB codes 2YKU, 2YKY, 4AO4, 2YKX and 2YKV (Supplemental Material, **Table S1**).

Enzyme assay and analytical methods

Aminotransferase assays were performed with 10 mM amino donor ((*S*)-*β*-phenylalanine), 10 mM amino acceptor (pyruvate) and enzyme at 37 °C in 50 mM MOPS buffer, pH 7.6, containing 50 µM PLP (Acros Organics). Samples were taken at different times and treated according to the following procedure: to 50 µl of sample, 50 µl of a 2M HCl was added to quench the reaction. The sample was left on ice for 5 min and neutralized by adding 45 µl of 2M NaOH followed by adding 50 µl of demineralized water. In an HPLC autosampler (Jasco), 1 µl sample was mixed with 2 µl of an *ortho*-phthalaldehyde (Sigma) (OPA)-solution [15 mg of OPA was dissolved in 50

µl absolute ethanol, which was then mixed with 4.42 ml 0.4 M sodium borate (pH 10.4), 15 µl 30% *w/v* Brij 35 (Fluka) and 11 µl β-mercaptoethanol] and 5 µl 0.4 M sodium borate (pH 10.4). The OPA-derivatized samples were analysed by HPLC using a C18 Alltech Adsorbosphere 5u column (5 µm, 4.6 mm x 100 mm) using a Jasco HPLC system. Separation of OPA-derivatized imines was achieved at room temperature at a flow rate of 1 ml/min using a gradient of eluent A (5% THF in 20 mM sodium acetate, pH 5.5) and eluent B (99% pure CH_3CN) as follows: start with 100:0 A:B for 5 min; in 7 min from 100:0 to 80:20 A:B; continue with 80:20 for 4 min, 8 min from 80:20 to 40:60; continue with 40:60 for 6 min; then change from 40:60 to 100:0 in 2 min and finally continue for 5 min at 100:0 for re-equilibration of the column. The eluate was analysed by UV (338 nm) using a Jasco UV-2075 Plus detector and with a Jasco FP-920 fluorescence detector (350 nm excitation and 450 nm emission). Retention times for derivatized L-α-alanine and (*S*)-*β*-phenylalanine were 7.7 min and 23.2 min, respectively. One unit of enzyme activity is defined as the amount of enzyme that produces 1 µmol/min of alanine from 10 mM pyruvate (sodium salt; Fluka) and 10 mM (*S*)-*β*-phenylalanine (Acros Organics).

To determine the V_{max} and K_m values of the R412A mutant of *Mes*AT, initial rate assays were done with varying concentrations of (*S*)-*β*-Phe or pyruvate, fixing the non-variant substrate at 10 mM. The reactions were started by adding 680 µg of purified protein, and incubated at 37 °C.

Inhibition studies were performed by pre-incubating the reaction mixture, lacking (*S*)-*β*-Phe but containing 40 µg of wild-type enzyme, with 5 mM 2-aminooxyacetic acid (AOA) (Aldrich) or 5 mM DL-propargylglycine (2-amino-4-pentynoic acid, PPG) (Sigma-Aldrich) for 5 min, after which (*S*)-*β*-Phe (PepTech. Corp.) was added.

Results

Overexpression, purification and enzyme activity measurements of wild-type and R412A *Mes*AT

Previously, an overexpression system of *Mes*AT was reported that gave a yield of 1.4 mg pure protein per liter of culture (Kim *et al.,* 2007). To obtain enhanced expression, we used a codon-optimized synthetic gene that was equipped with an *N*-terminal His tag, cloned it under control of the T7 promoter in a pET vector, and cultivated the transformed *E. coli* BL21(DE3) cells in TBS medium at 17 °C. This resulted in an expression level that allowed the isolation of about 10 mg of pure enzyme per liter of culture (**Table 4.1**). The specific activity of the purified wild-type

enzyme was 1.6 U • mg^{-1}, which is similar to what was reported earlier (Kim *et al.,* 2007).

Table 4.1. Purification of recombinant wild-type *Mes*AT.

Purification step	Volume (ml)	Total protein (mg)	Total activity (U)	Specific activity (U • mg^{-1})	Recovery (%)
CFE	75	4350	30.5	0.007	100
IMAC	9.2	21.1	23.1	1.1	76
IEXC	6.1	12.2	18.3	1.5	60
SEC	0.7	8.4	13.5	1.6	44

CFE: cell-free extract; IMAC: immobilized metal affinity chromatography; IEXC: ion exchange chromatography; SEC: size exclusion chromatography.

Structure determination of *Mes*AT

The holo-enzyme crystallizes in space group *C*2 with three molecules (chains A, B and C) per asymmetric unit. The 3D-structure of *Mes*AT was elucidated at 2.5 Å resolution by molecular replacement and refined at 1.65 Å resolution. No density is defined for the first 30 N-terminal residues and the C-terminal residue M445. The three molecules are very similar to each other with RMSD values of Cα atom positions of ~0.2-0.25 Å. They form 1½ dimer in the asymmetric unit; one dimer consists of chains A and B (**Fig. 4.2**), the other dimer is made up of chain C and a chain C from a neighboring asymmetric unit related by crystallographic two-fold symmetry. Both dimers are very similar, with RMSD values in the order of 0.2 Å (Cα atoms). The two chains in the dimer interact tightly, burying a surface area of about 4400 $Å^2$, which is a quarter of their total surface area. The presence of dimers in the crystal is in agreement with the occurrence of *Mes*AT dimers in solution (Kim *et al.,* 2006).

The structure of the *Mes*AT monomer

The *Mes*AT monomer has a curved shape and consists of a PLP-binding domain (residues 112-334) and a domain formed by the N- and C-termini of the polypeptide chain (NC-domain; residues 1-111 and 335-445) (**Fig. 4.2**). These two domains line a cleft into which the PLP cofactor protrudes. The monomer contains 11 α-helices (of at least 2 or more turns) and 12 β-strands that form a mixed central 7-stranded β-sheet in the large domain and a 3-stranded as well as a 2-stranded anti-parallel β-sheet in the NC-domain (**Fig. 4.2**). The overall structure is similar to that of aspartate aminotransferase, the archetypical representative of fold type I aminotransferases (Z-score 21, RMSD of 4.2 Å for 309 Cα atoms, 16 % sequence identity, PDB code: 1BGK) (Grishin *et al.,* 1995; Schneider *et al.,* 2000) and the aromatic α-amino acid aminotransferase from *Paracoccus denitrificans* (AroAT) (Z-

score 21, RMSD of 4.8 Å for 326 Cα atoms, 15 % sequence identity, PDB code: 1AY4) (Oue *et al.,* 1997; Okamoto *et al.,* 1998), which is specific for L-α-phenylalanine.

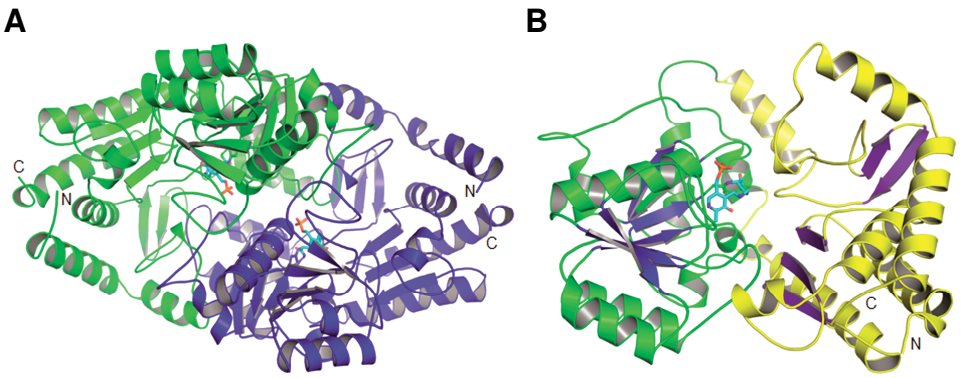

Figure 4.2 A) Three-dimensional structure of the *Mes*AT dimer. The 2 monomers (blue and green) are related by two-fold symmetry. Each monomer contains a PLP cofactor (magenta), bound to the enzyme *via* an imine bond to residue K280. **B**) Three-dimensional structure of a *Mes*AT monomer. The PLP cofactor (magenta) is positioned in a cleft that separates the large PLP-binding domain (left, green α-helices, blue 7-stranded β-sheet) from the NC-domain (right, yellow α-helices, deep blue β-sheets).

The PLP cofactor

Each *Mes*AT monomer contains a pyridoxal-5'-phosphate (PLP) cofactor, covalently anchored *via* an imine bond (Schiff base) to the ε-amino group of residue K280. The amide protons of residues G145, T146 and T314 (from monomer B in case of the AB dimer) anchor the phosphate group of the PLP cofactor to the protein backbone. The pyridine ring of the PLP cofactor is stacked between residues V255 (at the *si*-face of the pyridine ring (Soda *et al.,* 2001)) and Y172 (at the *re*-face of the pyridine ring). The nitrogen atom of the pyridine ring is at hydrogen bonding distance to residue D253. These interactions keep the PLP cofactor secured in the active site.

The binding of (*S*)-*β*-phenylalanine

To analyze how (*S*)-*β*-Phe binds in the active site, a crystal structure of *Mes*AT with bound (*S*)-*β*-Phe was solved at 1.7 Å resolution. (*S*)-*β*-Phe binds covalently to the PLP cofactor *via* its *β*-amino group, substituting the imine bond between the ε-amine of residue K280 and the C4A atom of the PLP cofactor (**Fig. 4.3A**). It binds with an estimated occupancy of about 80% in the three subunits. The carboxylate group of (*S*)-*β*-Phe has a salt bridge interaction with the Nε- and Nη2-atoms of R54. The aromatic ring of (*S*)-*β*-Phe is bound between the side chains of Y89 and Y172 with

edge-to-face interactions (**Fig. 4.3A**) and has also van der Waals interactions with residues I56, A225, M256 and M414 from monomer A as well as with residue A312 from monomer B; these residues line a hydrophobic binding pocket that is capped by residue R412 (monomer A).

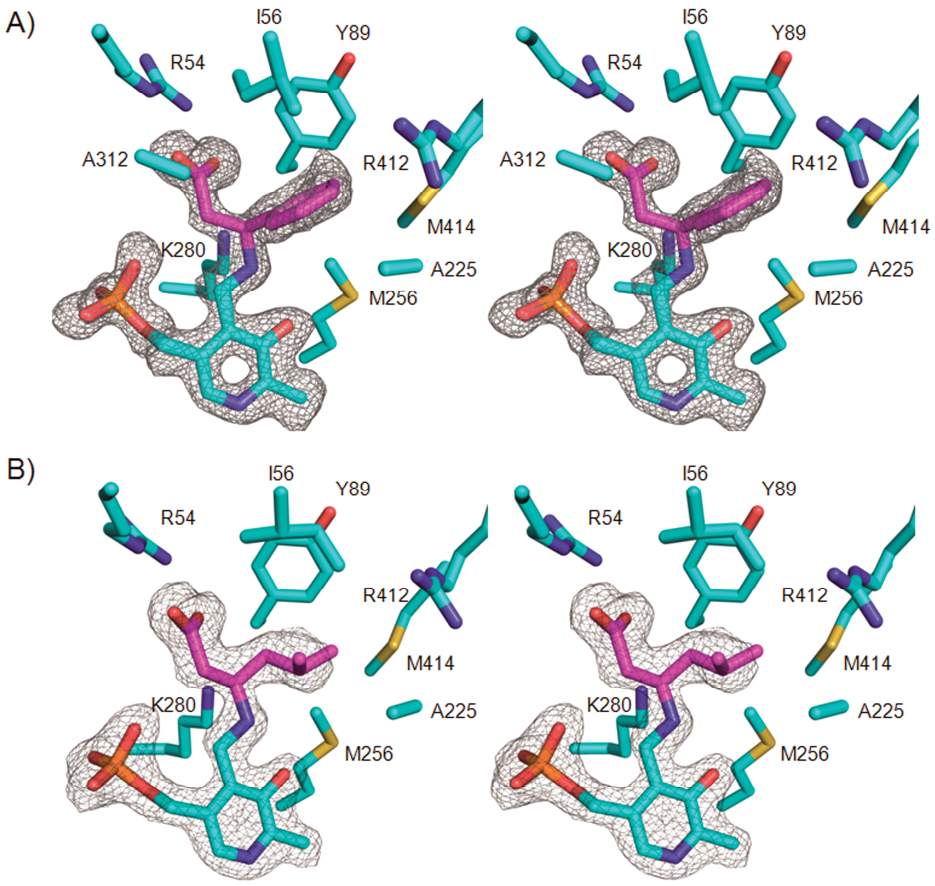

Figure 4.3 (A,B) Stereo figures of simulated annealing composite 2mFo-DFc omit maps contoured at 1σ. **A)** (*S*)-*β*-Phe (magenta) bound to the PLP cofactor. For clarity residue Y172 has been omitted from this figure as well as from figures 4.3B, 4.3C and 4.3D. **B)** (*R*)-3-amino-5-methylhexanoic acid (magenta). For clarity residue A312 has been omitted from this figure as well as from figures 4.3C and 4.3D.

Thus, residues from both monomer A and monomer B contribute to the binding of the aromatic side chain of (*S*)-*β*-Phe. The side chain amino group of K280 is close to the C*β* (*R*)-proton of (*S*)-*β*-Phe (3.3 Å), in agreement with its role in proton transfer (**Fig. 4.1**).

The binding of (*S*)-*β*-Phe does not induce large-scale conformational changes or domain movements in *Mes*AT. Only local conformational changes have occurred (see Discussion).

In monomer A, a second (*S*)-*β*-Phe molecule is present in a surface pocket, with its aromatic ring stacked between residues L269 and L368. Its carboxylate and amino groups point into the solvent and do not interact with the protein. However, in the surface pockets of monomers B and C electron density is only present for the aromatic ring of an (*S*)-*β*-Phe molecule, but not for the amino- and the carboxylate groups. From this we conclude that (*S*)-*β*-Phe binds non-specifically in this surface pocket.

The binding of (*R*)-3-amino-5-methylhexanoic acid

To investigate how an aliphatic *β*-amino acid such as (*R*)-3-amino-5-methylhexanoic acid (Kim *et al.,* 2007) binds in the active site, a 1.95 Å resolution crystal structure was determined of *Mes*AT in complex with this compound. (*R*)-3-amino-5-methylhexanoic acid binds covalently to the PLP cofactor *via* its *β*-amino group, substituting the imine bond between the ε-amine of residue K280 and the C4A atom of the PLP cofactor (**Fig. 4.3B**). It binds with an estimated occupancy of about 90% in the three subunits. The carboxylate group of (*R*)-3-amino-5-methylhexanoic acid has a salt bridge interaction with the Nε- and Nη2-atoms of residue R54, and the aliphatic side chain (atoms C4, C5 and C6) binds in the hydrophobic binding pocket where also the aromatic side chain of (*S*)-*β*-Phe was observed to bind (see above). Binding of (*R*)-3-amino-5-methylhexanoic acid only produces limited local conformational changes in *Mes*AT.

The binding of 2-oxoglutarate

To analyze how a keto-acid binds in the active site of *Mes*AT we determined the crystal structure of the enzyme with bound 2-oxoglutarate at 1.85 Å resolution (**Fig. 4.3C**). The compound binds non-covalently in the active site. Its *α*-carboxylate has a bidentate salt-bridge interaction with the Nη1- and Nη2-atoms of R412. The *γ*-carboxylate binds with one of its oxygen atoms to the Nε- and Nη2-atoms of R54; the other oxygen atom is not involved in hydrogen bond formation. The keto-oxygen atom of 2-oxoglutarate is located at 3.0 Å from the nitrogen atom of the K280 side chain, which is covalently bound to the C4A atom of the PLP cofactor. The binding of 2-oxoglutarate thus leaves the internal aldimine intact. The orientation of 2-oxoglutarate in the active site of *Mes*AT suggests that amino group transfer from PMP results in the synthesis of L-glutamate, in agreement with chiral HPLC analysis of the

product of a reaction with (*S*)-*β*-Phe as amino-donor and 2-oxoglutarate as amino-acceptor (data not shown). Binding of 2-oxoglutarate does not result in large-scale conformational changes of *Mes*AT. However, residue R412 reorients its side chain such that its Nη1- and Nη2-atoms can make a salt bridge interaction with the *α*-carboxylate of 2-oxoglutarate. This reorientation of the arginine side chain in response to the binding of an amino acid in the active site of an aminotransferase is referred to as the 'arginine switch' (Eliot *et al.,* 2004).

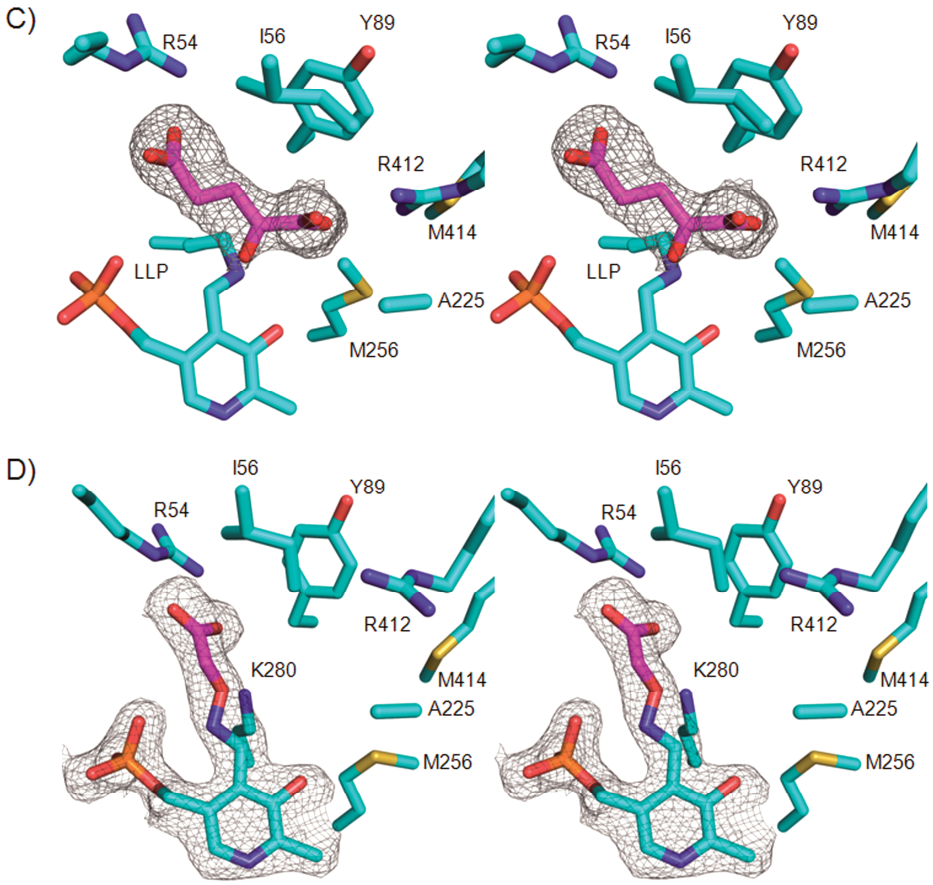

Figure 4.3 (C,D) Stereo figures of simulated annealing composite 2mFo-DFc omit maps contoured at 1σ. **C)** 2-oxoglutarate (magenta) bound in the active site of *Mes*AT [LLP = (2-lysine(3-hydroxy-2-methyl-5-phosphonooxymethyl-pyridin-4-ylmethane)], the internal aldimine. **D)** 2-aminooxyacetic acid (magenta), a *β*-alanine mimic, bound in the active site of *Mes*AT.

The binding of 2-aminooxyacetic acid (AOA)

AOA (John *et al.,* 1978) and 2-amino-4-pentynoic acid (L-PPG) (Marcotte *et al.,* 1975; Tanase *et al.,* 1976) are known inhibitors of aminotransferase activity. Pre-incubation of *Mes*AT with 5 mM of these inhibitors resulted in an activity decrease of 10 % upon treatment with L-PPG and a 96 % decrease upon treatment with AOA. Analysis of the 1.9 Å resolution crystal structure of *Mes*AT with bound AOA (**Fig. 4.3D**) shows that the amino group of AOA binds covalently to the C4A atom of PLP, as has also been observed for the interaction of AOA with aspartate aminotransferase (Markovic-Housley *et al.,* 1996). The ether oxygen atom (OX1) is close to K280 (2.9 Å) and the carboxylate group binds *via* a salt bridge to the Nε- and Nη2-atoms of R54. The binding of AOA to the PLP cofactor is irreversible; the amine-OX1 bond cannot be weakened by residue K280. Binding of AOA to the PLP cofactor thus prevents PMP formation and thereby inhibits aminotransferase activity. No significant conformational changes are observed upon AOA binding.

The importance of R412 for activity was confirmed by mutagenesis. The protein yield of the R412A variant was similar to that of the wild-type enzyme. The k_{cat} values of the R412A mutant were significantly lower than those of the wild-type enzyme (**Table 4.1**). Furthermore, the K_m value for pyruvate had increased by a factor of 28, whereas for (*S*)-*β*-Phe it had decreased by a factor of 4. The relationship between the reaction rate of the R412A mutant and the substrate concentration indicated substrate inhibition, as observed in the wild-type enzyme (Tipton *et al.,* 1996) (**Table 4.1**).

Table 4.1. Specific activity at 37 °C of wild-type *Mes*AT and the R412A mutant using (*S*)-*β*-Phe as amino-donor and pyruvate as amino-acceptor.

	Activity		(*S*)-*β*-Phe				Pyruvate				
*Mes*AT	Sp. act. (U • mg^{-1})[a]	Rel. act. (%)	K_m (mM)	k_{cat} (s^{-1})	k_{cat}/K_m (s^{-1} • mM^{-1})	K_i (mM)	K_m (mM)	k_{cat} (s^{-1})	k_{cat}/K_m (s^{-1} • mM^{-1})	K_i (mM)	Source
WT	1.6	100	1.2[b]	1.3	1.1	3.2[b]	3.9[b]	1.3	0.33	177[b]	Kim *et al*., 2007[b]
R412A	$6•10^{-3}$	0.4	0.29	$5•10^{-3}$	$2•10^{-2}$	47	109	$4.1•10^{-2}$	$3.8•10^{-4}$	2500	This study

[a] Abbreviations: Sp. act., specific activity; Rel. act., relative activity; WT, wild-type.
[b] Adopted from Kim and coworkers (2007).

Discussion

The structure of *Mes*AT

The structure of *Mes*AT presented here is the first structure of a transaminase with specificity towards *β*-amino acids as well as *α*-amino acids. The structure of the enzyme is similar to that of aspartate aminotransferase (Kirsch *et al.,* 1984), the archetypical fold type I aminotransferase. The enzyme assembles into a homo-dimer in which residues from both monomer A and B contribute to the binding of amino acid and their respective oxo-acid substrates. In contrast to aspartate aminotransferase, the binding of ligands does not induce large domain movements. Structural changes that do occur in *Mes*AT upon substrate/inhibitor binding are localized to the active site and consist of a 16° rotation of the pyridine ring of the PLP cofactor upon formation of the external aldimine. This rotation liberates K280 and allows it to function as the proton transferring lysine. Another structural change is the rearrangement of the R412 side chain, also known as the arginine switch (Eliot *et al.,* 2004), upon binding of 2-oxoglutarate (mentioned above).

Different binding modes of (*S*)-*β*-phenylalanine, (*R*)-3-amino-5-methylhexanoic acid and 2-oxoglutarate

The way in which 2-oxoglutarate binds in the active site of *Mes*AT and the manner in which (*S*)-*β*-phenylalanine and (*R*)-3-amino-5-methylhexanoic acid bind are very different. The side chains of (*S*)-*β*-Phe (**Fig. 4.3A**) and (*R*)-3-amino-5-methylhexanoic acid (**Fig. 4.3B**) bind in a pocket on the 3'-O side of the PLP cofactor, which we denote the O-pocket. However, the side chain of the *α*-keto acid 2-oxoglutarate, a model for the *α*-amino acid L-glutamate, binds with its *γ*-carboxylate group on the phosphate side of the PLP cofactor (**Fig. 4.3C**), in the P-pocket. Thus, *Mes*AT has two distinct side chain binding pockets, one for the side chains of *β*-amino acids (**O-pocket**, **Fig. 4.4**) and one, on the other end of the active site, for the side chain of *α*-keto acids and presumably also *α*-amino acids (**P-pocket**, **Fig. 4.4**). The enzyme has also two carboxylate binding pockets; one, involving R54 in the P-pocket, binds the *α*-carboxylate group of *β*-amino acids and of AOA, a *β*-alanine mimic (**Fig. 4.3D**), while the other, which contains R412 in the O-pocket, binds the *α*-carboxylate of *α*-keto acids such as 2-oxoglutarate (**Fig. 4.3C**). As a consequence, an *α*-amino acid and a *β*-amino acid have very different binding modes in *Mes*AT (**Fig. 4.4A,B**).

Intriguingly, the O-pocket that binds the aliphatic and hydrophobic side chain of *β*-amino acids also binds the *α*-carboxylate group of *α*-keto acids and presumably also of *α*-amino acids. This dual functionality is made possible by a switch in position

of the R412 side chain, the arginine switch residue (Eliot *et al.,* 2004). When a *β*-amino acid binds, the R412 side chain is oriented away from the active site, providing space in the O-pocket for the hydrophobic side chain of the *β*-amino acid (**Fig. 4.3A,B**). This orientation of R412 is stabilized by a hydrogen bond of its side chain Nη-atom to the carbonyl oxygen atom of A225 (monomer B, not shown). In contrast, upon 2-oxoglutarate binding, the side chain of R412 switches back towards the hydrophobic O-pocket (**Fig. 4.3C**); the hydrogen bond with A225 is broken and R412 now has a salt-bridge interaction with the *α*-carboxylate of 2-oxoglutarate. In this way the R412 side chain allows the enzyme to accept both *α*-keto/amino acids and aliphatic- or aromatic *β*-amino acids in the same active site.

Because of the dual functionality of the active site pockets of *Mes*AT we prefer to use O- and P-pocket, rather than L- and S-pocket nomenclature, which reflects the presumed size of these pockets (Shin *et al.,* 2002).

For aminotransferase activity R412 is virtually essential, as reflected by the 870-fold reduction of the catalytic efficiencies for pyruvate and (*S*)-*β*-Phe, respectively, upon mutation of this residue to Ala (**Table 4.1**). Whereas the decreased apparent K_m for (*S*)-*β*-Phe can be due to the reduced catalytic rate at 10 mM pyruvate, the increased K_m for pyruvate strongly supports that R412 is important for binding pyruvate through electrostatic interactions with its carboxylate.

Comparison of *Mes*AT and AroAT

To investigate how *Mes*AT differs from an aminotransferase that only accepts *α*-amino acids, the *Mes*AT structures were compared with that of the aromatic amino acid aminotransferase AroAT from *P. denitrificans* (Oue *et al.,* 1997). In both enzymes the PLP cofactor has a similar position and orientation. In contrast to *Mes*AT, AroAT has a single *α*-carboxylate binding pocket and charged as well as uncharged *α*-amino acids bind with their *α*-carboxylate groups to R386 in the O-pocket (**Fig. 4.4C,D**). In *Mes*AT, the *α*-carboxylate group of (*S*)-*β*-Phe binds to R54 in the P-pocket, while the side chain of (*S*)-*β*-Phe is bound in the O-pocket (**Fig. 4.4A**). As a consequence, in *Mes*AT, *β*-amino acids bind in a reverse orientation in comparison to the substrates of AroAT (**Fig. 4.4A,C,D**). Moreover, the arginine switch of *Mes*AT (R412) is located in the O-pocket of the enzyme, where it binds the *α*-carboxylate group of an *α*-amino acid, while in AroAT the arginine switch (R292), is located in the P-pocket of the enzyme and binds the side chain carboxylate group of *α*-amino/*α*-keto acids (**Fig. 4.4A-D**). These differences between *Mes*AT and AroAT show that, while these enzymes share the same fold, the architecture of their active site is very different. In *Mes*AT the active

site architecture has evolved to accommodate *β*-amino acids, while retaining the ability to accommodate *α*-amino/*α*-keto acids.

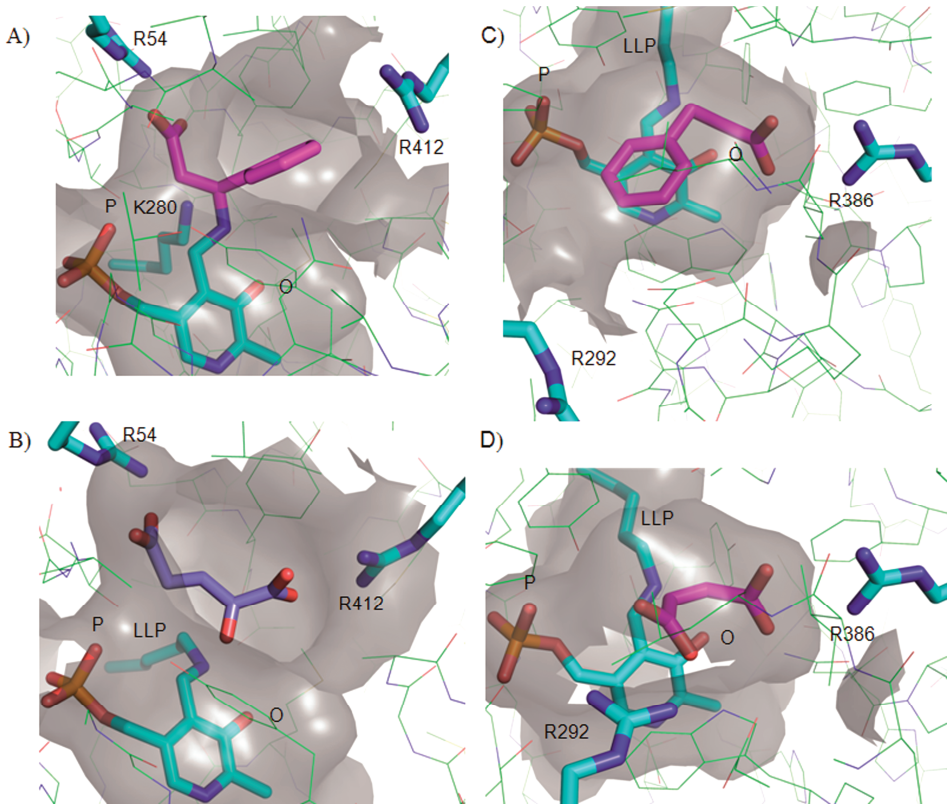

Figure 4.4 (A,B,C,D) Comparison of the active site architectures of the *β*-aminotransferase *Mes*AT (left column) and the *α*-aminotransferase AroAT (right column). **A)** Surface rendition of the active site of *Mes*AT bound with (*S*)-*β*-Phe (magenta) and **B)** with 2-oxoglutarate (magenta). **C)** Surface rendition of the active site of AroAT bound with 3-phenylpropionate (magenta) based on PDB entry 1AY8 (Okamoto *et al.,* 1998) and **D)** with maleate (magenta) based upon PDB entry 1AY5 (Okamoto *et al.,* 1998). The positions of the PLP cofactor as well as R412 and R386 in the active sites of *Mes*AT and AroAT, respectively, are similar. R412 represents the arginine switch of *Mes*AT, R292 represents the arginine switch of AroAT. LLP, the internal aldimine. P (P-pocket) and O (O-pocket), see text for explanation.

The covalent adducts in the active site of *Mes*AT represent external aldimine intermediates

Structures obtained from crystals soaked with (*S*)-*β*-Phe and (*R*)-3-amino-5-methylhexanoic acid show that covalent PLP-*β*-amino acid adducts have formed in the active site of *Mes*AT (**Fig. 4.3A,B**). These adducts represent external aldimine intermediates since the N*β*-, C*α*-, C*β*- and C*γ*-atoms are not coplanar, as would occur in the ketimine intermediate (**Fig. 4.1**). The non-coplanarity of the N*β*-, C*α*-, C*β*- and C*γ*-atoms suggests that the reaction has stopped before abstraction of the C*β*-proton.

Different explanations for the trapping of the external aldimine trapping may be considered. Proton abstraction is most efficient if, in the transition state, the bond to be broken is oriented perpendicular to the plane of the PLP ring system (Toney *et al.,* 2011). The crystal structures indicate that the C*β*-proton is indeed nearly perpendicular to the PLP plane, deviating 20-30° from the perpendicular position. Such a deviation is probably not sufficient to fully prevent proton abstraction.

Another explanation may be related to the observation that in none of the external aldimine intermediate bound structures density is present for a hydrolytic water molecule near the C*β*-atom that could convert the ketimine intermediate into the pyridoxamine intermediate (**Fig. 4.1**). The equilibrium of the aminotransferase reaction in the crystal structure of *Mes*AT may thus lie towards the external aldimine intermediate rather than the ketimine intermediate which could explain why the external aldimine intermediates of (*S*)-*β*-Phe and (*R*)-3-amino-5-methylhexanoic acid are trapped.

Enantioselectivity of *Mes*AT

*Mes*AT is enantioselective towards the *β*-amino acids (*S*)-*β*-Phe, (*R*)-3-amino-5-methylhexanoic acid and (*R*)-3-aminobutyric (Kim *et al.,* 2007). These preferred enantiomers have the same stereoconfiguration of functional groups on the C*β*-atom as (*S*)-*β*-Phe. The preference for these enantiomers can be fully explained by the architecture of the active site which forces these substrates to bind in an orientation in which the carboxylate group binds to R54 in the P-pocket and the side chain in the O-pocket followed by addition of an amino group at the *si*-face of the *β*-carbon of the *β*-keto acid.

The insights obtained from the 3D-structure of *Mes*AT on the enzyme's interaction with *α*- and *β*-amino/keto acids may facilitate structure-based protein engineering efforts aimed at enhancing the biocatalytic potential of *β*-transaminases for the production of *β*-amino acids of pharmacological interest.

Acknowledgements

We acknowledge the European Synchrotron Radiation Facility (ESRF) and the EMBL Outstation at DESY (Deutsches Elektronen Synchrotron) for provision of synchrotron radiation facilities. We thank the beam line staff of ID14-1 and ID14-2 (ESRF) and X13 (DESY) for their assistance. This project is financially supported by the Netherlands Ministry of Economic Affairs and the B-Basic partner organizations (www.b-basic.nl) through B-Basic, a public-private NWO-ACTS program (ACTS = Advanced chemical Technologies for Sustainability).

References

Adams, P.D., Afonine, P.V., Bunkoczi, G., Chen, V.B., Davis, I.W., Echols, N., Headd, J.J., Hung, L.W., Kapral, G.J., Grosse-Kunstleve, R.W., McCoy, A.J., Moriarty, N.W., Oeffner, R., Read, R.J., Richardson, D.C., Richardson, J.S., Terwilliger, T.C. and Zwart, P.H. (2010) PHENIX: a comprehensive Python-based system for macromolecular structure solution. *Acta Crystallogr Sect D: Biol Crystallogr* 66: 213–221.

Barth, S., Huhn, M., Matthey, B., Klimka, A., Galinski, E.A. and Engert, A. (2000) Compatible-solute-supported periplasmic expression of functional recombinant proteins under stress conditions. *Appl Environ Microbiol* 66: 1572–1579.

Bea, H.S., Park, H.J., Lee, S. H. and Yun, H. (2011) Kinetic resolution of aromatic *β*-amino acids by ω-transaminase. *Chem Commun* (Camb.) 47: 5894–5896.

Braunstein, A.E. (1964) Binding and reactions of the vitamin B6 coenzyme in the catalytic center of aspartate transaminase. *In* Vitamins & Hormones (Harris, R.S., Wool, I.G., Loraine, J.A., Marrian, G.F. and Thimann, K.V. eds.), *Academic Press*. p 451–484.

Chen, V.B., Arendall, W.B., 3rd, Headd, J.J., Keedy, D.A., Immormino, R.M., Kapral, G.J., Murray, L. W., Richardson, J. S. and Richardson, D.C. (2010) MolProbity: all-atom structure validation for macromolecular crystallography. *Acta Crystallogr Sect D: Biol Crystallogr* 66: 12–21.

Cole, D.C. (1994) Recent stereoselective synthetic approaches to *β*-amino acids. *Tetrahedron* 50: 9517–9582.

Claude, J.B., Suhre, K., Notredame, C., Claverie, J.M. and Abergel, C. (2004) CaspR: a web server for automated molecular replacement using homology modelling. *Nucl Acids Res* 32: W606–609.

Eliot, A.C. and Kirsch, J.F. (2004) Pyridoxal phosphate enzymes: mechanistic, structural, and evolutionary considerations. *Annu Rev Biochem* 73: 383–415.

Emsley, P., Lohkamp, B., Scott, W.G. and Cowtan, K. (2010) Features and development of Coot. *Acta Crystallogr Sect D: Biol Crystallogr* 66: 486–501.

Evans, P. (2006) Scaling and assessment of data quality. *Acta Crystallogr Sect D: Biol Crystallogr* 62: 72–82.

Grishin, N.V., Phillips, M.A. and Goldsmith, E.J. (1995) Modeling of the spatial structure of eukaryotic ornithine decarboxylases. *Prot Sci* 4: 1291–1304.

Holm, L. and Rosenstrom, P. (2010) Dali server: conservation mapping in 3D. *Nucl Acids Res* 38: W545–W549.

Jaroszewski, L., Rychlewski, L., Li, Z., Li, W. and Godzik, A. (2005) FFAS03: a server for profile-profile sequence alignments. Nucl Acids Res 33: W284–288.

John, R.A. and Charteris, A. (1978) The reaction of amino-oxyacetate with pyridoxal phosphate-dependent enzymes. *Biochem J* 171: 771–779.

Kabsch, W. (2010) Integration, scaling, space-group assignment and post-refinement. *Acta Crystallogr Sect D: Biol Crystallogr* 66: 133–144.

Kim, J., Kyung, D., Yun, H., Cho, B.K., Seo, J.H., Cha, M. and Kim, B.G. (2007) Cloning and characterization of a novel *β*-transaminase from *Mesorhizobium* sp. strain LUK: a new biocatalyst for the synthesis of enantiomerically pure *β*-amino acids. *Appl Environ Microbiol* 73: 1772–1782.

Kim, B., Park, O.K., Bae, J.Y., Jang, T.H., Yoon, J.H., Do, K.H., Kim, B.G., Yun, H. and Park, H.H. (2011) Crystallization and preliminary X-ray crystallographic studies of *β*-transaminase from *Mesorhizobium* sp. strain LUK. *Acta Crystallogr Sect F: Struct Biol Cryst Commun* 67: 231–233.

Kim, J., Kyung, D., Yun, H., Cho, B. K., and Kim, B. G. (2006) Screening and purification of a novel transaminase catalyzing the transamination of aryl *β*-amino acid from *Mesorhizobium* sp. LUK. *J Microbiol Biotechnol* 16: 1832–1836.

Kirsch, J.F., Eichele, G., Ford, G.C., Vincent, M.G., Jansonius, J.N., Gehring, H. and Christen, P. (1984) Mechanism of action of aspartate aminotransferase proposed on the basis of its spatial structure. *J Mol Biol* 174: 497–525.

Koeller, K.M. and Wong, C.H. (2001) Enzymes for chemical synthesis. *Nature* 409: 232–240.

Krissinel, E. and Henrick, K. (2007) Inference of macromolecular assemblies from crystalline state. *J Mol Biol* 372: 774–797.

Langer, G., Cohen, S.X., Lamzin, V.S. and Perrakis, A. (2008) Automated macromolecular model building for X-ray crystallography using ARP/wARP version 7. *Nat Protoc* 3: 1171–1179.

Liljeblad, A. and Kanerva, L.T. (2006) Biocatalysis as a profound tool in the preparation of highly enantiopure *β*-amino acids. *Tetrahedron* 62: 5831–5854.

Marcotte, P. and Walsh, C. (1975) Active site-directed inactivation of cystathionine *γ*-synthetase and glutamic pyruvic transaminase by propargylglycine. *Biochem Biophys Res Commun* 62: 677–682.

Markovic-Housley, Z., Schirmer, T., Hohenester, E., Khomutov, A.R., Khomutov, R.M., Karpeisky, M.Y., Sandmeier, E., Christen, P. and Jansonius, J.N. (1996) Crystal structures and solution studies of oxime adducts of mitochondrial aspartate aminotransferase. *Eur J Biochem* 236: 1025–1032.

McCoy, A.J., Grosse-Kunstleve, R.W., Adams, P.D., Winn, M.D., Storoni, L.C. and Read, R.J. (2007) Phaser crystallographic software. *J Appl Crystallogr* 40: 658–674.

Murshudov, G.N., Vagin, A.A. and Dodson, E.J. (1997) Refinement of macromolecular structures by the maximum-likelihood method. *Acta Crystallogr Sect D: Biol Crystallogr* 53: 240–255.

Okamoto, A., Nakai, Y., Hayashi, H., Hirotsu, K. and Kagamiyama, H. (1998) Crystal structures of *Paracoccus denitrificans* aromatic amino acid aminotransferase: a substrate recognition site constructed by rearrangement of hydrogen bond network. *J Mol Biol* 280: 443–461.

Oue, S., Okamoto, A., Nakai, Y., Nakahira, M., Shibatani, T., Hayashi, H. and Kagamiyama, H. (1997) *Paracoccus denitrificans* aromatic amino acid aminotransferase: a model enzyme for the study of dual substrate recognition mechanism. *J Biochem* 121: 161–171.

Schneider, G., Kack, H. and Lindqvist, Y. (2000) The manifold of vitamin B6 dependent enzymes. *Structure* 8: R1–6.

Schuttelkopf, A.W. and van Aalten, D.M. (2004) PRODRG: a tool for high-throughput crystallography of protein-ligand complexes. *Acta Crystallogr Sect D: Biol Crystallogr* 60: 1355–1363.

Shin, J.S. and Kim, B.G. (2002) Exploring the active site of amine:pyruvate aminotransferase on the basis of the substrate structure-reactivity relationship: how the enzyme controls substrate specificity and stereoselectivity. *J Org Chem* 67: 2848–2853.

Soda, K., Yoshimura, T. and Esaki, N. (2001) Stereospecificity for the hydrogen transfer of pyridoxal enzyme reactions. *Chem Rec* 1: 373–384.

Storici, P., De Biase, D., Bossa, F., Bruno, S., Mozzarelli, A., Peneff, C., Silverman, R.B. and Schirmer, T. (2004) Structures of γ-aminobutyric acid (GABA) aminotransferase, a pyridoxal 5'-phosphate, and [2Fe-2S] cluster-containing enzyme, complexed with γ-ethynyl-GABA and with the antiepilepsy drug Vigabatrin. *J Biol Chem* 279: 363–373.

Tanase, S. and Morino, Y. (1976) Irreversible inactivation of aspartate aminotransferases during transamination with L-propargylglycine. *Biochem Biophys Res Commun* 68: 1301–1308.

Taylor, P.P., Pantaleone, D.P., Senkpeil, R.F. and Fotheringham, I.G. (1998) Novel biosynthetic approaches to the production of unnatural amino acids using transaminases. *Trends Biotechnol* 16: 412–418.

The CCP4 suite: programs for protein crystallography. (1994) Acta Crystallogr Sect D: Biol Crystallogr 50: 760–763.

The PyMOL molecular graphics system, version 1.2r3pre. Schrodinger, LLC.

Tipton, K.F. (1996) Patterns of enzyme inhibition. *In* Enzymology LabFax (Engel, P. C. ed.), Academic Press, San Diego, CA p 115–174.

Toney, M.D. (2011) Controlling reaction specificity in pyridoxal phosphate enzymes. *Biochim Biophys Acta* 1814: 1407–1418.

Weiner, B., Szymanski, W., Janssen, D.B., Minnaard, A.J. and Feringa, B.L. (2010) Recent advances in the catalytic asymmetric synthesis of β-amino acids. *Chem Soc Rev* 39: 1656–1691.

Supplemental Material

Structural determinants of the β-selectivity of a bacterial aminotransferase

Gjalt G. Wybenga[1,a], Ciprian G. Crismaru[2,a], Dick B. Janssen[2] and Bauke W. Dijkstra[1]

[1]Laboratory of Biophysical Chemistry, University of Groningen, Nijenborgh 7, 9747 AG Groningen, The Netherlands and [2]Department of Biochemistry, University of Groningen, Nijenborgh 4, 9747 AG Groningen, The Netherlands

[a] These two authors contributed equally to this study.

Table S1. Data collection and refinement statistics of the crystal structures of *Mes*AT.

Entry	*Mes*AT holo	*Mes*AT + (*S*)-β-Phe	*Mes*AT + (*R*)-3-amino-5-methylhexanoic acid	*Mes*AT + 2-oxoglutarate	*Mes*AT + 2-aminooxyacetic acid
Beam line	ID14-2	ID14-1	X13	ID14-2	ID14-1
Data collection					
Resolution (Å) [a]	48.35-1.9 (2.0-1.9)	48.16-1.7 (1.78-1.69)	48.38-1.95 (2.06-1.95)	48.23-1.85 (1.95-1.85)	48.09-1.9 (2.0-1.9)
Space group	*C*2	*C*2	*C*2	*C*2	*C*2

Table S1. Data collection and refinement statistics of the crystal structures of *Mes*AT (*continued*).

Entry	*Mes*AT holo	*Mes*AT + (*S*)-*β*-Phe	*Mes*AT + (*R*)-3-amino-5-methylhexanoic acid	*Mes*AT + 2-oxoglutarate	*Mes*AT + 2-aminooxyacetic acid
Cell dimensions					
a, b, c (Å)	184.2, 94.8, 104.9	183.6, 94.5, 103.7	184.4, 94.9, 103.0	183.8, 94.4, 103.7	183.8, 94.3, 102.3
β (°)	113.7	113.8	113.8	113.6	114.0
R_{merge} [b]	0.07 (0.33)	0.04 (0.24)	0.07 (0.24)	0.01 (0.44)	0.07 (0.38)
Wavelength (Å)	0.933	0.9334	0.8123	0.933	0.9334
I/σ (I)	12.6 (3.2)	19.1 (4.5)	7.6 (3.3)	8.1 (2.6)	11.9 (2.8)
Completeness (%)	99.9 (99.8)	99.9 (100)	98.7 (99.6)	99.9 (100)	99.9 (100)
No. unique reflections	129742 (18883)	180581 (26294)	116568 (17122)	138206 (20113)	125289 (18287)
Multiplicity	2.6	2.7	3.0	2.8	3.0
Refinement					
Resolution (Å)	1.9	1.69	1.95	1.85	1.9
R_{work} [c]	0.16	0.16	0.18	0.18	0.18
R_{free} [d]	0.19	0.18	0.22	0.20	0.21
Rms deviations					
Bond lengths (Å)	0.01	0.012	0.018	0.006	0.012
Bond angles (°)	1.25	1.25	1.46	0.95	1.25
Ramachandran (MolProbity)					
Favored (%)	97.9	97.7	97.0	98.1	97.1
Outliers (%)	0.0	0.0	0.0	0.0	0.0
PDB entry	2YKU	2YKY	4AO4	2YKX	2YKV

[a] Values in parentheses are for the highest resolution shell.
[b] $R_{merge} = \Sigma_h\Sigma_i |I(h)_i - \langle I(h)\rangle| / \Sigma_h\Sigma_i \langle I(h)_i\rangle$, where I is the observed intensity and $\langle I\rangle$ is the average intensity of multiple observations of symmetry-related reflections.
[c] $R_{work} = \Sigma_h|F_{obs} - F_{calc}| / \Sigma_h|F_{obs}|$, where F_{obs} and F_{calc} are the observed and calculated structure factor amplitudes, respectively.
[d] R_{free} is calculated as R_{work} using 5 % of all reflections randomly chosen and excluded from structure factor calculation and refinement.

Chapter 5

Degradation of *β*-valine by *Pseudomonas* sp. strain SBV1

Ciprian G. Crismaru,[a] Christiaan Postema,[a] Matthew M. Heberling,[a] Wiktor Szymanski,[b] Stefaan De Wildeman,[c] Marleen Otzen,[a] and Dick B. Janssen[a]

[a]*Department of Biochemistry, Groningen Biomolecular Sciences and Biotechnology Institute, University of Groningen*

[b]*Center for Systems Chemistry, Stratingh Institute for Chemistry, University of Groningen*

[c]*DSM Pharmaceutical Products, Geleen, The Netherlands*

Manuscript in preparation

Abstract

Pseudomonas sp. strain SBV1 is a bacterium that can rapidly grow on glucose with *β*-valine as sole nitrogen source. The structure of the compound, with the amine group on a tertiary carbon atom, makes aminotransferase, amino acid dehydrogenase and amino acid oxidase reactions for direct deamination impossible. Lyase- or aminomutase-mediated conversion would be possible. A number of deamination reactions were tested using activity assays but no substrate disappearance or ammonia release was detected in cell-free extracts. A cosmid library was prepared and triparental mating was performed with a *Pseudomonas* strain that is very similar to SBV1 but cannot degrade *β*-valine. The library was screened by growth selection on minimal medium plates containing *β*-valine as sole nitrogen source. Two positive clones were found, of which one (p4-D1) was further investigated. The sequence of the 26 kb DNA insert of p4-D1 revealed the presence of genes that encode enzymes that are likely involved in the degradation of *β*-valine. Two putative enzymes have high sequence similarity to CoA-dependent phenylacetate ligase and enoyl-CoA hydratase. The results suggest that *β*-valine conversion proceeds with a CoA activation of the substrate followed by CoA-dependent deamination catalyzed by an ammonia lyase.

Introduction

Whereas the microbial metabolism of α-amino acids is well known, the conversion of *β*-amino acids by microorganisms and microbial enzymes has been poorly investigated. More insight in microbial enzymes that metabolize *β*-amino acids is desirable since it can lead to a toolbox of enzymes that can be used for synthetic purposes. Furthermore, enzymes converting *β*-amino acids may be suitable for incorporation in biosynthetic pathways that are of importance for synthetic biology.

In analogy to the conversion of α-amino acids, several reaction types can be envisaged (Fernandez & Zuniga, 2006; Massey *et al.,* 1976). The most common enzymes involved in α-amino acid deamination reactions are aminotransferases, which transfer the amino group to a keto-acceptor such as 2-ketoglutarate, pyruvate, or oxaloacetate. The amino acid itself is converted into a 2-keto acid. The same keto-acids can be formed by amino acid dehydrogenases, of which glutamate dehydrogenase is a good example (Brunhuber & Blanchard, 1994). Here, the amino group is released as ammonia and electrons are transferred to $NAD(P)^+$, producing NAD(P)H. Amino acid oxidases usually contain FAD and also produce a ketone and ammonia, but electrons are transferred to oxygen, producing H_2O_2. All these reactions are very common and have been detected for a wide range of compounds, including α-amino acids and primary amines (Fitzpatrick, 2010). Aspartic acids, which can also be considered *β*-amino acids, and aromatic amino acids can be deaminated by ammonia lyase reactions. There are at least three different classes: aspartase of the fumarase/aspartase superfamily, metal-containing methylaspartate ammonia lyases of the enolase superfamily, and MIO (4-methylideneimidazole-5-one)-containing aromatic ammonia lyases. These enzymes have drawn attention because of their possible use in biocatalysis (Asano *et al.,* 2004; Heberling *et al.,* 2013). The MIO cofactor is formed via a cyclization of three amino acids (alanine, serine and glycine) in the active site and is also present in some mutases (see below, Walker *et al.,* 2004).

In case of *β*-amino acids, aminotransferases are known to catalyze deamination, e.g. for *β*-(*R*)-phenylalanine (Kim *et al.,* 2007; Crismaru *et al.,* 2013). A special situation occurs with so-called blocked amino acids, which carry the amine substituent on a tertiary carbon atom. In that case, the three deamination reactions producing a keto-acid would not be possible, whereas lyase and mutase reactions can be envisaged (see below).

As an example of such a blocked amino acid is *β*-valine, of which we examine the metabolism in this paper. A bacterial culture that uses *β*-valine as sole nitrogen source was enriched earlier by one of us (S. De Wildeman) (**Fig. 5.1**). The organism

has a high growth rate in mineral medium when β-valine is the sole nitrogen source. Whereas the metabolism of L-α-valine and D-α-valine has been studied in detail (Leavitt & Umbarger, 1962; Gilbert & Migeon, 1975), the degradation of β-valine or related compounds has to our knowledge not been examined. Metabolism of L-α-valine often starts with a transamination to produce 3-methyl-2-oxobutanoate, a reaction catalyzed by a pyridoxal phosphate dependent valine aminotransferase (VAT, EC 2.6.1.42) (Magnus *et al.,* 2006; Berg *et al.,* 1983). Conversion can also involve L-amino acid oxidases (LAAOs, EC 1.4.3.2)(Boyer *et al.,* 1963) or D-amino acid oxidases (DAAOs, EC 1.4.3.3) (Pollegioni *et al.,* 2007).

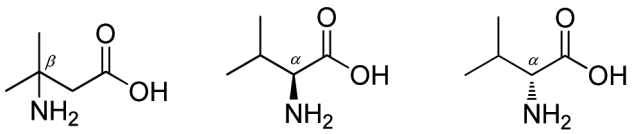

Figure 5.1. Chemical structure of β-valine, L-valine and D-valine.

Reactions that would be possible for β-valine are aminomutase-mediated conversion to L-α-valine or deamination by an ammonia lyase reaction. Ammonia lyases were mentioned above. Aminomutases (AM) catalyze a reversible intra-molecular amino group migration from one carbon atom to a neighboring one, and can act on leucine, lysine and also play a role in secondary metabolite synthesis (Walker *et al.,* 2004; Yin *et al.,* 2003; Wu *et al.,* 2011). Early reports describe the role of leucine 2,3-aminomutase in leucine metabolism (Poston, 1986; Poston, 1976), although to this date there is no sequence available of this enzyme. Other AMs are lysine 2,3-aminomutase from *Clostridium subterminale* (Aberhart *et al.,* 1981), lysine 5,6-aminomutase from *Clostridium sticklandii* (Tang *et al.,* 2003), arginine 2,3-aminomutase from *Streptomyces griseochromogenes* (Prabhakaran *et al.,* 1988) and glutamate 2,3-aminomutase from *Clostridium difficile* (Ruzicka & Frey, 2007). All these enzymes catalyze the aminomutase reaction with the involvement of several cofactors, such as S-adenosylmethionine (SAM), [4Fe-4S] clusters, and pyridoxal-5'-phosphate (PLP). AMs acting on aromatic amino acids contain the MIO group mentioned above. Activity has been shown with phenylalanine, tyrosine, and histidine deamination, but no activity has been reported for aliphatic α- or β-amino acids. Another pathway for the degradation of β-amino acids, although not very common, starts with coenzyme A (CoA-SH) activation of the substrate, in a reaction catalyzed by an ATP-dependent CoA ligase. This was shown for β-alanine (Herrmann *et al.,* 2005),

a naturally occurring *β*-amino acid found in vitamin B_5 (pantothenic acid), which is used to synthesize coenzyme A, and in the dipeptide carnosine (*β*-alanyl-L-histidine). After CoA activation to a *β*-alanyl-CoA-transferase, ammonia is eliminated by a *β*-alanyl-CoA:ammonia lyase.

In this chapter, the metabolism of *β*-valine by strain SBV1 is explored using different methods, including deamination assays with cell-free extracts, whole-cell conversion experiments, and a genetic approach that involves preparation and screening of a cosmid DNA library.

Materials and methods

Chemicals, strains and media

S-(5'-adenosyl)-L-methionine (SAM), coenzyme B_{12}, adenosine 5'-triphosphate (ATP), phenylmethanesulfonyl fluoride (PMSF), *ortho*-phthalaldehyde (OPA), sodium pyruvate, isopropyl β-D-1-thiogalactopyranoside (IPTG), 5-bromo-4-chloro-3-indolyl β-D-galactopyranoside (X-gal) and DL-propargylglycine (PAG) were obtained from Sigma. *β*-Valine (3-amino-3-methyl butyric acid) was purchased from Fluorochem (Germany). DL-*α*-valine, 2-oxoglutarate (α-ketoglutarate) disodium salt were purchased from Fluka. Aminooxy-acetic acid (AOA), and *O*-(carboxymethyl)-hydroxylamine were purchased from Aldrich. Other chemicals were purchased as follows: D-glucose, sodium phosphate dibasic and potassium phosphate monobasic, magnesium phosphate from Merck; pyridoxal 5'-phosphate (PLP) and deuterated water (D_2O) from Acros Organics. Yeast carbon base (YCB) and Luria-Bertani medium (LB) were obtained from Difco. *E. coli* TOP10 and *E. coli* C41(DE3) were purchased from Invitrogen, whereas *Pseudomonas fluorescens* Pf0-1 was kindly provided by prof. M.W. Silby (University of Massachusetts, Dartmouth, USA) and and *P. fluorescens* Pf-5 was obtained from ATCC (American Type Culture Collection). The restriction enzymes NdeI, BamHI, XhoI, HindIII, EcoRI, PstI and Sau3A were purchased from New England BioLabs Inc. and used according to the manufacturer's protocol. Plasmids pLAFR3, a modified pBAD (Invitrogen) and pET21 (Novagen) were used for DNA libraries and overexpression. The pBAD-NdeI-His expression vector is a pBAD/MycHisA derived expression vector (Invitrogen) in which the NdeI site is removed and the NcoI site is replaced by NdeI (Jin *et al.,* 2007). In this vector the myc-HisA epitope has also been removed and replaced by a 6x His-tag immediately downstream of the C-terminal PstI site.

Microorganism and cultivation conditions

The *β*-valine degrading bacterium strain SBV1 was isolated from garden soil and provided by Dr. Stefaan De Wildeman (DSM Pharmaceutical Products, Geleen, The Netherlands). It utilizes *β*-valine as sole nitrogen source.

All growth and selection media were based on YCB or on minimal medium. The latter was composed of 5.3 g $Na_2HPO_4 \cdot 12H_2O$, 1.4 g KH_2PO_4, 0.2 g $MgSO_4 \cdot 7H_2O$, 1 ml vitamin solution (Janssen *et al.,* 1984) and 5 ml trace elements solution (Gabor *et al.,* 2004) per l of medium. The pH was 7.5. In nitrogen-free minimal medium, $(NH_4)_2SO_4$ was replaced by Na_2SO_4, and $Ca(NO_3)_2 \cdot 4H_2O$ was omitted from the trace element solution. Stock solutions of *β*-valine and D-glucose were prepared in 100 mM sodium phosphate buffer (pH 7.5). In batch liquid cultures 10-20 mM glucose was used as carbon source and 5-10 mM *β*-valine as nitrogen source.

DNA sequencing

Total genomic DNA was isolated from cells of strain SBV1 grown at 30 °C on minimal medium containing 10 mM *β*-valine, 20 mM glucose, vitamins and nitrogen-free trace elements (Gabor *et al.,* 2004) using a described procedure (Poelarends *et al.,* 1998). DNA was dissolved in 10 mM Tris-HCl buffer (pH 7.2) containing 1 mM EDTA and 20 µg/mL RNase.

For 16S rRNA gene sequencing, first a PCR reaction was performed using two universal 16S rRNA gene primers: 27F (5'-AGAGTTTGATCMTGGCTCAG–3') and 1492R (5'-GGYTACCTTGTTACGACTT-3'). The PCR product was purified by PCR Purification Kit (Qiagen) and sequenced by GATC Biotech (Konstanz, Germany).

Bacterial chromosomal DNA was subjected to paired-end sequencing by Baseclear BV (Leiden, The Netherlands). The genome sequencing was done using Illumina (Solexa) GA*IIx* Genome Analyzer. For this, an amount of about 20 µg of genomic DNA was used with a concentration of 200 ng/µl. Sequencing yielded 7.2 million reads of about 50 bp reads as raw data. These were assembled using CLC-Bio (Aarhus, Denmark) software to yield 996 contigs of 188 to 63,169 bp.

Sequencing of cosmid clones was done at GATC (Konstanz, Germany). Standard primers (forward primer – BAC1: 5'-GCTCGTATGTTGTGTGGAATTG-3'; reverse primer – EGF2: 5'-GGGGATGTGCTGCAAGG-3') for pLAFR3 were used to start the sequencing. New primers were designed based on the 3' terminal parts of the contigs found by BLAST analysis of sequence reads against assembled contigs of genomic sequences.

Isolation of pLAFR3-clone DNA from *E. coli* TOP10 by alkaline lysis

An overnight culture of 5 mL of LB with tetracycline (12.5 µg/ml) was centrifuged (15,000 rpm) and the pellet was washed once in 1 ml of 10 mM Tris-HCl, pH 8, 100 mM NaCl, 1 mM EDTA. Next, the pellet was resuspended in 200 µL of 25 mM Tris-HCl, pH 8, 50 mM glucose, 10 mM EDTA at 4 °C. To the suspension was added 400 µl of 0.2 M NaOH, 1% (wt/vol) SDS and the sample was quickly mixed. After incubation for 1 min on ice, 300 µl of 3 M potassium acetate containing 11% (vol/vol) acetic acid glacial was added and kindly mixed. The mixture was incubated 5 min on ice and centrifuged for 10 min at 4 °C. The supernatant was taken for phenol/chloroform extraction. The whole procedure was performed on ice. To the supernatant one volume of phenol saturated with 10 mM Tris-HCl, pH 8, and 1 volume of chloroform : isoamyl alcohol (1:24) was added, followed by mixing and centrifugation for 2 min. The supernatant was taken and one volume of chloroform : isoamyl alcohol (1:24) was added, mixed and spinned down. Again the supernatant was taken and 0.1 volume of 3 M sodium acetate was added. Next 0.7 volumes isopropanol were added, followed by mixing and centrifugation for 20 min at 4 °C. The supernatant was discarded and the DNA-containing pellet was washed with ice-cold 70% ethanol and dried by air. The dried pellet was dissolved in 20 µl water and used for restriction analysis with EcoRI.

Whole-cell transformation of *β*-valine

Cells of strain SBV1 were grown on a 3 l minimal medium supplemented 10 mM glucose and 5 mM *β*-valine at 30 °C with shaking for 9 h to an optical density at 600 nm of 1.4. After harvesting by centrifugation, cells were washed with minimal medium and suspended in 40 ml 15 mM sodium phosphate in D_2O, pH 7.5. Next, the cells were incubated with 5 or 10 mM mM *β*-valine at 30 °C with rotary shaking at 200 rpm. Depletion of *β*-valine was followed in time by taking samples which were analyzed by HPLC with UV detection at 210 nm. Peaks that suggested potential degradation products of *β*-valine were manually collected and phosphates were precipitated by addition of excess of $CaCO_3$ to prepare the sample for ^{1}NMR and electrospray ionization mass spectrometry (ESI-MS). After complete consumption of *β*-valine, the remaining reaction mixture (2 x 24 ml) was lyophilized and the residue was dissolved in 1.5 ml D_2O, followed by HPLC analysis. Peaks that were observed (210 nm) were isolated and lyophilized, dissolved in 1.5 ml D_2O, and analyzed by ^{1}H NMR (Varian 400 MHz) and MS after removal of phosphates by precipitation. The MS analysis was performed using an MS ion-trapping system (Thermo Scientific,

Waltham, USA) by direct injection of the samples and spectra were recorded in positive and negative ionization modes.

Cosmid library generation and screening

The genomic DNA was partially digested with Sau3A to an average fragment size of 20 – 30 kb. Fragments were ligated in the BamHI linearized cosmid cloning vector pLAFR3 (Friedman *et al.,* 1982) that was isolated using a Maxi DNA purification kit (Nucleobond). Packaging was done in phage particles using the Gigapack III-XL kit according to manufacturer's instructions (Agilent). Phage particles were transfected to *E. coli* TOP10 (Invitrogen), which was subsequently plated on LB agar with tetracycline (12.5 µg/ml).

Triparental mating (Ditta *et al.,* 1980) was carried out by replica plating donor cells on LB-agar plates that were previously spread with 0.2 ml of an exponential culture (optical density at 450 nm of 0.6) of *E. coli* HB101(pRK600) (Kessler *et al.,* 1992). After overnight incubation these plates were replica plated on LB-agar that was previously spread with 0.2 ml of an overnight LB culture of the recipient strain *Pseudomonas fluorescens* Pf0-1. The plates were incubated overnight at 30 °C, and transconjugants were selected by replica-plating on minimal medium agarose plates containing 5 mM sodium citrate, 10 mM ammonium sulfate and tetracycline (12.5 µg/ml). Clones were screened by replicating on plates containing 5 mM citrate and 10 mM *β*-valine. From the positive clones plasmid DNA was isolated from the corresponding *E. coli* clone using alkaline lysis and the DNA insert was sequenced and compared to partial genome data.

Ammonia release assays were performed in microtiter plate (MTP) format using the Berthelot assay (Berthelot, 1859). A small amount of cell material was transferred from a fresh nutrient broth (NB) plate to an MTP well containing 150 µl of 5 mM *β*-valine in 1 mM KPi buffer (pH 7.5). The MTP was covered with BreathSeal (GE-Healthcare) and incubated overnight at 30 °C, with shaking at 1,050 rpm in a tabletop MTP shaker (Titramax 1000, Heidolph). The next day the MTP was centrifuged and 20 µl of supernatant was taken and added to 30 µl 0.025 % phenol (vol/vol) in 0.3 N NaOH. Immediately, 30 µl of 0.01% sodium nitroprusside and 30 µl of 20 mM NaOCl were added. The mixture was incubated for 15 min at 30 °C. Blue coloration indicated free ammonia present.

Preparation of cell-free extracts and enzyme assays

Strain SBV1 was grown (1.5 l, 200 rpm, 30 °C, 24 h) on minimal medium supplemented with 10 mM glucose and 5 mM *β*-valine, and harvested at an OD_{600} of

3.6, which gave about 5 g of wet cells. The cells were washed and resuspended in sonication buffer, which consisted of 50 mM of phosphate or HEPES buffer (pH 7.5), 0.01% (vol/vol) *β*-mercaptoethanol, 0.1 mM $MgCl_2$ and a tablet of protease inhibitors EDTA-free cocktail (Roche). After centrifugation, cell-free extract was obtained and used immediately for enzyme assays.

Aminomutase activity assays were performed using 10 mM *β*-valine in 50 mM sodium phosphate buffer (pH 7.5) and several potential cofactors (0.1 mM) such as PLP, coenzyme B_{12} (adenosylcobalamin, AdoCbl), and S-adenosylmethionine (SAM). Freshly prepared cell-free extract was used as enzyme source and conversion of *β*-valine into *α*-valine was monitored by HPLC with UV detection at 210 nm. Separation was achieved using a Thermo Aquasil C18 (250 x 4.6 mm, 5 µm) column coupled to a Jasco HPLC system which was connected to a Jasco Intelligent UV detector (210 nm). Analyses were run at 15 °C, isocratic mode using as eluent an aqueous solution that was brought to pH 1.25 with phosphoric acid and a flow rate of 1 ml/min. The retention time for *α*-valine was 6.6 min and for *β*-valine 5.6 min.

Aminotransferase (AT) activity assays were performed at 30 °C using an assay cocktail containing 10 mM α-valine, 5 mM 2-oxoglutarate (or pyruvate) and 50 µM PLP in 50 mM MOPS buffer, pH 7.6. Analysis was done as described (Crismaru *et al.,* 2013). Samples were analyzed by HPLC after derivatization with OPA (Roth, 1971). Depletion of *α*-valine and formation of L-*α*-glutamate or L-*α*-alanine was followed by means of UV (338 nm) and fluorescence (excitation at 350 nm, emission at 450 nm) spectroscopy using for separation a C18 Alltech OPA Adsorbosphere 5u column (5 µm, 4.6 mm x 100 mm) connected to a Jasco HPLC system, which was coupled to a Jasco UV and fluorescence detectors. The retention time for glutamate was 2.4 min and for alanine 7.7 min. One unit of AT activity is defined as the amount of enzyme (Val-AT) that catalyzes the formation of one µmol of L-*α*-glutamate or L-*α*-alanine from 10 mM *α*-valine, 10 mM 2-oxoglutarate or pyruvate in 1 minute in 50 mM MOPS buffer (pH 7.4) at 30 °C.

Inhibition studies of Val AT were performed using the potential AT inhibitors 2-aminooxy-acetic acid (AOA) (John & Charteris, 1978) and DL-propargylglycine (PAG) (Marcotte & Walsh, 1975). Freshly prepared cell-free extract was preincubated 5 min with 1 mM of the inhibitor, after which aminotransferase or aminomutase activity assays were performed as described above.

Ammonia release was also tested in cell-free extract. To a reaction mixture of 1.5 ml (50 mM HEPES, 100 mM NaCl, pH 8.0, 10 mM *β*-valine, 2 mM $MgCl_2$, 3 mM ATP, 1.5 mM CoA-SH) 50 µl (20 µl and 100 µl also tested) CFE was added. At different times, samples of 100 µl were taken and added to 100 µl 0.025 % phenol (vol/vol) in 0.3 N

NaOH. Immediately, 100 µl 0.01% sodium nitroprusside and 100 µl 20 mM NaOCl were added. The mixture was incubated 15 min at 30 °C. Absorption at 630 nm was measured to monitor ammonia release.

Protein concentrations were determined with the Bradford reagent.

Results

Properties of a *β*-valine degrading bacterium

Strain SBV1 was isolated from garden soil by enrichment culture with *β*-valine as sole nitrogen source. The degradation of *β*-valine in minimal medium cultures was followed in two distinct experiments using 5 mM and 10 mM *β*-valine, with glucose as carbon source (**Fig. 5.2**).

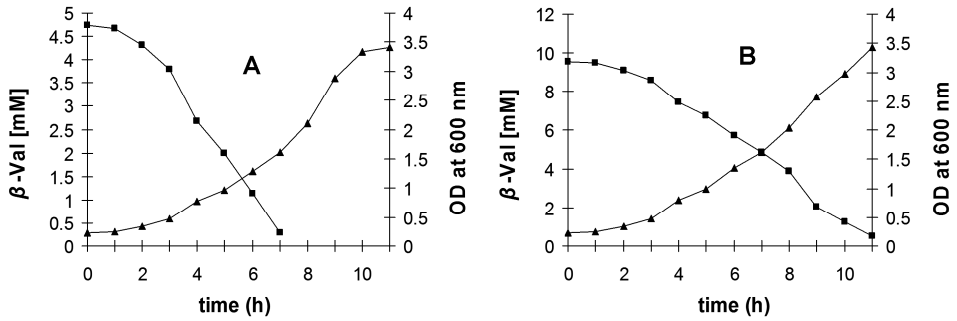

Figure 5.2 Conversion of *β*-valine by SBV1. Panel **A** – 5 mM *β*-valine with 20 mM glucose, panel **B** – 10 mM *β*-valine with 30 mM glucose, ■ – *β*-valine concentration, ▲ – optical density at 600 nm.

From the *β*-valine depletion curves and a relationship between cell mass (mg dry weight per ml) and OD_{600} (AU) of 0.4 ($mg \cdot ml^{-1} \cdot AU^{-1}$) we calculated a degradation rate of approximately 0.025-0.03 $\mu mol \cdot mg^{-1}$(cell dry weight)$\cdot min^{-1}$ during the mid-exponential phase for both growth cultures curves. The maximum growth rate observed with glucose and *β*-valine was approximately 0.20-0.22 h^{-1}. The growth curve in panel A indicates that cell density increased after depletion of *β*-valine, indicating temporary accumulation of a nitrogen source in the medium.

To identify strain SBV1, the 16S rRNA gene was sequenced. A BLAST search using the partial gene sequence showed that the SBV1 is a *Pseudomonas* sp. Partial genome analysis by paired-end sequencing confirmed this result by revealing a 1,410 bp 16S rRNA gene in contig 859 of 5,339 bp. A BLAST search using contig 859 as a

query sequence showed 98% sequence identity with a segment of the genome sequence of *Pseudomonas fluorescens* Pf0-1 (accession number CP000094.2) and 97% sequence identity with a segment of the genome sequence of *P. fluorescens* Pf-5 (accession number CP000076.1).

Possible pathways for *β*-valine degradation

The *β*-valine structure suggests that in comparison to *α*-valine few enzymatic reactions can theoretically take place (**Fig. 5.3**). For example, an amino acid oxidase or amino acid dehydrogenase reaction would not be possible since the position of the amino group on a *tert*-carbon atom does not allow formation of a keto functionality.

During *β*-valine degradation, significant amounts of *α*-ketoisovalerate were found as metabolite (S. De Wildeman, unpublished results), suggesting that an aminomutase could be responsible for the first step of the *β*-valine degradation pathway by forming *α*-valine (**Fig. 5.3**, reaction **1**). The latter is commonly converted by a branched amino acid aminotransferase to *α*-ketoisovalerate in bacteria, yeast or higher organisms (Massey *et al.,* 1976; Inoue *et al.,* 1988; Lange *et al.,* 2004). In several aerobic (e.g. *Bacillus subtilis, Burkholderia cepacia, Pseudomonas aeruginosa, P. fluorescens, Pseudomonas putida*), *α*-ketoisovalerate is converted by 2-oxoisovalerate dehydrogenase to isobutyryl-CoA, which can undergo degradation via the methylmalonyl pathway to succinyl-CoA, which enters the TCA cycle (**Fig. 5.5**). To investigate the possibility of this pathway, we checked the presence of *β*-valine aminomutase and α-valine aminotransferase. The results revealed that cell-free extracts incubated with *β*-valine did not show any *β*-valine depletion or α-valine formation, also when known cofactors of aminomutases were added, suggesting that an aminomutase that forms *α*-valine form *β*-valine is absent (or unstable).

Nevertheless, if we assume that an aminomutase is performing the first step in the degradation of *β*-valine, one would expect the presence of an *α*-valine aminotransferase catalyzing deamination, in agreement with the formation of 2-ketoisovalerate. Activity assays with cell-free extracts showed that *α*-valine aminotransferase activity was present when using 2-oxoglutarate as amino acceptor (specific activity 0.15 U·mg^{-1} protein). No AT activity was detected in the presence of pyruvate as amino acceptor. Similar levels of AT activity were found in cell-free extracts prepared from SBV1 cultures grown on minimal medium supplemented with *β*-valine, *α*-valine or NH_4^+ (5 mM) as nitrogen source and glucose (10 mM) as carbon source. This indicates that growth on *β*-valine does not induce aminotransferase activity for *α*-valine.

An even more straightforward deamination reaction would be the direct conversion of β-valine by an ammonia lyase to form 3-methyl-2-butenoic acid (**Fig. 5.3**, reaction **2**). However, incubations of cell free extracts with β-valine never showed any substrate depletion or ammonia release, suggesting that such an ammonia lyase is absent.

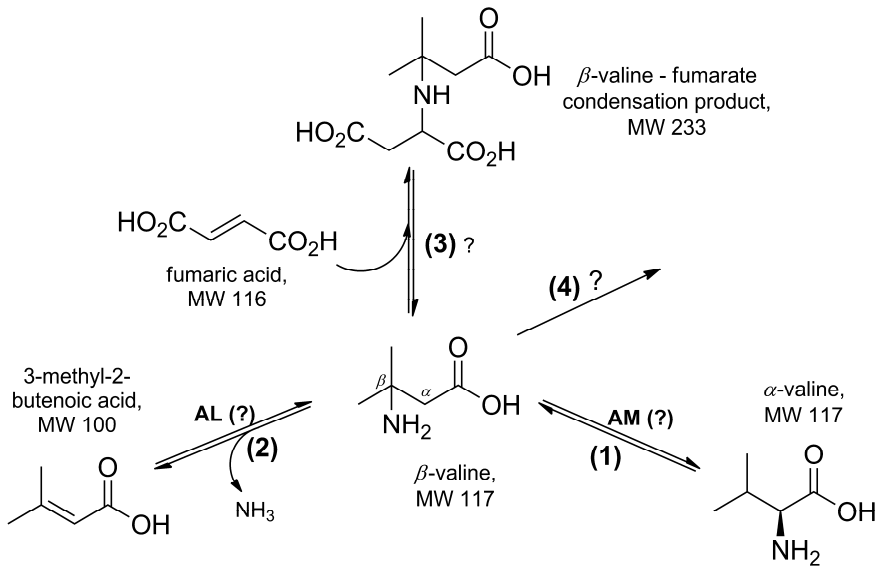

Figure 5.3 Possible degradation reactions of β-valine. Reactions: (**1**) – aminomutase; (**2**) – ammonia lyase; condensation (**3**); unknown reaction (**4**).

Enzyme assays

Since it is possible that the AM reaction is slow, we considered that α-valine eventually produced by the mutase enzyme is rapidly further converted by a valine aminotransferase (Val AT). In order to test this, we performed an experiment in which freshly prepared cell-free extract was incubated with α-valine, 2-oxoglutarate and AOA or PAG as potential inhibitors of Val AT. These assays showed that the aminotransferase activity was almost abolished when using AOA, whereas with PAG, Val AT activity was inhibited by 20%. However, our results showed no depletion of β-valine upon prolonged incubation with AT-inhibited cell-free extract. The same approach, using AOA and PAG for inhibition of Val AT was used with resting cells. Although β-valine was rapidly degraded within 1.5 h, no α-valine was detected in the whole-cell transformation supernatant.

In order to check if different proteins are expressed in cells of strain SBV1 during growth on β-valine, protein patterns were analyzed by SDS-PAGE. SBV1 cells

were grown under inducible (*β*-valine) and non-inducible conditions (cells grown on $NH4^+$ and glucose or succinate). The results showed no significant difference on the protein expression patterns between the cell-free extracts from induced and non-induced cells (**Fig. 5.4**) and thus provided no lead for a proteomics-based approach to discover the enzymes of the *β*-valine metabolic pathway.

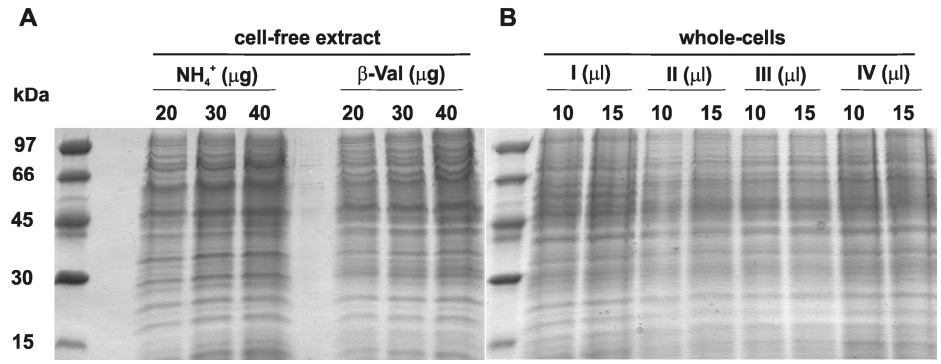

Figure 5.4 Protein expression pattern of SBV1 under inducible and non-inducible conditions in cell-free extract (**panel A**) and whole cells (**panel B**). Roman numbers represent growth conditions for SBV1: **I** - *β*-valine 15 mM; **II** - *β*-valine 5 mM with 10 mM glucose; **II** - NH_4^+ 5 mM with 10 mM glucose; **IV** - *β*-valine 5 mM with 10 mM succinate. Numbers located above the lanes represent the amount of protein (µg) analyzed (**panel A**) or the sample volume (µl) analyzed (**panel B**).

Ammonia release using the Berthelot assay in cell-free extract was found to be independent of *β*-valine but dependent of ATP. However, the background was too high to accurately quantify how much ammonia was formed in the reaction mixture, and it was concluded that no enzymes for direct ammonia release from *β*-valine were present in cell-free extracts.

Whole-cell transformation of *β*-valine

In some cases, a pulse addition of a substrate leads to transient accumulation of early metabolites in the culture fluid (Hollywood *et al.,* 2006; Villas-Boas *et al.,* 2005; Winkelmann *et al.,* 1999). Therefore, we performed whole-cell transformation experiment and investigated the formation of metabolites by HPLC and ESI-MS. Using a suspension of cells precultivated in the presence of *β*-valine (5 mM), the degradation of *β*-valine was monitored over time and was complete after about 1.5 h in the case of 5 mM *β*-valine (37.5 mg of cells ml^{-1}) or 2.5 h when using 10 mM *β*-valine (75 mg of cells ml^{-1}). Samples of the supernatant were taken and subjected to HPLC, MS and ^{1}NMR analysis. By HPLC-UV analysis with detection at 210 nm, seven (7) peaks

(including *β*-valine) were observed as possible products. Control experiments showed that none of these peaks appeared when no *β*-valine was added to the cell suspension. The ^{1}NMR spectra obtained with samples of culture fluid were not very informative because no clear signals were detected that could be associated with possible products of *β*-valine catabolism.

Isolated fractions of the seven observed HPLC peaks were prepared for ESI-MS analysis. After lyophilization, the sample material of each peak was dissolved in D_2O. The compounds present will have different masses due to varying degrees of proton:deuterium exchange and as a consequence clusters of masses were observed for most peaks (**Table 5.1**). Few peaks indicated lower molecular masses than 118 Da (*β*-valine). This may suggest that *β*-valine degradation does not take place directly, but possibly via a condensation reaction with a metabolite (**Fig. 5.3**, reaction **3**), which would yield a product more suitable to eliminate nitrogen and allow growth. Since we repeatedly observed a mass of 231-234 Da in different isolated peaks (**Table 5.1**), we considered the possibility that *β*-valine is condensed with fumarate in a reverse lyase reaction.

Table 5.1 Mass clusters observed by ESI-MS analysis (positive mode) on possible products peaks of *β*-valine by whole-cell transformation.

Mass clusters (Da)	peak I	peak II	peak III	peak IV	peak V	peak VI	peak VII
103			103.25	103.17		103.17	
113					113.17-116.25		
118	118.17	118.25					
121			121.25-124.25				
139						139.25 140.25	
195	195.33			195.33		195.33	195.33
204		204.33 205.25					
217				217.17			
231-234			234.17	233.25 234.17	231.17-237.17	232.17-234.17	233.25-234.17

These peaks were not seen in control experiments where no *β*-valine was added. This type of reaction has been reported in the literature for ethylene diaminodisuccinate lyase (EDDS lyase) and iminodisuccinate lyase (IDS lyase), which convert their substrates to fumarate and N-(2-aminoethyl)-aspartate and to fumarate and aspartate, respectively (Bauerle *et al.,* 2006; Cokesa *et al.,* 2004). However, when we attempted to measures such activities using cell-free extracts, no depletion of *β*-valine

was observed in the presence of fumarate. From the ^{1}NMR spectra (data not shown) and also from the HPLC data, it was clear that fumarate was consumed and converted to oxaloacetate, but *β*-valine remained unconverted.

Partial genome sequencing of SBV1

By sequencing the chromosomal DNA of SBV1, we could possibly obtain information about genes coding an enzyme for *β*-valine degradation (**Table 5.2**). Using BLAST searches, it appeared that the SBV1 genome is highly similar those of *P. fluorescens* Pf-5 and *P. fluorescens* Pf0-1 but when the latter two strains were tested for growth with *β*-valine as sole nitrogen source in liquid cultures, no visible growth was observed within 3 weeks. This suggests that the latter two strains lack genes and enzymes for *β*-valine metabolism.

Table 5.2 Processing of paired-end sequencing data from SBV1.

de novo gene assembly stats	SBV1
Total matched base pairs from reads	354 M bp
Average read length	49 bp
# contigs	996
Average contig length	6,400 bp
Coverage of contigs	6.4 M bp
Fold-coverage	55

A BLAST search using several known amino acid aminomutase sequences [lysine 2,3-aminomutase from *C. subterminale* SB4 (AF159146.1), two lysine 2,3-aminomutases from *E. coli* K-12 strain w3110 (AP004647.1 and BAE78148.1), arginine aminomutase from *S. griseochromogenes* (AAP03121.1) and arginine aminomutase from *P. syringae p.v phaseolicola* (AAZ35479.1)] was performed. The results showed no relevant hits. Using the MIO-type tyrosine aminomutase from *Streptomyces globisporus* (PDB code 2OHY) as query, three hits were found (contigs 873 (two copies) and contig 526. BLAST searches performed with Artemis showed that the two putative MIO-enzyme genes in contig 873 are highly similar to genes encoding histidine ammonia lyases, and that this region also contains other genes of histidine metabolism. The same holds for the gene in contig 526, although the closest hit with a protein of known structure was tyrosine aminomutase. Thus, the genomic analysis did not provide convincing indications for a mutase involved in *β*-valine degradation.

A BLAST search with known branched-chain aminotransferase sequences from yeast, *Pseudomonas* sp., *E. coli*, and *Bacillus* sp. gave a promising hit in contig 839 (1,422 bp). The hit is a putative branched chain aminotransferase gene (339 codons), which shares 95% sequence identity at the amino acid sequence level to a putative aminotransferase from *P. fluorescens* Pf0-1 (ABA75205.1) and 94% sequence identity to a putative aminotransferase from *P. fluorescens* Pf-5 (AAY91803.1). The last two share 93% sequence identity with respect to each other. Due to the shortness of this contig, no regulatory regions or other potential pathway related genes could be found. The putative Val AT in contig 839 possibly is responsible for the α-valine AT activity that was detected and quantified in cell-free extract of SBV1 (**Fig. 5.5**, reaction **2**).

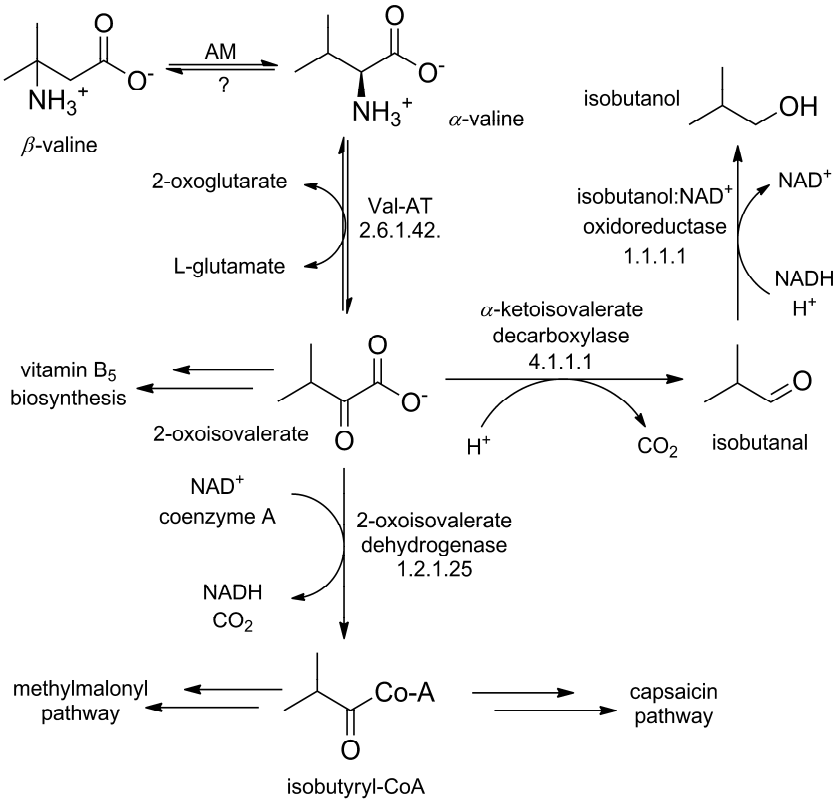

Figure 5.5 Hypothetical aminomutase-based degradation pathways of *β*-valine.

The analysis of the partial genome sequence of strain SBV1 further identified several genes for enzymes of the biosynthesis and catabolic pathways of all three branched chain amino acids (leucine, isoleucine and valine). To consider the possibility that the

first step of *β*-valine degradation is catalyzed by an EDDS-lyase like enzyme, we performed BLAST searches using two EDDS C-N lyase (EC 4.3.2.1) sequences from *Ralstonia* sp. SLRS7 (AAZ80812.1) and the one from *Agrobacterium tumefaciens* strain BY6 (AAZ80811.1) as queries. In contig 636 (14,564 bp) a putative protein sequence that shares 36% sequence identity with EDDS-lyase from *Ralstonia* sp. SLRS7 and 35% sequence identity with EDDS-lyase from *A. tumefaciens* BY6 was found. However, this hit was 97% sequence identical to an argininosuccinate lyase from *P. fluorescens* Pf0-1 (ABA77226.1) and 95% sequence identical to another argininosuccinate-lyase from *P. fluorescens* Pf-5 (AAY95193.1). Argininosuccinate lyases catalyze the splitting of 2-[N-(omega)-L-arginino]-succinate into fumarate and L-arginine. From the same BLAST search, a hit was found in contig 463 (29,139 bp) that shares at the amino acid sequence level 30% sequence identity with EDDS-lyase from *Ralstonia* sp. SLRS7 and 31% sequence identity with EDDS-lyase from *A. tumefaciens* BY6. This putative protein was found to be 83% sequence identical to an argininosuccinate-lyase from *P. fluorescens* Pf0-1 (ABA74593.1).

Identification of a gene cluster for *β*-valine degradation

Since neither of the above approaches identified the mechanism of *β*-valine transformation, a classical genetic approach was followed. A cosmid library of about 2,300 clones was constructed using genomic DNA isolated from the strain SBV1, with an estimated DNA average size of 20-30 kb. Initial screening of the SBV1 cosmid library in *E. coli* by plating cells on minimal medium supplemented with *β*-valine (5 mM) and glucose (10 mM) did not yield any positive clones after 3 weeks of incubation at 30 °C. Therefore, screening was performed in *P. fluorescens* Pf0-1, which is similar to strain SBV1 at the DNA sequence level, but is not able to use *β*-valine as a nitrogen source, suggesting that genes for the deamination of *β*-valine are absent. Replica plating of the SBV1 cosmid library on plates containing *β*-valine (10 mM) and citrate (5 mM) gave two positive clones (p5-F12 and p4-D1), out of which the latter was further investigated. Screening was also performed using the Berthelot assay for whole cells which confirmed ammonia release by the clones, p5-F12 (**Fig. 5.6**) and p4-D1 (data not shown). Ammonia production exceeded the upper detection limit of 1 mM, whereas the other clones produced less than 0.2 mM ammonia.

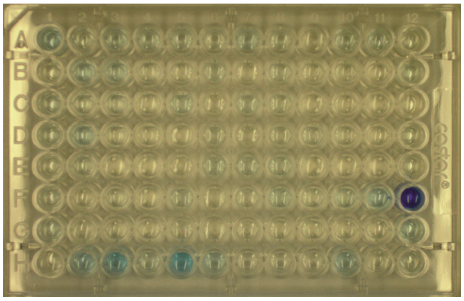

Figure 5.6 Screening of *P. fluorescens* Pf0-1 pLAFR3 SBV1 library for ammonia release from β-valine using the Berthelot assay. The positive clone shown is called p5-F12, and gave the same result as p4-D1 (not shown).

The sequence of the 26 kb insert of plasmid p4-D1 was determined with a combination of primer walking with dideoxy sequencing and assembly with the contigs of the partial genome sequence. This yielded the complete sequence of the 26,347 bp insert. Translation using Artemis software and sequence analysis by BLAST searches revealed the presence of 19 relevant open reading frames (**Table 5.3**, **Fig. 5.7**).

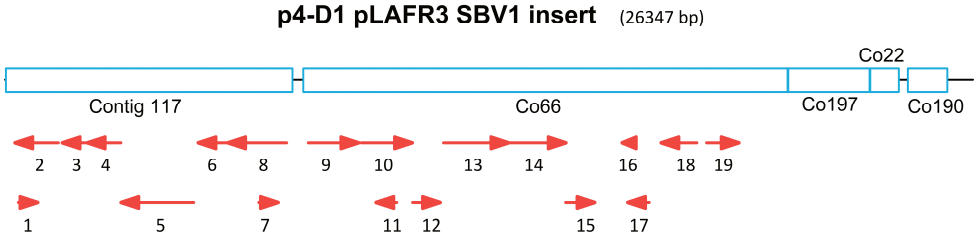

Figure 5.7 Organization of the 26,347 bp insert of plasmid p4-D1 harboring the β-valine degradation gene cluster. Arabic numbers represent the open reading frames that are potentially relevant for β-valine degradation (**Table 5.3**).

Proposed pathway for β-valine metabolism

The sequence of the open reading frames detected in the insert of clone p4-D1, which endows *P. fluorescens* Pf0-1 with the capacity to degrade β-valine, suggests a possible pathway for β-valine metabolism in strain SBV1 (**Fig. 5.8**). Since the sequence of several putative enzymes is similar to enzymes of the leucine catabolic pathway (Aquilar *et al.,* 2006), it seems that β-valine is transformed in a similar way. First, uptake of β-valine may be facilitated by a transport protein (**Fig. 5.8**, **ORF 9**) that has 50% sequence identity to a putative γ-aminobutyrate pearmease from *Rhodococcus opacus* PD630 (EHI41568.1). Inside the cell, β-valine may undergo

activation by coenzyme A in an ATP-dependent reaction catalyzed by a CoA-dependent ligase (**Fig. 5.8**, **ORF 10**). The translated sequence of **ORF 10** shares 36% sequence identity with phenylacetate-CoA ligase from *Burkholderia cenocepacia* of which crystal structures bound with phenylacetate and ATP were reported (Law & Boulanger, 2011).

Table 5.3 List of relevant open-reading frames found in the 26 kb insert of the p4-D1 pLAFR3 positive clone of the SBV1 cosmid library.

ORF No	Position in the insert (bp)	Enzyme	Number of amino acids	EC number	Seq. identity to known proteins (%)	PDB
1	366-902	acyl-CoA DH	178	1.3.99.3	38	
2	1456-272 (C)	acetyl-CoA acetyltransferase	424	2.3.1.9	45	
3	2231-1557 (C)	gluathione S-transferase	224	2.5.1.18	64	
4	3159-2242 (C)	hydroxymethylglutaryl-CoA lyase	305	4.1.3.4	61	2CW6
5	5141-3156 (C)	3-methyl-crotonyl-CoA carboxylase	661	6.4.1.4	73	3U9S
6	6051-5257 (C)	methylglutaconyl-CoA hydratase	264	4.2.1.18	74	
7	6910-7446	Hypothetical protein	178	-	48	
8	7671-6064 (C)	propionyl-CoA carboxylase	535	6.4.1.3	66	3N6R
9	8255-9634	gamma-aminobutyrate permease	459	-	50	
10	9696-11096	phenylacetate CoA-ligase	466	6.2.1.30	36	2Y4N
11	10667-10095 (C)	3-hydroxybutyryl-CoA dehydratase	190	4.2.1.55	41	
12	11096-11857	enoyl-CoA hydratase	253	4.2.1.17	36	3HRX
13	11936-13717	transcription regulator	593	-	49	
14	13762-15276	acetyl-CoA acetyltransferase	504	2.3.1.9	51	
15	15261-16061	enoyl-CoA hydratase	266	4.2.1.17	38	1DUB
16	17183-16791 (C)	D-isomeric 2-hydroxyacid DH short	130	1.1.99.6	38	
17	17536-16946 (C)	D-isomeric 2-hydroxyacid DH long	196	1.1.99.6	52	
18	18834-17854 (C)	phage cointegrase	326	-	74	
19	19096-19984	conintegrate resolution protein T	322	-	62	

In the next step, the *β*-valinyl-CoA adduct is proposed to release ammonia by the activity of an aminoacyl-CoA ammonia lyase, forming 3-methyl-crotonyl-CoA. This is based on the fact that **ORFs 4-6** in the gene cluster share sequence similarity to genes involved in conversion of 3-methyl-crotonyl-CoA, which is a common intermediate in the leucine degradation pathway (Aguilar *et al.,* 2006). However, no ammonia lyases that are active on *β*-aminoacyl-CoAs have been described in the literature, with the exception of two *β*-alanine CoA ammonia lyases found in *Clostridium propionicum* (Herrmann *et al.,* 2005). The gene encoding the *β*-alanyl-CoA ammonia lyase II is located next to the gene that encodes the *β*-alanine CoA ligase. Since the *β*-alanine CoA ligase is somewhat homologous to the putative CoA ligase described here (**ORF 10**), we inspected the complementary strand for the presence of

a homolog of the described *β*-alanyl-CoA ammonia lyase, but no such ORF was detected. However, further inspection of the sequenced region showed the presence of two ORFs (**Fig. 5.8**, **ORFs 12** and **15**), which encode protein sequences that share sequence similarity to an enoyl-CoA-hydratase from *Rattus norvegicus* (38%) with known structure(s) (PDB code 1EY3 (Bahnson *et al.,* 2002); PDB code 1MJ3 (Bell *et al.,* 2002); PDB code 2DUB (Engel *et al.,* 1998)), an enoyl-Coa hydratase from *Thermus thermophilus* HB8 (36%) with solved crystal structure (PDB code 3HRX (Kichise *et al.,* 2009)) and to an enoyl-CoA hydratase (35%) from *Bacillus anthracis* (PDB code 3KQF).

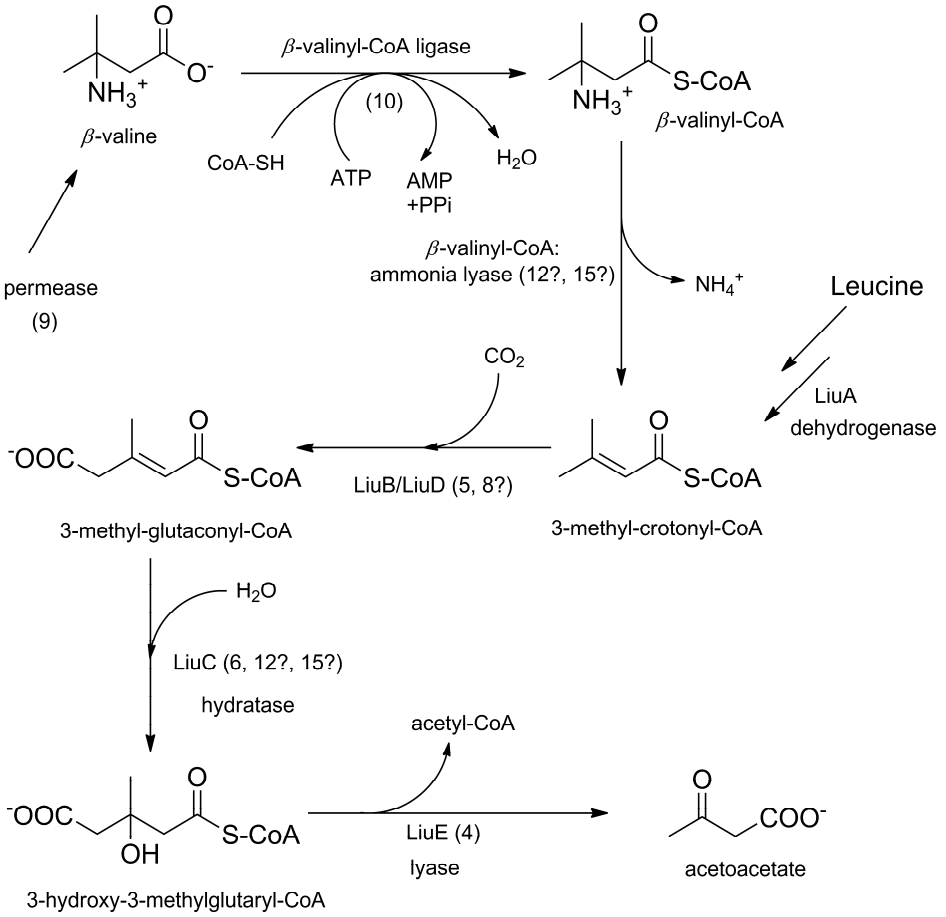

Figure 5.8 Proposed degradation pathway of *β*-valine by *Pseudomonas* sp. strain SBV1. Numbers in the parenthesis correspond to the ORFs of clone p4-D1 that are homologous to the enzymes from the leucine degradation pathway (Aguilar *et al.,* 2006).

According to the literature enoyl-CoA hydratases are hexamers containing six identical subunits (dimer of trimers). Keeping in mind the sequence similarity between hydratase and ammonia lyase (e.g. fumarase and aspartate ammonia lyase (Puthan Veetil *et al.,* 2012)) it is conceivable that one of these genes encodes the enzyme that carries out the deamination step.

The product of the reaction catalyzed by the expected *β*-valinyl-CoA ammonia lyase is 3-methyl-crotonyl-CoA, which is a common intermediate in the leucine degradation pathway. It can undergo a carboxylation reaction to form to 3-methyl-glutaconyl-CoA, which is catalyzed by 3-methyl-crotonyl-CoA carboxylase (Huang *et al.,* 2011). Indeed, **ORF 5** (**Fig. 5.8**) shares 73% sequence identity to 3-methyl-crotonyl-CoA carboxylase from *P. aeruginosa* (PDB code 3U9S). In the next step, 3-methyl-glutaconyl-CoA can be hydrated by a hydratase (**Fig. 5.8**, **ORF 6**) which shares 74% sequence identity to 3-methyl-crotonyl-CoA hydratase from *Pseudomonas chlororaphis* subsp. *aureofaciens* 30-84 (EJL05953.1), and 46% sequence identity to an enoyl-CoA hydratase (crotonase) from *Legionella pneumophila* subsp. *pneumophila* (PDB code 3I47), forming 3-hydroxy-3-methylglutaryl-CoA. In the last step, the latter metabolite is cleaved into acetyl-CoA and acetoacetate by hydroxymethylglutaryl-CoA lyase (**Fig. 5.8**, **ORF 4**), which shares 61% sequence identity to the human homolog (PDB code 2CW6) (Fu *et al.,* 2006).

Discussion

Multiple options exist for solving the pathway of microbial metabolism of an exogenous compound: 1) performing enzyme assays to detect conversion of the substrate and identify products (Kim *et al.,* 2006; Yun *et al.,* 2004; Iwasaki *et al.,* 2003); 2) searching for metabolites in culture fluids after pulse addition of the substrate (Hollywood *et al.,* 2006; Villas-Boas *et al.,* 2005; Winkelmann *et al.,* 1999); 3) measuring the inducibility of oxygen uptake activity upon addition of possible intermediates to resting cell suspensions; 4) construction of gene libraries, followed by functional screening (Gabor *et al.,* 2004); 5) genome sequence analysis, if possible using comparative genomics (Becker & Palsson, 2005); 6) gene inactivation experiments using transposon mutagenesis (de Lorenzo *et al.,* 1994); 7) proteomics experiments, looking for differential induction of protein synthesis. In this work we have tried approaches 1, 2, 4 and to a certain extent 5 and 7.

Based on earlier work on *β*-valine degradation, the most likely route was conversion by an aminomutase to α-valine, followed by an α-valine:α-ketoglutarate

aminotransferase reaction. The latter activity was detected in cell-free extracts, and it was observed earlier that 2-oxoisovalerate is formed when whole cells were exposed to *β*-valine (De Wildeman, unpublished observation). However, aminomutase assays using cell-free extract as well as whole-cell incubations did not result in the detection of aminomutase activity. However, we cannot rule out completely the presence of an unstable or oxygen sensitive mutase, as found in anaerobic bacteria such as *Clostridium sticklandii, Pseudomonas gingivalis, Clostridium subterminale, Clostridium sporogenes* (Poston, 1976, Chirpich *et al.,* 1970). Often, these enzymes are difficult to purify and need reactivation by reduction with sodium dithionite due to oxidation of cofactors (AdoCbl, SAM or [4Fe-4S] cluster). Since strain SBV1 grows aerobically we did not consider an anaerobic purification protocol. Furthermore, the genome sequence did not provide indications of such a pathway.

Another straightforward route for *β*-valine metabolism would be a lyase reaction. Again, neither incubations of cell-free extracts nor genomic analysis suggested the presence of such a lyase. Furthermore, ^{1}NMR and HPLC analysis of culture fluids failed to identify. A promising mass cluster in the range of 231-234 Da (due to H-D exchange) appeared in different HPLC peak samples, and some material was unstable. The possibility that suggestion *β*-valine starts with a condensation reaction with fumarate, which would yield a product of 231 Da, was examined, but no activity was detected in cell-free extracts, and also the genome sequence provided no support for this. Possibly, these peaks are due to some side reaction that has little to do with productive metabolism.

A more convincing clue for the *β*-valine degradation pathway was obtained by following a genetic approach. After construction of a gene library in a broad-host range vector, followed by conjugation into *P. fluorescens* Pf0-1 and screening, a clone was discovered that allowed growth of the host on *β*-valine. The sequence data suggest that the key genes for the deamination of *β*-valine are likely to encode a CoA-dependent ligase that activates *β*-valine, and a *β*-valinyl-CoA ammonia lyase that deaminates and produces 3-methyl-crotonyl-CoA (**Fig 5.8**). Thus, the most successful approach for elucidating the *β*-valine pathway was similar to the strategy used to solve the deamination mechanism of *β*-phenylalanine by *Variovorax paradoxus* strain CBF3 (Crismaru *et al.,* 2013). Expression studies by C. Postema and M. Otzen in our laboratory (data not shown) have recently demonstrated that the purified His-tagged CoA ligase encoded by ORF10 indeed has CoA-ligase activity with *β*-valine. The *β*-valinyl-CoA adduct was detected by mass spectrometry and could be deaminated by addition of the purified overexpressed *β*-valinyl-CoA ammonia lyase proteins encoded by ORF12 and ORF15. The ammonia lyase product 3-methylglutaconic acid was

identified by mass spectrometry. These results confirm that the sequence-based predictions provided here are correct.

Since there is little information on the *β*-valine-CoA ligase protein homologs it is quite difficult to predict how exactly the activation takes place or what type of residues are involved during the reaction. Nevertheless, BLAST searches using the protein sequence of the identified CoA ligase demonstrated high sequence similarity with several phenylacetate-CoA ligases, including the published *Burkholderia cenocepacia* phenylacetate-CoA ligases PaaK1 and Paak2. Structural analyses of Paak1 and PaaK2 in complex with either ATP or phenylacetyl adenylate revealed several important residues for proper activity (PDB codes 2Y27, 2Y4O and 2Y4N (Law & Boulanger, 2011)). Sequence alignments using the identified *β*-valine-CoA ligase PaaK1 and PaaK2 demonstrated that the ATP binding pocket is also present in *β*-valine-CoA ligase. However, the residues involved in the binding of phenylacetyl adenylate (PDB code 2Y4N) differ from the residues present in *β*-valine-CoA ligase (**ORF 10**). The following substitutions were observed (Y136→L167, F141→W172, A147→D178, A214→G245, I236→N270 and Pro245→Ile278). This large number of substitutions of residues that contact the phenyl ring in Paak1 (2Y4N) has to result in differences in shape and polarity of the substrate binding site that may explain why the activity with *β*-valine CoA ligase instead of phenylacetic acid.

Sequence analysis of the two putative *β*-valinyl-CoA ammonia lyases that we detected in the *β*-valine gene cluster (**Fig. 5.7**, **ORFs 12** and **15**) indicated that there are several crystal structures available of sequence-related enoyl-CoA hydratases from different sources (PDB codes: 1EY3, 1MJ3, 2DUB, 3HRX, 3KQF) complexed with various CoA-bound substrates (e.g. hexadienoyl-CoA, octanoyl-CoA, 4-(N,N-dimethylamino)cinnamoyl-COA). These enzymes belong to the crotonase/enoyl coenzyme A (CoA) hydratase superfamily with conserved domain structure cd06558 (Marchler-Bauer *et al.,* 2013). A close homolog of which the structure is known is the enoyl-CoA hydratase from rat. This enzyme is active with cinnamic acid and a structure containing the substrate 4-(N,N-dimethylamino)cinnamoyl-CoA was solved (Bahnson *et al.,* 2002). At least three amino acid residues are known to be important for substrate activation and catalysis in such hydratases, i.e. Gly141 (Bell *et al.,* 2001), Glu144 and Glu164 (Agnihotri *et al.,* 2003; Hofstein *et al.,* 1999).

A sequence alignment including the two **ORFs** (**12** and **15**) that are suspected to correspond to *β*-valinyl-CoA ammonia lyase and the structurally related enoyl-CoA hydratases from *Rattus norvegicus* and *Bacillus anthracis* showed that Gly141, Glu144 and Glu164 were strictly conserved in all enzymes. In enoyl CoA hydratase, the glutamate residues are bridged by a catalytic water that has a lone pair of electrons

that can react with C(3) of the enzyme-bound α,β-unsaturated thioester (Bahnson *et al.,* 2002). In case of the *β*-valinyl-CoA ammonia lyase, this position might correspond to the binding site for the amino group of the substrate. Deamination would probably require a different hydrogen bonding pattern around the leaving groups as compared to (de) hydration, and a structure is likely required to explain the deamination mechanism.

The ammonia lyase reaction proposed here for the *β*-valine catabolic pathway is a rare example of an ammonia lyase acting on *β*-amino functionality of a carboxylic acid other than aspartate. Whereas ammonia lyase reactions acting on aspartate and methylaspartate are strictly dependent on two carboxylate functionalities (or at least a carboxylate and an amide group), the CoA activation apparently allows deamination without a second electron-withdrawing substituent flanking the amine hat is eliminated. Although this is an elegant way of allowing (de)amination of a *β*-substituted amino acid, applications to an industrial process would not benefit from this pathway since it requires the use of the expensive component coenzyme A, and also of ATP. Possible applications of the discovered β-elimination and the reverse addition reaction seem most realistic for conversions involving whole cells, e.g. using engineered microorganisms in which the relevant genes (CoA-dependent ligase and *β*-valinyl-CoA ammonia lyase genes) are integrated in a biosynthetic pathway with coenzyme recycling.

Acknowledgements

This research was financially supported by the BE-Basic Foundation (http://www.be-basic.org). The authors acknowledge Dr. B. Kaptein from (DSM, Geleen, The Netherlands) for support and helpful discussions and Piet Wietzes for assistance with MS analysis.

References

Aberhart, D.J., Lin, H.J. and Weiller, B.H. (1981) Stereochemistry of lysine 2,3-aminomutase. *J Am Chem Soc* 103: 6750–6752.

Agnihotri, G. and Liu, H.W. (2003) Enoyl-CoA hydratase. reaction, mechanism, and inhibition. *Bioorg Med Chem* 11: 9–20.

Aguilar, J.A., Zavala, A.N., Diaz-Perez, C., Cervantes, C., Diaz-Perez, A.L. and Campos-Garcia, J. (2006) The atu and liu clusters are involved in the catabolic pathways for acyclic monoterpenes and leucine in *Pseudomonas aeruginosa*. *Appl Environ Microbiol* 72: 2070–2079.

Asano, Y., Kato, Y., Levy, C., Baker, P. and Rice, D. (2004) Structure and function of amino acid ammonia-lyases. *Biocatal Biotransfor* 22: 131–138.

Bahnson, B.J., Anderson, V.E. and Petsko, G.A. (2002) Structural mechanism of enoyl-CoA hydratase: three atoms from a single water are added in either an E1cb stepwise or concerted fashion. *Biochemistry* 41: 2621–2629.

Banerjee, A., Sharma, R. and Banerjee, U.C. (2003) A rapid and sensitive fluorometric assay method for the determination of nitrilase activity. *Biotechnol Appl Biochem* 37: 289–93.

Bauerle, B., Cokesa, Z., Hofmann, S. and Rieger, P.G. (2006) Sequencing and heterologous expression of an epimerase and two lyases from iminodisuccinate-degrading bacteria. *Appl Environ Microbiol* 72: 2824–2828.

Becker, S.A. and Palsson, B.Ø. (2005) Genome-scale reconstruction of the metabolic network in *Staphylococcus aureus* N315: an initial draft to the two-dimensional annotation. *BMC Microbiol* 5: 8.

Bell, A.F., Feng, Y., Hofstein, H.A., Parikh, S., Wu, J., Rudolph, M.J., Kisker, C., Whitty, A. and Tonge, P.J. (2002) Stereoselectivity of enoyl-CoA hydratase results from preferential activation of one of two bound substrate conformers. *Chem Biol* 9: 1247–1255.

Bell, A.F., Wu, J., Feng, Y. and Tonge, P.J. (2001) Involvement of glycine 141 in substrate activation by enoyl-CoA hydratase. *Biochemistry* 40: 1725–33.

Berg, C.M., Whalen, W.A. and Archambault, L.B. (1983) Role of alanine-valine transaminase in *Salmonella typhimurium* and analysis of an avtA::Tn5 mutant. *J Bacteriol* 155: 1009–1014.

Berthelot, M. (1859) *Répert Chim Appl* 1: p. 284.

Boyer, P.D., Lardy, H. and Myrback, K. (1963) (Eds.), The Enzymes, 2nd ed., vol. 7, Academic Press, New York: 609–648.

Brunhuber, N.M. and Blanchard, J.S. (1994) The biochemistry and enzymology of amino acid dehydrogenases. *Crit Rev Biochem Mol Biol* 29: 415–67.

Chirpich, T.P., Zappia, V., Costilow, R.N. and Barker, H.A. (1970) Lysine 2,3-aminomutase. Purification and properties of a pyridoxal phosphate and S-adenosylmethionine-activated enzyme. *J Biol Chem* 245: 1778–1789.

Cokesa, Z., Knackmuss, H.J. and Rieger, P.G. (2004) Biodegradation of all stereoisomers of the EDTA substitute iminodisuccinate by *Agrobacterium tumefaciens* BY6 requires an epimerase and a stereoselective C-N lyase. *Appl Environ Microbiol* 70: 3941–3947.

Crismaru, C.G., Wybenga, G.G., Szymanski, W., Wijma, H.J., Wu, B., Bartsch, S., De Wildeman, S., Poelarends, G.J., Dijkstra, B.W. and Janssen, D.B. (2013) Biochemical properties and crystal structure of a *β*-phenylalanine aminotransferase from *Variovorax paradoxus*. *Appl Environ Microbiol* 79: 185–195.

DeFelice, M., Levinthal, M., Iaccarino, M. and Guardiola, J. (1979) Growth inhibition as a consequence of antagonism between related amino acids: effect of valine in *Escherichia coli* K-12. *Microbiot Rev* 43: 42–58.

de Lorenzo, V. and Timmis, K.N. (1994) Analysis and construction of stable phenotypes in gram-negative bacteria with Tn5- and Tn10-derived minitransposons. *Methods Enzymol* 235: 386–405.

Ditta, G., Stanfield, S., Corbin, D. and Helinski, D.R. (1980) Broad host range DNA cloning system for gram-negative bacteria: Construction of a gene bank of *Rhizobium meliloti*. *Proc Natl Acad Sci* 77: 7347–7351.

Engel, C.K., Kiema, T.R, Hiltunen, J.K. and Wierenga, R.K. (1998) The crystal structure of enoyl-CoA hydratase complexed with octanoyl-CoA reveals the structural adaptations required for binding of a long chain fatty acid-CoA molecule. *J Mol Biol* 275: 847–859.

Fernandez, M. and Zuniga, M. (2006) Amino acid catabolic pathways of lactic acid bacteria. *Crit Rev Microbiol* 32:155–83.

Fernandez de Palencia, P., de la Plaza, M., Amarita, F., Requena, T. and Pelaez, C. (2006). Diversity of amino acid converting enzymes in wild lactic acid bacteria. *Enzyme Microb Technol* 38: 88–93.

Fitzpatrick, P.F. (2010) Oxidation of amines by flavoproteins. *Arch Biochem Biophys* 493: 13–25.

Friedman, A.M., Long, S.R., Brown, S.E., Buikema, W.J. and Ausubel, F.M. (1982) Construction of a broad host range cosmid cloning vector and its use in the genetic analysis of *Rhizobium* mutants. *Gene* 18: 289–296.

Fu, Z., Runquist, J.A., Forouhar, F., Hussain, M., Hunt, J.F., Miziorko, H.M. and Kim, J.J. (2006) Crystal structure of human 3-hydroxy-3-methylglutaryl-CoA Lyase: insights into catalysis and the molecular basis for hydroxymethylglutaric aciduria. *J Biol Chem* 281: 7526–32.

Gabor, E.M, de Vries, E.J. and Janssen, D.B. (2004) Construction, characterization, and use of small-insert gene banks of DNA isolated from soil and enrichment cultures for the recovery of novel amidases. *Environ Microbiol* 6: 948–958.

Gilbert, S.F. and Migeon, B.R. (1975) D-valine as a selective agent for normal human and rodent epithelial cells in culture. *Cell* 5: 11–17.

Glover, S.W. (1962) Valine-resistant mutants of *Escherichia coli* K-12. *Genetical Research* 3: 448–460.

Heberling, M.M., Wu, B., Bartsch, S. and Janssen, DB. (2013) Priming ammonia lyases and aminomutases for industrial and therapeutic applications. *Curr Opin Chem Biol* 17: 250–260.

Herrmann, G., Selmer, T., Jessen, H.J., Gokarn, R.R., Selifonova, O., Gort, S.J. and Buckel, W. (2005) Two beta-alanyl-CoA:ammonia lyases in *Clostridium propionicum*. *FEBS J* 272: 813–821.

Hofstein, H.A., Feng, Y., Anderson, V.E. and Tonge, P.J. (1999) Role of glutamate 144 and glutamate 164 in the catalytic mechanism of enoyl-CoA hydratase. *Biochemistry* 38: 9508–9516.

Hollywood, K., Brison, D.R. and Goodacre, R. (2006) Metabolomics: current technologies and future trends. *Proteomics* 6: 4716–4723.

Huang, C.S., Ge, P., Zhou, Z.H. and Tong, L. (2011) An unanticipated architecture of the 750-kDa α6β6 holoenzyme of 3-methylcrotonyl-CoA carboxylase. *Nature* 481: 219–223.

Inoue, K., Kuramitsu, S., Aki, K., Watanabe, Y., Takagi, T., Nishigai, M., Ikai, A. and Kagamiyama, H. (1988) Branched-chain amino acid aminotransferase of *Escherichia coli*: overproduction and properties. *J Biochem* 104: 777–784.

Iwasaki, A., Yamada, Y., Ikenaka, Y. and Hasegawa, J. (2003) Microbial synthesis of (*R*)- and (*S*)-3,4-dimethoxyamphetamines through stereoselective transamination. *Biotechnol Lett* 25: 1843–1846.

Jin, J., Mazon, H., van den Heuvel, R.H., Janssen, D.B. and Fraaije, M.W. (2007) Discovery of a eugenol oxidase from *Rhodococcus* sp. strain RHA1. *FEBS J* 274: 2311–2321.

John, R.A. and Charteris, A. (1978) The reaction of amino-oxyacetate with pyridoxal phosphate-dependent enzymes. *Biochem J* 171: 771–779.

Kanda, M., Hori, K., Kurotsu, T., Ohgishi, K., Hanawa, T. and Saito, Y. (1995) Purification and properties of branched chain amino acid aminotransferase from gramicidin S-producing *Bacillus brevis*. *J Nutr Sci Vitaminol* 41: 51–60.

Kessler, B., de Lorenzo, V. and Timmis, K.N. (1992) A general system to integrate lacZ fusions into the chromosomes of gram-negative eubacteria: regulation of the Pm promoter of the TOL plasmid studied with all controlling elements in monocopy. *Mol Gen Genet* 233: 293–301.

Kichise, T., Hisano, T., Takeda, K. and Miki, K. (2009) Crystal structure of phenylacetic acid degradation protein PaaG from *Thermus thermophilus* HB8. *Proteins* 76: 779–786.

Kim, J., Kyung, D., Yun, H., Cho, B.K., Seo, J.H., Cha, M. and Kim, B.G. (2007) Cloning and characterization of a novel beta-transaminase from *Mesorhizobium* sp strain LUK: a new biocatalyst for the synthesis of enantiomerically pure beta-amino acids. *Appl Environ Microbiol* 73: 1772–1782.

Kim, J., Kyung, D., Yun, H., Cho, B.K. and Kim, B.G. (2006) Screening and purification of a novel transaminase catalyzing the transamination of aryl beta-amino acid from *Mesorhizobium* sp. LUK. *J Microbiol Biotechnol* 16: 1832-1836.

Lange, P.R., Eastmond, P.J., Madagan, K. and Graham, I.A. (2004) An *Arabidopsis* mutant disrupted in valine catabolism is also compromised in peroxisomal fatty acid beta-oxidation. *FEBS Lett* 571: 147–153.

Law, A. and Boulanger, M.J. (2011) Defining a structural and kinetic rationale for paralogous copies of phenylacetate-CoA ligases from the cystic fibrosis pathogen *Burkholderia cenocepacia* J2315. *J Biol Chem* 286: 15577–15585.

Leavitt, R.I. and Umbarger, H.E. (1962) Isoleucine and valine metabolism in *Escherichia coli*. XI. Valine inhibition of the growth of *Escherichia coli* strain K-12. *J Bacteriol* 83: 624–630.

Magnus, J.B., Hollwedel, D., Oldiges, M. and Takors, R. (2006) Monitoring and modeling of the reaction dynamics in the valine/leucine synthesis pathway in *Corynebacterium glutamicum*. *Biotechnol Prog* 22: 1071–1083.

Marchler-Bauer, A., Zheng, C., Chitsaz, F., Derbyshire, M.K., Geer, L.Y., Geer, R.C., Gonzales, N.R., Gwadz, M., Hurwitz, D.I., Lanczycki, C.J., Lu, F., Lu, S., Marchler, G.H., Song, J.S., Thanki, N., Yamashita, R.A., Zhang, D. and Bryant, S.H. (2013) CDD: conserved domains and protein three-dimensional structure. *Nucleic Acids Res* 41: D348–D352.

Marcotte, P. and Walsh, C. (1975) Active site-directed inactivation of cystathionine γ-synthetase and glutamic pyruvic transaminase by propargylglycine. *Biochem Biophys Res Commun* 62: 677–682.

Massey, L.K., Sokatch, J.R. and Conrad, R.S. (1976) Branched-chain amino acid catabolism in bacteria. *Bacteriol Rev* 40: 42–54.

Narkates, A.J. and Pittillo, R.F. (1965) Influence of inoculum media on sensitivity of *Escherichia coli* to azaserine. *J Bacteriol* 90: 710–714.

Pollegioni, L., Piubelli, L., Sacchi, S., Pilone, M.S. and Molla, G. (2007) Physiological functions of D-amino acid oxidases: from yeast to humans. *Cell Mol Life Sci* 64: 1373–1394.

Poelarends, G.J., Wilkens, M., Larkin, M.J., van Elsas, J.D. and Janssen, D.B. (1998) Degradation of 1,3-dichloropropene by *Pseudomonas cichorii* 170. *Appl Environ Microbiol* 64: 2931–2936.

Poston, J.M. (1986) Beta-leucine and the beta-keto pathway of leucine metabolism. *Adv Enzymol Relat Areas Mol Biol* 58: 173–189.

Poston, J.M. (1976) Leucine 2,3-aminomutase, an enzyme of leucine catabolism. *J Biol Chem* 251: 1859–1863.

Puthan Veetil, V., Fibriansah, G., Raj, H., Thunnissen, A.M. and Poelarends, G.J. (2012) Aspartase/fumarase superfamily: a common catalytic strategy involving general base-catalyzed formation of a highly stabilized aci-carboxylate intermediate. *Biochemistry* 51: 4237–4243.

Prabhakaran, P.C., Woo, N.T., Yorgey, P.S. and Gould, S.J. (1988) Biosynthesis of blasticidin S from L-α-arginine. Stereochemistry in the arginine-2,3-aminomutase reaction. *J Am Chem Soc* 110: 5785–5791.

Roth, M. (1971) Fluorescence reaction for amino acids. *Anal Chem* 43: 880–882.

Ruzicka, F.J. and Frey, P.A. (2007) Glutamate 2,3-aminomutase: a new member of the radical SAM superfamily of enzymes. *Biochim Biophys Acta* 1774: 286–296.

Sambrook, J., Fritsch, E.F. and Maniatis, T. (1989) Molecular cloning: a laboratory manual. New York (USA): Cold Spring Harbor Laboratory Press.

Tang, K.H., Casarez, A.D., Wu, W. and Frey, P.A. (2003) Kinetic and biochemical analysis of the mechanism of action of lysine 5,6-aminomutase. *Arch Biochem Biophys* 418: 49–54.

Tatum, E.L. (1946) Induced biochemical mutations in bacteria. *Cold Spring Harbor Symposia Quant Biol* 11: 278–284.

Umbarger, H.E. and Brown, B. (1955). Isoleucine and valine metabolism in *E. coli*. V. Antagonism between isoleucine and valine. *J Bacteriol* 70: 241–248.

Villas-Boas, S.G., Mas, S., Akesson, M., Smedsgaard, J. and Nielsen, J. (2005) Mass spectrometry in metabolome analysis. *Mass Spectrom Rev* 2: 613–646.

Walker, K.D., Klettke, K., Akiyama, T. and Croteau, R. (2004) Cloning, heterologous expression, and characterization of a phenylalanine aminomutase involved in taxol biosynthesis. *J Biol Chem* 279: 53947–53954.

Weatherburn, M.W. (1967) Phenol-hypochlorite reaction for determination of ammonia. *Anal Chem* 39: 971–974.

Winkelmann, G., Busch, B., Hartmann, A., Kirchhof, G., Süssmuth, R. and Jung, G. (1999) Degradation of desferrioxamines by *Azospirillum irakense*: assignment of metabolites by HPLC/electrospray mass spectrometry. *Biometals* 12: 255–264.

Witschel, M. and Egli, T. (1998) Purification and characterization of a lyase from the EDTA-degrading bacterial strain DSM 9103 that catalyzes the splitting of [S,S]-ethylenediaminedisuccinate, a structural isomer of EDTA. *Biodegradation* 8: 419–428.

Wu, B., Szymanski, W., Heberling, M.M., Feringa, B.L. and Janssen, D.B. (2011) Aminomutases: mechanistic diversity, biotechnological applications and future perspectives. *Trends Biotechnol* 29: 352–362.

Yin, X., O'Hare, T., Gould, S.J. and Zabriskie, T.M. (2003) Identification and cloning of genes encoding viomycin biosynthesis from *Streptomyces vinaceus* and evidence for involvement of a rare oxygenase. *Gene* 312: 215–224.

Yun, H., Lim, S., Cho, B.K. and Kim, B.G. (2004) omega-Amino acid:pyruvate transaminase from *Alcaligenes denitrificans* Y2k-2: a new catalyst for kinetic resolution of beta-amino acids and amines. *Appl Environ Microbiol* 70: 2529–2534.

Chapter 6

Summary and Outlook

Introduction

β-Amino acids occur as intermediates in the synthesis of a diversity of bioactive compounds, both in laboratory-developed chemical production schemes and in naturally evolved biosynthetic routes. Examples of compounds synthetically prepared from *β*–amino acids are *β*-peptides (Seebach and Matthews, 1997) and cytotoxic agents containing *β*-amino acid building blocks (Wani *et al.,* 1971; Shih *et al.,* 1999; Namikoshi *et al.,* 1989). The presence of *β*-amino acid moieties in various antibiotics and other compounds with pharmacological activity stimulated research on the properties and preparation of these compounds, and several efficient methods to synthesize *β*-amino acids and intermediates by organic chemistry have been developed (Liu & Sibi, 2002; Juaristi & Soloshonok, 2005; Weiner *et al.,* 2010). Among these, the Mannich reaction and hydrogenation of enamines are particularly attractive (**Fig. 6.1**). Advantages of these methods are the high conversion rates and the high enantioselectivity, but disadvantages are that some of the transition metals that are used are environmentally unattractive and the lack of compatibility with biological production strategies. In such cases, biocatalytic conversions leading to enantiopure amino acids would represent a good alternative. Enzymatic conversions can potentially be applied in engineered biosynthetic pathways for fermentative production. However, there are only a few reports describing enzymes that can be used for the preparation of *β*-amino acids (Liljeblad & Kanerva, 2006; Weiner *et al.,* 2010; Rudat *et al.,* 2012). Furthermore, most of the described conversions rely on kinetic resolution, which implies that only 50% of the starting compound is converted to the desired product.

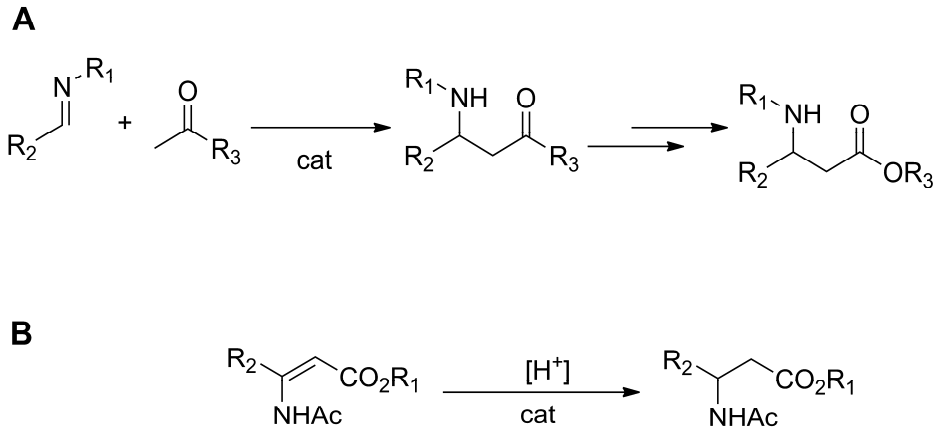

Figure 6.1 Chemical conversions for preparing *β*-amino acids. **A**) Mannich reaction in which an imine reacts with a ketone to yield a *β*-substituted ketone that can be converted to a *β*-amino acid by Baeyer-Villiger oxidation; **B**) Hydrogenation reaction of an enamine to yield an N-substituted *β*-amino acid.

As described in **Chapter 1** of this thesis and papers cited there, production of enantiomerically pure *β*-amino acids by means of biocatalytic methods can be catalyzed by different types of enzymes (**Fig. 6.2**). This includes: (a) acylases that catalyze hydrolysis of *N*-acetylated *β*-amino acids (Groger *et al.,* 2004); (b) acylation of *β*-amino acids and deacetylation of *N*-phenylacetylated *β*-amino acids by penicillin acylase (Soloshonok *et al.,* 1995; Cardillo *et al.,* 1999; Li *et al.,* 2007); (c) kinetic resolution of aliphatic *β*-amino acid amides by aminopeptidases (Heck *et al.,* 2009); (d) deacylation of *β*-amino acid esters using lipases or esterases (Liljeblad & Kanerva, 2006); (e) enantioselective addition of ammonia to cinnamic acid derivatives using phenylalanine aminomutase (Szymanski *et al.,* 2009); (f) production of *β*-amino acid esters from aminoketones using Baeyer-Villiger monooxygenases (BVMOs) (Rehdorf *et al.,* 2010); (g) kinetic resolution of aromatic *β*-amino acids by transaminases (ATs) (Crismaru & Wybenga *et al.,* 2013; Bea *et al.,* 2011); (h) transaminae-catalyzed asymmetric amination of *β*-keto acids or esters (Yun *et al.,* 2004; Kim *et al.,* 2007). Most of these conversions still suffer from some enzyme-related difficulties, such as the low catalytic activity (phenylalanine aminomutase), product inhibition (transaminases with keto acids), the need for more than one enzyme (asymmetric synthesis by lipase/transaminase), or cofactor requirement (Baeyer-Villiger monooxygenases). On the other hand, there are also important advantages, such as high enantioselectivity of transaminases and most hydrolases, and the fact that hydrolases do not require expensive cofactors.

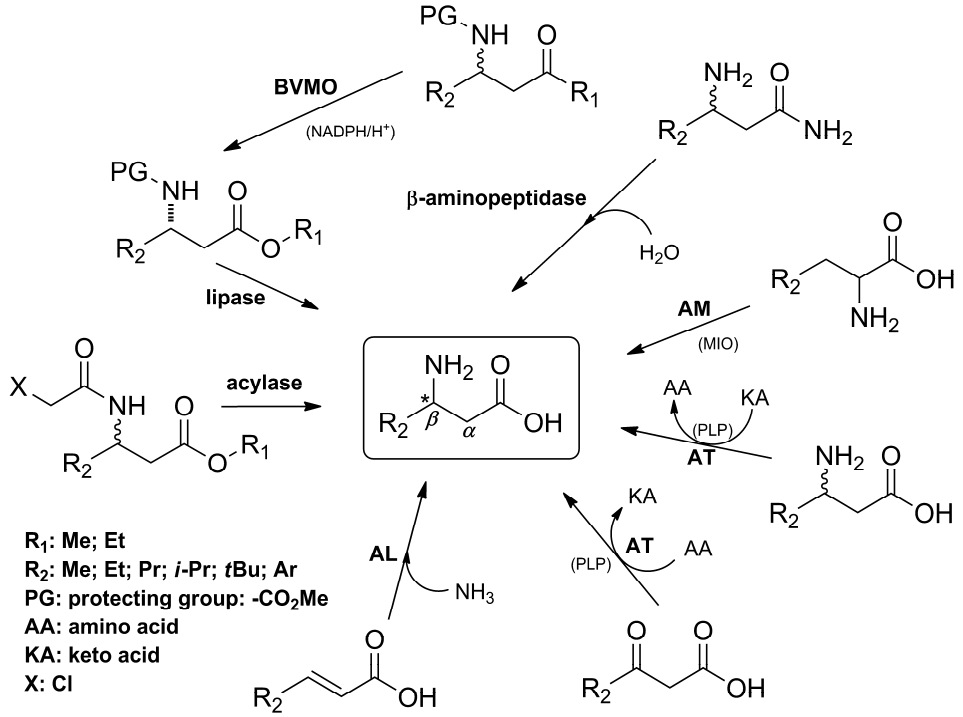

Figure 6.2 Enzymatic routes towards *β*-amino acids.

The research presented in this thesis aims to discover new enzymes for *β*-amino acid metabolism that can be used in biocatalysis. Our work started with enrichment experiments to obtain microorganisms that are able to use *β*-amino acids as nitrogen source. Microbial cultures that are isolated by selective enrichment were expected to possess enzymes that metabolize *β*-amino acids. Next, the newly discovered *β*-amino acid-converting enzymes can be characterized and overproduced by cloning and heterologous expression. In combination with a biochemical characterization, kinetic studies, establishment of substrate scope and enantioselectivity as well as crystal structure determination, this was expected to contribute to the development of a toolbox for biocatalytic production of *β*-amino acids.

Isolation of β-amino acid-degrading microorganisms

In **Chapter 2** we explore the metabolism of β-amino acids in microorganisms. By enrichment cultivation, a collection of 18 bacterial strains was obtained that use different β-amino acids as sole nitrogen source, including β-alanine, D-aspartate, β-glutamate, β-asparagine, β-leucine, β-phenylalanine and β-tyrosine (**Fig. 6.3**).

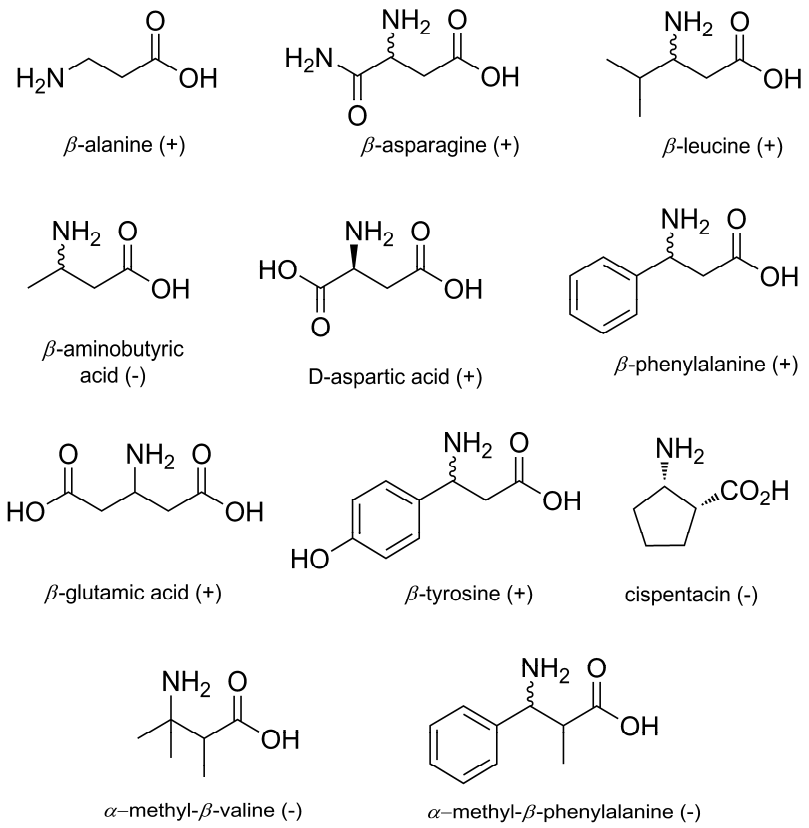

Figure 6.3 Various β-amino acids used for enrichment of β-amino acid-degrading microorganisms. Signs represent compounds that were metabolized and for which pure isolates were obtained **(+)** or compounds that were not metabolized or for which no pure cultures could be isolated **(-)**.

In case of β-aminobutyric acid and cispentacin, no pure isolates were obtained because bacteria could not be separated from contaminating fungi. Enrichment experiments with α-methyl-β-valine and α-methyl-β-phenylalanine as sole nitrogen source did not result in detectable growth, suggesting that microorganisms that

release ammonia from these compounds are rare or do not exist. Both these compounds have a second substituent on the Cα carbon atom, which makes amine oxidase, dehydrogenase and transferase reactions impossible.

The cultures that were obtained were examined for enzymes that could catalyze deamination, including amino acid dehydrogenase, amino acid oxidase, ammonia lyase, aminotransferase and aminomutase activity. Amino acid dehydrogenase, amino acid oxidase, and ammonia lyase reactions should yield direct release of nitrogen as ammonia. Such enzymes acting on *α*-amino acids are well investigated, their reaction mechanisms are known and several crystal structures are available. A culture that was investigated in detail is *Variovorax paradoxus* strain CBF3. This *β*-phenylalanine-degrading bacterium was found to use a *β*-phenylalanine-aminotransferase (*Vp*AT) for deamination.

Characterization of *β*-phenylalanine aminotransferase from *Variovorax paradoxus*

Chapter 3 describes the biochemical characterization of the *β*-phenylalanine aminotransferase (*Vp*AT) that was discovered in the *β*-phenylalanine-degrading bacterium *V. paradoxus* strain CBF3. Initially, attempts to isolate the enzyme from the wild-type strain failed, mainly due to the very low expression level. Therefore, a genetic approach was followed. The gene that encodes the aminotransferase was isolated from a cosmid library prepared from genomic DNA and sequenced. Paired-end whole genome sequence analysis extended the contig harboring the *Vp*AT-encoding gene to a DNA fragment of 20.6 kb. No regulatory regions flanking the aminotransferase gene were identified. The *Vp*AT protein sequence shares 90%, 87% and 87% identity with the sequence of three putative aminotransferases from *Variovorax* sp. CF313, *V. paradoxus* S110 and *V. paradoxus* EPS, respectively. The closest homolog (51% identity) that is known to catalyze a similar reaction is the *β*-transaminase from *Mesorhizobium* sp. strain LUK (*Mes*AT) (Kim *et al.,* 2007). Sequence comparison of *Vp*AT and *Mes*AT did not indicate the presence of conserved regions that would have permitted the isolation by PCR of the *vp*AT gene from genomic DNA of CBF3.

The newly identified *Vp*AT was overexpressed in *E. coli* and purified to homogeneity. Biochemical studies showed that *Vp*AT has a high catalytic activity (17.5 $U \cdot mg^{-1}$ at 30 °C and 33 $U \cdot mg^{-1}$ at 55 °C). Moreover, the pH profile showed that the enzyme is active at a range of pH values between 4 and 11.2. Additionally, *Vp*AT is

about 10-fold more active with (*S*)-*β*-phenylalanine than *Mes*AT (Kim *et al.,* 2007) and about 2-fold more active than *Po*GSAM (Bea *et al.,* 2011).

The enzyme is highly enantioselective towards the (*S*)-enantiomer of *β*-phenylalanine, producing (*R*)-*β*-phenylalanine from racemic *β*-phenylalanine (*ee* >99%, *E* >200). The same enantiopreference holds for a range of phenyl-ring substituted *β*-phenylalanines, especially *meta* and *para* ring-substituted *β*-phenylalanine derivatives (**Fig. 6.4**). Interestingly, *Vp*AT does not convert *α*-phenylalanines or other *α*-amino acids. Together, these results suggest that *Vp*AT can be used for preparing *β*-amino acids by kinetic resolution.

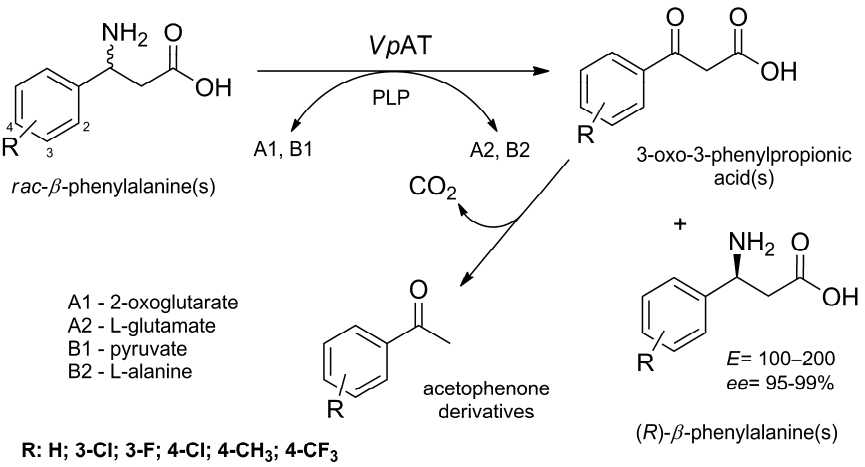

Figure 6.4 Kinetic resolution of *rac*-*β*-phenylalanines to obtain (*R*)-*β*-phenylalanines using *Vp*AT (**Chapter 3**).

In order to obtain more information about the reaction mechanism, the crystal structure of the enzyme was solved at 1.5 Å resolution using molecular replacement with the recently solved structure of *Mes*AT (Wybenga & Crismaru *et al.,* 2012) as the template. A second structure was obtained by complexation of *Vp*AT crystals with the uncompetitive inhibitor 2-aminooxyacetic acid (AOA). By forming a covalent bond to PLP, AOA prevents formation of pyridoxamine 5'-phosphate (PMP), thus inhibiting the enzyme.

Based on the B6 database that compiles information on PLP-dependent enzymes, seven-fold types of PLP enzymes can be distinguished (Percudani & Perrachi, 2009). The aminotransferases occur in fold-types I and IV. Representative examples of fold type I ATs are aspartate AT, aromatic amino acid AT and ω-ATs (Finn

et al., 2010). The structure of *Vp*AT reveals that it is a fold-type I enzyme, which was also found for the *β*-transaminase from *Mesorhizobium* sp. strain LUK (*Mes*AT) (Kim *et al.,* 2007; Wybenga & Crismaru *et al.,* 2012).

According to a classification introduced in the 1980s based on the reaction that is catalyzed, ATs are divided in two subgroups: (I) α-ATs, which catalyze transamination of amino groups at the α-carbon; and (II) ω-ATs, which perform transamination at a β-, γ-, or another more distal amino group of the substrate (Yonaha *et al.,* 1983). According to this older non-phylogenetic classification, all ATs that convert *β*-amino acids are confusingly considered to be ω-ATs, which would place ATs acting on *β*-amino acid in subgroup II with *β*-alanine AT, 4 aminobutyrate AT, ornithine AT, acetylornithine AT and 7,8-diaminopelargonic acid AT (Christen & Mehta, 2001; Mehta *et al.,* 1993).

Comparison of the structures showed that the active site architecture of *Vp*AT is very similar to that of *Mes*AT. By computer docking of (*S*)-*β*-phenylalanine, it was found that the binding pose of the substrate in the active site of *Vp*AT (**Fig. 6.5**) is likely very similar to that described for *Mes*AT. Most of the residues flanking the active sites are conserved, with three exceptions: *S298 (monomer B), V43 and F400 from *Vp*AT correspond in *Mes*AT to *A312 (monomer B), I56 and M414, respectively.

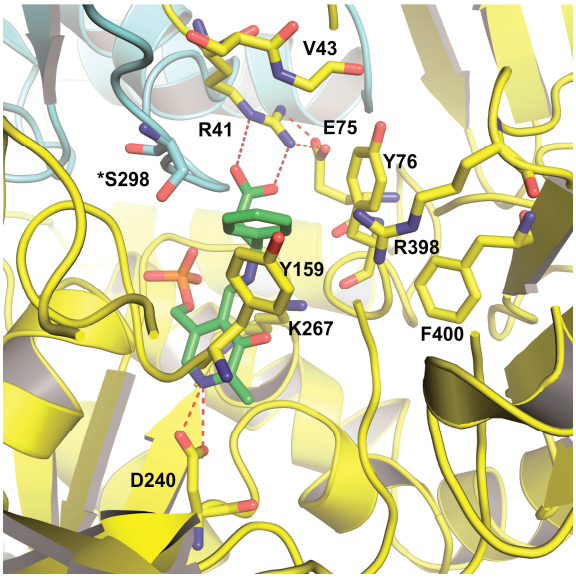

Figure 6.5 Active site of *Vp*AT with docked (*S*)-*β*-phenylalanine, monomer A (yellow). Residue *S298 is present in a loop from monomer B (magenta). The external aldimine (PLP bound to (*S*)-*β*-phenylalanine) is shown in green. Docking was performed using the Rosetta software (Das & Baker, 2008).

By combining sequence analysis, structural data and information on substrate range, aminotransferase sequence motifs can be defined that allow the discovery of aminotransferases with a specific substrate selectivity (Hohne *et al.,* 2010). Inspection of the *Vp*AT structure with AOA bound and of the modeled *Vp*AT-(*S*)-*β*-phenylalanine structure indicated that residues R41 and E75 are shaping the carboxylate binding site in this enzyme (P-pocket). Since E75 is conserved in the *β*-amino acid selective enzymes *Vp*AT, *Mes*AT and *Po*GSAM (**Fig. 6.6**), but not in *Tt*GSAM and *Ps*D-PhgAT which do not convert *β*-amino acids, we used the conserved R41/E75 pair as the starting point to identify a motif that may distinguish ATs with activity towards aromatic *β*-amino acids from ATs with a similar fold but a different activity.

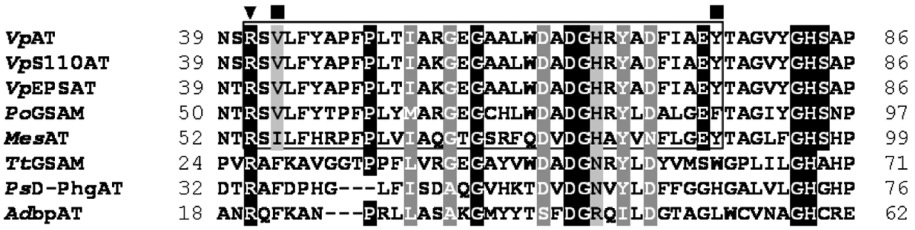

Figure 6.6 Partial sequence alignment of *Vp*AT and the transaminase subgroup II enzymes. Two structurally related proteins (*Tt*GSAM and *Ps*D-PhgAT) with *Vp*AT and *Mes*AT are included. Highly conserved residues are highlighted in black, and moderately conserved residues are shown in gray boxes. Symbols: ▼, amino acid residues involved in the binding of the carboxylate group of (*S*)-*β*-Phe, the carboxylate group of pyruvate and/or the α/γ-carboxylate group(s) of 2-oxoglutarate; ■, amino acid residues having hydrophobic interactions with the phenyl ring of (*S*)-*β*-phenylalanine. Proteins: *Vp*AT, *β*-transaminase in this study (CCE46017.1); *Vp*S110AT, putative aminotransferase of *Variovorax paradoxus* strain S110 (YP_002944294.1); *Vp*EPSAT, putative aminotransferase of *Variovorax paradoxus* strain EPS (YP_004154921.1); *Po*GSAM, glutamate-1-semialdehyde 2,1-aminomutase of *Polaromonas* sp. strain JS666 (ABE43415.1); *Mes*AT, *β*-transaminase of *Mesorhizobium* sp. strain LUK (ABL74379.1); *Tt*GSAM, glutamate-1-semialdehyde 2,1-aminomutase from *Thermus thermophilus* HB8 (2E7U, BAD70757.1); *Ps*D-PhgAT, D-phenylglycine aminotransferase of *Pseudomonas stutzeri* ST-201 (2CY8, AAQ82900.1); *Ad*bpAT, *β*-alanine:pyruvate transaminase of *Alcaligenes denitrificans* (AAP92672.1).

The suggested motif consists of R-X-[AVI]-X(6)-P-X(14)-D-G-X(8)-[EDNQ]-[YFW] and comprises 36 residues in the N-terminal segment of the NC domain. Although this motif may be applied to identify aminotransferases in a set of fold-type I aminotransferases it can probably not predict *β*-aminotransferase activity in less related sequences or enzymes lacking activity with aromatic substrates. For example, an *Alcaligenes denitrificans* AT (*Ad*bpAT, Yun *et al.,* 2004) that is inactive with aromatic *β*-amino acids and has an opposite enantiopreference for aliphatic *β*-amino

acids as compared to *Vp*AT and *Mes*AT (Kim *et al.,* 2007), is not covered by the motif. This suggests that *Ad*bpAT belongs to a different phylogenetic cluster and has a different mode of substrate binding. Using the sequence motif proposed above, at least 46 unique protein sequences of putative *β*-selective ATs could be retrieved from a collection of about 2,000 sequences that share sequence identity from 18 to 90% to *Vp*AT, *Mes*AT and *Po*GSAM.

Crystal structure of *β*-phenylalanine aminotransferase from *Mesorhizobium* sp. strain LUK

A *β*-phenylalanine transaminase (*Mes*AT) from a different source (*Mesorhizobium* sp. strain LUK), that shares 51% sequence identity with *Vp*AT was investigated in **Chapter 4**. *Mes*AT was discovered and biochemically characterized by Kim *et al.* (2007). This enzyme has transaminase activity with *β*-phenylalanine as amino donor and *α*-ketoglutarate or pyruvate as amino acceptor. The apparent K_m and k_{cat} values with *β*-phenylalanine were 1.2 mM and 1.3 s^{-1}, respectively. For pyruvate the apparent K_m and k_{cat} were 3.9 mM and 1.3 s^{-1}, respectively. Kim and coworkers showed that the enzyme has low activity with *α*-phenylalanine and other *α*-amino acids.

Since no structure of such an enzyme was available, our work was aimed at obtaining its crystal structure and to understand the reaction mechanism of the enzyme. Five different crystal structures of *Mes*AT were obtained: apo-holoenzyme structure (1.65 Å); (*S*)-*β*-phenylalanine bound structure; a structure with (*R*)-3-amino-5-methylhexanoic acid; a structure with *α*-ketoglutarate; and a structure with the uncompetitive inhibitor 2-aminooxyacetic acid.

The overall structures of *Mes*AT and *Vp*AT are rather similar (**Fig. 6.7**). However, as mentioned above, three substitutions are observed in the active sites of the two enzymes. The role of the different amino acids (I56, A312, R412, and M414 in *Vp*AT) was then tested by making mutants (**Fig. 6.8**). The role of the different amino acids (I56, A312, R412, and M414 in *Vp*AT) was then tested by making mutants (**Fig. 6.8**). The *Mes*AT A312S/I56V/M414F triple mutant proved to be 2-fold more active than the wild-type. Thus, by using sequence information and structural data it was possible to obtain *Mes*AT mutants with enhanced activity towards *β*-phenylalanine, even though a structural explanation of the mechanism by which these mutations enhance activity is missing.

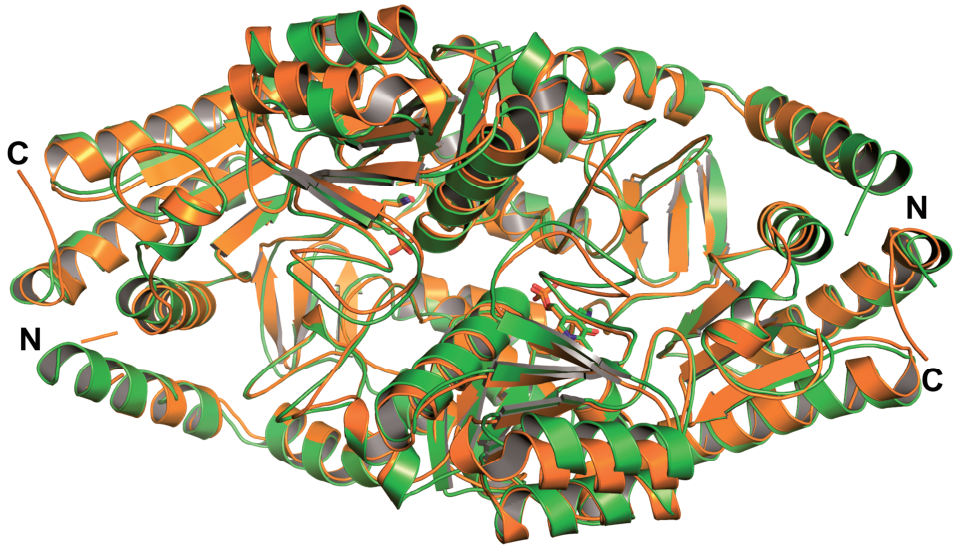

Figure 6.7 Structures of the dimers of *Mes*AT (green) and *Vp*AT (orange). Each monomer of the dimeric enzymes contains one PLP cofactor covalently bound to the enzyme *via* residues K280 and K267, respectively.

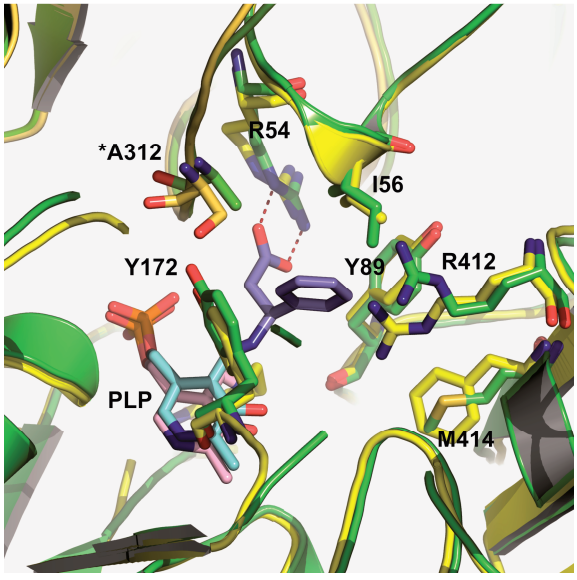

Figure 6.8 Active site residues of *Mes*AT (green) vs. *Vp*AT (yellow). The substrate *β*-phenylalanine is indicated in blue-slate. The PLP cofactor from *Vp*AT is shown in light pink and from *Mes*AT in cyan. Residue numbers are for *Mes*AT. Residue *A312 is positioned on a loop of the opposite monomer of *Mes*AT.

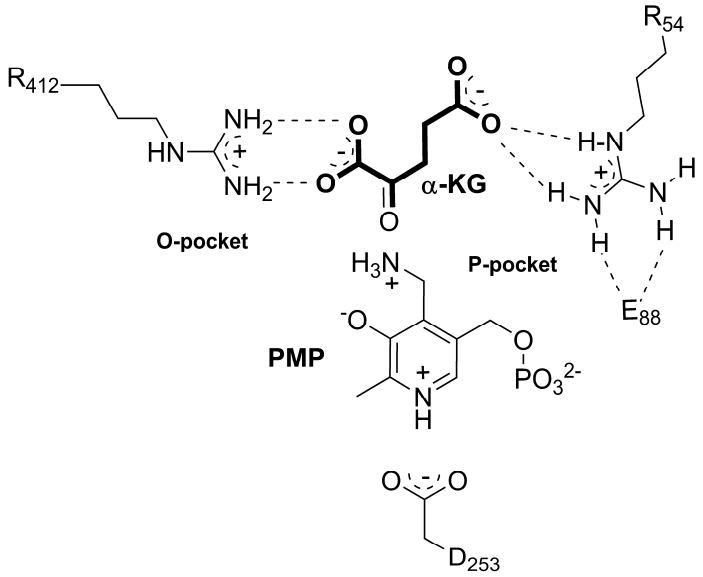

Figure 6.9 Binding of α-ketoglutarate (α-KG) in the active site of *Mes*AT. The orientation of the amino-acceptor with respect to the PMP cofactor is in agreement with the production of (*S*)-L-glutamate from α-ketoglutarate.

The binding of (*S*)-β-phenylalanine occurs through an interaction of its carboxylate group with Arg54 in the so-called P-pocket (Wybenga & Crismaru *et al.,* 2012), which is located approximately in the same direction as the phosphate group of the PLP cofactor. Indeed, the R41A mutant of *Vp*AT showed no detectable activity. The binding of α-ketoglutarate occurs in a different manner: the α-carboxylate group is positioned in the so-called O-pocket, which is more close to the hydroxyl side of the PLP ring, and has a salt bridge with Arg412. The γ-carboxylate group of α-ketoglutarate is hydrogen bonded to Arg54 in the P-pocket (**Fig. 6.9**). In agreement with this, the *Mes*AT R412A mutant has very low activity (0.006 U·mg^{-1} at 30°C) compared to the wild type (1.6 U·mg^{-1}). The K_m for pyruvate increased by a factor of 28 in this mutant. Substrate inhibition was observed with WT enzyme as well as with the R412A mutant.

In contrast to what was observed by Kim and coworkers (2007), we could not detect transaminase activity of *Mes*AT towards α-phenylalanine. Moreover, soaking or co-crystallization using a high concentration of α-phenylalanine did not result in binding in the active site of *Mes*AT. To understand the lack of conversion of α-phenylalanine, we compared the binding mode of α-phenylalanine in α-transaminases

to the binding of β-phenylalanine in *Mes*AT (**Fig. 6.10, panel A**). So far, there is no report of an aromatic AT structure bound with α-phenylalanine. However, Okamoto and co-workers (1998) described an aromatic AT from *Paracoccus denitrificans* (*Pd*AroAT, PDB code 1AY8) bound with 3-phenylpropionic acid, a substrate analog of α-phenylalanine. The carboxylate binding site of this aminotransferase contains an arginine (R386) that donates a salt bridge, just like R54 in *Mes*AT (**Fig. 6.10, panel B**).

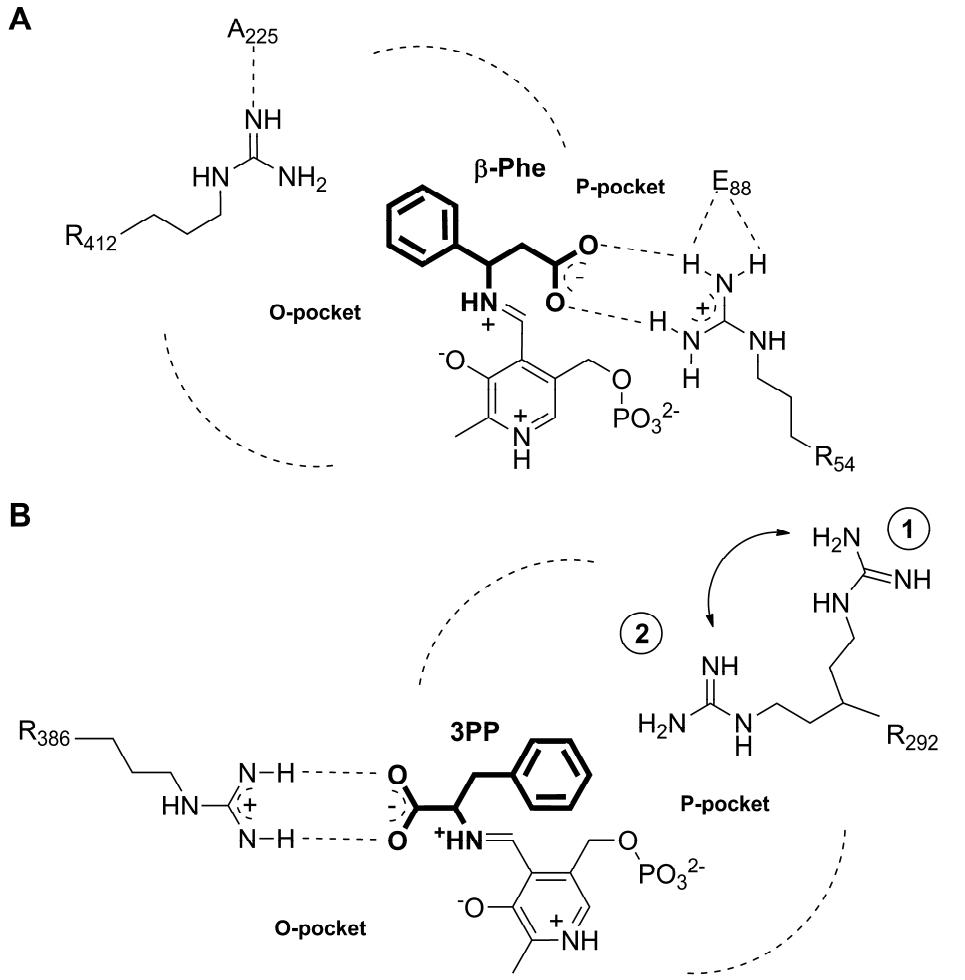

Figure 6.10 Comparison between the binding of β-phenylalanine (β-Phe) in *Mes*AT (**panel A**) and the proposed binding of α-phenylalanine in *Pd*AroAT (**panel B**). Conformations 1 (open form) and 2 (closed form) (panel B) of the guanidino group of R292 in *Pd*AroAT occur when 3-phenylpropionic acid (3PP) and maleic acid, respectively, are bound to in the active site of the enzyme (PDB codes 1AY8 and 1AY5).

Thus, it seems that binding of α-phenylalanine occurs in an inverted manner in *Pd*AroAT as compared the β-phenylalanine binding in *Mes*AT. On the other side, the hydrophobic binding pocket (P-pocket in AroAT, O-pocket in *Mes*AT and *Vp*AT) that accommodates the phenyl ring of 3-phenylpropionic acid in *Pd*AroAT, contains an arginine residue (R292, monomer B, PDB code 1AY8) that corresponds to R412 in *Mes*AT. However, the guanidine group of R292 is positioned in an "open" conformation quite far away (~7Å) from the phenyl ring of 3-phenylpropionate as compared to the distance (~3.5Å) between the guanidine group of R412 and the phenyl ring of β-phenylalanine in *Mes*AT. In the structure of *Pd*AroAT complexed with maleate (PDB code 1AY5), one carboxylate group is anchored by R386 and the other carboxylate group interacts with R292 of monomer B. In this case, the guanidine group of R292 is oriented more into the active site and approaches the substrate, forming the closed form of the enzyme and suggesting that binding of maleate triggers a conversion from the open form to the closed form (**Fig. 6.10, panel B**).

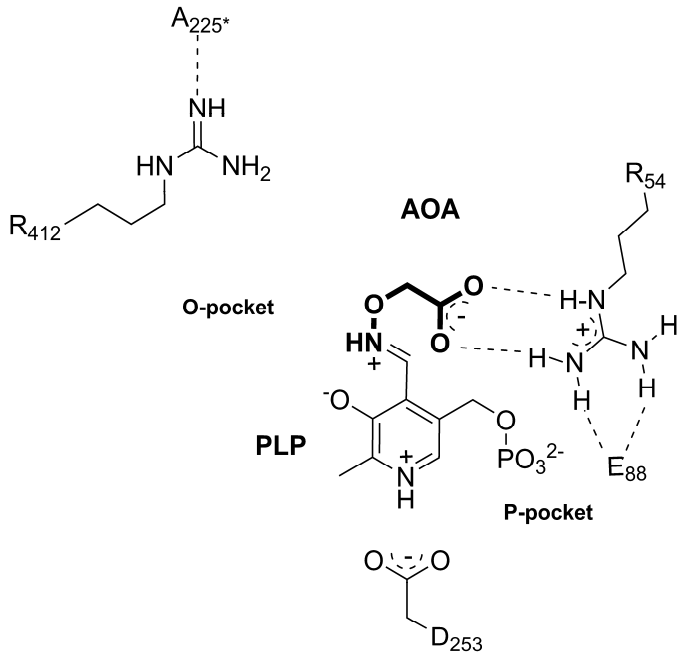

Figure 6.11 The binding of the aminooxyacetate (AOA) inhibitor to the PLP cofactor in the active site of *Mes*AT.

Another interesting aspect of *Mes*AT was the inhibition observed with 2-aminooxyacetic acid, which almost completely abolished its activity under standard

conditions. This is due to the fact that the amino group of 2-aminooxyacetate binds covalently to the C4' atom of PLP and the carboxylate group anchors via a salt bridge to the Nε and Nη2 atoms of residue R54, thereby preventing PMP formation and inhibiting catalytic activity (**Fig. 6.11**).

Biodegradation of *β*-valine by *Pseudomonas* sp. strain SBV1

The biodegradation of *β*-valine by *Pseudomonas* sp. strain SBV1 is discussed in **Chapter 5**. Since the structure of *β*-valine excludes amino acid dehydrogenase, amine oxidase, and aminotransferase reactions, we envisaged that this substrate might possibly be deaminated by a novel type of *β*-amino acid selective ammonia lyase.

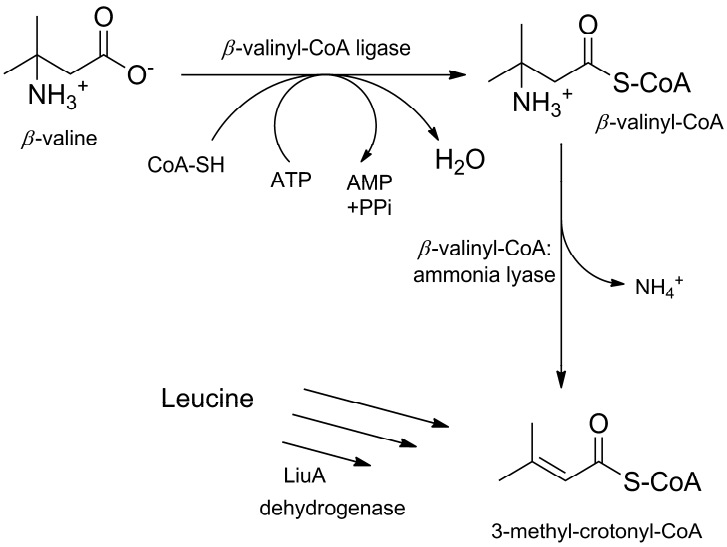

Figure 6.12 Degradation of *β*-valine by *Pseudomonas* sp. strain SBV1 proceeds via a CoA activation of the substrate followed by elimination of ammonia in a CoA-dependent manner.

Various deamination activities were tested using cell-free extracts prepared from *β*-valine-grown cells. Furthermore, the degradation of *β*-valine by whole cells was investigated by HPLC-MS and ^{1}H-NMR. Since these experiments did not provide evidence for a certain deamination mechanism or catabolic pathway, we adopted a genetic approach. A cosmid library from genomic DNA of strain SBV1 was constructed in *E. coli* and screened by growth selection in *Pseudomonas fluorescens* Pf0-1, which is

a strain that is very similar at the genetic level to SBV1 but that cannot degrade *β*-valine. A positive clone found (p4D1) contained a DNA insert of about 25 kb, which revealed the presence of a cluster of genes that likely encodes all the enzymes needed for *β*-valine catabolism.

The sequence analysis suggests that *β*-valine is not transformed by any of the initially considered reactions (aminomutase or ammonia lyase) that are known for *α*-amino acids. Instead, the sequence suggests that *β*-valine degradation proceeds via CoA activation of the substrate, catalyzed by a CoA-dependent ligase, followed by elimination of ammonia in a reaction catalyzed by a CoA-dependent ammonia lyase (**Fig. 6.12**). A similar route was reported for the conversion of *β*-alanine by *Clostridium propionicum* (Herrmann *et al.,* 2005). The product of the *β*-valinyl-CoA-dependent ammonia lyase-catalyzed reaction would be 3-methyl-crotonyl-CoA, which is a common intermediate in one of the catabolic pathways of leucine (Aguilar *et al.,* 2006). Further work should be aimed at expression of the CoA-dependent ligase and CoA-dependent ammonia lyase genes and confirmation of the catalytic activities of the encoded proteins.

Outlook

The use of enrichment cultures and environmental gene libraries to discover *β*-amino acid-converting enzymes was successful only with first approach. The lack of success with environmental gene libraries must be due to the rareness of genes encoding enzymes that liberate ammonia from *β*-amino acids (data not shown). Rare genes will normally escape discovery by screening non-enriched libraries, even if a reliable screening method for the desired enzymatic activity is available. In our view, enrichment experiments are necessary to recover genes and enzymes involved in microbial metabolism of *β*-amino acids. Unfortunately, this approach is far more laborious, usually implying isolation of pure isolates, identification of the respective enzymatic activities, purification of the enzymes and gene identification followed by cloning and overexpression of the recombinant enzymes.

The results in this thesis suggests that the two approaches may be combined. Enrichment is probably required to recover rare metabolic activities, such as the capacity to convert *β*-amino acids. Isolation of pure cultures may not be necessary. Instead, the use of mixed enrichment cultures may help to maintain a certain diversity of relevant enzymes in the next step, which preferably consists of library construction for screening. In this step, large-insert libraries may be much more efficient, or even

essential, since small-insert libraries may be ineffective if a pathway for converting the target substrate to a common central metabolite involves several enzymes. In any case, it may be better not to isolate pure cultures, and in the cases we examined, activity detection and enzyme isolation did not significantly help with the discovery of the target enzymes or genes for *β*-phenylalanine and *β*-valine metabolism. In case of the *Vp*AT from *Variovorax paradoxus* CBF3, enzyme yield after a laborious purification procedure was very low, and no protein sequence information could be obtained. The availability of a fast screening assay for the known enzymatic activity (e.g. detection of AT activity by the colorimetric acetophenone formation assay), and the availability of a host strain in which selection can be carried out, led to rapid discovery of the required genes from broad-host range cosmid genome libraries.

The elucidation of the crystal structures of the *β*-ATs from *Mesorhizobium* sp LUK and *Variovorax paradoxus* CBF3, as described in this thesis, will serve both the discovery of new *β*-amino acid aminotransferase and the engineering of the *β*-ATs that are now available. Structure-guided directed evolution is a highly efficient tool for engineering enzymes with enhanced activity or with an enlarged substrate range. A particularly interesting target would be the use of *β*-keto esters as amino acceptors. At this moment, synthesis of (*S*)-*β*-phenylalanine from its ethyl *β*-keto ester precursor is only described for a coupled assay using a lipase to generate the free *β*-keto acid, which is then immediately converted by the aminotransferase (Kim *et al.,* 2007). This tandem reaction thus yields an attractive asymmetric synthesis. Structure-based directed evolution may yield an enzyme that can achieve synthesis of enantiomerically pure substituted *β*-phenylalanine esters from the *β*-keto esters. Such a conversion would have significant advantages over the kinetic resolution of *rac β*-phenylalanine and its derivatives using an ω-AT (Crismaru & Wybenga *et al.,* 2013; Bea *et al.,* 2011). The growing understanding of the relation between active site architecture and substrate selectivity will contribute to an efficient strategy for structure-based engineering, which may also be aimed at more bulky substrates such as alkyl or aryl *β*-keto esters or *β*-ketones.

Recently, a transaminase has been engineered by directed evolution for its use at industrial scale for the production of enantiomerically pure chiral amines that can be incorporated as building blocks in pharmaceuticals (Savile *et al.,* 2010). Especially discovery and engineering of (*R*)-selective transaminases has generated interest, since very few (*R*)-selective transaminases have been reported as compared to (*S*)-selective transaminases (Iwasaki *et al.,* 2003; Koszelewski *et al.,* 2008). Although, preparation of (*R*)-amines can be achieved by kinetic resolution of the racemic amines with the use of (*S*)-selective transaminases, the disadvantage of this

approach is that a maximum of 50% yield can be obtained (Hanson *et al.,* 2008). Since the produced ketone has low economic value, this is not an economically attractive process. If the ketone cannot be reused, sustainability parameters of the process will also be very poor. In contrast, an asymmetric synthesis is far more economical with yields up to 100%. It obviously requires a separate enzyme for each enantiomer, and therefore a toolbox of enzymes that have either (*R*)- or (*S*)-selectivity is needed.

In general, strategies to obtain enzymes with complementary enantioselectivity encompass at least three approaches: (1) screening of strain collections (or selective enrichment) for identification of complementary enzymes (Mugford *et al.,* 2008); (2) protein engineering for widening the substrate range, which may also yield enzymes with opposite enantioselectivity (Ivancic *et al.,* 2007; Magnusson *et al.,* 2005; May *et al.,* 2000; Zha *et al.,* 2001; van Leeuwen *et al.,* 2012); (3) definition of sequence features that predict substrate specificity and enantiopreference in combination with genome mining (Hohne *et al.,* 2010). The last strategy is very attractive and may yield a collection of enzymes with the desired properties. The structure-based description of sequence motifs that can be used for the discovery of *β*-selective amino acid aminotransferases described in this thesis will contribute to the applicability of genome mining for finding such enzymes.

References

Aguilar, J.A., Zavala, A.N., Diaz-Perez, C., Cervantes, C., Diaz-Perez, A.L. and Campos-Garcia, J. (2006) The atu and liu clusters are involved in the catabolic pathways for acyclic monoterpenes and leucine in *Pseudomonas aeruginosa*. *Appl Environ Microbiol* 72: 2070–2079.

Bea, H.S., Park, H.J., Lee, S.H. and Yun, H. (2011) Kinetic resolution of aromatic *β*-amino acids by ω-transaminase. *Chem Commun* 47: 5894–5896.

Cardillo, G., Tolomelli, A. and Tomasini, C. (1999) A new diastereoselective synthesis of anti-α-alkyl α-hydroxy β-amino acids. *Eur J Org Chem* 1: 155–161.

Christen, P. and Mehta, P. (2001) From cofactor to enzymes. The molecular evolution of pyridoxal-5'-phosphate-dependent enzymes. *Chem Rec* 1: 436–447.

Crismaru, C.G., Wybenga, G.G., Szymanski, W., Wijma, H.J., Wu, B., Bartsch, S., de Wildeman, S., Poelarends, G.J., Feringa, B.L., Dijkstra, B.W. and Janssen, D.B. (2013) Biochemical properties and crystal structure of a β-phenylalanine aminotransferase from *Variovorax paradoxus*. *Appl Environ Microbiol* 79: 185–195.

Das, R. and Baker, D. (2008) Macromolecular modeling with Rosetta. *Annu Rev Biochem* 77: 363–382.

Finn, R.D., Mistry, J., Tate, Coggill, J.P., Heger, A., Pollington, J.E., Gavin, O.L., Gunasekaran, P., Ceric, G., Forslund, K., Holm, L., Sonnhammer, E.L., Eddy, S.R. and Bateman, A. (2010) The Pfam protein families database. *Nuc Acids Res* 38: D211–222.

Groger, H., Trauthwein, H., Buchholz, S., Drauz, K., Sacherer, C., Godfrin, S. and Werner, H. (2004) The first aminoacylase-catalyzed enantioselective synthesis of aromatic beta-amino acids. *Org Biomol Chem* 2: 1977–1978.

Hanson, R.L., Davis, B.L., Yijun, C., Goldberg, S.L., Parker, W.L., Tully, T.P., Montana, M.A. and Patel, R.N. (2008) Preparation of (*R*)-amines from racemic amines with an (*S*)-amine transaminase from *Bacillus megaterium*. *Adv Synth Catal* 350: 1367–1375.

Heck, T., Seebach, D., Osswald, S., Ter Wiel, M.K., Kohler, H.P. and Geueke, B. (2009) Kinetic resolution of aliphatic beta-amino acid amides by beta-aminopeptidases. *ChemBioChem* 10: 1558–1561.

Herrmann, G., Selmer, T., Jessen, H.J., Gokarn, R.R., Selifonova, O., Gort, S.J. and Buckel, W. (2005) Two beta-alanyl-CoA:ammonia lyases in *Clostridium propionicum*. *FEBS J* 272: 813–821.

Hohne, M., Schatzle, S., Jochens, H., Robins, K., and Bornscheuer, U.T. (2010) Rational assignment of key motifs for function guides in silico enzyme identification. *Nat Chem Biol* 6: 807–813.

Ivancic, M., Valinger, G., Gruber, K. and Schwab, H. (2007) Inverting enantioselectivity of *Burkholderia gladioli* esterase EstB by directed and designed evolution. *J Biotechnol* 129: 109–122.

Iwasaki, A., Yamada, Y., Ikenaka, Y. and Hasegawa, J. (2003) Microbial synthesis of (R)- and (S)-3,4-dimethoxyamphetamines through stereoselective transamination. *Biotechnol Lett* 25: 1843–1846.

Jansonius, J.N. (1998) Structure, evolution and action of vitamin B6-dependent enzymes. *Curr Opin Struct Biol* 8: 759–769.

Juaristi, E. and Soloshonok, V. (2005) Enantioselective synthesis of β-amino acids. Wiley-Interscience, New York, 2nd ed.

Kim, J., Kyung, D., Yun, H., Cho, B.K., Seo, J.H., Cha, M. and Kim, B.G. (2007) Cloning and characterization of a novel beta-transaminase from *Mesorhizobium* sp strain LUK: a new biocatalyst for the synthesis of enantiomerically pure beta-amino acids. *Appl Environ Microbiol* 73: 1772–1782.

Koszelewski, D., Lavandera, I., Clay, D., Rozzell, D. and Kroutil, W. (2008) Asymmetric synthesis of optically pure pharmacologically relevant amines employing ω-transaminases. *Adv Synth Catal* 350: 2761–2766.

van Leeuwen, J.G., Wijma, H.J., Floor, R.J., van der Laan, J.M. and Janssen, D.B. (2012) Directed evolution strategies for enantiocomplementary haloalkane dehalogenases: from chemical waste to enantiopure building blocks. *ChemBioChem* 13: 137–148.

Liljeblad, A. and Kanerva, L.T. (2006) Biocatalysis as a profound tool in the preparation of highly enantiopure β-amino acids. *Tetrahedron* 62: 5831–5854.

Li, D., Cheng, S., Wei, D., Ren Y. and Zhang, D. (2007) Production of enantiomerically pure (*S*)-β-phenylalanine and (*R*)-β-phenylalanine by penicillin G acylase from *Escherichia coli* in aqueous medium. *Biotechnol Lett* 29: 1825–1830.

Liu, M. and Sibi, M.P. (2002) Recent advances in the stereoselective synthesis of β-amino acids. *Tetrahedron* 58: 7991–8035.

Magnusson, A.O., Takwa, M., Hamberg, A. and Hult, K. (2005) An *S*-selective lipase was created by rational redesign and the enantioselectivity increased with temperature. *Angew Chem Int Edn Engl* 44: 4582–4585.

May, O., Nguyen, P.T. and Arnold, F.H. (2000) Inverting enantioselectivity by directed evolution of hydantoinase for improved production of L-methionine. *Nat Biotechnol* 18: 317–320.

Mehta, P.K., THale, T.I. and Christen, P. (1993) Aminotransferases - demonstration of homology and division into evolutionary subgroups. *Eur J Biochem* 214: 549–561.

Mugford, P.F., Wagner, U.G., Jiang, Y., Faber, K. and Kazlauskas, R.J. (2008) Enantiocomplementary enzymes: classification, molecular basis for their enantiopreference, and prospects for mirror-image biotransformations. *Angew Chem Int Ed* 47: 8782–8793.

Namikoshi, M., Rinehart, K.L., Dahlem, A.M., Beasley, V.R. and Carmichael, W.W. (1989) Total synthesis of Adda, the unique C20 amino acid of cyanobacterial hepatotoxins. *Tetrahedron Lett* 30: 4349–4352.

Okamoto, A., Nakai, Y., Hayashi, H., Hirotsu, K. and Kagamiyama, H. (1998) Crystal structures of *Paracoccus denitrificans* aromatic amino acid aminotransferase: A substrate recognition site constructed by rearrangement of hydrogen bond network. *J Mol Biol* 280: 443–461.

Percudani, R. and Peracchi, A. (2009) The B6 database: a tool for the description and classification of vitamin B6-dependent enzymatic activities and of the corresponding protein families. *BMC Bioinformatics* 10: 273.

Rudat, J., Brucher, B.R. and Syldatk, C. (2012) Transaminases for the synthesis of enantiopure beta-amino acids. *AMB Express* 2:11

Rehdorf, J., Mihovilovic, M.D. and Bornscheuer, U.T (2010) Exploiting the regioselectivity of Baeyer–Villiger monooxygenases for the formation of *β*-amino acids and *β*-amino alcohols. *Angew Chem Int Ed* 49: 4506–4508.

Savile, C.K., Janey J.M., Mundorff, E.C., Moore, J.C., Sarena, Tam, S., Jarvis, W.R., Colbeck, J.C., Krebber, A., Fleitz, F.J., Brands, J., Devine, P.N., Huisman, G.W. and Hughes G.J. (2010) Biocatalytic asymmetric synthesis of chiral amines from ketones applied to sitagliptin manufacture. *Science* 329: 305–309.

Seebach, D., Beck, A.K., Capone, S., Deniau, G., Groselj, U. and Zass E. (2009) Enantioselective preparation of β^2-amino acid derivatives for β-peptide synthesis. *Synthesis* 1: 1–32.

Seebach, D. and Matthews, J.L. (1997) β-Peptides: a surprise at every turn. *Chem Commun* 2015–2022.

Shih, C., Gossett, L.S., Gruber, J.M., Grossman, C.S., Andis, S.L., Schultz, R.M., Worzalla, J.F., Corbett, T.H. and Metz J.T. (1999) Synthesis and biological evaluation of novel cryptophycin analogs with modification in the β-alanine region. *Bioorg Med Chem Lett* 9: 69–74.

Soloshonok, V.A., Fokina, N.A., Rybakova, A.V., Shishkina, I.P., Galushko, S.V., Sochorinsky, A.E., Kukhar, V.P., Savchenko, M.V. and Svedas, V. K. (1995) Biocatalytic approach to enantiomerically pure β-amino acids. *Tetrahedron: Asymmetry* 6: 1601–1610.

Szymanski, W., Wu, B., Weiner, B., de Wildeman, S., Feringa, B.L. and Janssen, D.B. (2009) Phenylalanine aminomutase-catalyzed addition of ammonia to substituted cinnamic acids: a route to enantiopure alpha- and beta-amino acids. *J Org Chem* 74: 9152–9157.

Wani, M.C., Taylor, H.L., Wall, M.E., Coggon, P. and McPhail, A.T. (1971) Plant antitumor agents. VI. Isolation and structure of taxol, a novel antileukemic and antitumor agent from *Taxus brevifolia*. *J Am Chem Soc* 93: 2325–2327.

Weiner, B., Szymański, W., Janssen, D.B., Minnaard, A.J. and Feringa, B.L. (2010) Recent advances in the catalytic asymmetric synthesis of beta-amino acids. *Chem Soc Rev* 39: 1656–1691.

Wybenga, G.G., Crismaru, C.G., Janssen, D.B. and Dijkstra, B.W. (2012) Structural determinants of the *β*-selectivity of a bacterial aminotransferase. *J Biol Chem* 287: 28495–28502.

Yonaha, K., Suzuki, K., Minei, H. and Toyama, S. (1983) Distribution of omega-amino acid - pyruvate transaminase and aminobutyrate - alpha-ketoglutarate transaminase in microorganisms. *Agr Biol Chem Tokyo* 47: 2257–2265.

Yun, H., Lim, S., Cho, B.K. and Kim, B.G. (2004) omega-Amino acid:pyruvate transaminase from *Alcaligenes denitrificans* Y2k-2: a new catalyst for kinetic resolution of beta-amino acids and amines. *Appl Environ Microbiol* 70: 2529–2534.

Zha, D.X., Wilensek, S., Hermes, M., Jaeger, K.E. and Reetz, M.T. (2001) Complete reversal of enantioselectivity of an enzyme-catalyzed reaction by directed evolution. *Chem Commun (Camb)* 24: 2664–2665.

Chapter 7

Nederlandse samenvatting

β-Aminozuren komen voor als intermediairen bij de synthese van diverse bioactieve stoffen, zowel in laboratorium-ontwikkelde chemische productieschema's, alsook in natuurlijk geëvolueerde bio-synthetische routes. Voorbeelden van dergelijke synthetische verbindingen zijn *β*-peptiden, cytotoxische stoffen die opgebouwd zijn uit *β*-aminozuren. De aanwezigheid van *β*-aminozuur groepen in verscheidene antibiotica en farmacologisch actieve verbindingen heeft onderzoek naar de eigenschappen en bereiding van deze stoffen gestimuleerd, en heeft geleid tot de ontwikkeling van verschillende efficiënte methoden voor de organische synthese van *β*-aminozuren. Daarbij dient in het bijzonder de Mannich-reactie en de hydrogenering van enamines te worden vermeld (**Fig. 7.1**). Het belang van deze methode is een hoge conversie en enantioselectiviteit, maar daar staat tegenover dat de overgangsmetalen die gebruikt worden als katalysator bij deze reactie nadelig zijn voor het milieu en moeilijk verenigbaar zijn met biologische productiemethoden. In zulke gevallen zijn biokatalytische reacties die resulteren in enantiomeer zuivere aminozuren een goed alternatief. Enzymatische reacties kunnen ook toegepast worden in te ontwikkelen biosynthetische routes voor productie met behulp van fermentatie, hoewel er momenteel weinig bekend is in de literatuur over enzymatische routes die leiden tot productie van *β*-aminozuren. Daar komt bij dat de bekende biokatalytische routes voor productie van optisch actieve verbindingen gebruik maken van een kinetische resolutie, waarbij in het gunstigste geval toch slechts 50% van het startmateriaal omgezet kan worden in het gewenste product.

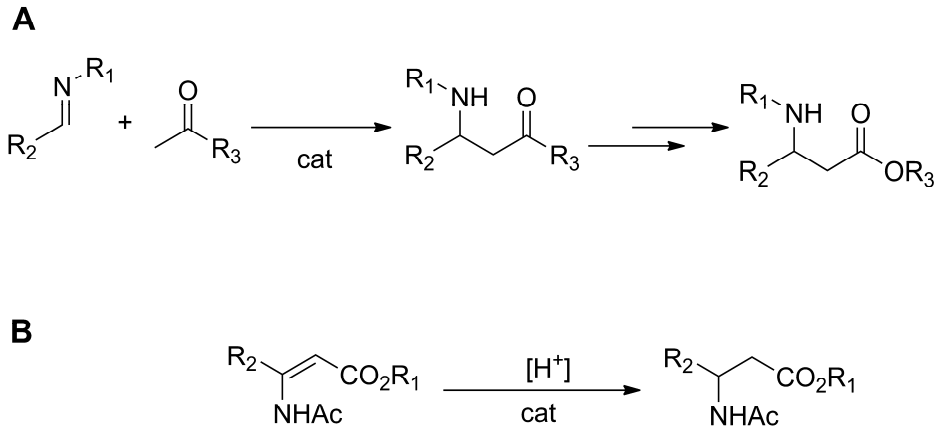

Figuur 7.1 Chemische reacties voor de bereiding van *β*-aminozuren. **A)** De Mannich-reactie, waarbij een imine-groep reageert met een keton tot een zogenaamd *β*-gesubstitueerd keton, dat vervolgens kan worden omgezet in een *β*-aminozuur via de Baeyer-Villiger oxidatie; **B)** Hydrogenering van een enamine-groep tot een N-gesubstitueerd *β*-aminozuur.

In **Hoofdstuk 1** van dit proefschrift en de hierin geciteerde artikelen wordt beschreven hoe de productie van enantiomeer zuivere *β*-aminozuren via biokatalytische methoden wordt uitgevoerd met verschillende typen enzymen (**Fig. 7.2**). De volgende enzymen en enzymreacties worden genoemd: (a) acylasen die de hydrolyse van N-geacetyleerde *β*-aminozuren katalyseren; (b) de acylering van *β*-aminozuren en de-acylering van *N*-fenyl-geacetyleerde *β*-aminozuren door penicilline acylase; (c) de kinetische omzetting van alifatische *β*-aminozure amines door aminopeptidasen; (d) de de-acylering van *β*-aminozuur-esters door lipasen en esterases; (e) de enantio- en regio-selectieve additie van ammonia aan kaneelzuur-afgeleide stoffen door fenylalanine aminomutasen; (f) de productie van *β*-aminozuur-esters van aminoketonen door Baeyer-Villiger mono-oxygenasen; (g) de omzetting van aromatische *β*-aminozuren door transaminasen (TA's); en (h) de transaminase-gekatalyseerde asymmetrische aminering van *β*-ketozuren en -esters.

Hoewel ze in principe attractief zijn voor biokatalytische processen, gaan de bovengenoemde omzettingen vaak gepaard met enzym-gerelateerde problemen zoals een lage katalytische activiteit (fenylalanine aminomutasen), product-inhibitie (transaminasen met ketozuren), de noodzaak meerdere enzymen te gebruiken (asymmetrische synthese door lipase en transaminase), of de noodzaak cofactoren toe te voegen (Baeyer-Villiger mono-oxygenasen). Daar staan potentieel belangrijke

voordelen tegenover, bijvoorbeeld de hoge enantioselectiviteit van transaminasen en veel hydrolasen, en het feit dat hydrolasen geen dure cofactoren nodig hebben.

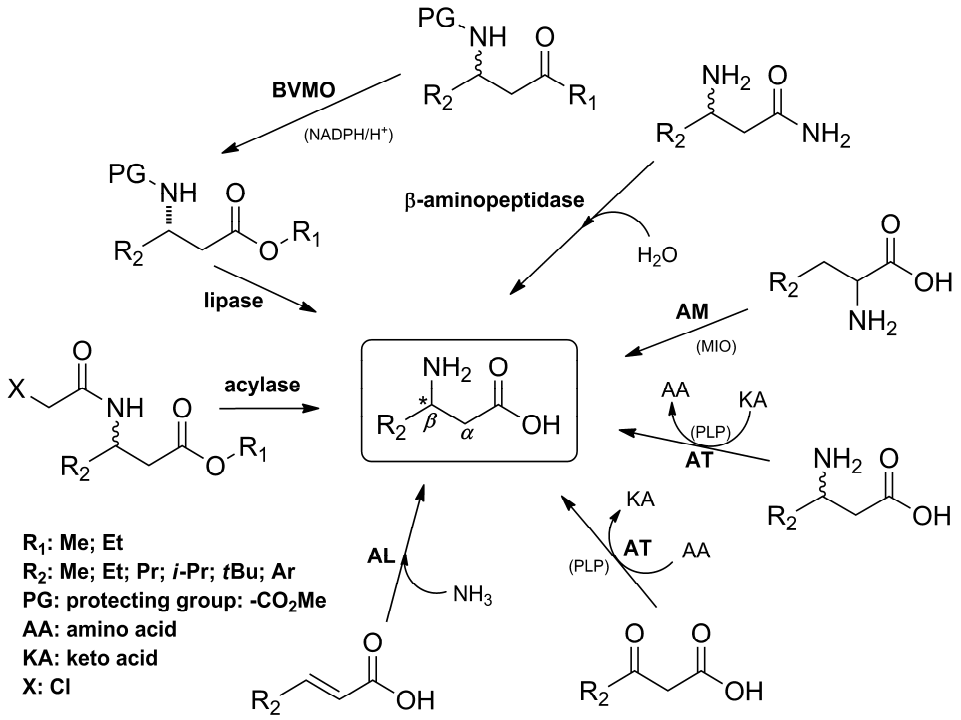

Figuur 7.2 Enzymatische routes voor de productie van *β*-aminozuren.

Dit proefschrift is het resultaat van het onderzoeksproject "Selectie en karakterisering van nieuwe enantioselectieve (de-)amінerings-enzymen", onderdeel van het publiek-private NWO-ACTS programma B-Basic, waaraan de Rijksuniversiteit Groningen deelnam. Het doel was het ontdekken van nieuwe (de-)amінerings-enzymen die betrokken zijn of toegepast kunnen worden bij de omzetting en productie van *β*-aminozuren. Omdat enkele *β*-aminozuren vrij in de natuur voorkomen, als zelfstandige moleculen of als onderdeel van grotere molecuulstructuren, is het te verwachten dat enzymen die *β*-aminozuren produceren en afbreken in de natuur te vinden zijn. Om deze te vinden zijn twee verschillende methoden gebruikt: (a) het verrijken van microbiële culturen waarna organismen geïsoleerd worden die groeien op *β*-aminozuren als enige bron van stikstof; en (b) het onderzoeken van gen-bibliotheken, afgeleid uit het milieu, waarbij geselecteerd wordt voor *β*-aminozuren

als enige stikstofbron. De eerste methode gaat ervan uit dat de gezochte enzymen *β*-aminozuren omzetten in tussenproducten of in ammonium, hetgeen vervolgens de groei van microbiële culturen mogelijk maakt. In dergelijke ophopings-cultures werd een *β*-aminozuur gebruikt als enige stikstofbron en een verwante verbinding als koolstofbron.

In **Hoofdstuk 2** worden de resultaten van dergelijke ophopings-cultures beschreven. In totaal 18 microbiële stammen zijn geïsoleerd en gedeeltelijk gekarakteriseerd. De *β*-aminozuren waarvoor omzetting werd gevonden zijn: *β*-alanine, *β*-asparagine, *β*-glutamaat, *β*-leucine, *β*-fenylalanine, *β*-aminoboterzuur, D-asparaginezuur en *β*-tyrosine. Een *Variovorax paradoxus* stam die groeit op *β*-fenylalanine is vervolgens geselecteerd voor verder onderzoek.

De ontdekking van een nieuw *β*-fenylalanine aminotransferase van *V. paradoxus* (*Vp*AT) is beschreven in **Hoofdstuk 3**. Het gen dat codeert voor dit enzym is geïsoleerd na het screenen van een gen-bibliotheek voor klonen die in staat zijn *β*-fenylalanine om te zetten in acetofenon. Nadat de gensequentie was geanalyseerd, is het gen tot overexpressie gebracht in *E. coli* en kon het eiwit (het nieuwe *β*-fenylalanine aminotransferase) biochemisch en structureel worden gekarakteriseerd in samenwerking met Dr. Gjalt G. Wybenga van de Röntgenkristallografie-groep van de Rijksuniversiteit Groningen. Gebaseerd op een analyse van de aminozuurvolgorde en vergelijking van structuren van aminotransferasen is een aminozuurvolgorde-motief voor het actieve centrum voorgesteld dat van nut kan zijn voor het ontdekken van meer aminotransferasen die *β*-aminozuren kunnen omzetten.

In **Hoofdstuk 4** beschrijven we een tweede aminotransferase: het *β*-fenylalanine aminotransferase van *Mesorhizobium* sp. stam LUK (*Mes*AT). Dit eiwit was oorspronkelijke beschreven door Kim *et al.* in Korea, maar een structuur was onbekend. Het enzym is verder onderzocht en gebruikt voor vergelijkend onderzoek met betrekking tot de katalytische activiteit en de 3D structuur, weer in samenwerking met Gjalt Wybenga. De resultaten laten zien dat dit enzym behoort tot ”fold-type I PLP enzymen”, en dat het een omgekeerde oriëntatie van *β*-fenylalanine in het actieve centrum heeft, vergeleken met de positionering van *α*-aminozuren in andere leden van dezelfde familie van aminotransferasen.

Hoofdstuk 5 beschrijft de omzetting van *β*-valine door *Pseudomonas* sp. stam SBV1, een bacteriële stam die is geïsoleerd en verstrekt door Dr. Stefaan De Wildeman van DSM. Dit organisme kan *β*-valine omzetten tijdens groei op een mineraal medium. De omzettingssnelheid is hoog en *β*-valine wordt gebruikt als enige bron van stikstof. Het substraat is een zogenaamd geblokkeerd aminozuur: omdat de aminogroep zich op een tertiair koolstofatoom bevindt kunnen de meest voorkomende deamineringsmechanismen (aminotransferase, aminozuur dehydrogenase, amine oxidase) niet plaatsvinden, waardoor de kans om een mutase- of een lyase-reactie te vinden toeneemt. We ontdekten een deamineringsroute die gebaseerd is op eerst een activering van *β*-valine door een coenzym A koppeling, gevolgd door een deaminering onder invloed van een lyase. Een genetische analyse van deze route is uitgevoerd: de genen die coderen voor de meest relevante enzymen zijn geïsoleerd en gekarakteriseerd. Een nieuw type lyase dat reageert met het CoA-conjugaat van *β*-valine en gerelateerd is aan enoyl-CoA hydratasen is verondersteld de deamineringsreactie te katalyseren.

In **Hoofdstuk 6** worden de resultaten van dit proefschrift samengevat en bediscussieerd in de context van nieuwe uitdagingen. De mogelijkheid andere nieuwe enzymen te vinden die deamineringsreacties katalyseren, en de kans deze te gebruiken bij biokatalyse, worden besproken.

Het onderzoek dat in dit proefschrift beschreven is begon met verrijkingsexperimenten om micro-organismen de vinden die *β*-aminozuren kunnen gebruiken als enige bron van stikstof. Via activiteits-bepaling assays is gezocht naar nieuwe enzymreacties. Daarna werden nieuw ontdekte *β*-aminozuur omzettende enzymen gekarakteriseerd en geproduceerd door middel van kloneren en heterologe expressie. In combinatie met biochemische karakterisering, kinetische analyse, het bepalen van substraatspecificiteit en enantioselectiviteit, en ook structuurbepaling is nieuw inzicht gegenereerd in de mogelijkheden van enzymatische omzetting van *β*-aminozuren, waarvan verwacht wordt dat het bijdraagt aan de ontwikkeling van een moleculaire gereedschapskist voor de biokatalytische productie van *β*-aminozuren.

Acknowledgements / Mulţumiri

I've made it! After quite some time I managed to finish my PhD research and to put on paper the results that I obtained. I have to mention though that this experience was very challenging and I could have not succeeded without the support, contribution and guidance of several people. For these reasons I would like to acknowledge them.

I shall start with my first promoter, prof. Dick Janssen. I might be a bit "wordy" now, but I take my chances. Dick, you have my deep appreciation, respect and gratitude for the manner you guided me during this research project. I had a rather difficult start with the project but you were everything a (PhD)student could possibly wish from his supervisor, and that is motivating, focusing, enthusiastic spirit and systematic way of conducting research, interpret the data and draw clear conclusions. I learned many things from you during these years not only from the scientific perspective but also from many other areas. I enjoyed always our conversations especially during the long trips to our DSM partners in Geleen, about science, politics, history or whatever we and our colleagues came across to discuss. Thank you for having me in your group, I wish you many years in the field and keep at least the same level of performing research in the famous "systematic" manner that I always found exciting and remarkable.

I would like to express my respect and sincere acknowledgements to my second promoter, prof. Bauke Dijkstra. From the moment I arrived to the Netherlands (October 24, 2004), when I started my MSc project in your group, Protein Crystallography, you were my first contact with the laboratory research at this university. I admire your talent, your perfectionism and kindness. Thank you for having me in your group then and I am also thankful to Cyril Hamiaux, my close supervisor in the lab. Remarkably, we came to collaborate later again through the work performed by Gjalt Wybenga, within the B-Basic programme. Thank you for your guidance, for reviewing my thesis and for very useful comments.

I am very thankful to my very first lab supervisor, prof. Gerrit Poelarends. I remember as it happened yesterday Gerrit, when we went to Haren to ask prof. Dirk van Elsas for soil samples, which I used to enrich the first bacterial cultures on *β*-amino acids. I am happy that I had the opportunity to work with you and I am very grateful for your support and guidance not only in the beginning of the project but also later when you left our group and founded yours at the Pharmaceutical Biology Department (UMC Groningen). Thank you also for your critical comments, suggestions and advices throughout my PhD project.

I am thankful to prof. Dirk van Elsas from the Microbial Ecology research group for providing me the very first soil samples to start my bacterial isolation experiments.

I would like to thank my close co-workers during this research. Gjalt Wybenga, thank you for your input in our fruitful collaboration, which yielded two chapters in this thesis. Gjalt, you are great guy, we had very nice results and I admired your motivation and skills, thanks for solving the structures of *Vp*AT and *Mes*AT. Dank je wel! Veel succes in je carrière! Wu Bian, we were also colleagues in the B-Basic programme. Thank you for your support, nice ideas and valuable suggestions. I wish you and your beautiful family (Andy is a big boy now!) all the best and I hope to meet you guys again, maybe in China! You can be the best guide for us! Wiktor Szymanski, you are the "most" chemist I know, and now with lots of "bio" views acquired in the last period: you deliver not only great chemistry but you become a good biochemist over the years, performing remarkably good from gene cloning, protein expression to analytical assays – brilliant scientist ! Thank you for your contribution to my research, in particular for the work done in chapter 3 and 5. I wish you success in your academic career! Many thanks to Christiaan Postema ! Without your help Christiaan, the chapter 5 could not have been what it is now in the book. Heel graag bedankt, Christiaan ! Many thanks to all the other B-Basic colleagues: Barbara (cool chemist), Alja (great person, always "to the point"!), Jan (look forward to your defense & good luck at DSM!), Hans and Vinod (we had nice time in this research!). Good luck to you all guys and all the best in

your professional and personal life.

This research could not reach this far without the support and assistance of our collaborators from DSM. Many thanks to Dr. Stefaan De Wildeman (for SBV1 – the "speedy" strain, deamination mechanisms solved in chapter 5), Dr. Oliver May, Dr. Frisso van Assema, Dr. Bernard Kaptein and Dr. Jan-Metske van der Laan.

My appreciation and many thanks are also for the "beoordelingscommissie" members: prof. Wolfgang Kroutil, prof. Lubert Dijkhuizen and prof. Adriaan Minnaard. This thesis looks now better after going through your hands. Thank you for your comments and suggestions.

I would like to express my warm thanks to my former colleagues from the Biotransformation and Biocatalysis research group. I shall start with prof. Marco Fraaije, thank you for your advices and valuable suggestions. Many thanks to Danny and Matthew for your help and for being my "paranimfen". Further, I would like to thank Erik (probably saved my life when I fainted on the corridor!), Dominic, Chiara (nice cakes and ice cream made in house with liquid N_2), Martijn (always enjoying borrels with you!), Roga (good luck with finishing your thesis!), Ana (we shall visit your country, it's one of our top destinations!), Edwin (great to be your office mate & good luck in the industry!), Remko (you are majestic!), Robert (stay motivated & I look forward to your defense!), Hein (very organized guy!), Marcus and Anett (you have a blessed family!), Anette and Sebastian (I wish you a happy marriage!), Willem (good luck with your PhD project!), Hassan, Irfan (thanks for your help with DNA libraries & good luck with finishing your thesis!), Samin (all the best in Pakistan!), Hanna (nice person, always helpful!) Hugo, Gosia (you guys, shall defend soon, good luck!). In addition, I would like to thank Piet, Jaap, Nico for all the technical support in the lab. Mijne heren, dank u wel! Bovendien, ik wil graag Sandra en Karlien bedanken! Lieve dames dank u, voor jullie hulp met het administratieve dingen en beschikbarheid, maar ook voor jullie bijdrage om mijn Nederlandse taal te verbeteren. I would like also to thank my students during my PhD research, Djoke Hendriks, Marius Uebel and Ruslan

Vietrov. I wish you success with your studies.

I would like to thank Menno Tol, from my current research group (Molecular Microbiology) for his contribution with *Nederlandse samenvatting*.

I would like to address sincere thanks to my former professors and staff from my home university in Iaşi, România, prof. D. Cojocaru, prof. V. Artenie, prof. O. Toma, lecturer S. Dunca, lecturer E. Ungureanu and lecturer E. Ciornea who taught me things like biochemistry, metabolic pathways, DNA, and microbiology. In addition I am thankful to Mihaela Bucşă, chief secretary of the Faculty of Biology at Alexandru Ioan Cuza University, Iasi, România for her support with administrative matters regarding my Erasmus exchange scholarship (2004-2005).

I would like to thank my Romanian fellows and their families with brilliant children here in Groningen but also within the Netherlands or abroad for their support, encouragement and constant help throughout these years. It was a real pleasure for me and my family to meet you here and become your friends in this Dutch adventure. To mention them, I hope not to forget any of them: Dragoş and Oana Vârnav, Orest and Maria Iftime, Mihai and Mia Brăgaru, Laura Maruşter and George Oltean, Laurenţiu and Aurora Alexe, Marc Zoetendal and Carmen Zoetendal-Popa, Ana Arteni, Marius and Mădălina Costache, Mihaela Folea, Aurora Batinaş-Geurts and Koen Geurts, Cătălina Lomoş, Magda Isac, Mihai and Ileana Rădulescu, Rodica Ioan, Alex Simu, Roxana Teodor. I would like to thank also vader Onufry and Jewsewy from the Russian Orthodox church in Groningen, for their unconditional support and good faith! Mai departe, aş dori să mulţumesc părintelui Costel Ionaşcu, familiei dânsului dar şi comunităţii românilor de la parohia ortodoxă română din Groningen pentru sprijinul si înţelegerea acordate.

I would like to thank also Wissam Chemissany and his wife Lana for their friendship and congratulate them for the beautiful children they have. All the best to you guys!

I am very grateful and respectful to my parents, who offered me a great education and supported me in many matters at all times. Dragă mamă şi tată, voi mi-aţi oferit atât de multe! Am să vă fiu mereu recunoscător pentru sacrificiile voastre şi am să vă port respectul întotdeauna. Dragă Simona, sora mea mai mică îţi mulţumesc si ţie pentru sprijinul tău, te felicit pentru familia deosebită, si fetiţa voastră, nepoţica noastră, Shara Maria, frumoasă foc!

The most wonderful thing in life is family. Last but not least, I must say that this thesis could not be finalized without my family's affection, support and encouragement. Mihaela, my lovely wife, the kindest, warmest and most understanding person I know, you were constantly supportive and caring. During my PhD project our son Matei was born, bringing us enormous happiness and joy ☺ !

I thank you both and I love you so very much! Vă iubesc din toată inima !!!

Ciprian Crîşmaru

May 2014

List of publications

Crismaru, C.G.*, Wybenga, G.G.*, Szymanski, W., Wijma, H.J., Wu, B., Bartsch, S., De Wildeman, S., Poelarends, G.J., Feringa, B.L., Dijkstra, B.W. and Janssen, D.B. (**2013**) Biochemical properties and crystal structure of a *β*-phenylalanine aminotransferase from *Variovorax paradoxus*. *Appl Environ Microbiol* 79: 185–195.

Wybenga, G.G.*, **Crismaru, C.G.***, Janssen, D.B. and Dijkstra, B.W. (**2012**) Structural determinants of the *β*-selectivity of a bacterial aminotransferase. *J Biol Chem* 287: 28495–28502.

Wu, B., Szymanski, W., **Crismaru, C.G.**, Feringa B.L. and Janssen, D.B. (**2012**) C-N lyases catalyzing addition of ammonia, amines and amides to C=C and C=O bonds, p 749–778. *In* Drauz K, Groger H, May O (ed), *Enz Catal Org Synth* Wiley-VCH, New York, NY.

Wu, B., Szymanski, W., Wijma, H.J., **Crismaru, C.G.**, De Wildeman, S., Poelarends, G.J., Feringa, B.L. and Janssen, D.B. (**2010**) Engineering of an enantioselective tyrosine aminomutase by mutation of a single active site residue in phenylalanine aminomutase. *Chem Commun (Camb)* 46: 8157–8159.

Crismaru, C.G., Otzen, M., Postema, C.P., Heberling, M.M., De Wildeman, S. and Janssen, D.B. (**2014**) Degradation of *β*-valine by *Pseudomonas* sp. strain SBV1. To be submitted.

* these authors contributed equally to this study